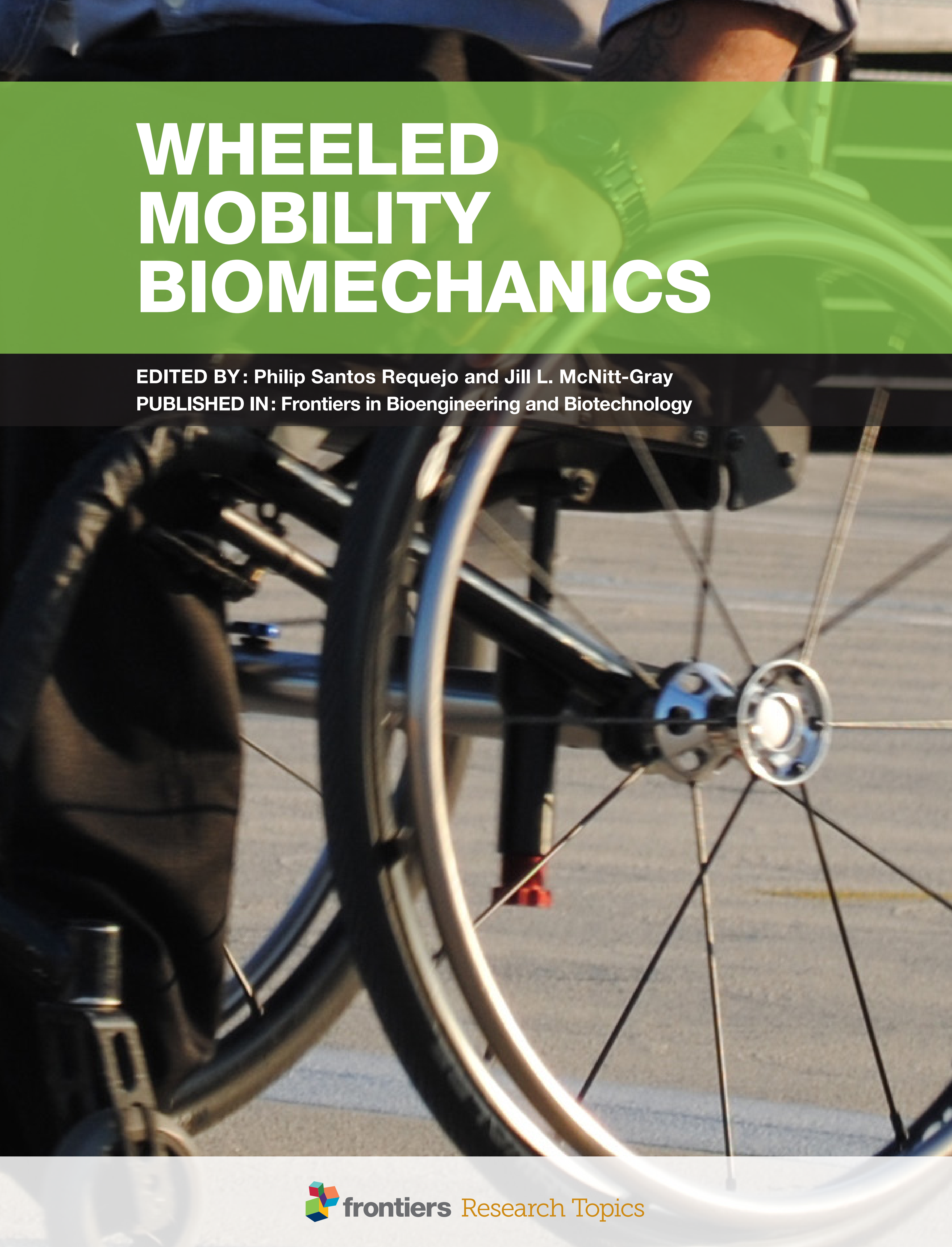

WHEELED MOBILITY BIOMECHANICS

EDITED BY: Philip Santos Requejo and Jill L. McNitt-Gray
PUBLISHED IN: Frontiers in Bioengineering and Biotechnology

frontiers Research Topics

ISSN 1664-8714
ISBN 978-2-88919-938-9
DOI 10.3389/978-2-88919-938-9

About Frontiers

Frontiers is more than just an open-access publisher of scholarly articles: it is a pioneering approach to the world of academia, radically improving the way scholarly research is managed. The grand vision of Frontiers is a world where all people have an equal opportunity to seek, share and generate knowledge. Frontiers provides immediate and permanent online open access to all its publications, but this alone is not enough to realize our grand goals.

Frontiers Journal Series

The Frontiers Journal Series is a multi-tier and interdisciplinary set of open-access, online journals, promising a paradigm shift from the current review, selection and dissemination processes in academic publishing. All Frontiers journals are driven by researchers for researchers; therefore, they constitute a service to the scholarly community. At the same time, the Frontiers Journal Series operates on a revolutionary invention, the tiered publishing system, initially addressing specific communities of scholars, and gradually climbing up to broader public understanding, thus serving the interests of the lay society, too.

Dedication to quality

Each Frontiers article is a landmark of the highest quality, thanks to genuinely collaborative interactions between authors and review editors, who include some of the world's best academicians. Research must be certified by peers before entering a stream of knowledge that may eventually reach the public - and shape society; therefore, Frontiers only applies the most rigorous and unbiased reviews.
Frontiers revolutionizes research publishing by freely delivering the most outstanding research, evaluated with no bias from both the academic and social point of view.
By applying the most advanced information technologies, Frontiers is catapulting scholarly publishing into a new generation.

What are Frontiers Research Topics?

Frontiers Research Topics are very popular trademarks of the Frontiers Journals Series: they are collections of at least ten articles, all centered on a particular subject. With their unique mix of varied contributions from Original Research to Review Articles, Frontiers Research Topics unify the most influential researchers, the latest key findings and historical advances in a hot research area! Find out more on how to host your own Frontiers Research Topic or contribute to one as an author by contacting the Frontiers Editorial Office: **researchtopics@frontiersin.org**

WHEELED MOBILITY BIOMECHANICS

Topic Editors:
Philip Santos Requejo, Rancho Los Amigos National Rehabilitation Center, USA
Jill L. McNitt-Gray, University of Southern California, USA

Manual wheelchair user propelling a wheelchair.

Photo by Philip Santos Requejo

For the manual wheelchair (MWC) user, loss of lower extremity function often places the burden for mobility and activities of daily living on the upper extremities. This e-book on Wheeled Mobility Biomechanics contains current research that provides insights into the mechanical demands and performance techniques during tasks associated with MWC. Our intent was to contribute to advancing the knowledge regarding the variables that promote or hinder an individual's capacity to handle the daily manual wheeled mobility demands and gain greater insights into upper extremity loading consequences, predictors of pain onset and injury, and ultimately identify strategies for preserving health and functional mobility for the MWC user.

Citation: Requejo, P. S., McNitt-Gray, J. L., eds. (2016). Wheeled Mobility Biomechanics. Lausanne: Frontiers Media. doi: 10.3389/978-2-88919-938-9

Table of Contents

frontiers in Bioengineering and Biotechnology

EDITORIAL
published: 28 June 2016
doi: 10.3389/fbioe.2016.00053

Editorial: Wheeled Mobility Biomechanics

Philip Santos Requejo[1] and Jill L. McNitt-Gray[2,3]*

[1] Rehabilitation Engineering, Rancho Los Amigos National Rehabilitation Center, Downey, CA, USA, [2] Biomechanics Research Laboratory, Department of Biological Sciences, University of Southern California, Los Angeles, CA, USA, [3] Biomechanics Research Laboratory, Department of Biomedical Engineering, University of Southern California, Los Angeles, CA, USA

Keywords: wheelchair, mobility, shoulder, pain, spinal cord injuries, propulsion, car transfer, ultrasonography

The Editorial on the Research Topic

Wheeled Mobility Biomechanics

For the manual wheelchair (MWC) user, loss of lower extremity function often places the burden for mobility and activities of daily living on the upper extremities. People who use a MWC commonly report fatigue and musculoskeletal pain in the shoulder, most often due to increased demands of mobility (Kemp and Mosqueda, 2004; Kemp, 2005). Because individuals who rely on MWC are dependent on their upper extremities for mobility and requisite activities (sitting, transfers, and pressure reliefs), as well as activities initiated from the wheelchair (exercise, reaching, and lifting), shoulder pain and dysfunction (Vissers et al., 2008; Mulroy et al., 2011a) can limit independence and functional mobility (Gerhart et al., 1993; Pentland and Twomey, 1994; Ballinger et al., 2000; McCasland et al. 2006) and negatively impact community participation and quality of life (Gutierrez et al., 2007; Chang et al., 2012). While the exact relationship between the physical demands of wheelchair use and the development of shoulder pathology is not yet fully understood, ergonomics studies consistently suggest that there is a link between highly repetitive tasks and the occurrence of upper extremity pain and injury (Frost et al., 2002; Silverstein et al., 2008). Therefore, to prevent further loss of independence and functional mobility, it is imperative to find ways to preserve shoulder function for the MWC user.

In preparing for this Research Topic in Wheeled Mobility Biomechanics, we were particularly interested in receiving contributions about current research that provided insights into the mechanical demands and performance techniques during tasks associated with MWC use in order to gain a greater insight into upper extremity loading consequences, predictors of pain onset and injury, and identifying strategies that can preserve functional mobility for the MWC user.

In organizing the Research Topic issue, we invited a number of experts who study wheeled mobility from different perspectives with the intent of advancing the knowledge regarding the variables that promote or hinder an individual's capacity to handle the daily manual wheeled mobility demands. This is highlighted in the contribution by Gil-Agudo and colleagues who provided insights into the acute changes to the shoulder's soft tissues by evaluating the echographic and kinetic changes in the shoulder joint after MWC propulsion under two different workload settings (Gil-Agudo et al.). Zhao and colleagues presented an analysis of the scapular motion in three common tasks performed by individuals who use a MWC to gain insights into potentially detrimental shoulder kinematics experienced during wheelchair use and related activities (Zhao et al.). To provide a comprehensive approach for MWC prescription, training, and long-term care for children who use a MWC, Slavens and colleagues characterized the upper extremity biomechanics of MWC mobility in children and adolescents during propulsion, starting, and stopping (Slavens et al.). They identified the greatest demand occurring during the starting task, with distinct propulsion patterns that were unlike those seen in adults.

OPEN ACCESS

Edited and Reviewed by:
Yih-Kuen Jan,
University of Illinois at Urbana-Champaign, USA

****Correspondence:***
Philip Santos Requejo
requejo@usc.edu

Specialty section:
This article was submitted to Biomechanics, a section of the journal Frontiers in Bioengineering and Biotechnology

Received: *16 May 2016*
Accepted: *15 June 2016*
Published: *28 June 2016*

Citation:
Requejo PS and McNitt-Gray JL (2016) Editorial: Wheeled Mobility Biomechanics. Front. Bioeng. Biotechnol. 4:53. doi: 10.3389/fbioe.2016.00053

Manual wheelchair Propulsion (WCP) technique is one aspect of wheelchair use that is believed to be associated with upper limb overuse injury (Boninger et al., 2002). Two contributions provided excellent insights into the relationship between propulsion technique and upper limb biomechanics (Dysterheft et al.). First, Dysterheft and colleagues studied the changes in adolescents' WCP biomechanics pre- and post-video and verbal feedback in order to maximize contact angle, while minimizing stroke frequency at the handrim (Paralyzed Veterans of America Consortium for Spinal Cord Medicine, 2005). Second, to gain insights into the relationship between WCP technique and loading consequences, Russell et al. showed how individuals with paraplegia modify WCP biomechanics to accommodate expected increases in reaction forces generated at the pushrim with self-selected increases in WCP speed.

There is growing theoretical and empirical evidence that fluctuations in movement (i.e., motor variability), including asymmetry between each arm during WCP, are related to musculoskeletal pain. In a perspective paper, Sosnoff and colleagues argue that the variability of WCP is impacted by shoulder pain and recommend inclusion of variability metrics can yield insights into shoulder pain development (Sosnoff et al.). Also, drawing from a large sample size, Soltau et al. establish the validity of bilateral symmetry during MWC propulsion in those without significant upper extremity pain or impairment.

For the MWC user, being able to self-transfer is essential for independence and community participation. But independent transfer, particularly car transfer, is complex, physically demanding, and known to provoke shoulder pain (Fliess-Douer et al., 2012). To gain insights into the relationship between movement technique and shoulder loading in activities associated with MWC use, Haubert and colleagues described techniques and factors influencing car transfer and WC loading for individuals with paraplegia driving their own vehicles and using their personal MWC (Haubert et al.). They provide an evidence-based recommendation for safe and effective car transfer technique for maintaining independence and preserving mobility for the MWC user.

We claim that creation and application of evidence-based strategies aimed at preserving shoulder function must be personalized and must address multiple factors related to ergonomics and equipment selection, performance techniques, and load-bearing capability of the individual. These include recommendations for reducing the mechanical loads and muscular demands through ergonomics, wheelchair selection and configuration, and environmental adaptations and personal factors for increasing the capacity to handle the daily mobility demands (Requejo et al., 2008, 2015). By integrating up-to-date knowledge of the musculoskeletal system, individual's capacity to generate and withstand external demands, preferred multijoint control strategies including propulsion technique, and repetitive load exposure through biomechanical modeling and simulations, feasible interventions can be identified and implemented (Munaretto et al., 2012, 2013; Slowik et al., 2015, 2016a,b).

In practice, we highlight the need for individualization of the wheelchair prescription process such that the characteristics of the wheelchair matched the functional capacity of the individual. Individually configured MWCs and seating systems can change postural alignment that improves comfort by decreasing pain from poor posture and improves the ability and efficiency to self-propel, prolonging mobility and endurance and preventing the development of secondary problems. An appropriate wheelchair and seating system provides a stable base for using upper and lower extremities for all mobility-related daily activities and, most important, propelling a wheelchair to maintain independent functional mobility to maximize quality of life. What is important is that clinicians must identify the wheelchair characteristics that are crucial for each individual and then identify the appropriate wheelchair that results in a fit that is specific and unique to a single MWC user. The ability to prescribe, order, modify, or configure the frame or components, to achieve a final system that meets the medical and functional needs of the individual, remains a key ingredient for preserving wheeled mobility.

AUTHOR CONTRIBUTIONS

Drs. PR and JM-G contributed equally to the writing of the contents of this editorial.

FUNDING

Some contents of this article were developed under a grant from the US Department of Health and Human Services, Administration for Community Living, National Institute on Disability, Independent Living, and Rehabilitation Research (NIDILRR). However, these contents do not necessarily represent the policy of the Department of Health and Human Services, and you should not assume endorsement by the Federal Government.

REFERENCES

Ballinger, D. A., Rintala, D. H., and Hart, K. A. (2000). The relation of shoulder pain and range-of-motion problems to functional limitations, disability, and perceived health of men with spinal cord injury: a multifaceted longitudinal study. *Arch. Phys. Med. Rehabil.* 81, 1575–1581. doi:10.1053/apmr.2000.18216

Boninger, M. L., Souza, A. L., Cooper, R. A., Fitzgerald, S. G., Koontz, A. M., and Fay, B. T. (2002). Propulsion patterns and pushrim biomechanics in manual wheelchair propulsion. *Arch. Phys. Med. Rehabil.* 83, 718–723. doi:10.1053/apmr.2002.32455

Chang, F.-H., Wang, Y.-H., Jang, Y., and Wang, C.-W. (2012). Factors associated with quality of life among people with spinal cord injury: application of the international classification of functioning, disability and health model. *Arch. Phys. Med. Rehabil.* 93, 2264–2270. doi:10.1016/j.apmr.2012.06.008

Fliess-Douer, O., Vanlandewijck, Y. C., and Van der Woude, L. H. (2012). Most essential wheeled mobility skills for daily life: an international survey among paralympic wheelchair athletes with spinal cord injury. *Arch. Phys. Med. Rehabil.* 93, 629–635. doi:10.1016/j.apmr.2011.11.017

Frost, P., Bonde, J. P., Mikkelsen, S., Andersen, J. H., Fallentin, N., Kaergaard, A., et al. (2002). Risk of shoulder tendinitis in relation to shoulder loads in monotonous repetitive work. *Am. J. Ind. Med.* 41, 11–18. doi:10.1002/ajim.10019

Gerhart, K. A., Bergstrom, E., Charlifue, S. W., Menter, R. R., and Whiteneck, G. G. (1993). Long-term spinal cord injury: functional changes over time. *Arch. Phys. Med. Rehabil.* 74, 1030–1034. doi:10.1016/0003-9993(93)90057-H

Gutierrez, D. D., Thompson, L., Kemp, B., and Mulroy, S. J. (2007). The relationship of shoulder pain intensity to quality of life, physical activity, and community participation in persons with paraplegia. *J. Spinal. Cord. Med.* 30, 251–255.

Kemp, B. J. (2005). What the rehabilitation professional and the consumer need to know. *Phys. Med. Rehabil. Clin. N. Am.* 16, 1–18, vii. doi:10.1016/j.pmr.2004.06.009

Kemp, B. J., and Mosqueda, L. (2004). *Aging with a Disability: What the Clinician Needs to Know*. Baltimore: JHU Press.

McCasland, L. D., Budiman-Mak, E., Weaver, F. M., Adams, E., and Miskevics, S. (2006). Shoulder pain in the traumatically injured spinal cord patient: evaluation of risk factors and function. *J. Clin. Rheumatol.* 12, 179–186. doi:10.1097/01.rhu.0000230532.54403.25

Mulroy, S. J., Winstein, C. J., Kulig, K., Beneck, G. J., Fowler, E. G., DeMuth, S. K., et al. (2011a). Secondary mediation and regression analyses of the PTClinResNet database: determining causal relationships among the International Classification of Functioning, Disability and Health levels for four physical therapy intervention trials. *Phys. Ther.* 91, 1766–1779. doi:10.2522/ptj.20110024

Munaretto, J. M., McNitt-Gray, J. L., Flashner, H., and Requejo, P. S. (2012). Simulated effect of reaction force redirection on the upper extremity mechanical demand imposed during manual wheelchair propulsion. *Clin. Biomech. (Bristol, Avon)* 27, 255–262. doi:10.1016/j.clinbiomech.2011.10.001

Munaretto, J. M., McNitt-Gray, J. L., Flashner, H., and Requejo, P. S. (2013). Reconfiguration of the upper extremity relative to the pushrim affects load distribution during wheelchair propulsion. *Med. Eng. Phys.* 35, 1141–1149. doi:10.1016/j.medengphy.2012.12.002

Paralyzed Veterans of America Consortium for Spinal Cord Medicine. (2005). Preservation of upper limb function following spinal cord injury: a clinical practice guideline for health-care professionals. *J. Spinal Cord Med.* 28, 434–470.

Pentland, W. E., and Twomey, L. T. (1994). Upper limb function in persons with long term paraplegia and implications for independence: part II. *Paraplegia* 32, 219. doi:10.1038/sc.1994.41

Requejo, P., Mulroy, S., Haubert, L. L., Newsam, C., Gronley, J., and Perry, J. (2008). Evidence-based strategies to preserve shoulder function in manual wheelchair users with spinal cord injury. *Top. Spinal Cord Inj. Rehabil.* 13, 86–119. doi:10.1310/sci1304-86

Requejo, P. S., Furumasu, J., and Mulroy, S. J. (2015). Evidence-based strategies for preserving mobility for elderly and aging manual wheelchair users. *Top. Geriatr. Rehabil.* 31, 26–41. doi:10.1097/TGR.0000000000000042

Silverstein, B. A., Bao, S. S., Fan, Z. J., Howard, N., Smith, C., Spielholz, P., et al. (2008). Rotator cuff syndrome: personal, work-related psychosocial and physical load factors. *J. Occup. Environ. Med.* 50, 1062–1076. doi:10.1097/JOM.0b013e31817e7bdd

Slowik, J. S., McNitt-Gray, J. L., Requejo, P. S., Mulroy, S. J., and Neptune, R. R. (2016a). Compensatory strategies during manual wheelchair propulsion in response to weakness in individual muscle groups: a simulation study. *Clin. Biomech. (Bristol, Avon)* 33, 34–41. doi:10.1016/j.clinbiomech.2016.02.003

Slowik, J. S., Requejo, P. S., Mulroy, S. J., and Neptune, R. R. (2015). The influence of speed and grade on wheelchair propulsion hand pattern. *Clin. Biomech. (Bristol, Avon)* 30, 927–932. doi:10.1016/j.clinbiomech.2015.07.007

Slowik, J. S., Requejo, P. S., Mulroy, S. J., and Neptune, R. R. (2016b). The influence of wheelchair propulsion hand pattern on upper extremity muscle power and stress. *J. Biomech.* 49, 1554–1561. doi:10.1016/j.jbiomech.2016.03.031

Vissers, M., van den Berg-Emons, R., Sluis, T., Bergen, M., Stam, H., and Bussmann, H. (2008). Barriers to and facilitators of everyday physical activity in persons with a spinal cord injury after discharge from the rehabilitation centre. *J. Rehabil. Med.* 40, 461–467. doi:10.2340/16501977-0191

Conflict of Interest Statement: The authors declare that the research was conducted in the absence of any commercial or financial relationships that could be construed as a potential conflict of interest.

frontiers in
BIOENGINEERING AND BIOTECHNOLOGY

ORIGINAL RESEARCH ARTICLE
published: 23 December 2014
doi: 10.3389/fbioe.2014.00077

Echographic and kinetic changes in the shoulder joint after manual wheelchair propulsion under two different workload settings

Ángel Gil-Agudo[1]*, Marta Solís-Mozos[1], Beatriz Crespo-Ruiz[1], Antonio J. del-Ama Eng[1], Enrique Pérez-Rizo[1], Antonio Segura-Fragoso[2] and Fernando Jiménez-Díaz[3]

[1] *Biomechanics and Technical Aids Unit, Department of Physical Medicine and Rehabilitation, National Hospital for Paraplegics, Servicio de Salud de Castilla-La Mancha, Toledo, Spain*
[2] *Health Sciences Institute of Castilla-La Mancha, Toledo, Spain*
[3] *Laboratory of Performance and Sports Rehabilitation, Faculty of Sport Science, University of Castilla-La Mancha, Toledo, Spain*

Edited by:
Philip Santos Requejo, Rancho Los Amigos National Rehabilitation Center, USA

Reviewed by:
Henrique De Amorim Almeida, Polytechnic Institute of Leiria, Portugal
Glen Lichtwark, The University of Queensland, Australia

****Correspondence:***
Ángel Gil-Agudo, Biomechanics and Technical Aids Unit, Department of Physical Medicine and Rehabilitation, National Hospital for Paraplegics, Finca la Peraleda s/n, Toledo 45071, Spain
e-mail: amgila@sescam.jccm.es

Manual wheelchair users with spinal cord injury (SCI) have a high prevalence of shoulder pain due to the use of the upper extremity for independent mobility, transfers, and other activities of daily living. Indeed, shoulder pain dramatically affects quality of life of these individuals. There is limited evidence obtained through radiographic techniques of a relationship between the forces acting on the shoulder during different propulsion conditions and shoulder pathologies. Today, ultrasound is widely accepted as a precise tool in diagnosis, displaying particularly effectiveness in screening the shoulder rotator cuff. Thus, we set out to perform an ultrasound-based study of the acute changes to the shoulder soft tissues after propelling a manual wheelchair in two workload settings. Shoulder joint kinetics was recorded from 14 manual wheelchair users with SCI while they performed high- and low-intensity wheelchair propulsion tests (constant and incremental). Shoulder joint forces and moments were obtained from inverse dynamic methods, and ultrasound screening of the shoulder was performed before and immediately after the test. Kinetic changes were more relevant after the most intensive task, showing the significance of high-intensity activity, yet no differences were found in ultrasound-related parameters before and after each propulsion task. It therefore appears that further studies will be needed to collect clinical data and correlate data regarding shoulder pain with both ultrasound images and data from shoulder kinetics.

Keywords: kinetics, shoulder injury, wheelchair propulsion, biomechanics, ultrasonography, spinal cord injury

INTRODUCTION

Manual wheelchair users with spinal cord injury (SCI) have a high prevalence of shoulder pain (Bayley et al., 1987; Sie et al., 1992; Subbarao et al., 1995; Escobedo et al., 1997; Curtis et al., 1999; Ballinger et al., 2000; Boninger et al., 2001; Mercer et al., 2006), with estimates ranging from 30% (Ballinger et al., 2000) to 73% (Pentland and Twomey, 1991). As the life expectancy of patients with SCI continues to increase, the prevalence of shoulder impingement related to damage of the rotator cuff is rising (Bayley et al., 1987). Since wheelchair users depend strongly on the upper extremity for independent mobility and their daily activities, shoulder pain has a strong negative impact on their quality of life.

The shoulder joint experiences a repetitive and continuous load during the push phase of the wheelchair propulsion cycle. Since the upper limb is not specialized for this action, this repetitive loading may cause musculoskeletal disorders at the shoulder joint, predisposing manual wheelchair users to upper limb pathologies (Bayley et al., 1987). Indeed, this mechanical stress leads to overuse syndrome, which is a possible factor influencing the development of shoulder pain in this population and commonly, injuries of the rotator cuff (Subbarao et al., 1995). High-intensity wheelchair propulsion increases upward shoulder joint forces, which could result in upward translation of the humeral head and subsequent compression of the subacromial structures against the overlying acromion (Kulig et al., 1998). Repetitive strains of rotator cuff tendons can potentially induce microinjuries, which may facilitate tendon degeneration. Therefore, it is important to define the biomechanical factors that may predispose wheelchair users to shoulder pathologies in order to recommend interventions that minimize the shoulder load during propulsion (Rodgers et al., 1994; Kulig et al., 1998; Cooper et al., 1999; Finley et al., 2004; Mulroy et al., 2005; Mercer et al., 2006; Moon et al., 2013), contemplating different lesion levels (Gil-Agudo et al., 2010a). Recommendations to prevent shoulder injury based solely on pushrim biomechanics are available (Boninger et al., 2005). However, research using inverse dynamics techniques revealed that posterior and superior forces both act on the shoulder joint during the push phase of propulsion, these probably being related to coracoacromial ligament edema and compression of the rotator cuff, respectively (Koontz et al., 2002; Van Drongelen et al., 2005; Mercer et al., 2006; Collinger et al., 2008; Gil-Agudo et al., 2010a).

Despite the logic of these claims, there is limited radiographic evidence for the relationship between shoulder joint forces in different propulsion conditions and shoulder pathologies. Several radiographic abnormalities have been reported in the shoulder of the SCI population (Bayley et al., 1987; Wylie and Chakera, 1988; Boninger et al., 2001; Kivimäki and Ahoniemi, 2008; Akbar et al., 2010). Acute changes in the shoulder tendons upon high-intensity wheelchair propulsion may contribute to the pathological process that leads to a chronic pathology and pain (Van Drongelen et al., 2007). Indeed, acute exercise induces changes in tendon metabolism and increased inflammation (Landberg et al., 1999). Nevertheless, to the best of our knowledge only one previous study has addressed the relationship between kinetics and shoulder pathologies (Mercer et al., 2006), assessing the shoulder pathology by magnetic resonance imaging (MRI). However, MRI is a complex technique that is not easy to conduct immediately after propelling the wheelchair. In fact, musculoskeletal ultrasound techniques have several advantages over MRI when diagnosing shoulder pathologies, such as portability, ease to implement in clinics, and the capability to assess joint dynamics during motion. Thus, this technique allows the shoulder joint to be readily assessed immediately before and after conducting a propulsion test in laboratory settings. Moreover, ultrasound is a technique that is widely available in clinical settings due to its diagnostic precision (Landberg et al., 1999; Teefey et al., 2004; Iannotti et al., 2005) and it is particularly effective in assessing the shoulder rotator cuff (Allen, 2008). The acute changes in shoulder tendons that might follow strong demands on propulsion could contribute to chronic shoulder pathologies and pain. Such acute changes can be rapidly screened using ultrasound immediately after completing the propulsion task in a controlled environment.

Tangential forces acting on the hand rim have been shown to be directly linked to net shoulder moments, indicative of a higher risk of shoulder injury (Koontz et al., 2002; Desroches et al., 2008). Therefore, it can be assumed that the greater the demand on propulsion, the higher the net shoulder moments, and hence, the risk of shoulder injury increases. Acute changes in shoulder tendons have been studied previously by ultrasound after two different high-intensity propulsion activities. In both cases, ultrasound findings were not correlated with kinetic data from the shoulder joint, probably because these measurements were not made in the two different intensity and standardized exercises employed (Van Drongelen et al., 2007; Collinger et al., 2010).

We hypothesize here that (1) shoulder joint forces would be greater in the more intensive propulsion task and cuff rotator tendon ultrasound changes would be consequently more notable; and (2) it would be possible to establish a link between shoulder joint kinetics and ultrasound-derived metrics. Accordingly, the aim of this study was to compare shoulder joint forces and moments between early and late propulsion instances in two different propulsion protocols: low- and high-intensity activities. In addition, we set out to compare changes in the shoulder evident by ultrasound after performance of the same two different wheelchair propulsion protocols.

MATERIALS AND METHODS

SUBJECTS

Subjects were recruited from the discharge records from a monographic in-patient SCI hospital, sending a letter inviting them to participate in the research study. For inclusion in the study, subjects had to have traumatic SCI at level T2 or below, with AIS grade A or B (Marino et al., 2003), which occurred after the age of 18 and before 45, and with an evolution longer than 18 months at time of the study. Volunteers must use manual wheelchairs as their primary means of mobility. Subjects were excluded if they had had fractures or dislocations in the non-dominant shoulder at any time, upper limb pain that prevented them from propelling a manual wheelchair, progressive or degenerative disability, or a history of cardiopulmonary disease. This study was approved by the ethics review board and all the participants signed an informed consent form prior to enrollment.

INSTRUMENTATION

A standard adjustable wheelchair (Action3 Invacare, Invacare Corp, Elyria, OH, USA), was properly fitted for each subject and placed on a treadmill (Bonte Zwolle B.V., BO Systems, Netherlands). A force transducer (Revere ALC 0.5, Vishay Revere Transducers BV, Breda, The Netherlands) was situated in front of the treadmill in order to estimate the rolling resistance, and a custom dead weight and pulley system that can be attached to the back of the wheelchair (van der woude et al., 1986; Van Drongelen et al., 2013) (**Figure 1**) was also available to regulate the propulsion power output (see below). Propulsion trials were conducted using a safety system, which prevented lateral movements.

Non-dominant upper limb kinematic data were collected at 50 Hz (maximum recording frequency) using passive markers and four camcorders (Kinescan-IBV, Instituto de Biomecánica de Valencia, Valencia, Spain). All subjects were right-hand dominant so that the left upper limb was analyzed and spatial marker coordinates were smoothed out using a procedure of mobile means. Reflective markers were positioned following ISB recommendations to define local reference systems on the hand, forearm, and arm (Wu et al., 2005). The local trunk reference system was defined using markers placed on the seventh cervical vertebra (C7), and on the right (ACRR) and left (ACRL) acromioclavicular joints [the axes of this reference system have been described previously (Gil-Agudo et al., 2010b)]. Markers were also placed on the wheel hub during data collection.

Both wheels of the chair were replaced by two SMART^{Wheels} (Three Rivers Holdings, LLC, Mesa, AZ, USA) to balance the inertial characteristics of both axes and ensure symmetrical propulsion. A synchronization pulse from the Kinescan-IBV was used to trigger the start of the kinetic and kinematic data collection. Kinetic data were recorded at a frequency of 240 Hz and filtered using a Butterworth, fourth-order, low-pass filter with a cutoff frequency of 20 Hz and a zero phase lag. Spatial marker coordinates were interpolated by cubic spline to synchronize with the kinetic data.

DATA COLLECTION

Upon arrival at the laboratory, the participants provided their demographic information and a physical examination was

FIGURE 1 | Overview of the test set-up where the subject is working against extra resistance applied through a pulley system and including the positions of the markers.

performed that included a study of the range of shoulder movement and that identification of the painful point. A visual analog scale (VAS) was used to measure current pain, with 0 indicating a painless shoulder and 100 indicating an intensely painful shoulder. Functional status was assessed using the wheelchair user's shoulder pain index (WUSPI) (Curtis et al., 1995). Subjects then underwent a base-line ultrasound screening of the non-dominant shoulder before completing the wheelchair propulsion test and ultrasound screening immediately after finishing it.

All subjects performed two different wheelchair propulsion tests, one at high intensity with an incremental workload (Protocol A) and another at low intensity with a constant workload (Protocol B). In order to comply with recommendations on resting periods described in physiology studies (Schuenke et al., 2002), the tests were performed with at least 48 h difference, thereby ensuring complete recovery of the patient. Movements like turning or going backwards were excluded because these could not be performed in the same experimental set up. The four camcorders were fixed above the treadmill, and hence, manual wheelchair propulsion was the only movement that could be registered in such conditions.

To simulate the conditions of wind resistance, the treadmill slope was fixed at 0.7° for both protocols (Mason et al., 2014). The order in which the tests were performed was randomized for each subject, and before testing the subjects were allowed to familiarize themselves with the wheelchair and the experimental set up. Afterwards, the individual rolling resistance was determined in a separate drag test (Marino et al., 2003; Mason et al., 2014). The mean and SD of the friction coefficient was 0.010 ± 0.002, which falls among optimal limits set by previous studies (van der woude et al., 1986; de Groot et al., 2006) regardless of the constraints in lateral movements imposed by our safety system.

Once the rolling resistance was determined, the propulsion power output could be regulated by an additional external force that acted via a pulley system on the wheelchair-user combination (**Figure 1**). The propulsion power output (PO external) was calculated as Power (W) = Force (N) × Speed (km h^{-1}), and the minimum load imposed by the pulley system was 20 W. The speed necessary to adjust the resistance power of each subject to 20 W was therefore calculated using the sum of F_{drag} and the dead weight acting via the pulley system ($F_{\text{additional}}$). Therefore, by varying the dead weight acting through the pulleys and/or the speed of the treadmill, the PO external could be set to a desired value, independently of the experimental subject.

The treadmill speed in protocol A was calculated in order to set the PO external for all subjects at 20 W. Discrete increases of 5 W were introduced every 2 min without rest between stages using the dead weights in the pulley system. The trial was finished either when the subject was exhausted and could not propel the wheelchair any longer or when the security system stopped the propulsion. The maximum criteria were then obtained following the ACSM guidelines (ACSM, 2006).

In protocol B, the treadmill speed was also adjusted to a PO external of 20 W for all subjects, and it remained constant during this protocol. The maximum test duration was fixed at 20 min and the test terminated when the subject stopped propelling the wheelchair or the time limit was reached. A subjective perception of fatigue (Borg scale) was recorded immediately after completing each protocol (Borg, 1970).

MEASURES OF SHOULDER PATHOLOGY

The same physician conducted a physical examination on all the subjects that focused on shoulder injury, as reported previously

(Boninger et al., 2001). All ultrasound screenings were also performed by the same physician, who has more than 15 years of training and experience in musculoskeletal ultrasound. Ultrasound was performed with a General Electric Healthcare (Logiq S8) apparatus and using 8–12 MHz linear array transducer. Images of the long head of the biceps tendon and supraspinatus tendon were captured before and immediately after the propulsion task. During the base-line ultrasound examination, external reference landmarks were taped to the shoulder skin. These were not removed until the end of the second propulsion task, allowing ultrasound measurements at the two different time points to be obtained with minimal variation in transducer location, making the procedure more reliable (Collinger et al., 2009). The protocol used in both ultrasound examinations to examine the structures in the shoulder was the same and it was based on previously described techniques (Mack et al., 1985; Middleton et al., 1986; Crass et al., 1987; Middleton, 1992). To examine the transverse image of the biceps tendon, the subject's hand was placed on their thigh with the palm facing upwards. Supination of the hand with external rotation of the shoulder improved the visualization of the bicipital groove. The transducer was then turned 90° to obtain the long-axis image of the biceps tendon. The supraspinatus tendon was observed with the hand placed behind the back with the shoulder in internal rotation. The acromio-humeral distance was recorded with the arm in internal rotation.

DATA ANALYSIS

Biomechanical data

The total pushrim force (Ftot) was calculated as the vector sum of the SMART^{Wheel} components (Fx, Fy, Fz). Mechanical effective force (MEF) was calculated as the proportion of the force at the pushrim that contributes to the forward motion ($Ft^2/Ftot^2$), where Ft is the tangential force obtained by dividing the measured mean propulsion moment around the wheel axle by the radius of the pushrim. These kinetics parameters were only calculated over the push phase of the stroke (Koontz et al., 2005).

We used an inverse dynamic model described previously to calculate the shoulder joint forces and moments (Gil-Agudo et al., 2010b). The model was used to calculate the net shoulder joint forces and moments from segment kinematics, the forces acting on the pushrim, and the subject's anthropometric measurements (Clauser et al., 1969). Net joint forces and moments were calculated on a global reference system and then expressed through the joint reference system (Cooper et al., 1999; Mercer et al., 2006). The analysis focused on the glenohumeral joint, and movements of the scapula, clavicle, and thoracic spine were not considered. The forces reported constituted the reaction forces on the joint and moments were reported as the action moments.

In order to obtain the biomechanical data as close as possible to ultrasound examination, the first and last 20 s of each test were recorded for analysis. For protocol A, the last 20 s corresponded to the maximum step achieved. For protocol B, it corresponded to the last 20 s before finishing the test.

Five consecutive cycles were selected from the 20 s recording of data, and the cycles were normalized from 0 to 100% since the time spent in each cycle varied between individuals and cycles. The push phase started/finished at the instant at which the propulsive moment exerted by the user during hand contact with the pushrim was higher/lower than 1 Nm. The peaks were determined for each stroke individually and then averaged over five cycles. The output variables of the biomechanical model were the time-varying 3D joint net forces and moments. The following sign convention was used:

Forces

- Fx: +anterior, −posterior.
- Fy: +superior, −inferior.
- Fz: +lateral, −medial.

Moments

- Mx: +adduction, −abduction.
- My: +internal rotation, −external rotation.
- Mz: +flexion, −extension.

Ultrasound data

The ultrasound images were screened by two reviewers to assess their usability. The anatomical shoulder references, and the biceps and supraspinatus tendon characteristics, were analyzed with custom software written in Matlab (The Mathworks Inc., Natick, MA, USA). The most common ultrasound finding related to the shoulder of SCI manual wheelchair users is an increase in the glenohumeral joint space (Kivimäki and Ahoniemi, 2008), and the most common ultrasound finding after high-intensity wheelchair propulsion activity is an increase in the biceps tendon diameter (Van Drongelen et al., 2007). Nevertheless, a comprehensive analysis of shoulder ultrasound parameters was carried out, including anatomical shoulder references such as acromioclavicular distance (ACD) and acromio-humeral distance using the Cholewinski (CHI) method (acromion to greater tuberosity of humerus) (Seitz and Michener, 2010) (see **Figure 2**). Several tendon characteristics, such as long-axis biceps tendon thickness (LBTT), long-axis biceps sonoelasticity (LBS), short-axis supraspinatus thickness (SST), and short-axis supraspinatus sonoelasticity (SSS) were also analyzed (Farin et al., 1995; Turrin and Capello, 1997; Park and Kwon, 2011) (**Figures 3** and **4**). In the longitudinal images of the biceps

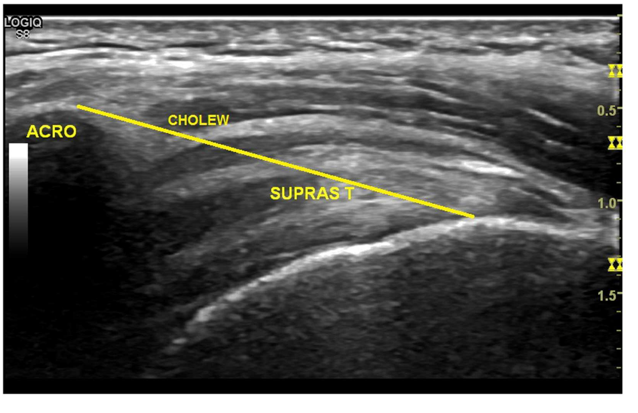

FIGURE 2 | Measurement of the greater acromion tuberosity distance (Cholewinski index).

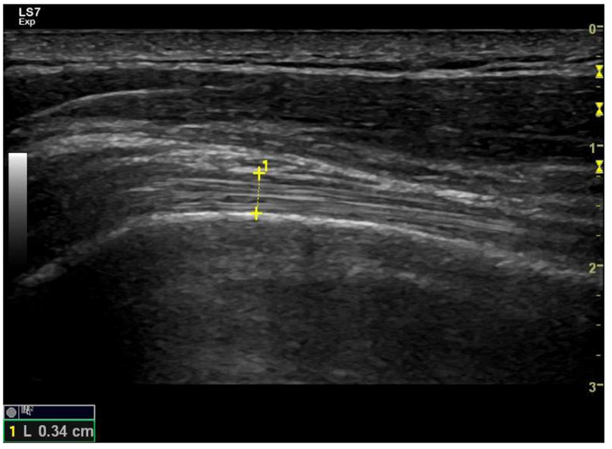

FIGURE 3 | Long-axis ultrasound examination which shows the fibrillar pattern of the long-biceps tendon.

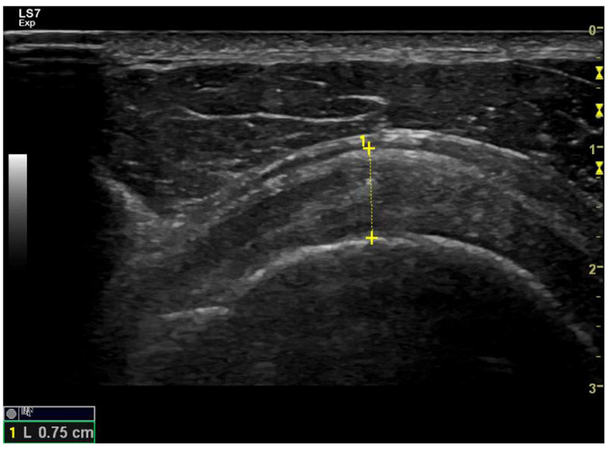

FIGURE 4 | Examination of the short axis of the supraspinatus tendon to measure its thickness and check the hyperechoic fibrillar pattern.

Table 1 | Subject's characteristics, mean (SD).

Characteristics	SCI subjects		
n	14		
Sex (male/female)	14 male		
Age (years)	35.2 (6.11)		
Weight (kg)	68.3 (8.96)		
Height (m)	1.77 (0.07)		
Time since injury (months)	90.2 (54.78)		
Shoulder pain (no pain/pain)	7/7		
WUSPI (0–150)	25.46 (25.75)		
	Subjects with non-pain: 5.7 (4.98)		
	Subjects with pain: 45.23 (22.37)		
VAS (0–100)	53.8 (5.03)		
	Pain: 74.3 (5.21)		
	Non-pain: 21.4 (4.32)		
Level of injury	D2–D6	D7–D11	D12–L3
	7	2	5

tendon, a 2 cm length was selected by the researcher that included the part of the tendon located inside the bicipital groove, and the average diameter of this selection was calculated (Van Drongelen et al., 2007).

Statistics

Descriptive analysis, including the means and SD for the continuous variables, was performed initially to describe the subject's characteristics. Differences in the shoulder joint forces, moments, and ultrasound parameters between the two wheelchair propulsion tests were analyzed and all statistical analysis was carried out using SPSS® V.17 for Windows (SPSS Inc., Chicago, IL, USA).

Peak shoulder forces and moments were averaged to create a representative value for each direction. Shoulder joint kinetics was calculated as the average of the peak force or moment for the two wheelchair propulsion test. Differences between early and late propulsion for each protocol and between protocols were analyzed. In order to calculate the differences in shoulder joint forces and moments between both conditions, a Shapiro–Wilk test was applied to the normal distribution of the sample. A Student's *t*-test for independent samples was applied to those variables that followed a normal distribution. A Mann–Whitney *U* test for independent samples was used to compare those variables that showed a non-parametric distribution. Additionally, correlations between ultrasound parameters and shoulder kinetic data were evaluated using Spearman's rho. These correlations were performed considering differences obtained in ultrasound and kinetic examinations before and after each protocol. Significance level was set at $p < 0.05$.

RESULTS

SUBJECTS

Fourteen subjects with SCI participated in this study, all males. They had an average height of 1.77 m (SD = 0.07; range 1.67–1.87) and weight 68.3 kg (SD = 8.96; range 53–87), and their average age was 35.2 years (SD = 6.11; range 25–43) with an average time since injury of 90.2 months (SD = 54.78; range 37–282: **Table 1**). As only half of subjects suffered from shoulder pain, we considered all SCI subjects as a single group rather that conducting a separate analysis for those who referred to shoulder pain.

BIOMECHANICS

The performance of the subjects in both the protocols was considered and the effective mechanical force was similar in both protocols (**Table 2**), although the increase in the forces and moments was greater after protocol A (high intensity). Considering only protocol A, significant differences were found between early and late propulsion for all the parameters analyzed, except for the adduction and abduction shoulder peak moments (**Table 3**).

The increments in biomechanical parameters for each protocol were analyzed and they were higher in protocol A for all the parameters except for lateral peak force, and for peak adduction and abduction moments (**Table 4**). **Figures 5** and **6** show representative mean cycle of shoulder joint forces and moments data, respectively, for the group analyzed for both protocols.

Table 2 | Performance in both protocols, mean (SD).

	Test duration (min)	Speed (km/h)	Power output (W)	Increasing steps (kg)	Borg scale (0–20)	Mechanical effective force (*N*)
High-intensity task						
SCI subjects	14.85 (2.17)	1.44 (0.08)	53.21 (4.20)	1.24 (0.10)	17.42 (1.01)	0.84 (0.11)
Low-intensity task						
SCI subjects	20	1.47 (0.08)	20		8.46 (1.94)	0.85 (0.08)

Table 3 | Raw mean of the biomechanical variables in the two wheelchair propulsion tasks, mean (SD).

		High-intensity task			Low-intensity task		
		Early propulsion	Late propulsion	*p*-Value	Early propulsion	Late propulsion	*p*-Value
Fx (N) (+anterior, −posterior)	Max	41.89 (9.32)	51.28 (10.13)	**<0.05**	43.42 (9.83)	41.38 (10.30)	0.59
	Min	−44.00 (8.04)	−82.14 (18.49)	**<0.01**	−42.54 (9.22)	−45.24 (10.43)	0.47
Fy (N) (+superior, −inferior)	Max	−0.45 (9.33)	21.07 (21.91)	**<0.01**	0.47 (9.91)	−0.12 (11.81)	0.88
	Min	−47.45 (11.60)	−67.16 (21.96)	**<0.01**	−45.35 (8.66)	−49.44 (10.05)	0.25
Fz (N) (+lateral, −medial)	Max	13.84 (5.27)	19.42 (8.39)	**<0.05**	16.29 (7.37)	17.51 (9.57)	0.70
	Min	−9.93 (3.53)	−15.36 (6.72)	**<0.05**	−11.71 (5.25)	−10.98 (2.91)	0.65
Mx (N·m) (+adduction, −abduction)	Max	3.08 (1.53)	6.10 (5.83)	0.07	3.35 (2.47)	3.03 (1.90)	0.71
	Min	−5.43 (1.93)	−7.71 (4.15)	0.07	−4.94 (1.16)	−5.14 (1.68)	0.71
My (N·m) (+int. rotation, −ext. rotation)	Max	2.45 (0.93)	4.65 (1.99)	**<0.01**	2.60 (1.31)	2.58 (1.25)	0.96
	Min	−3.09 (1.29)	−5.23 (2.71)	**<0.05**	−3.19 (0.99)	−3.22 (0.83)	0.93
Mz (N·m) (+flexion, −extension)	Max	13.16 (2.79)	24.84 (7.25)	**<0.01**	13.26 (3.10)	14.08 (3.45)	0.51
	Min	−7.09 (2.39)	−11.70 (7.18)	**<0.05**	−7.34 (2.09)	−7.96 (2.30)	0.45

Bold font indicates statistical significance at p < 0.05.

Table 4 | Intra-protocol differences (early and late propulsion) for peak forces (N) and moments (N·m) acting on the shoulder joint, mean (SD).

	SCI subjects			
	High-intensity task	Low-intensity task	Inter-protocols	*p*-Value
Cadence	−0.01 (0.15)	−0.05 (0.12)	0.03	0.50
Fx (+anterior, −posterior)				
Max	11.07 (12.98)	−2.04 (3.52)	13.11	**<0.01**
Min	−38.94 (18.60)	−2.70 (8.77)	−36.23	**<0.01**
Fy (+superior, −inferior)				
Max	21.14 (19.41)	−0.59 (7.55)	21.74	**<0.01**
Min	−19.91 (27.46)	−4.09 (6.82)	−15.81	**<0.05**
Fz (+lateral, −medial)				
Max	4.81 (8.23)	1.21 (5.66)	3.59	0.19
Min	−5.65 (7.90)	0.73 (3.77)	−6.38	**<0.05**
Mx (+adduction, −abduction)				
Max	2.80 (5.94)	−0.03 (1.62)	3.11	0.07
Min	−2.63 (4.67)	−0.20 (0.77)	−2.43	0.06
My (+int.rotation, −ext.rotation)				
Max	2.47 (2.08)	−0.02 (0.65)	2.49	**<0.01**
Min	−2.45 (2.94)	−0.02 (0.79)	−2.42	**<0.01**
Mz (+flexion, −extension)				
Max	12.16 (7.37)	0.82 (2.43)	11.34	**<0.01**
Min	−4.89 (7.61)	−0.62 (1.15)	−4.26	**<0.05**

Statistical significance (p-value) is related to the inter-protocol differences.
Bold font indicates statistical significance at p < 0.05.

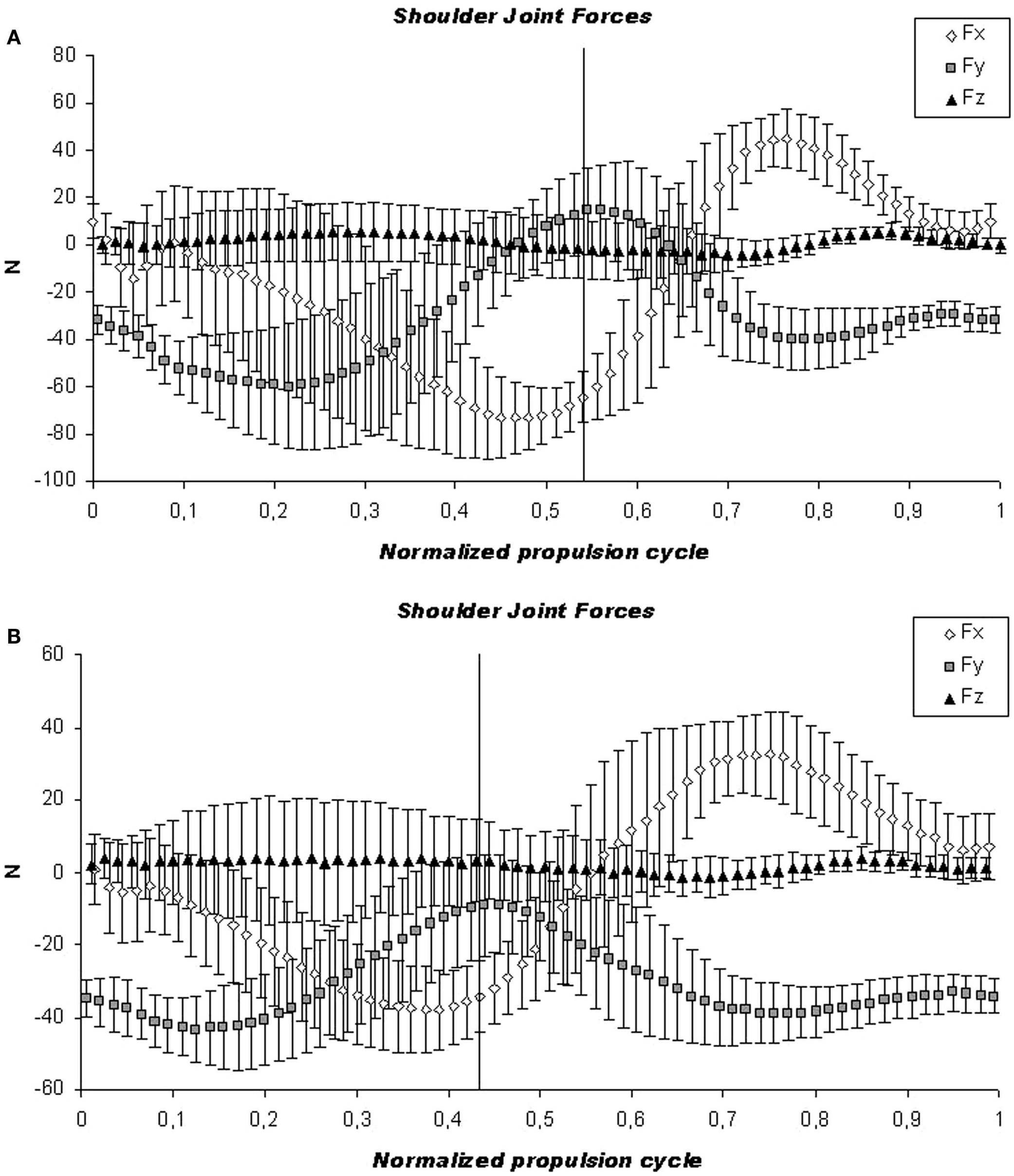

FIGURE 5 | Kinetic analysis. Illustration of the mean cycle of shoulder joint forces for the group analyzed. The mean (continuous line) and SD (dashed line) are shown for the high-intensity **(A)** and low-intensity protocol **(B)**. The vertical line indicates the push and recovery phase of the forces on the shoulder joint.

SHOULDER BIOMECHANICS AND ULTRASOUND PARAMETERS

No differences were found for the ultrasound parameters before and after each protocol (**Table 5**). Regarding the correlations between changes in kinetic and ultrasound findings before and after protocol A, increases in medial peak shoulder force were correlated with increases in LBTT ($\rho = 0.594$, $p < 0.05$) and with decreases in subacromial space measured following Cholewinsk index ($\rho = -0.534$, $p < 0.05$) (**Table 6**).

DISCUSSION

To the best of our knowledge, this is the first study to address changes in shoulder joint kinetics with anatomical shoulder soft tissue changes recorded in ultrasound images after performing two different propulsion tasks that exert stronger or weaker physical demands. In accordance with our hypothesis, shoulder joint forces were stronger in the more intense manual propulsion task (protocol A) with respect to the less intense (protocol B). However, no differences were found for the ultrasound parameters before and after each propulsion task.

Regarding the kinetic variables, these are difficult to compare directly with data in the literature due to the different testing procedures, units of measurement, equipment employed, and characteristics of the population studied (Gil-Agudo et al., 2010a). A high-intensity wheelchair propulsion test was chosen

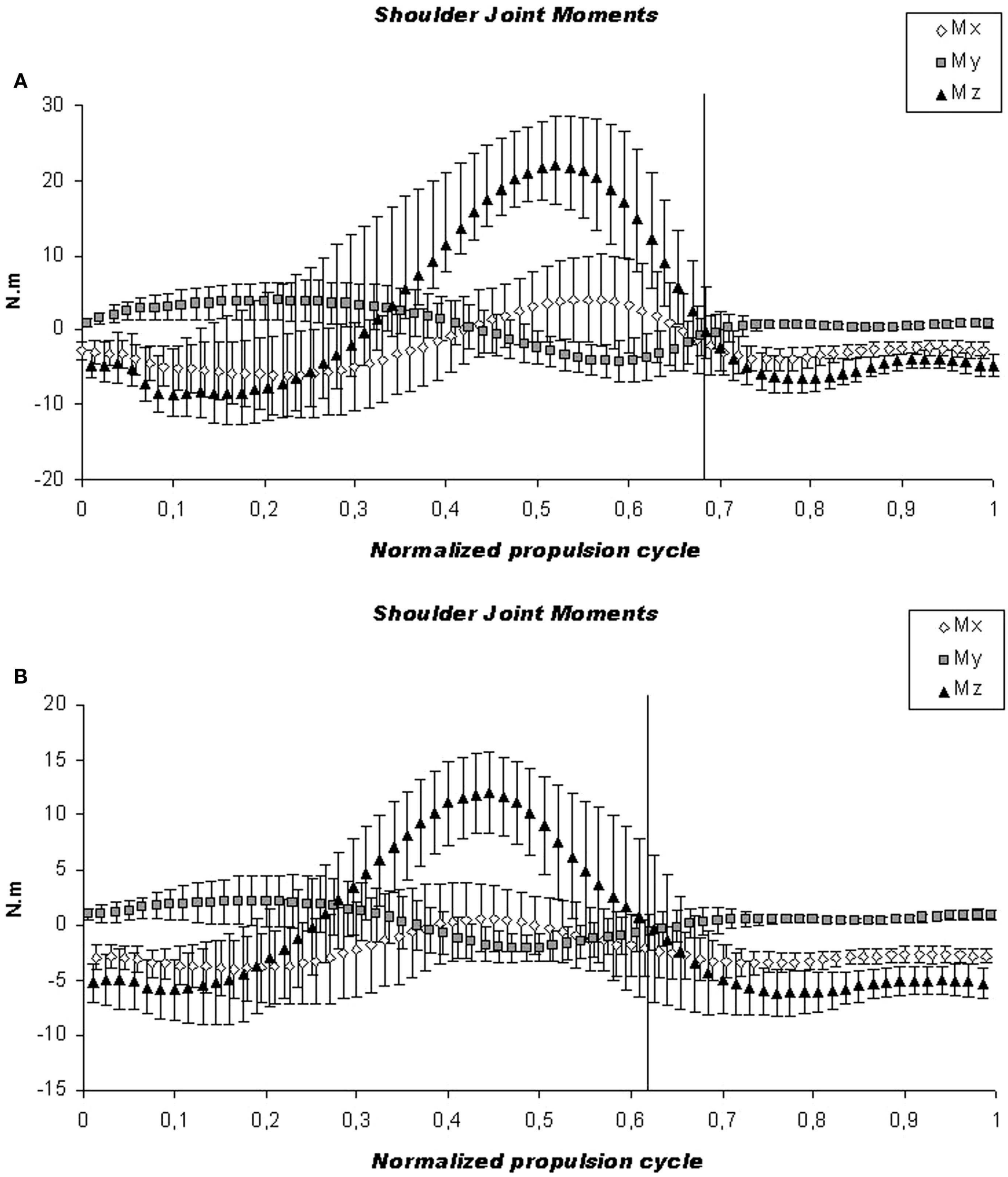

FIGURE 6 | Kinetic analysis. Illustration of the mean cycle of shoulder joint moments for the group analyzed. The mean (continuous line) and SD (dashed line) are shown for the high-intensity **(A)** and low-intensity protocol **(B)**. The vertical line indicates the push and recovery phase of the forces on the shoulder joint.

considering that greater shoulder joint forces and moments were more likely to provoke shoulder pathology (Mercer et al., 2006). Moreover, such pathological changes might be easier to detect with ultrasound examination. Owing to the use of a treadmill for the experimental set up, we modified the resistance to be overcome by the subject by increasing the weight attached to a pulley system, a method that is safer than increasing the treadmill speed. However, we considered it interesting to compare these results with a lower intensity protocol that cause weaker shoulder joint forces and to correlate these with ultrasound findings.

Thus, we analyzed two specific workload settings and in both protocols, treadmill speed was individualized in order to normalize the power demand for all subjects to 20 W and this speed remained constant in both protocols. From our previous experience, we choose to develop a high-intensity wheelchair propulsion test on a treadmill without increasing the slope for safety and mechanical reasons (Hartung et al., 1993). Increasing the speed of the treadmill might cause heterogeneous increases on the loads that the subject has to overcome depending on its own weight. Therefore, to normalize the power to be overcome by the subject, we employed a procedure that calculates the increasing weights to be imposed by a pulley system in order to normalize every 5 W increase in this incremental test. For the low-intensity propulsion task, the speed and weight required to propel at 20 W remained constant during 20 min adapted from a previous long-term wheelchair propulsion protocol (Gass et al., 1981).

In the present study, the more intensive task produced increases in all directions of shoulder joint forces and almost all moments, as found previously when increasing speed (Mercer et al., 2006; Collinger et al., 2008). The greater posterior and lateral shoulder forces were previously related to pathological findings (Mercer et al., 2006). However, we did not find an increase in the LBTT after the high-intensity task, in contrast to a previous report (Van Drongelen et al., 2007), probably because our test was performed in less time. The subjects included in our study were experienced in manual wheelchair propulsion (time since injury 90.2 ± 54.78 months) and it is likely that the participants were accustomed to such exercise, possibly explaining why no differences could be detected in the ultrasound parameters before and after the propulsion tests.

With respect to the relation between kinetic and ultrasound findings, we found that in high-intensity protocols long-biceps tendon thickness increases when medial and inferior forces increases. Also, subacromial space measured following Cholewinsk index decreases when shoulder medial forces increases. Subjects need to propel the wheelchair everyday. So, instead of limiting subject's activity, the need is to reduce the overall force to propel the wheelchair by accomplishing an alternative wheelchair set up or propelling with different technique. Bigger changes after high-intensity protocol were expected in relation to low-intensity task because the amount of work might be a risk factor for developing overuse injuries.

Table 5 | Mean (SD) ultrasound values before and after wheelchair propulsion tasks.

	High-intensity task			Low-intensity task		
	Before	**After**	***p*-Value**	**Before**	**After**	***p*-Value**
LBTT	0.41 (0.09)	0.42 (0.07)	0.86	0.40 (0.09)	0.40 (0.06)	0.90
LBS	4.03 (0.66)	3.75 (0.93)	0.35	4.27 (0.65)	4.3 (0.87)	0.92
ACD	0.66 (0.16)	0.70 (0.15)	0.52	0.71 (0.15)	0.75 (0.15)	0.56
CHI	2.46 (0.45)	2.35 (0.59)	0.55	2.42 (0.49)	2.39 (0.51)	0.87
SST	0.64 (0.08)	0.61 (0.08)	0.48	0.62 (0.06)	0.60 (0.07)	0.56
SSS	4.41 (0.54)	4.42 (0.44)	0.96	4.46 (0.71)	4.30 (0.72)	0.55

LBTT, long-axis biceps tendon thickness; LBS, long-axis biceps sonoelasticity; ACD, acromioclavicular distance; CHI, Cholewinski index; SST, short-axis supraspinatus thickness; SSS, short-axis supraspinatus sonoelasticity.

Although the biceps tendon diameter was similar to the reported elsewhere, those results are not directly comparable since we focused on potentially pathological parameters, such as decreased tendon thickness rather than other parameters like echogenicity (Van Drongelen et al., 2007). Similarly, we did not use grayscale-based quantitative ultrasound (Collinger et al., 2010), which may provide indicators of more microscopic damage. A lower echogenicity ratio of the biceps tendon has been reported, which might indicate the presence of a shoulder pathology after exercise but not an increase in biceps tendon diameter (Van Drongelen et al., 2007). Grayscale-based quantitative ultrasound proved to be useful to study the development of repetitive strain shoulder injury, although the appearance of supraspinatus post-propulsion was not significantly influenced by the biomechanics of propulsion (Collinger et al., 2010). We did not find differences in ultrasound images before and after both propulsion tasks in reference to the anatomic shoulder references and macroscopic tendon characteristics. We expected that more evident shoulder ultrasound changes would be produced by the high-intensity workload imposed. However, we also considered that the changes in the characteristics of the biceps and supraspinatus tendons are not only directly related to wheelchair propulsion but also the amount of change was related to the specific workload (Van Drongelen et al., 2007). Indeed, it appears that risk of developing shoulder joint damage is higher in subjects with long-term SCI using a wheelchair than after a high-intensity wheelchair propulsion task (Akbar et al., 2010). However, some correlation between shoulder kinetics and ultrasound images has been shown.

No relationship has been found between pain and imaging abnormalities (Boninger et al., 2001) and we agree that pathological findings in ultrasound images are not necessarily symptomatic, and thus, we also believe risk factors for clinical pathology should be identified before the individual becomes symptomatic (Mercer et al., 2006).

One limitation of this study was the small sample size and likewise, the number of subjects with and without shoulder pain. This limitation prevented us from performing a comparative analysis, and assessing the correlations between clinical data and kinetic or ultrasound findings. It should be noted that pain may confound the relationship between propulsion and ultrasound

Table 6 | Correlation between shoulder joint kinetics and ultrasound variables considering the changes in each protocol.

	Fymin (inferior)		Fzmax (lateral)		Fzmin (medial)		Mxmax (adduction)	
	R. spear	***p***	**R. spear**	***p***	**R. spear**	***p***	**R. spear**	***p***
High-intensity task								
LBTT	0.554	<0.05			0.594	<0.05		
CHI					−0.534	<0.05		
Low-intensity task								
SST			0.538	<0.05	0.574	<0.05	0.578	<0.05

LBTT, long-axis biceps tendon thickness; CHI, Cholewinski index; SST, short-axis supraspinatus thickness.

variables. In any case, we consider the findings presented here to be of interest considering that correlations between shoulder joint kinetics and ultrasound examination before and immediately after a propulsion task are a novelty itself. Nevertheless, further research will be necessary to identify relationships between kinetic data, ultrasound parameters, and clinical findings.

CONCLUSION

Shoulder joint forces and moments increase in an intense propulsion task allowing the relationship between intensity and loads on the development of shoulder pain to be seen. However, no differences were found in ultrasound images after a high-intensity wheelchair propulsion task was carried out. More research is needed to collect clinical information and correlate data on shoulder pain with ultrasound images and kinetic information.

ACKNOWLEDGMENTS

This work was supported by Ministerio de Economía y Competitividad: DEP 2011-29222-C02-02 (Spain).

REFERENCES

ACSM. (2006). *Guidelines for Exercise Testing and Prescription*, 7 Edn. Philadelphia: Lippincott & Wilkins.

Akbar, M., Balean, G., Brunner, M., Seyler, T. M., Bruckner, T., Munzinger, J., et al. (2010). Prevalence of rotator cuff tear in paraplegic patients compared with controls. *J. Bone Joint Surg. Am.* 92, 23–30. doi:10.2106/JBJS.J.00769

Allen, G. M. (2008). Shoulder ultrasound imaging-integrating anatomy, biomechanics and diseases processes. *Eur. J. Appl. Radiol.* 68, 137–146. doi:10.1016/j.ejrad.2008.02.024

Ballinger, D., Rintala, D., and Hart, K. (2000). The relation of shoulder pain and range-of-motion problems to functional limitations, disability, and perceived health of men with spinal cord injury: a multifaceted longitudinal study. *Arch. Phys. Med. Rehabil.* 81, 1575–1581. doi:10.1053/apmr.2000.18216

Bayley, J. C., Cochran, T. P., and Sledge, C. B. (1987). The weight-bearing shoulder. The impingement syndrome in paraplegics. *J. Bone Joint Surg. Am.* 69, 676–678.

Boninger, M., Koontz, A., Sisto, S., Dyson-Hudson, T., Chang, M., Price, R., et al. (2005). Pushrim biomechanics and injury prevention in spinal cord injury: recommendations based on CULP-SCI investigations. *J. Rehabil. Res. Dev.* 42(3 Suppl. 1), 9–19.

Boninger, M. L., Towers, J. D., Cooper, R. A., Dicianno, B. E., and Munin, M. C. (2001). Shoulder imaging abnormalities in individuals with paraplegia. *J. Rehabil. Res. Dev.* 38, 401–408.

Borg, G. (1970). Perceived exertion as an indicator of somatic stress. *Scand. J. Rehabil. Med.* 2, 92–98.

Clauser, C. E., McConville, J. T., and Young, J. W. (1969). *Weight, Volume and Center of Mass of Segments of the Human Body*. Boca Raton, FL: Taylor & Francis.

Collinger, J. L., Boninger, M. L., Koontz, A. M., Price, R., Sisto, S. A., Tolerico, M. L., et al. (2008). Shoulder biomechanics during the push phase of wheelchair propulsion: a multisite study of persons with paraplegia. *Arch. Phys. Med. Rehabil.* 89, 667–676. doi:10.1016/j.apmr.2007.09.052

Collinger, J. L., Gagnon, D., Jacobson, J., Impink, B. G., and Boninger, M. L. (2009). Reliability of quantitative ultrasound measures of the biceps and the supraespinatus tendons. *Acad. Radiol.* 16, 1424–1432. doi:10.1016/j.acra.2009.05.001

Collinger, J. L., Impink, B. G., Ozawa, H., and Boninger, M. L. (2010). Effect of an intense wheelchair propulsion task on quantitative ultrasound of shoulder tendons. *Am. Acad. Phys. Med. Rehabil.* 2, 920–925. doi:10.1016/j.pmrj.2010.06.007

Cooper, R., Boninger, M., Shimada, S., and Lawrence, B. (1999). Glenohumeral joint kinematics and kinetics for three coordinate system representations during wheelchair propulsion. *Am. J. Phys. Med. Rehabil.* 78, 435–446. doi:10.1097/00002060-199905000-00019

Crass, J. R., Craig, E. V., and Feinberg, S. B. (1987). The hyperextended internal rotation view in rotator cuff ultrasonography. *J. Clin. Ultrasound* 15, 416–420. doi:10.1002/jcu.1870150613

Curtis, K. A., Drysdale, G. A., Lanza, R. D., Kolber, M., Vitolo, R. S., and West, R. (1999). Shoulder pain in wheelchair users with tetraplegia and paraplegia. *Arch. Phys. Med. Rehabil.* 80, 453–457. doi:10.1016/S0003-9993(99)90285-X

Curtis, K. A., Roach, K. E., Applegate, E. B., Amar, T., Benbow, C. S., Genecco, T. D., et al. (1995). Development of the wheelchair user's shoulder pain index (WUSPI). *Paraplegia* 33, 435–446. doi:10.1038/sc.1995.65

de Groot, S., Zuidgeest, M., and van der Woude, L. H. (2006). Standardization of measuring power output during wheelchair propulsion on a treadmill pitfalls in a multi-center study. *Med. Eng. Phys.* 28, 604–612. doi:10.1016/j.medengphy.2005.09.004

Desroches, G., Aissaoui, R., and Bourbonnais, D. (2008). Relationship between resultant force at the pushrim and the net shoulder joint moments during manual wheelchair propulsion in elderly persons. *Arch. Phys. Med. Rehabil.* 89, 1155–1161. doi:10.1016/j.apmr.2007.10.040

Escobedo, E., Hunter, J., Hollister, M., Patten, R., and Goldstein, B. (1997). MR imaging of rotator cuff tears in individuals with paraplegia. *Am. J. Roentol.* 168, 919–923. doi:10.2214/ajr.168.4.9124140

Farin, P. U., Jaroma, H., Harju, A., and Soimakallio, S. (1995). Medial displacement of the biceps brachii tendon: evaluation with dynamic sonography during maximal external shoulder rotation. *Radiology* 195, 845–848. doi:10.1148/radiology.195.3.7754018

Finley, M., Rasch, E., Keyser, R., and Rodgers, M. (2004). The biomechanics of wheelchair propulsion in individuals with and without upper-limb impairment. *J. Rehabil. Res. Dev.* 41, 395–402. doi:10.1682/JRRD.2004.03.0385

Gass, G. C., Camp, E. M., Davis, H. A., Eager, D., and Grout, L. (1981). The effects of prolonged exercise on spinally injured subjects. *Med. Sci. Sports Exerc.* 13, 277–283. doi:10.1249/00005768-198105000-00001

Gil-Agudo, A., Del Ama-Espinosa, A., Pérez-Rizo, E., Pérez-Nombela, S. P., and Rodriguez-Rodriguez, P. (2010a). Upper limb joint kinetics during manual wheelchair propulsion in patients with different levels of spinal cord injury. *J. Biomech.* 43, 2508–2515. doi:10.1016/j.jbiomech.2010.05.021

Gil-Agudo, A., Del Ama-Espinosa, A., Pérez-Rizo, E., Pérez-Nombela, S. P., and Crespo-Ruiz, B. (2010b). Shoulder joint kinetics during wheelchair propulsion on a treadmill at two different speeds in spinal cord injury patients. *Spinal Cord* 48, 290–296. doi:10.1038/sc.2009.126

Hartung, G. H., Lally, D. A., and Blancq, R. J. (1993). Comparison of treadmill exercise testing protocols for wheelchair users. *Eur. J. Appl. Physiol. Occup. Physiol.* 66, 362–365. doi:10.1007/BF00237783

Iannotti, J. P., Ciccone, J., Buss, D. D., Visotsky, J. L., Mascha, E., Cotman, K., et al. (2005). Accuracy of office-based ultrasonography of the shoulder for the diagnosis of rotator cuff tears. *J. Bone Joint Surg. Am.* 87, 1305–1311. doi:10.2106/JBJS.D.02100

Kivimäki, J., and Ahoniemi, E. (2008). Ultrasonographic findings in shoulders of able-bodied, paraplegic and tetraplegic subjects. *Spinal Cord* 46, 50–52. doi:10.1038/sj.sc.3102061

Koontz, A., Cooper, R., Boninger, M., Yusheng Yang, M. A., Impink, B. G., and Van der Woude, L. H. (2005). A kinetic analysis of manual wheelchair propulsion during start-up on select indoor and outdoor surfaces. *J. Rehabil. Res. Dev.* 42, 447–458. doi:10.1682/JRRD.2004.08.0106

Koontz, A. M., Cooper, R. A., Boninger, M. L., Souza, A. L., and Fay, B. T. (2002). Shoulder kinematics and kinetics during two speeds of wheelchair propulsion. *J. Rehabil. Res. Dev.* 39, 635–649.

Kulig, K., Rao, S., Mulroy, S., Newsam, C. J., Gronley, J. K., Bontrager, E. L., et al. (1998). Shoulder joint kinetics during the push phase of wheelchair propulsion. *Clin. Orthop. Relat. Res.* 354, 132–143. doi:10.1097/00003086-199809000-00016

Landberg, H., Skovgaard, D., Karamuzis, M., Bulow, J., and Kjaer, M. (1999). Metabolism and inflammatory mediators in the peritendinous space measured by microdyalisis during intermittent isometric exercise in humans. *J. Physiol.* 515, 919–927. doi:10.1111/j.1469-7793.1999.919ab.x

Mack, L. A., Matsen, F. A., Kilcoyne, R. F., Davies, P. K., and Sickler, M. E. (1985). US evaluation of the rotator cuff. *Radiology* 157, 205–209. doi:10.1148/radiology.157.1.3898216

Marino, R. J., Barros, T., Biering-Sorensen, F., Burns, S. P., Donovan, W. H., Graves, D. E., et al. (2003). International standards for neurological classification of spinal cord injury. *J. Spinal Cord Med.* 26(Suppl. 1), S50–S56.

Mason, B., Lenton, J., Leicht, C., and Goosey-Tolfrey, V. (2014). A physiological and biomechanical comparison of over-ground, treadmill and ergometer wheelchair propulsion. *J. Sports Sci.* 32, 78–91. doi:10.1080/02640414.2013.807350

Mercer, J. L., Boninger, M. L., Koontz, A., Ren, D., Dyson-Hudson, T., and Cooper, R. A. (2006). Shoulder joint kinetics and pathology in manual wheelchair users. *Clin. Biomech.* 21, 781–789. doi:10.1016/j.clinbiomech.2006.04.010

Middleton, W. D. (1992). Ultrasonography of the shoulder. *Radiol. Clin. North Am.* 30, 927–940.

Middleton, W. D., Reinus, W. R., Totty, W. G., Melson, C. L., and Murphy, W. A. (1986). Ultrasonographic evaluation of the rotator cuff and biceps tendon. *J. Bone Joint Surg. Am.* 68, 440–450.

Moon, Y., Chandrasekaran, J., Hsu, I. M. K., Rice, I. M., Hsiao-Wecksler, E. T., and Sosnoff, J. J. (2013). Variability of peak shoulder force during wheelchair propulsion in manual wheelchair users with and without shoulder pain. *Clin. Biomech. (Bristol Avon)* 28, 967–972. doi:10.1016/j.clinbiomech.2013.10.004

Mulroy, S., Newsam, C. J., Gutierrez, D., Requejo, P., Gronley, J. K., and Haubert, L. L. (2005). Effect of fore-aft seat position on shoulder demands during wheelchair propulsion: part 1. A kinetic analysis. *J. Spinal Cord Med.* 28, 214–221.

Park, G. Y., and Kwon, D. R. (2011). Application of real-time sonoelastography in musculoskeletal diseases related to physical medicine and rehabilitation. *Am. J. Phys. Med. Rehabil.* 90, 875–886. doi:10.1097/PHM.0b013e31820ff67a

Pentland, W. E., and Twomey, L. T. (1991). The weight-bearing upper extremity in women with long term paraplegia. *Paraplegia* 29, 521–531. doi:10.1038/sc.1991.75

Rodgers, M., Gayle, G. W., Figoni, S., Kobayashi, M., Lieh, J., and Glaser, R. (1994). Biomechanics of wheelchair propulsion during fatigue. *Arch. Phys. Med. Rehabil.* 75, 85–93.

Schuenke, M. D., Mikat, R. P., and McBridge, J. M. (2002). Effect of an acute period of resistance exercise on excess post-exercise oxygen consumption: implications for body mass management. *Eur. J. Appl. Physiol.* 86, 411–417. doi:10.1007/s00421-001-0568-y

Seitz, A. L., and Michener, L. A. (2010). Ultrasonographic measures of subacromial space in patients with rotator cuff disease: a systematic review. *J. Clin. Ultrasound* 39, 146–154. doi:10.1002/jcu.20783

Sie, I. H., Waters, R. L., Adkins, R. H., and Gellman, H. (1992). Upper extremity pain in the postrehabilitation spinal cord injured patient. *Arch. Phys. Med. Rehabil.* 73, 44–48.

Subbarao, J., Klopfstein, J., and Turpin, R. (1995). Prevalence and impact of wrist and shoulder pain in patients with spinal cord injury. *J. Spinal Cord Med.* 18, 9–13.

Teefey, S. A., Rubin, D. A., Middleton, W. D., Hildebolt, C. F., Leibold, R. A., and Yamaguchi, K. (2004). Detection and quantification of rotator cuff tears. Comparison of ultrasonographic, magnetic resonance imaging, and arthroscopic findings in seventy-one consecutive cases. *J. Bone Joint Surg. Am.* 86, 708–716.

Turrin, A., and Capello, A. (1997). Sonographic anatomy of the supraespinatus tendon and adjacent structures. *Skeletal Radiol.* 26, 89–93. doi:10.1007/s002560050199

van der woude, L. H. V., de Groot, G., Hollander, A. P., van Ingen, G. J., and Rozendal, R. H. (1986). Wheelchair ergonomics and physiological testing of prototypes. *Ergonomics* 29, 1561–1573. doi:10.1080/00140138608967269

Van Drongelen, S., Arnet, U., Veeger, D., and Van der Woude, L. H. V. (2013). Effect of workload setting on propulsion technique in handrim wheelchair propulsion. *Med. Eng. Phys.* 35, 283–288. doi:10.1016/j.medengphy.2012.04.017

Van Drongelen, S., Boninger, M. L., Impink, B. G., and Khalaf, T. (2007). Ultrasoung imaging of acute biceps tendon changes after wheelchair sports. *Arch. Phys. Med. Rehabil.* 8, 381–385. doi:10.1016/j.apmr.2006.11.024

Van Drongelen, S., Van der Woude, L. H., Janssen, T. W., Angenot, E. L., Chadwick, E. K., and Veeger, D. H. (2005). Mechanical load on the upper extremity during wheelchair activities. *Arch. Phys. Med. Rehabil.* 86, 1214–1220. doi:10.1016/j.apmr.2005.03.014

Wu, G., van der Helm, F., Veeger, H. E. F., Makhsous, M., Van Roy, P., Anglin, C., et al. (2005). ISB recommendation on definitions of joint coordinate systems of various joints for the reporting of human joint motion. Part II: shoulder, elbow, wrist and hand. *J. Biomech.* 38, 981–992. doi:10.1016/j.jbiomech.2004.05.042

Wylie, E. J., and Chakera, T. M. (1988). Degenerative jopint abnormalities in patients with paraplegia of duration greater than 20 years. *Paraplegia* 26, 101–106. doi:10.1038/sc.1988.20

Conflict of Interest Statement: The authors declare that the research was conducted in the absence of any commercial or financial relationships that could be construed as a potential conflict of interest.

Received: 02 September 2014; accepted: 07 December 2014; published online: 23 December 2014.

Citation: Gil-Agudo Á, Solís-Mozos M, Crespo-Ruiz B, del-Ama Eng AJ, Pérez-Rizo E, Segura-Fragoso A and Jiménez-Díaz F (2014) Echographic and kinetic changes in the shoulder joint after manual wheelchair propulsion under two different workload settings. Front. Bioeng. Biotechnol. ***2****:77. doi: 10.3389/fbioe.2014.00077*

This article was submitted to Biomechanics, a section of the journal Frontiers in Bioengineering and Biotechnology.

frontiers in Bioengineering and Biotechnology

ORIGINAL RESEARCH
published: 20 November 2015
doi: 10.3389/fbioe.2015.00183

Scapulothoracic and Glenohumeral Kinematics During Daily Tasks in Users of Manual Wheelchairs

Kristin D. Zhao[1], Meegan G. Van Straaten[2], Beth A. Cloud[1], Melissa M. Morrow[3], Kai-Nan An[4] and Paula M. Ludewig[5]*

[1] Rehabilitation Medicine Research Center, Department of Physical Medicine and Rehabilitation, Mayo Clinic, Rochester, MN, USA, [2] Motion Analysis Laboratory, Division of Orthopedic Research, Mayo Clinic, Rochester, MN, USA, [3] Department of Health Sciences Research, Mayo Clinic, Rochester, MN, USA, [4] Biomechanics Laboratory, Division of Orthopedic Research, Mayo Clinic, Rochester, MN, USA, [5] Program in Rehabilitation Science, Department of Physical Medicine and Rehabilitation, University of Minnesota, Minneapolis, MN, USA

Background: Rates of shoulder pain in individuals who use manual wheelchairs (MWCs) as their primary means of mobility have been reported to be as high as 70% during activities of daily living. Current prevailing thought is that mechanical impingement of the soft tissues that reside within the subacromial space between the humeral head and coracoacromial arch is a major contributor to the shoulder pain in users of MWCs. The subacromial space size is directly related to the kinematics at the shoulder joint. Yet to be answered are questions about which common daily tasks are characterized by the most potentially detrimental kinematics.

Objective: The purpose of this analysis was to quantify and compare potentially detrimental kinematics in three common tasks performed by individuals with spinal cord injury and shoulder pain. These data will add to the body of knowledge and test common assumptions about relative risk of tasks.

Design: A cross-sectional study of 15 MWC users with shoulder pain.

Methods: Electromagnetic surface sensor measures of mean and peak scapulothoracic (ST) internal and downward rotation, anterior tilt, and glenohumeral (GH) internal rotation were compared across propulsion, weight relief, and scapular plane abduction tasks using one-way repeated-measure ANOVA.

Results: Statistical differences were observed between the tasks for all rotations. Mean ST anterior tilt was greater in weight relief and propulsion than during scapular plane abduction (24°, 23°, and 13° of anterior tilt, respectively). Mean GH axial rotation during weight relief was more internally rotated than during propulsion and scapular plane abduction (9°, 26°, and 51° of external rotation, respectively).

Limitations: Surface-based measures of kinematics are subject to skin motion artifact, especially in translation which was not addressed in this study.

Conclusion: Each task presented with specific variables that might contribute to risk of developing shoulder "impingement" and pain. These data may assist therapists in their assessment of movement contributions to shoulder pain in this population, as well as in subsequent treatment planning.

Keywords: kinematics, shoulder pain, activities of daily living, manual wheelchair users, spinal cord injury

OPEN ACCESS

Edited by:
Philip Santos Requejo, Rancho Los Amigos National Rehabilitation Center, USA

Reviewed by:
Ángel Gil-Agudo, National Hospital for Spinal Cord Injury (SESCAM), Spain
Lisa Lighthall Haubert, Rancho Los Amigos National Rehabilitation Center, USA

****Correspondence:***
Kristin D. Zhao
zhao.kristin@mayo.edu

Specialty section:
This article was submitted to Biomechanics, a section of the journal Frontiers in Bioengineering and Biotechnology

Received: *11 March 2015*
Accepted: *26 October 2015*
Published: *20 November 2015*

Citation:
Zhao KD, Van Straaten MG, Cloud BA, Morrow MM, An K-N and Ludewig PM (2015) Scapulothoracic and Glenohumeral Kinematics During Daily Tasks in Users of Manual Wheelchairs. Front. Bioeng. Biotechnol. 3:183. doi: 10.3389/fbioe.2015.00183

INTRODUCTION

Over 1.5 million persons in the United States use manual wheelchairs (MWCs) (Kaye et al., 2000), and ~20% are users of MWCs secondary to a traumatic or non-traumatic spinal cord injury (SCI) (Kaye et al., 2002). Users of MWCs with SCI are forced to perform many movements within the confines of the MWC. Therefore, they rely heavily on their shoulders as a means of locomotion, to perform weight relief lifts in order to avoid skin breakdown due to pressure on insensate skin, to reach for objects from a seated position, and to perform other activities of daily living. Thus, rates of shoulder pain in individuals with SCI have been reported to be as high as 70% during activities of daily living, negatively affecting their quality of life and independence (McCasland et al., 2006). Therefore, it is imperative that we better understand the secondary chronic conditions users of MWCs are confronted with, to preserve independence over the life span.

Current prevailing thought is that mechanical impingement of the soft tissues that reside within the subacromial space between the humeral head and coracoacromial arch (Dyson-Hudson and Kirshblum, 2004) is a major contributor to the shoulder pain in users of MWCs. The rotator cuff tendons, biceps tendon, and bursa reside within the subacromial space; therefore, reduction in this space, because of the tasks MWC users perform, provides a potential mechanism for injury or pain to the shoulder joint (Flatow et al., 1994; Schneeberger et al., 1998; Soslowsky et al., 2000). The subacromial space is defined and directly affected by the orientations of the humerus and scapula and the resulting rotation angles of the glenohumeral (GH) and scapulothoracic (ST) joints. Clinicians and biomechanists use slightly different language to describe the same movement, and this is important to keep in mind when reviewing kinematic literature. Biomechanists describe GH motions as: (1) humeral elevation, (2) motion in the horizontal plane during humeral elevation (anterior or posterior to the scapular plane), and (3) axial rotation (internal/external) about the humeral long axis (**Figure 1**). Clinicians describe these motions as: (1) flexion/extension/abduction/adduction, (2) horizontal abduction/adduction, and (3) internal/external rotation. Biomechanists describe ST motions as internal/external rotation, upward/downward rotation, and posterior/anterior tilting. The protraction/retraction terminology that clinicians use is a combination of scapular internal rotation and translation of the scapula on the thorax due to sternoclavicular joint protraction/retraction.

When comparing individuals with and without shoulder pain/subacromial impingement symptoms, kinematics have been shown to differ among able-bodied individuals during humeral elevation (Ludewig and Reynolds, 2009). Therefore, it is believed that altered kinematics may negatively impact the subacromial space. These potentially detrimental kinematics are as follows (compared with asymptomatic group values): (1) increased ST internal rotation, (2) increased ST downward rotation, (3) increased ST anterior tilt, and (4) increased GH internal rotation (Lukasiewicz et al., 1999; Ludewig and Cook, 2000; Endo et al., 2001). We believe that some of the tasks MWC users perform on a daily basis predispose them to these potentially detrimental kinematics, regardless of the presence or absence of pain.

A few investigations that include both ST and GH kinematics have been performed to characterize activities commonly performed by users of MWCs, and kinematics presumed to reduce the subacromial space were reported. Morrow et al. (2011) quantified ST and GH kinematics during level and ramp propulsion as well as during weight relief lifts in 12 users of MWCs using an optical-based motion capture system and a scapula tracker. Subjects tested were all pain free. At the point of peak shoulder loading, the weight relief lift displayed significantly less GH external rotation (or more relative GH internal rotation) than the level and ramp propulsion (16° and 19° differences, respectively). Riek et al. (2007) analyzed the shoulder kinematics of various activities of daily living in five individuals with SCI using an electromagnetic system and found that during the initial and maximum loading phases of weight relief, the humerus was significantly more internally rotated than in standing posture using a standing frame (15° and 38° differences, respectively). Nawoczenski et al. (2012) evaluated weight relief and transfer kinematics in individuals with and without shoulder pain. Throughout the transfer task, the group experiencing shoulder pain demonstrated increased anterior tilt of the trailing arm compared with the asymptomatic group. Overall, very little comparative data are available assessing the kinematics of common tasks theorized to contribute to subacromial impingement risk.

With limited data, the understanding of how kinematics during wheelchair-based tasks influence mechanical subacromial impingement and rotator cuff soft tissue compression has not matured. Yet to be answered are questions about which movement and/or environmental optimization interventions will have the biggest impact on maintenance of shoulder health. Yet, clinicians must make decisions on a daily basis as to how to intervene for MWC users who have developed shoulder pain. In

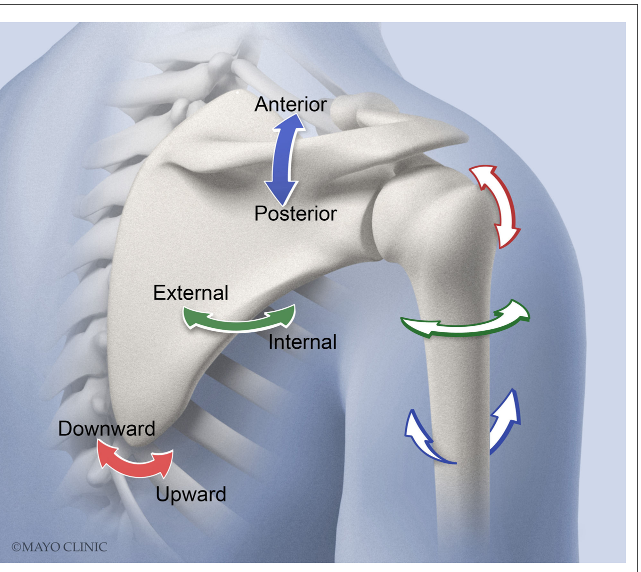

FIGURE 1 | Scapulothoracic (ST) rotation is comprised of internal/external rotation (solid green arrow), upward/downward rotation (solid red arrow), and posterior/anterior tilting (solid blue arrow). Glenohumeral (GH) motions of interest (not shown for clarity) include plane of elevation (anterior or posterior to the scapular plane) (blue outlined arrow), elevation (red outlined arrow), and axial rotation (internal/external) about the humeral long axis (green outlined arrow).

order to test current clinical theories and assumptions regarding task-related development of shoulder pain in MWC users, further direct comparison of shoulder kinematics are needed in common wheelchair-based tasks. In particular, there are no direct comparisons of tasks presumed most detrimental, such as MWC propulsion and weight relief raise, to the kinematics of raising the arm while in a seated position. Based on the literature in able-bodied individuals (Kebaetse et al., 1999), the latter task may be of equivalent risk for development of shoulder subacromial impingement in MWC users functioning from a seated position.

GH and ST kinematics during level MWC propulsion, weight relief, and humeral elevation in the scapular plane were collected as part of a study investigating the effects of an exercise intervention for individuals experiencing mild-to-moderate amounts of shoulder pain during daily activities (Van Straaten et al., 2014). We sought to compare these three wheelchair-based tasks to each other ergonomically, rather than to compare between subjects with and without shoulder pain. Subjects with shoulder pain may differ from those without due to causative or compensatory kinematic changes (Nawoczenski et al., 2012; Lawrence et al., 2014). We sought a symptomatic group to not confound the analysis with both presence and absence of pain and to allow for the high likelihood and relevance of pain in this population. The purpose of this analysis was to quantify and compare potentially detrimental kinematics in three common tasks performed by individuals with SCI and shoulder pain. We hypothesized that differences existed in ST internal rotation, ST downward rotation, ST anterior tilt, and GH internal rotation between the tasks of MWC propulsion, weight relief, and humeral elevation in the scapular plane. These data will add to the body of knowledge and test common assumptions about relative risk of tasks.

MATERIALS AND METHODS

Subject Population

Fifteen individuals who use MWCs as their primary means of mobility participated in the study. These subjects were recruited and signed written informed consent as part of a study approved by the Mayo Clinic Institutional Review Board, investigating shoulder kinematics as well as effects of an exercise intervention for shoulder pain. The kinematic data used for this analysis were recorded at the baseline time point, prior to intervention. Inclusion criteria were assessed by a licensed physical therapist and included: 18–65 years; SCI; shoulder pain during daily activities with clinical symptoms consistent with mechanical subacromial impingement (Park et al., 2005; Michener et al., 2009); use of a MWC as the primary means of mobility in the home and community; and ability to perform independent transfers and sit independently. Sixty-five years was selected as the upper limit for recruitment as we felt this represented the limit of fairly active MWC users whose results may not be confounded by age-related degenerative shoulder complaints. Exclusion criteria were cognitive impairments that limited the ability to independently follow instructions; pain deemed to be of cervical origin; presence of adhesive capsulitis (loss of >25% of range of motion in at least three directions; this included assessment of GH internal/external rotation with the arm at 90° abduction, as well as flexion, and abduction); significant injury to the tested shoulder in which pre-injury status was not attained; gross instability; or suspected labral tears. Finally, subjects were not included in the study if they had allergies to the adhesive tape that was used to attach the motion sensors.

Subject Setup

The subjects were asked to sit in their own MWC in a comfortable seated posture while sensors were applied. Electromagnetic sensors (RX2, Polhemus, Inc.; Colchester, VT, USA) were attached to the painful limb via double-sided medical-grade adhesive tape to the sternum (just beneath the sternal notch), the acromion (on the superior surface of the posteromedial aspect of the acromion, at the junction with the scapular spine), and to the humerus (on the lateral side of a thermoplastic cuff secured to the distal humerus, just proximal to the epicondyles) (Karduna et al., 2001; Hamming et al., 2012). Care was taken to ensure that the acromial sensor was placed on the flat superior surface of the posteromedial aspect of the acromion, at the junction with the spine of the scapula. The arm was elevated prior to securing the sensor so that the sensor was placed medial to the muscle bulk of the deltoid. Thin medical tape was secured over the sensors and attached to ~0.5 cm of adjacent skin to minimize sensor movement (**Figure 2**). Data were collected at 240 Hz using MotionMonitor (Innovative Sports Training, Inc., Chicago, IL, USA) software, and a standard range transmitter (Polhemus, Inc., Colchester, VT, USA).

All subjects' MWCs were tested for interference with the recording equipment and were deemed acceptable (i.e., the distance between two electromagnetic sensors rigidly attached to a wand in close proximity to the MWC remained constant). Each subject sat in his/her own MWC atop aluminum rollers with a resistance that was pre-determined to be similar to overground propulsion from pilot testing; the resistance of the rollers was not changed between the subjects. Local anatomical coordinate systems were defined on each body segment according to International Society of Biomechanics standards (X positive anterior, Y positive superior, Z positive to the right) (Wu et al., 2005). The shoulder joint center was defined using a functional (i.e., movement-based) approach (Meskers et al., 1999; Biryukova et al., 2000).

Experimental Conditions

Before each activity, the movements were explained to the subjects and they were encouraged to become familiar with the experimental setup and practice the movements. Two movements, propulsion and weight relief, were closed-chain tasks that required a load through the hand; scapular plane abduction was an open-chain task, without a weight in the hand. The subjects were asked to perform two repetitions of scapular plane abduction, treadmill propulsion, and weight relief raises, without taking a break between repetitions of each task. However, between tasks, subjects were asked to take as much time as needed for a break period. The beginning position for scapular plane abduction trials was with the humerus next to the trunk, the elbow extended, and the palm of the hand facing forward so that the subjects' ulnar side of the

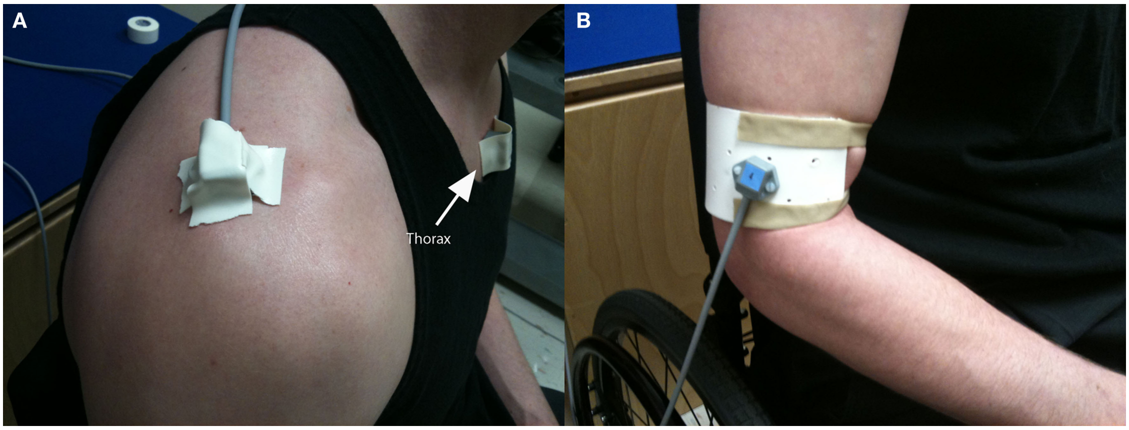

FIGURE 2 | Attachment of electromagnetic sensors on thorax and scapula (A), and distal humeral cuff (B).

forearm or hand rested on their MWC rim. Then, they were asked to move their arm through 90° of abduction, at an angle oriented ~40° anterior to the coronal plane, and then reverse the movement in the same plane by adducting to the starting position. Plane of movement of 40° anterior to the coronal plane was verified using the MotionMonitor software at the time of data collection and adjusted if needed. Subjects were asked to perform the movement at a consistent speed, with verbal counting "up, two, three, four, down, two, three, four" by the investigator, returning to contact the hand rim between trials. For the weight relief movement, the individual was asked to start with his/her hands in their lap, and then after a verbal clue, move at a comfortable pace and place their hands on the MWC hand rim or wheel, lift their weight until their elbows were fully extended, and hold for 2 s before lowering their body weight; the second trial was performed identically. For propulsion, subjects were asked to start with their hands in their lap and then when verbally prompted to begin, proceed with placing their hands on the hand rim followed by at least two full propulsion movements in the style they normally use to propel.

Just prior to the data collection, subjects were asked to complete the Wheelchair Users Shoulder Pain Index (WUSPI) (Curtis et al., 1995a,b), a validated survey for assessing shoulder pain during daily activities. The WUSPI requires that participants rate their shoulder pain intensity on a 0–10 visual analog scale anchored by "no pain" and "worst pain ever experienced" during 15 common daily activities, and is rated for each activity over the preceding 7 days. A total score of zero indicates no pain, while 150 indicates severe pain.

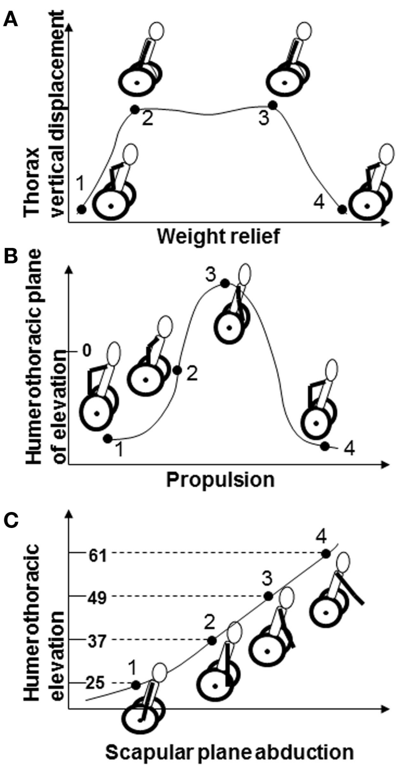

FIGURE 3 | Events 1–4 for (A) weight relief include initiation of lift, beginning of hold, end of hold, and end of lowering phases; (B) propulsion include beginning of push, mid-push, end of push, and end of recovery phases; (C) scapular plane abduction including 25°, 37°, 49°, and 61° of humerothoracic elevation.

Data Analysis

Euler angles were generated to describe the position and orientation of the scapula relative to the thorax (ST), the humerus relative to the scapula (GH), and the humerus relative to the thorax (HT) at each frame across the times series. The International Society of Biomechanics standard definitions were used for the ST (YX′Z″) and HT (YX′Y″) rotations; however, an alternative sequence (Phadke et al., 2011) was used to describe GH rotations (XZ′Y″) to avoid singular positions near the neutral position and provide a more clinically interpretable rotation sequence.

From the time series kinematics, four movement events were defined for each task so that they represented the overall excursion across the movements (**Figure 3**). The four events for weight relief were chosen interactively based on the vertical displacement of the trunk sensor. The start of the raise (event 1) was chosen as an upward vertical displacement. The start of the hold (event 2) was chosen as the end of the upward vertical displacement. The end of the hold (event 3) was chosen as the initiation of downward vertical movement of the trunk sensor. And, the return to the start position (event 4) was chosen as the end of downward vertical movement of the trunk. The four propulsion events were also selected interactively but were based on the HT plane of elevation rotation values. The start of propulsion (event 1) was chosen as the initiation of forward movement of the humerus. The point where the hand left the hand rim at the end of the push phase (event 3) was chosen as the end of forward movement of the humerus. Half way through the push phase (event 2) was calculated as half the time to event 3. The end of propulsion (event 4) was chosen as the end of backward movement of the humerus. This approach for identifying propulsion cycles has been validated against measurements of force applied on the push wheels during propulsion using a SMARTWheel (Three Rivers Holdings, LLC) (unpublished). There is a synchronous relationship between the application of force to the wheels and the HT plane of elevation when propelling on the rollers. Scapular plane abduction events were determined automatically based on the HT elevation values. The start of scapular plane abduction (event 1) was selected as the time at which 25° of elevation occurred. Events 2, 3, and 4 were defined as the times at which 37°, 49°, and 61° of elevation occurred, respectively. Twenty-five degrees was chosen as the minimum elevation value that all subjects could attain while seated in their MWC, 61° was chosen as the expected peak elevation for the other two tasks and was chosen so that all three tasks were taking place in similar regions of the movement space to prevent confounding of humeral elevation angle differences on task comparisons of kinematics. Peak kinematic values were also selected from the original time series curves for the kinematics in the direction of motion believed to be responsible for a reduction in the subacromial space (ST internal and downward rotation, ST anterior tilt, and GH internal rotation).

Statistics

Descriptive analyses of the mean and standard deviations of the time series data for each of the ST and GH rotations were performed. Repeatability of trial event data for outcome variables, for all three movement tasks, were determined using intraclass correlation coefficients ICC(1,1) and standard errors of measurement (SEMs). Separate analyses were performed for the mean kinematic values and peak kinematic values for all dependent variables (the three ST rotations and one GH rotation believed to influence subacromial space). The normality of the data was determined prior to performing one-way repeated-measure ANOVAs with the task condition (propulsion, weight relief, and scapular plane abduction) as the within-subject factor. The data were checked for sphericity. If the Mauchly's criterion was violated, the p values were corrected. Bonferroni *post hoc* t-tests were performed when a significant effect of task was found. All statistical analyses were performed using SAS Enterprise Guide 4.3 (Cary, NC, USA), and the significance level was set at 0.05. Potential covariates for this analysis included age, injury level, years of MWC use, and level of pain (WUSPI). Correlations were determined between these values and the dependent variables with a threshold of 0.5 for inclusion in the statistical model.

RESULTS

Subject Population

Fifteen subjects (13 males and 2 females) were recruited according to the recruitment criteria for study participation (**Table 1**). Subjects had a mean age of 39 (SD 12) years, mean weight of 81 (SD 18) kg, averaged 14 (SD 9) years of MWC use, and presented with mild-to-moderate levels of pain [WUSPI 37.9 (SD 24.4)]. Subjects' injury levels ranged from C6–C7 to L2 with one subject who was post-polio, presenting clinically as a lower lumbar SCI.

Kinematics

The ICC values for the trial-to-trial event data ranged from 0.92 to 0.98 and SEMs ranged from 1.1° to 2.3° across the three tasks. As the data were relatively repeatable, the second trial was used for further analysis in the study so that the data represented actual movement kinematics rather than means across trials. None of the covariate regressions reached a correlation of 0.5 (the highest correlation was 0.15), so covariates were not included in subsequent analyses. Parametric statistics were used for all analyses as kinematic data were deemed to be normally distributed.

Mean time series data across all subjects for each ST and GH rotation and each task are depicted (**Figure 4**). There were significant effects of task on event *means* of all kinematics of interest: GH axial rotation ($F(2,28) = 121.42$, $p < 0.0001$), ST internal rotation ($F(2,28) = 11.14$, $p = 0.0003$), upward rotation ($F(2,28) = 22.79$, $p < 0.0001$), and tilt ($F(2,28) = 51.03$, $p < 0.0001$). *Post hoc* testing demonstrated that mean GH axial rotation during weight relief was more internally rotated than during propulsion and scapular plane abduction (9°, 26°, and 51° of external rotation, respectively). Scapular plane abduction had greater mean ST internal rotation than both weight relief and propulsion tasks (32° versus 26° and 29° of ST internal rotation respectively, **Figure 5**). ST downward rotations were greater during propulsion (3° upward rotation) than weight relief (8° upward rotation) and scapular plane abduction (10° upward rotation, **Figure 5**). No differences were found between scapular plane abduction and weight relief in *post hoc* testing. Mean ST anterior tilt was greater in weight relief and propulsion than during scapular plane abduction (24°, 23°, and 13° of anterior tilt, respectively, **Figure 5**). Weight relief and propulsion were not significantly different with respect to mean ST anterior tilt (**Figure 5**).

Results from the one-way repeated-measure ANOVA analysis of the *peak* kinematic values show similar trends to the event *means* for all kinematics measures except ST internal rotation;

TABLE 1 | Subject demographics.

Characteristic	Participants ($n = 15$, mean ± SD)
Age (years)	39 ± 12
Gender	13 males, 2 females
Weight (kg)	81 ± 18
Injury level (range)	C6/7 to L2, post-polio
Time using MWC (years)	14 ± 9

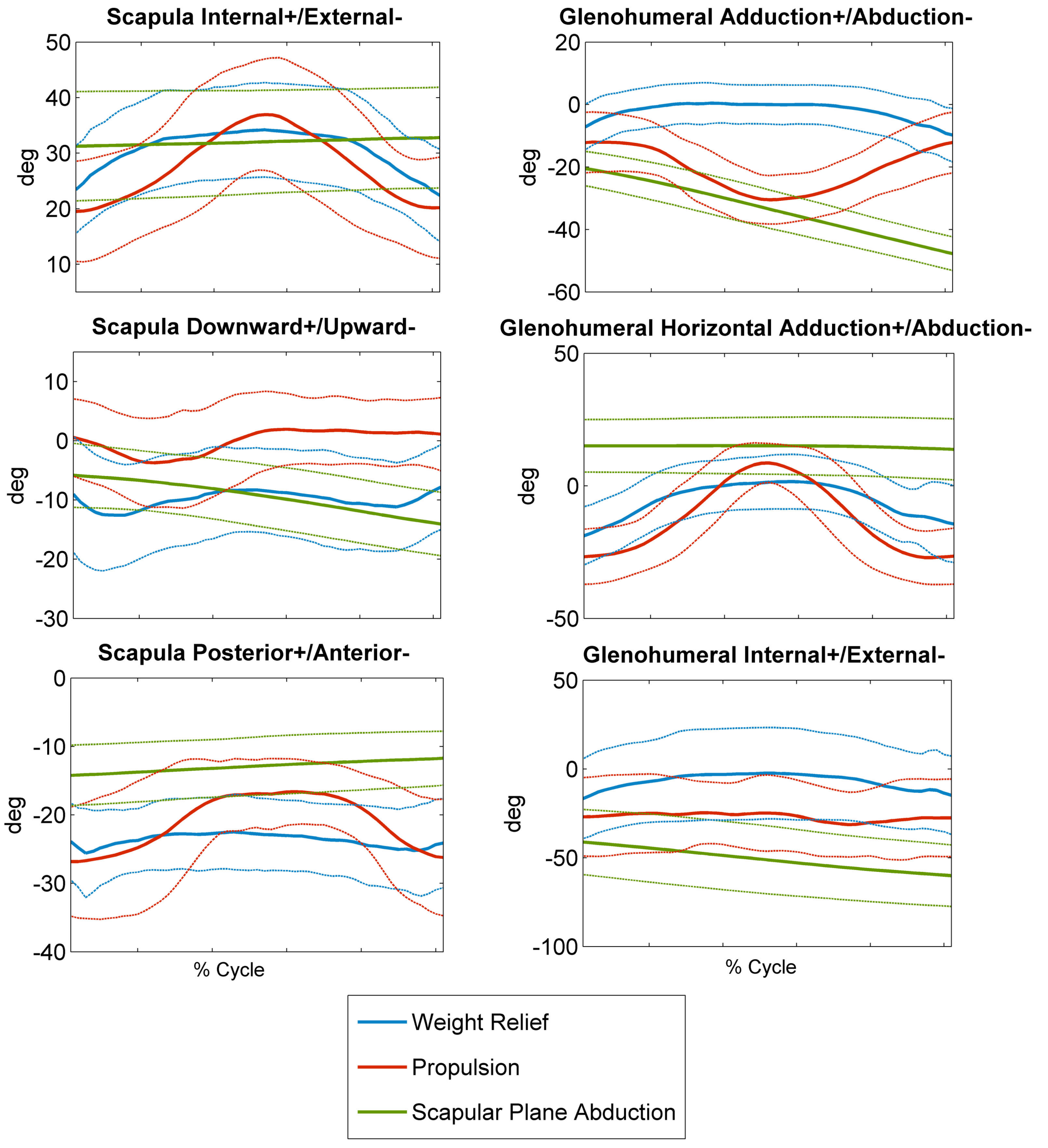

FIGURE 4 | Subjects' mean (±1 SD, dashed lines) scapulothoracic (internal+/external−, downward+/upward−, posterior+/anterior−) and glenohumeral (lowering+/elevation−, horizontal adduction+/abduction−, internal+/external−) rotations for weight relief, propulsion, and scapular plane abduction movements.

peak values reached in each of the rotations during each task can be found in **Figure 6**. Maximum GH internal rotation was greater during weight relief than propulsion and scapular plane abduction [$F(2,28) = 75.44$, $p < 0.0001$]. Propulsion resulted in greater peak ST internal rotation (39°) than scapular plane abduction (34°); it did not significantly differ from weight relief values (35°) [$F(2,28) = 4.07$, $p = 0.0282$]. Peak ST downward rotation was greater during propulsion (5° downward) than during weight relief (5° upward) and scapular plane abduction (6° upward) [$F(2,28) = 25.06$, $p < 0.0001$]. Peak anterior tilt during weight relief (28°) was greater than during scapular plane abduction (14°), but not significantly different than during propulsion (28°) [$F(2,28) = 40.83$, $p < 0.0001$].

DISCUSSION

Currently, the tasks most problematic for MWC users in the development of shoulder pain are often assumed to be MWC propulsion, weight relief raises, and transfers. However, this assumption has never directly been tested, and many other activities, such as arm elevation from a seated position, have the potential to be equally detrimental. Our investigation sought to begin to test these assumptions. Due to our working assumption that a reduction in the subacromial space is related to development of shoulder pain, we have chosen to investigate the kinematics of these movements as a more direct indication of the space, and not the kinetics that led to the ensuing motions. This study compared ST and GH kinematics believed to reduce the subacromial space between

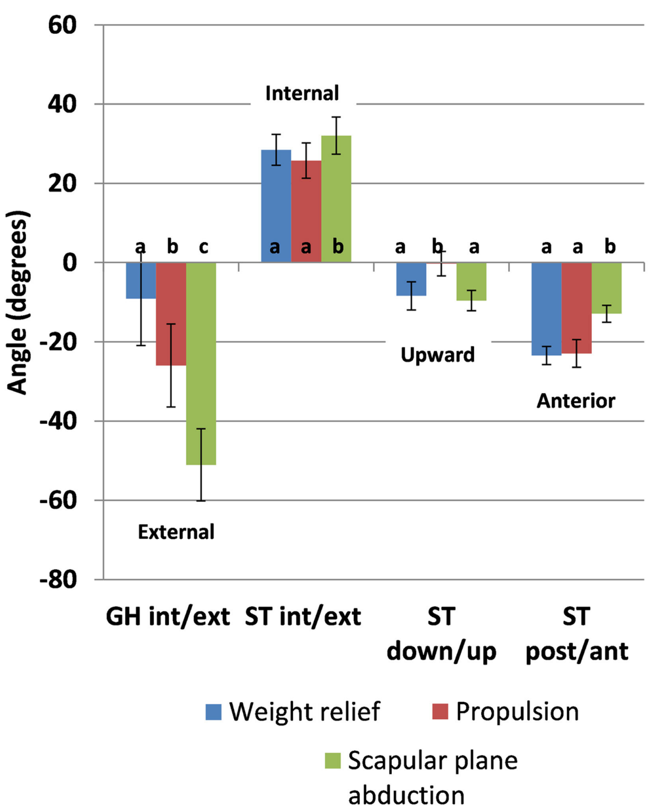

FIGURE 5 | Kinematic means and 95% confidence interval values for between-task comparison of the mean for the three tasks. Letters indicate significance ($p < 0.05$); the same letter indicates no significant difference between values (GH, glenohumeral; ST, scapulothoracic; int, internal; ext, external; down, downward; up, upward; post, posterior; ant, anterior).

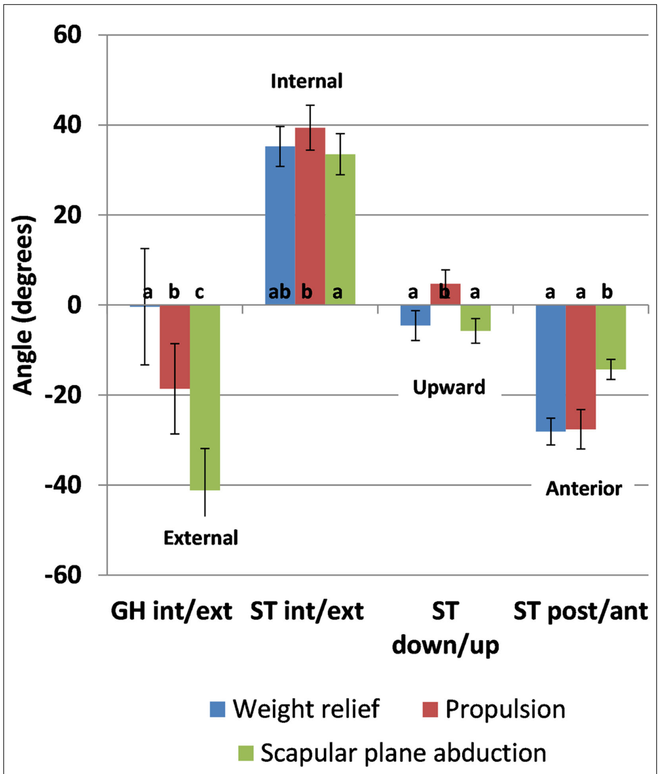

FIGURE 6 | Peak kinematic values in GH internal rotation (-0.4°, -18.7°, and -41.2°), ST internal rotation (35.2°, 39.4°, and 33.5°), downward rotation (-4.6°, 4.7°, and -5.7°), and anterior tilt (-28.1°, -27.6°, and -14.3°) and 95% confidence interval values for between-task comparison for the weight relief, propulsion, and scapular plane abduction, respectively. Letters indicate significance ($p < 0.05$); the same letter indicates no significant difference between values (GH, glenohumeral; ST, scapulothoracic; int, internal; ext, external; down, downward; up, upward; post, posterior; ant, anterior).

level propulsion, a weight relief maneuver, and an arm raise in the scapular plane. Not surprisingly, there were significant differences in the kinematics of different tasks. The meaningful part of these comparisons lie in the interpretation of the magnitude of these differences as well as the value that these findings will bring to the topic when combined with more direct measurements of subacromial space. The kinematics observed in this study provide some of the evidence needed to prioritize detrimental motions and tasks warranting further investigation.

In addition to determining that kinematics are different, one method of interpreting the potential importance of magnitudes of differences between the kinematic tasks is to qualitatively assess the differences from a neutral hanging posture. Neutral hanging arm posture has been defined in healthy subjects in a standing posture using bone-pin mounted sensors (Ludewig et al., 2009). It is known that in the hanging arm position, the soft tissue structures that reside within the space have adequate clearance, so deviations away from the hanging arm position (for both ST and GH articulations) in certain directions are thought to be detrimental. In the ISB coordinate system used in this study, the natural hanging posture is ~29° of ST internal rotation, 5° of ST downward rotation, 10° of ST anterior tilt, and 2° of GH external rotation (Ludewig et al., 2009).

Mean event data revealed a slightly greater overall ST internal rotation during scapular plane abduction than during the other two movements, with differences ranging from 3° to 6°. While these differences are statistically significant, we believe the differences to be small and likely do not have a substantial impact on the underlying subacromial space. Further, the values are very similar to the neutral hanging arm posture in healthy subjects. Therefore, we do not believe our ST internal rotation data are concerning for the MWC user population during these three tasks. ST upward/downward rotation differed by only 7° between tasks and, on average, the scapula remained in an upwardly rotated position. However, the peak rotation during propulsion reached a downward rotated position, which may place users at risk during this task given the elevated position of the humerus. Given the nature of the reduced upward rotation data during propulsion, therapists planning interventions for shoulder pain in MWC users should consider an assessment of an individual's upward rotation during propulsion. If reduced upward rotation is present, exercises to improve lower serratus anterior (primary scapular upward rotator) activation and function during propulsion may be important to consider in treatment planning.

ST anterior tilt and GH internal rotations exhibited larger differences between tasks and deviations from the neutral hanging arm position were greater for anterior tilt. Mean ST anterior tilt was greater in weight relief and propulsion than during scapular plane abduction by up to 11° and also represented deviations away from the hanging arm position, while scapular plane abduction did not (**Figure 5**). GH internal rotation values during weight relief were significantly greater, but did not deviate substantially from the neutral hanging arm posture. Based on current assumptions regarding relationships between angular kinematics and the subacromial space, weight relief and propulsion tasks warrant further investigation and more direct measurements of subacromial space. These study results suggest potentially greater focus on improving upward rotation angles during propulsion tasks, and reducing anterior tilt angles during weight relief raise. The data also suggest that the ST muscle groups deserve attention in rehabilitation interventions.

ST and GH time series data during weight relief were similar in ranges and values to previous data obtained from individuals with spinal cord injury without presence of pain (Morrow et al., 2011) except for ST anterior tilt values (52°–55° versus 20°–28° of anterior tilt in the current study). The anterior tilt differences are likely attributed to the use of a scapular tracker (versus an acromial sensor) for tracking scapula motion in the Morrow et al. investigation. A scapula tracker is most sensitive to error in the anterior/posterior tilt rotation values due the nature of its attachment to the scapular spine. Further, subject-specific coordinate systems were not assigned for each subject in the Morrow study. A transformation based on cadaveric data was used to reference the scapula tracker motion to the anatomical coordinate system of the scapula. As such, our data for anterior tilt cannot be directly compared to the Morrow et al. investigation.

When comparing to previously published data in able-bodied subjects during propulsion (Lu et al., 2002), differences in ST and GH internal rotation ranges (ST: 12°–29° versus 19°–39° of internal rotation in the current study, GH: 5°–10° internal rotation versus 19°–35° of external rotation in the current study) may be attributed to the study populations. Due to variable innervation of the trunk musculature in our spinal cord injured subjects, we have noted that subjects often have a more kyphotic posture and forward head position. This posture would encourage ST internal rotation, which would in turn cause GH rotation to be more externally rotated given a similar humeral position. ST rotations during propulsion in a spinal cord injured population (Morrow et al., 2011) had similar internal/external rotation values (33°–40° of external rotation) to the current study.

Comparisons of our data were made to previous scapular plane abduction studies in able-bodied subjects that included time series data from 25° to 61° of HT elevation (McClure et al., 2001; Ludewig et al., 2009) from a standing position. Ranges of rotations were similar between the previous work and the current study; however, in the current study, the scapula was in greater internal rotation [35°–38° (McClure et al., 2001; Ludewig et al., 2009) versus 45° of internal rotation in the current study] and anterior tilt [7°–12° of anterior tilt (McClure et al., 2001; Ludewig et al., 2009), and 2°–4° of posterior tilt (McClure et al., 2001) versus 16°–18° of anterior tilt in the current study]. These findings can potentially be attributed to the seated posture of users of MWCs who may lack postural stability and may have greater spinal kyphosis.

There are limited studies reporting on the kinematics of activities of daily living in users of MWCs, and none that we are aware of interpreting the findings as they relate to a potential reduction in the subacromial space. Therefore, there are limited relevant studies to compare to. While results of this study do not directly test a clinical intervention, we feel these findings will add important information to the literature that will help guide clinical decision-making of therapists addressing shoulder movement disorders in this population, as well as informing future research.

It is important to note that this investigation was not a comparison between painful and pain-free subjects, but rather a comparisons of the tasks themselves in MWC users with shoulder pain. We believe that the constraints of performing these tasks from a MWC likely have greater impact on kinematics than the presence or absence of pain. This presumption is supported by the lack of substantial association of the kinematics of subjects with their WUSPI scores. Pain also does not have a clear and consistent outcome with regard to affecting movement patterns (Ludewig and Cook, 2000; Nawoczenski et al., 2012). Subjects with shoulder pain have demonstrated disparate results as compared to controls, demonstrating both increases and decreases in key variables such as ST upward rotation. These disparate results have been suggested to represent both causation and compensation. Some subjects may alter kinematics in a compensatory pattern in response to pain, while others may have altered kinematics leading to pain. In addition, our analysis focused only on presumed kinematic mechanisms of subacromial rotator cuff compression, which occurs at lower arm elevation angles. Future work is intended to investigate tasks in this population at higher angles of elevation, where mechanical internal impingement may occur.

Limitations

When interpreting our study findings, it is important to understand its limitations. Surface markers are known to have error as compared to bone-mounted sensors or imaging techniques for recording shoulder kinematics. However, comparison of bone-mounted and skin sensor data have shown errors in humerus and scapula skin sensor acquisitions of $\leq 4°$ during shoulder movements $<60°$ of humeral elevation (Karduna et al., 2001; Ludewig et al., 2002), which is the range we investigated. This investigation focused on the effect of rotational changes during the tasks rather than including the humeral head translation values.

Additionally, this study focused specifically on kinematics thought to be detrimental for subacromial space. Through kinematic results, we can begin to infer which tasks may be putting the shoulder in disadvantageous positions. However, further investigation is warranted to understand the forces acting on the upper extremity and focused evaluations of the subacromial space during MWC-based tasks. An additional limitation is that task kinematics were collected in the same order for all subjects, so it is possible that an order effect existed in the data. No subjects complained of fatigue, and subjects were allowed a break between tasks if desired. It is also possible that study outcomes for the scapular plane abduction may have differed if the subjects had lifted a hand-held weight; however, this seems unlikely based on previous research (de Groot et al., 1999). Further, each subject sat in his/her MWC atop aluminum rollers with a resistance that was not changed between subjects (i.e., not personalized to subject weight). In addition, all subjects underwent a clinical exam by a physical therapist to ensure appropriate innervation and function of their shoulder musculature. While it is possible that the two subjects with higher level spinal cord injuries had some undetected differences in shoulder muscle innervation, it is unlikely.

CONCLUSION

Current assumptions regarding relationships between angular kinematics and the subacromial space implicate greater amounts of ST internal rotation, downward rotation, anterior tilt, and GH internal rotation as disadvantageous. Based on these assumptions and the overall kinematics observed in this study of the tasks evaluated, weight relief and propulsion seem to be most detrimental for the shoulder. However, each task presented with specific variables that might contribute to risk of developing shoulder "impingement" and pain. These data may assist therapists in their assessment of movement contributions to shoulder pain in this population, as well as in subsequent treatment planning. This data add to our understanding of the relative risks associated with various MWC-based activities.

ACKNOWLEDGMENTS

This study was funded by Paralyzed Veterans of America (#2745). Select resources and personnel were supported by NIH grants UL1 RR024150 and TL1 TR000137 from the National Center for Advancing Translational Science (NCATS). Its contents are solely the responsibility of the authors and do not necessarily represent the official views of the NIH or the Paralyzed Veterans of America.

REFERENCES

Biryukova, E. V., Roby-Brami, A., Frolov, A. A., and Mokhtari, M. (2000). Kinematics of human arm reconstructed from spatial tracking system recordings. *J. Biomech.* 33, 985–995. doi:10.1016/S0021-9290(00)00040-3

Curtis, K. A., Roach, K. E., Applegate, E. B., Amar, T., Benbow, C. S., Genecco, T. D., et al. (1995a). Reliability and validity of the wheelchair user's shoulder pain index (WUSPI). *Paraplegia* 33, 595–601. doi:10.1038/sc.1995.126

Curtis, K. A., Roach, K. E., Applegate, E. B., Amar, T., Benbow, C. S., Genecco, T. D., et al. (1995b). Development of the wheelchair user's shoulder pain index (WUSPI). *Paraplegia* 33, 290–293. doi:10.1038/sc.1995.126

de Groot, J. H., van Woensel, W., and van der Helm, F. C. (1999). Effect of different arm loads on the position of the scapula in abduction postures. *Clin. Biomech.* 14, 309–314. doi:10.1016/S0268-0033(98)90094-8

Dyson-Hudson, T. A., and Kirshblum, S. C. (2004). Shoulder pain in chronic spinal cord injury, part I: epidemiology, etiology, and pathomechanics. *J. Spinal Cord Med.* 27, 4–17.

Endo, K., Ikata, T., Katoh, S., and Takeda, Y. (2001). Radiographic assessment of scapular rotational tilt in chronic shoulder impingement syndrome. *J. Orthop. Sci.* 6, 3–10. doi:10.1007/s007760170017

Flatow, E. L., Soslowsky, L. J., Ticker, J. B., Pawluk, R. J., Hepler, M., Ark, J., et al. (1994). Excursion of the rotator cuff under the acromion. Patterns of subacromial contact. *Am. J. Sports Med.* 22, 779–788. doi:10.1177/036354659402200609

Hamming, D., Braman, J., Phadke, V., LaPrade, R., and Ludewig, P. (2012). The accuracy of measuring glenohumeral motion with a surface humeral cuff. *J. Biomech.* 45, 1161–1168. doi:10.1016/j.jbiomech.2012.02.003

Karduna, A. R., McClure, P. W., Michener, L. A., and Sennett, B. (2001). Dynamic measurements of three-dimensional scapular kinematics: a validation study. *J. Biomech. Eng.* 123, 184. doi:10.1115/1.1351892

Kaye, H. S., Kang, T., and LaPlante, M. (2000). *Mobility Device Use in the United States*. San Francisco, CA: University of California.

Kaye, H., Kang, T., and LaPlante, M. (2002). *Wheelchair Use in the United States*. Washington, DC: U.S. Department of Education, National Institute on Disability and Rehabilitation Research.

Kebaetse, M., McClure, P., and Pratt, N. A. (1999). Thoracic position effect on shoulder range of motion, strength, and three-dimensional scapular kinematics. *Arch. Phys. Med. Rehabil.* 80, 945–950. doi:10.1016/S0003-9993(99)90088-6

Lawrence, R. L., Braman, J. P., Staker, J. L., Laprade, R. F., and Ludewig, P. M. (2014). Comparison of 3-dimensional shoulder complex kinematics in individuals with and without shoulder pain, part 2: glenohumeral joint. *J. Orthop. Sports Phys. Ther.* 44, 646–655. doi:10.2519/jospt.2014.5556

Lu, T. W., Li, G. J., Kuo, M. Y., Chang, L. Y., and Hsu, H. C. (2002). *Measurement of Three-Dimensional Kinematics of the Glenohumeral Joint During Manual Wheelchair Propulsion Using Skeletal Markers*. Calgary, Canada: IV World Congress of Biomechanics.

Ludewig, P., Cook, T., and Shields, R. (2002). Comparison of surface sensor and bone-fixed measurement of humeral motion. *J. Appl. Biomech.* 18, 163–170.

Ludewig, P. M., and Cook, T. M. (2000). Alterations in shoulder kinematics and associated muscle activity in people with symptoms of shoulder impingement. *Phys. Ther.* 80, 276–291.

Ludewig, P. M., Phadke, V., Braman, J. P., Hassett, D. R., Cieminski, C. J., and LaPrade, R. F. (2009). Motion of the shoulder complex during multiplanar humeral elevation. *J. Bone Joint Surg. Am.* 91, 378–389. doi:10.2106/JBJS.G.01483

Ludewig, P. M., and Reynolds, J. F. (2009). The association of scapular kinematics and glenohumeral joint pathologies. *J. Orthop. Sports Phys. Ther.* 39, 90–104. doi:10.2519/jospt.2009.2808

Lukasiewicz, A. C., McClure, P., Michener, L., Pratt, N., and Sennett, B. (1999). Comparison of 3-dimensional scapular position and orientation between subjects with and without shoulder impingement. *J. Orthop. Sports Phys. Ther.* 29, 574–583. doi:10.2519/jospt.1999.29.10.574

McCasland, L. D., Budiman-Mak, E., Weaver, F. M., Adams, E., and Miskevics, S. (2006). Shoulder pain in the traumatically injured spinal cord patient: evaluation of risk factors and function. *J. Clin. Rheumatol.* 12, 179–186.

McClure, P., Michener, L., Sennett, B., and Karduna, A. (2001). Direct 3-dimensional measurement of scapular kinematics during dynamic movements in vivo. *J. Shoulder Elbow. Surg.* 10, 269–277. doi:10.1067/mse.2001.112954

Meskers, C. G., Fraterman, H., van der Helm, F. C., Vermeulen, H. M., and Rozing, P. M. (1999). Calibration of the "Flock of Birds" electromagnetic tracking device and its application in shoulder motion studies. *J. Biomech.* 32, 629–633. doi:10.1016/S0021-9290(99)00011-1

Michener, L. A., Walsworth, M. K., Doukas, W. C., and Murphy, K. P. (2009). Reliability and diagnostic accuracy of 5 physical examination tests and combination of tests for subacromial impingement. *Arch. Phys. Med. Rehabil.* 90, 1898–1903. doi:10.1016/j.apmr.2009.05.015

Morrow, M. M., Kaufman, K. R., and An, K. N. (2011). Scapula kinematics and associated impingement risk in manual wheelchair users during propulsion and a weight relief lift. *Clin. Biomech. (Bristol, Avon)* 26, 352–357. doi:10.1016/j.clinbiomech.2010.12.001

Nawoczenski, D. A., Riek, L. M., Greco, L., Staiti, K., and Ludewig, P. M. (2012). Effect of shoulder pain on shoulder kinematics during weight-bearing tasks in persons with spinal cord injury. *Arch. Phys. Med. Rehabil.* 93, 1421–1430. doi:10.1016/j.apmr.2012.02.034

Park, H. B., Yokota, A., Gill, H. S., El Rassi, G., and McFarland, E. G. (2005). Diagnostic accuracy of clinical tests for the different degrees of subacromial impingement syndrome. *J. Bone Joint Surg. Am.* 87, 1446–1455. doi:10.2106/JBJS.D.02335

Phadke, V., Braman, J. P., LaPrade, R. F., and Ludewig, P. M. (2011). Comparison of glenohumeral motion using different rotation sequences. *J. Biomech.* 44, 700–705. doi:10.1016/j.jbiomech.2010.10.042

Riek, L. M., Ludewig, P. M., and Nawoczenski, D. A. (2007). Comparative shoulder kinematics during free standing, standing depression lifts and daily functional activities in persons with paraplegia: considerations for shoulder health. *Spinal Cord* 46, 335–343. doi:10.1038/sj.sc.3102140

Schneeberger, A. G., Nyffeler, R. W., and Gerber, C. (1998). Structural changes of the rotator cuff caused by experimental subacromial impingement in the rat. *J. Shoulder Elbow Surg.* 7, 375–380. doi:10.1016/S1058-2746(98)90026-X

Soslowsky, L. J., Thomopoulos, S., Tun, S., Flanagan, C. L., Keefer, C. C., Mastaw, J., et al. (2000). Neer award 1999. Overuse activity injures the supraspinatus tendon in an animal model: a histologic and biomechanical study. *J. Shoulder Elbow Surg.* 9, 79–84. doi:10.1067/mse.2000.101962

Van Straaten, M. G., Cloud, B. A., Morrow, M. M., Ludewig, P. M., and Zhao, K. D. (2014). Effectiveness of home exercise on pain, function, and strength of manual wheelchair users with spinal cord injury: a high-dose shoulder program with telerehabilitation. *Arch. Phys. Med. Rehabil.* 95, 1810e–1817e. doi:10.1016/j.apmr.2014.05.004

Wu, G., van der Helm, F. C., Veeger, H. E., Makhsous, M., Van Roy, P., Anglin, C., et al. (2005). ISB recommendation on definitions of joint coordinate systems of various joints for the reporting of human joint motion – part II: shoulder, elbow, wrist and hand. *J. Biomech.* 38, 981–992. doi:10.1016/j.jbiomech.2004.05.042

Conflict of Interest Statement: The authors declare that the research was conducted in the absence of any commercial or financial relationships that could be construed as a potential conflict of interest.

frontiers in Bioengineering and Biotechnology

ORIGINAL RESEARCH
published: 10 September 2015
doi: 10.3389/fbioe.2015.00137

Biomechanics of pediatric manual wheelchair mobility

Brooke A. Slavens[1,2,3], Alyssa J. Schnorenberg[1], Christine M. Aurit[1], Sergey Tarima[4], Lawrence C. Vogel[2] and Gerald F. Harris[2,3]*

[1] Movement Analysis for Biomedical Innovation & Technology (Mobility) Laboratory, Department of Occupational Science and Technology, University of Wisconsin-Milwaukee, Milwaukee, WI, USA, [2] Shriners Hospitals for Children – Chicago, Chicago, IL, USA, [3] Orthopaedic and Rehabilitation Engineering Center (OREC), Medical College of Wisconsin and Marquette University, Milwaukee, WI, USA, [4] Department of Biostatistics, Medical College of Wisconsin, Milwaukee, WI, USA

OPEN ACCESS

Edited by:
Jill L. McNitt-Gray,
University of Southern California, USA

Reviewed by:
Ru-Lan Hsieh,
Shin Kong Wu Ho-Su Memorial Hospital, Taiwan
Henrique De Amorim Almeida,
Polytechnic Institute of Leiria, Portugal

***Correspondence:**
Brooke A. Slavens,
Movement Analysis for Biomedical Innovation & Technology (Mobility) Laboratory, Department of Occupational Science and Technology, University of Wisconsin-Milwaukee, 1225 Discovery Parkway, Wauwatosa, WI 53226, USA
slavens@uwm.edu

Specialty section:
This article was submitted to Biomechanics, a section of the journal Frontiers in Bioengineering and Biotechnology

Received: *16 June 2015*
Accepted: *26 August 2015*
Published: *10 September 2015*

Citation:
Slavens BA, Schnorenberg AJ, Aurit CM, Tarima S, Vogel LC and Harris GF (2015) Biomechanics of pediatric manual wheelchair mobility. Front. Bioeng. Biotechnol. 3:137. doi: 10.3389/fbioe.2015.00137

Currently, there is limited research of the biomechanics of pediatric manual wheelchair mobility. Specifically, the biomechanics of functional tasks and their relationship to joint pain and health is not well understood. To contribute to this knowledge gap, a quantitative rehabilitation approach was applied for characterizing upper extremity biomechanics of manual wheelchair mobility in children and adolescents during propulsion, starting, and stopping tasks. A Vicon motion analysis system captured movement, while a SmartWheel simultaneously collected three-dimensional forces and moments occurring at the handrim. A custom pediatric inverse dynamics model was used to evaluate three-dimensional upper extremity joint motions, forces, and moments of 14 children with spinal cord injury (SCI) during the functional tasks. Additionally, pain and health-related quality of life outcomes were assessed. This research found that joint demands are significantly different amongst functional tasks, with greatest demands placed on the shoulder during the starting task. Propulsion was significantly different from starting and stopping at all joints. We identified multiple stroke patterns used by the children, some of which are not standard in adults. One subject reported average daily pain, which was minimal. Lower than normal physical health and higher than normal mental health was found in this population. It can be concluded that functional tasks should be considered in addition to propulsion for rehabilitation and SCI treatment planning. This research provides wheelchair users and clinicians with a comprehensive, biomechanical, mobility assessment approach for wheelchair prescription, training, and long-term care of children with SCI.

Keywords: biomechanics, manual wheelchair, pediatrics, propulsion, mobility

Introduction

Of the ~10,000 individuals who sustain a spinal cord injury (SCI) each year in the United States (U.S.), 3–5% occur in individuals younger than 15 years of age and ~20% occur in those younger than 20 years of age (Vogel et al., 2004). An estimated 1455 children are admitted for SCI treatment to US hospitals each year (Vitale et al., 2006; Riddick-Grisham and Deming, 2011). SCI

Abbreviations: 3-D, three-dimensional; ARC, arcing; DLOP, double looping over propulsion; FIR, finite impulse response; GH, glenohumeral; LMM, linear mixed models; MR, magnetic resonance; RMS, root mean square; ROM, range of motion; SC, semicircular; SCI, spinal cord injury; SF-12, Short Form 12 Health Questionnaire; SLOP, single looping over propulsion; UE, upper extremity; UEs, upper extremities; VAS, Visual Analog Scale.

often occurs as a result of an accidental injury or traumatic event and may result in physical limitations that can affect functional mobility. Individuals with SCI are often reliant upon wheelchairs for mobility and contribute to the 3.7 million wheelchair users in the U.S. (Brault and U.S. Census Bureau, 2012). Among children under the age of 18, the wheelchair is the most widely used assistive mobility device impacting over 88,000 children, 90% of which use manual wheelchairs (Kaye et al., 2000). In adults with SCI shoulder pain and degenerative changes, especially at the acromioclavicular joint, may develop prematurely due to overuse and altered mechanical stresses, particularly in those with high levels of manual wheelchair activity (Lal, 1998; Mercer et al., 2006). Reported upper extremity injuries associated with manual wheelchair usage in adults with SCI include destructive shoulder arthropathy, degenerative arthritis of the shoulder and elbow, rotator cuff tendonitis, coracoacromial pathology, and carpal tunnel syndrome (Pentland and Twomey, 1991; Sie et al., 1992; Lal, 1998; Ballinger et al., 2000; Boninger et al., 2001; Mercer et al., 2006; Yang et al., 2009). It has been reported that adult manual wheelchair users with SCI have a high prevalence of shoulder pain and injury (Boninger et al., 2001; Mercer et al., 2006; Schnorenberg et al., 2014) with shoulder pain occurrence in paraplegics ranging from 30 to 73% (Pentland and Twomey, 1991; Sie et al., 1992; Boninger et al., 2002, 2005; Mercer et al., 2006). Due to longer-term wheelchair use in those with pediatric-onset SCI, upper extremity pain and injuries may occur earlier in their lifespan and severely limit independence, function, and quality of life (Vogel et al., 2011). Previous work by our group has shown that the incidence of shoulder pain in adults with pediatric-onset SCI is 48–54% (Hwang et al., 2014); however, there is limited information on functional mobility and pain in those with pediatric-onset SCI.

Children who have sustained a SCI often use a manual wheelchair for functional mobility in the home, school, and community environments. Functional mobility includes propulsion, starting from a stationary position, stopping their wheelchair, and moving over various terrains (Case-Smith and O'Brien, 2013). Studies have examined adult manual wheelchair users during mobility tasks including level propulsion, ramp ascent, start and stop, and weight relief and found significantly different upper extremity joint demands across tasks (Morrow et al., 2010). However, children are not physically proportionate to adults and we cannot assume that scaling dynamics information will give an accurate representation of the true demands of wheelchair mobility. A study by Jensen confirmed changes in force and moment curves due to differences in proportionality and a redistribution of mass that occurs with age (Jensen, 1989). Although children are proportionately different than adults, with developing musculoskeletal systems, there is limited research of pediatric wheelchair mobility (Schnorenberg et al., 2014; Slavens et al., 2015). It is, therefore, vital that research address the unique biomechanics of pediatric wheelchair mobility and provide insight to the differences from adults. Despite this, current literature contains many studies that consider the biomechanics of adult manual wheelchair mobility, and few focused on the biomechanics in the pediatric population (Koontz et al., 2005; Petuskey et al., 2007; Rice et al., 2009; Schnorenberg et al., 2014). Pediatric manual wheelchair propulsion repetitively places increased load demands on the upper extremities (Schnorenberg et al., 2014), leading to a level of high concern for the development of pain and injury over the long-term duration of usage. Further insight into the biomechanics of pediatric wheelchair users is critical for ultimately preserving upper extremity function and joint integrity. More so, a deeper understanding of the relationship among upper extremity biomechanics, pain, and function is necessary. We aim to quantify upper extremity kinematics and kinetics during functional manual wheelchair mobility in children with SCI and identify their related pain and health-related quality of life.

In adults, four primary wheelchair stroke patterns, the motion the hand makes during the recovery phase of the stroke cycle, have been defined. These include (1) single looping over propulsion (when the hands rise above the handrim), (2) double looping over propulsion (when the hands rise above and then fall below the handrim), (3) semicircular (when the hands fall below the handrim), and (4) arcing (ARC) (when the hand follows the path of the pushrim) (Shimada et al., 1998; Boninger et al., 2002, 2005). Research has demonstrated that in adults, the semicircular pattern allows the user to apply force to the handrim over a greater angle and for a longer duration. These characteristics correlated to a reduction of injury risk in adults. Therefore, the semicircular pattern is the recommended technique for adult manual wheelchair propulsion (Boninger et al., 2002, 2005). However, it is important to note that there is a void of propulsion stroke pattern characterization in the pediatric population and studies supporting the recommendation of the semicircular propulsion pattern are limited to adult wheelchair users with paraplegia and were cautioned for application to other groups, such as pediatrics (Boninger et al., 2005). We will, thus, examine pediatric stoke patterns in this study.

The primary purpose of this study is to quantify upper extremity joint kinematics and kinetics of pediatric manual wheelchair users during functional manual wheelchair mobility. We will investigate three functional tasks: (1) propulsion, (2) starting from rest, and (3) stopping during propulsion. We hypothesize that three-dimensional (3-D) upper extremity joint motions, forces, and moments will be significantly different among the three tasks. We will also identify pediatric wheelchair stroke patterns during the propulsion task and evaluate pain and health-related quality of life outcomes.

Materials and Methods

Upper Extremity Biomechanical Model

A custom, bilateral, pediatric, upper extremity model was utilized to determine 3-D joint angles, forces, and moments (Schnorenberg et al., 2014). This biomechanical model comprises 11 segments, including the thorax, clavicles, scapulae, humeri, forearms, and hands. The joints of interest are three degree-of-freedom thorax, acromioclavicular, glenohumeral (GH), and wrist joints; and two degree-of-freedom sternoclavicular and elbow joints. These segments are represented by strategically placing reflective markers on bony anatomical landmarks and technical locations of the subject, including the suprasternal notch, xiphoid process, spinal process C7, acromioclavicular joint, inferior angle (IA), trigonum spinae (TS), scapular spine, acromial angle, coracoid process, humerus technical marker, olecranon, radial and ulnar styloids, and the third and fifth metacarpals (Schnorenberg et al., 2014).

The upper extremity model includes novel features (Schnorenberg et al., 2014), some of which we will highlight. First, the markers defining the thorax segment are placed directly on the torso, with no indirect placement on the clavicles. This reduces the amount of error introduced when calculating the thorax joint angles due to clavicle motion relative to the thorax (Nguyen and Baker, 2004). Second, the elbow joint is modeled using a technique that does not require the use of a marker placed on the medial epicondyle, which is often obstructed and inadvertently interacts with the wheelchair. By using a single marker on the olecranon, inaccuracies and marker dropout are reduced (Hingtgen et al., 2006). Third, the model incorporates a scapula marker tracking technique developed by Senk et al. utilizing rigid body theory, which enables accurate calculation of markers placed on the TS and the IA of the scapulae despite the subcutaneous nature of scapula motion. This method captures the TS and IA scapula marker positions during a static position with precisely palpated positions. The TS and AI markers are then removed for dynamic trials and their trajectories calculated based on their position and orientation relative to the other scapula markers, which move more reliably during dynamic tasks. This was shown to be appropriate for scapular motion tracking, especially during tasks with <120–150° of arm elevation. This method has low root mean square (RMS) errors (5.4–10.3°), similar to those of the commonly used tracker (3.2–10.0°) and acromion (4.8–11.4°) methods (Senk and Cheze, 2010). Fourth, the ability to track these scapula positions allows the use of a more accurate method of GH joint center calculation. For this calculation, Meskers developed regression equations involving the positions of the scapula markers. These equations have since been updated by the International Shoulder Group (ISG) and were shown to be accurate when compared to magnetic resonance (MR) images of the actual joint center (Campbell et al., 2009). Lastly, we used pediatric appropriate body segment parameters and anthropometric measures (Jensen, 1989), specifically customizing our model to children and adolescents.

Segment coordinate systems were determined for each of the model's 11 segments. Following ISB recommendations, the segment coordinate systems' axes are aligned such that the Z-axis points laterally toward the subject's right side, the X-axis points anteriorly, and the Y-axis points superiorly (Wu et al., 2005). The joint angles were determined by the relative motion between two adjacent segment coordinate systems, distal relative to proximal. The segment coordinate systems follow the right-hand rule with the Z-axis as the flexion/extension axis; the X-axis as the abduction/adduction axis; and the Y-axis as the internal/external rotation axis. A Z–X–Y Euler sequence is used to calculate the GH, elbow, wrist, and thorax joint angles, and a Y–X–Z Euler sequence is used for the acromioclavicular and sternoclavicular joint angle computation.

Subjects

Approval from the Shriners Hospital for Children – Chicago's Institutional Review Board (IRB) was obtained for the study. Fourteen pediatric manual wheelchair users with SCI were recruited and an assent form or informed consent form were signed by the child and/or their parent/guardian. All subjects were evaluated at Shriners Hospitals for Children – Chicago. Subjects included in this study were under 21 years of age, had a SCI diagnosis, were at least 1 year post-injury and used a manual wheelchair for their primary mode of mobility. The mean subject age was 13.7 ± 4.8 years, with an average time since injury of 5.3 ± 3.9 years. The bony level of SCI ranged from the third cervical (C3) vertebra to the tenth thoracic (T10) vertebra. Levels A, B, and C of the American Spinal Injury Association (ASIA) Classification, which grades the severity of an individual's neurological loss, were represented. Subject characteristics are described in **Table 1**.

Data Collection

A pain outcome, the Visual Analog Scale (VAS), and a quality of life outcome, the Short Form 12 Health Questionnaire (SF-12), were administered prior to motion analysis. The VAS was utilized since it serves as a standard outcome tool for clinical assessment at Shriners Hospital for Children – Chicago. Subjects were asked to indicate their average daily pain level by marking it on the scale with a pen, or pointing, to indicate their rating, with 0 being no pain at all and 100 being the worst pain imaginable (Wewers and Lowe, 1990). The SF-12 assessed the subjects' health-related quality of life. Subjects were asked to respond to each of the 12 questions, which are used to calculate a physical composite score (PCS) and a mental health composite score (MCS) on a scale of 0–100, with the national norm score for healthy individuals being 50 (Office of Public Health Assessment, 2004).

Subject-specific measurements were obtained for all participants. The 27 passive reflective markers, previously described, were adhered to the subject to prepare for motion capture (**Figure 1**). A SmartWheel (Outfront, Mesa, AZ, USA), replaced the wheel on the dominant side of the subject's wheelchair for kinetic data collection; the SmartWheel companion wheel replaced the subject's wheel on the non-dominant side. Both the SmartWheel and its companion are air tires. No subject required the use of plastic-coated handrims or gloves to assist with their propulsion.

The subject propelled his or her manual wheelchair along a 15-m path at a self-selected speed and self-selected propulsion pattern to simulate community/home mobility. A 14-camera Vicon MX System captured 3-D marker trajectories at 120 Hz, while the SmartWheel simultaneously collected tri-axial forces and moments occurring at the hand–handrim interface at 240 Hz. Subsequently, the collected kinetic data was low-pass filtered using a 32-tap finite impulse response (FIR) filter. Multiple trials were collected, with adequate rest provided to the subject as needed.

All participants performed a series of functional mobility tasks, including propulsion, starting, and stopping (**Figure 2**). Propulsion involved subjects propelling their manual wheelchair across the room while staying on a colored walkway in the center

TABLE 1 | Subject characteristics for each subject and the calculated group averages and SDs.

Subject	Age (years)	Height (cm)	Weight (kg)	Time since injury (years)	SCI (ASIA) level	SCI classification	Gender	Arm dominance
1	11.1	177.8	24.4	2.9	T9 (A)	Paraplegia	Male	Right
2	17.3	169.9	63.8	1.1	C6 (B)	Quadriplegia	Male	Right
3	16.8	183.1	63.8	1.3	C7 (B)	Paraplegia	Male	Right
4	11.8	152.4	58.5	NR	C8 (A)	Paraplegia	Male	Right
5	20.9	167.6	51.1	3.8	T10 (A)	Quadriplegia	Female	Left
6	19.5	193	93	1.5	C6 (C)	Paraplegia	Male	Left
7	7.2	121.9	26.5	5.8	C3-T1 (C)	Paraplegia	Male	Left
8	6.5	119.4	28.5	6.2	L3 (C)	Paraplegia	Male	Right
9	10.2	121.9	24.0	8.1	T4 (A)	Paraplegia	Female	Right
10	16.6	133.1	31.6	10.9	T10 (C)	Paraplegia	Male	Right
11	19.0	178.0	76.0	6.5	T9 (A)	Paraplegia	Male	Right
12	14.5	139.7	42.5	14.0	T8 (A)	Paraplegia	Female	Right
13	13.0	153.4	44.0	3.1	C8 (B)	Paraplegia	Female	Right
14	7.8	118.1	22.6	4.1	T10 (A)	Quadriplegia	Female	Right
Average	13.7	152.1	46.5	5.3				
SD	4.8	26.4	22.1	3.9				

NR, not reported.

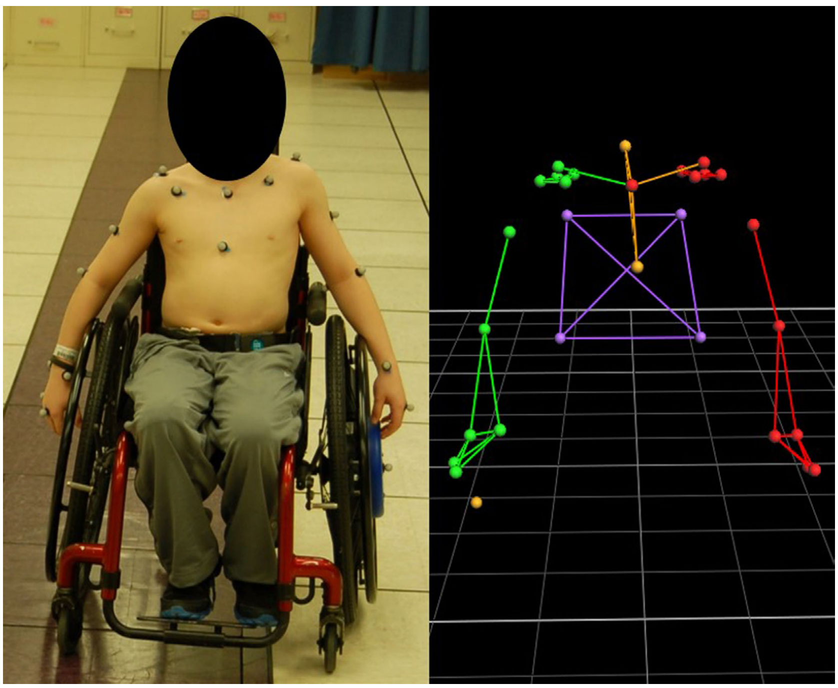

FIGURE 1 | Subject with marker set applied and SmartWheel replacing the dominant, left-hand side wheel (left) and the model rendering in Vicon Nexus software.

of the capture volume. Ten stroke cycles, obtained from multiple trials, were analyzed. Within a trial, the start-up strokes and stopping strokes were always excluded from evaluation to eliminate effects of acceleration and deceleration. The start task began with subjects at a static position in the center of the capture volume and then propelled themselves to the far side of the room (the end of the capture volume). The first stroke was analyzed for each of the three trials. The stop task began with subjects outside of the capture volume in a static position. They then propelled themselves into the capture volume and stopped when they reached the center. The last stroke was analyzed for each of the three trials.

Data Processing

Vicon Nexus was used to process the marker trajectories. The resulting marker trajectories were filtered using a Woltring filter with a mean squared error setting of 20 (Woltring, 1986). The kinetic data was then resampled to 120 Hz in MATLAB

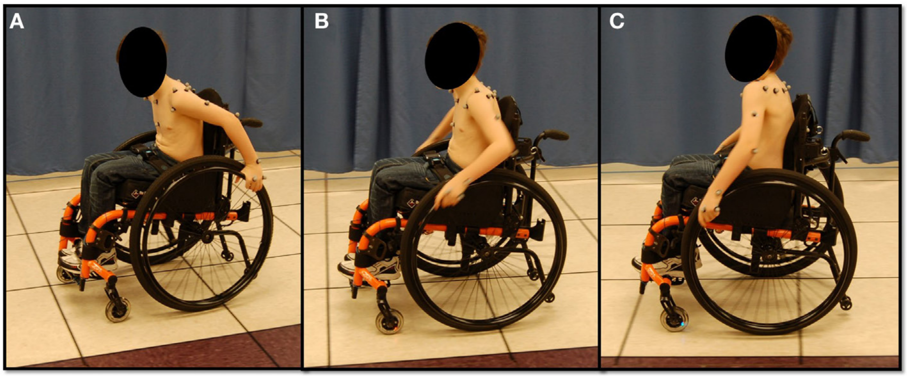

FIGURE 2 | Subject performing functional manual wheelchair mobility tasks. **(A)** Starting, **(B)** propulsion, and **(C)** stopping.

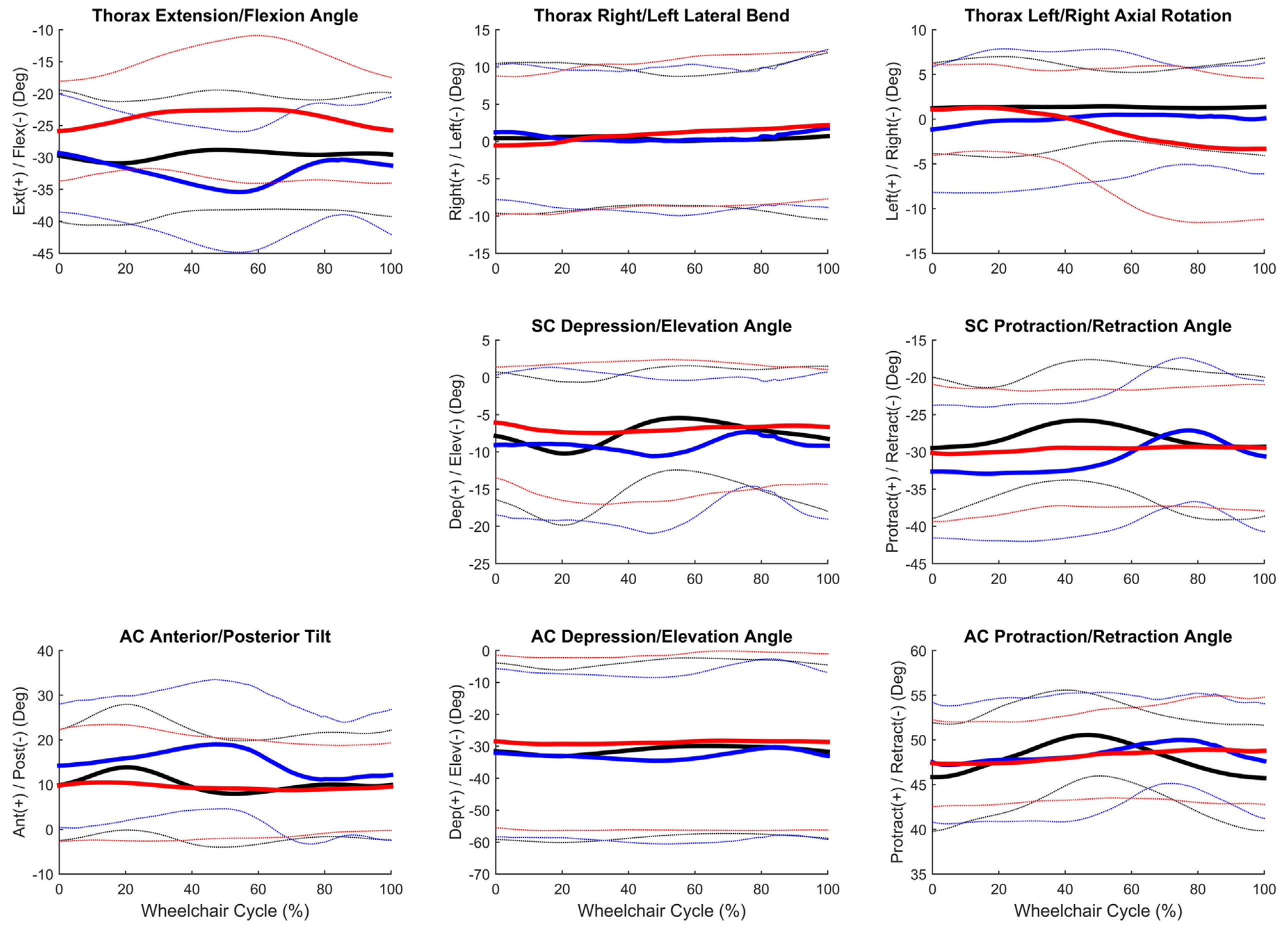

FIGURE 3 | Group mean (bold) and ±1 SD for the thorax joint angles (top row), sternoclavicular joint angles (middle row), and sternoclavicular joint angles (bottom row) during the steady-state propulsion (black), start stroke (blue), and stopping stroke (red).

(The Mathworks, Inc., Natick, MA, USA) to match the kinematic sampling rate.

For each subject, the wheelchair stroke cycles were analyzed to compute the mean group parameters of interest. Mean time series data of the joint angles, forces, and moments were all time normalized to the percent of the wheelchair stroke cycle. The stroke cycles were separated into two phases, contact and recovery phases, based on total force applied to the handrim, following

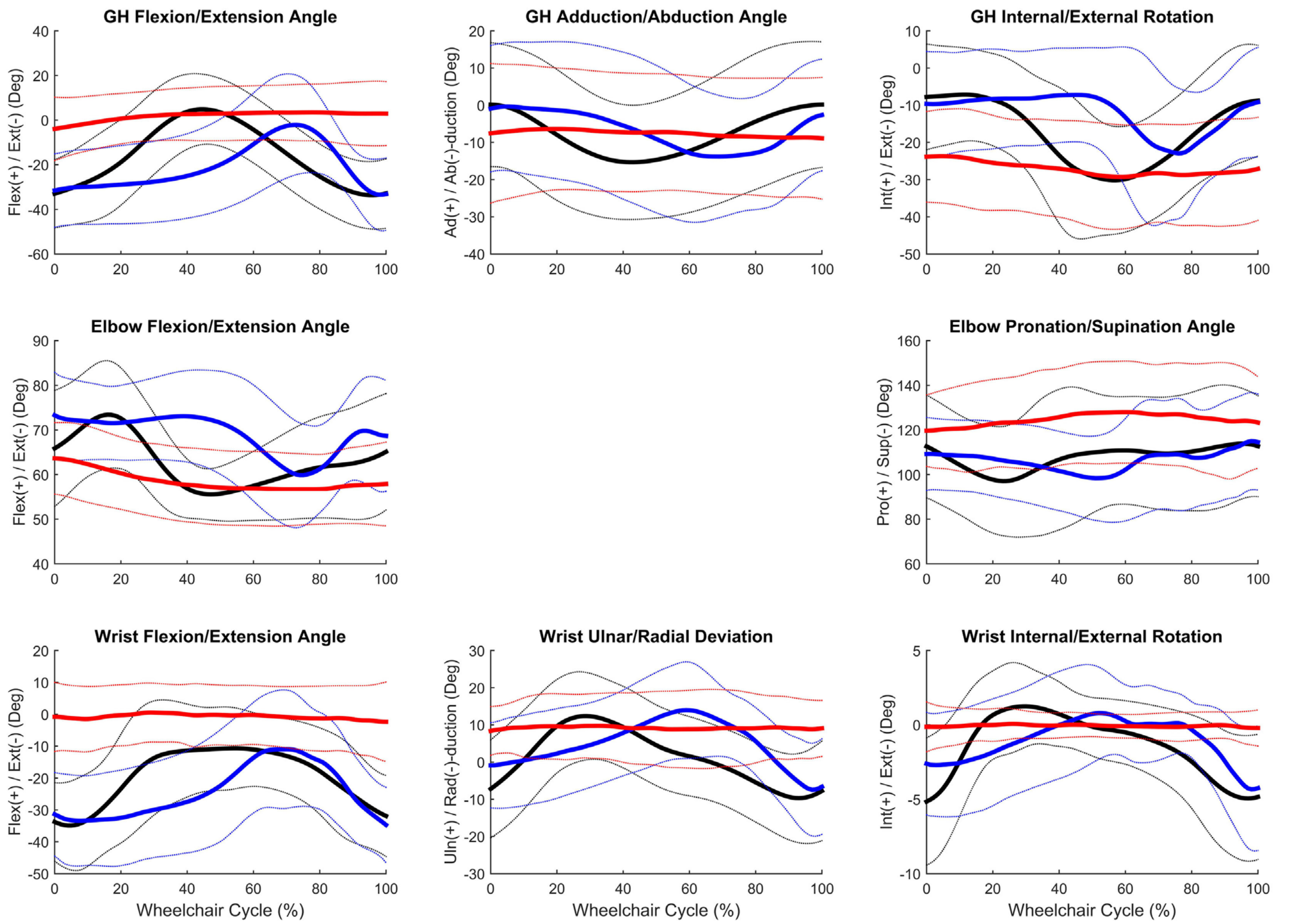

FIGURE 4 | Group mean (bold) and ±1 SD for the glenohumeral joint angles (top row), elbow joint angles (middle row), and wrist joint angles (bottom row) during the steady-state propulsion (black), start stroke (blue), and stopping stroke (red).

the definitions of Kwarciak et al. (2009). The stroke pattern was determined using the sagittal plane motion of the marker on the third metacarpal, plotting the vertical position versus fore–aft position (Shimada et al., 1998; Boninger et al., 2002, 2005). Peak joint angles (maximum and minimum) were identified and used to compute angular ranges of motion (ROMs). Maximum and minimum joint forces and moments were also identified and are referred to as peak forces and moments.

Statistical Analyses

Linear mixed models (LMM) were used for statistical comparisons amongst group joint ROMs and peak dynamics separately for each task. Random subject effect was used to control for possible within subject correlation. LMM were also used to investigate statistical significance of differences in biomechanical outcomes of the joints among the tasks.

Results

Joint Kinematics

Group mean joint angles were characterized in all three planes of motion over the wheelchair stroke cycle for the propulsion, start, and stop tasks. The mean and ±1 SD for the thorax, sternoclavicular, and acromioclavicular joints are shown in **Figure 3** and for the GH, elbow, and wrist joints in **Figure 4**. The mean peak joint angles (**Figures 5** and **6**) and mean joint ROMs (**Figure 7**) over the wheelchair stroke cycle were also calculated. Statistically significant differences ($p < 0.01$) in mean peak joint angles and mean ROMs among tasks were identified and are depicted in **Figures 5–7**.

Joint Kinetics

Group mean joint forces and moments were characterized three-dimensionally over the wheelchair stroke cycle for the propulsion, start, and stop tasks. The mean and ±1 SD joint forces and moments for the GH, elbow, and wrist joints are displayed in **Figures 8** and **9**, respectively. The mean peak joint forces (**Figure 10**) and mean peak joint moments (**Figure 11**) over the wheelchair stroke cycle were also calculated. Statistically significant differences ($p < 0.01$) in mean peak joint forces and moments among tasks were identified and are depicted in **Figures 10** and **11**.

Propulsion Stroke Patterns

The stroke patterns utilized during the propulsion task were analyzed qualitatively. While it is currently recommended for

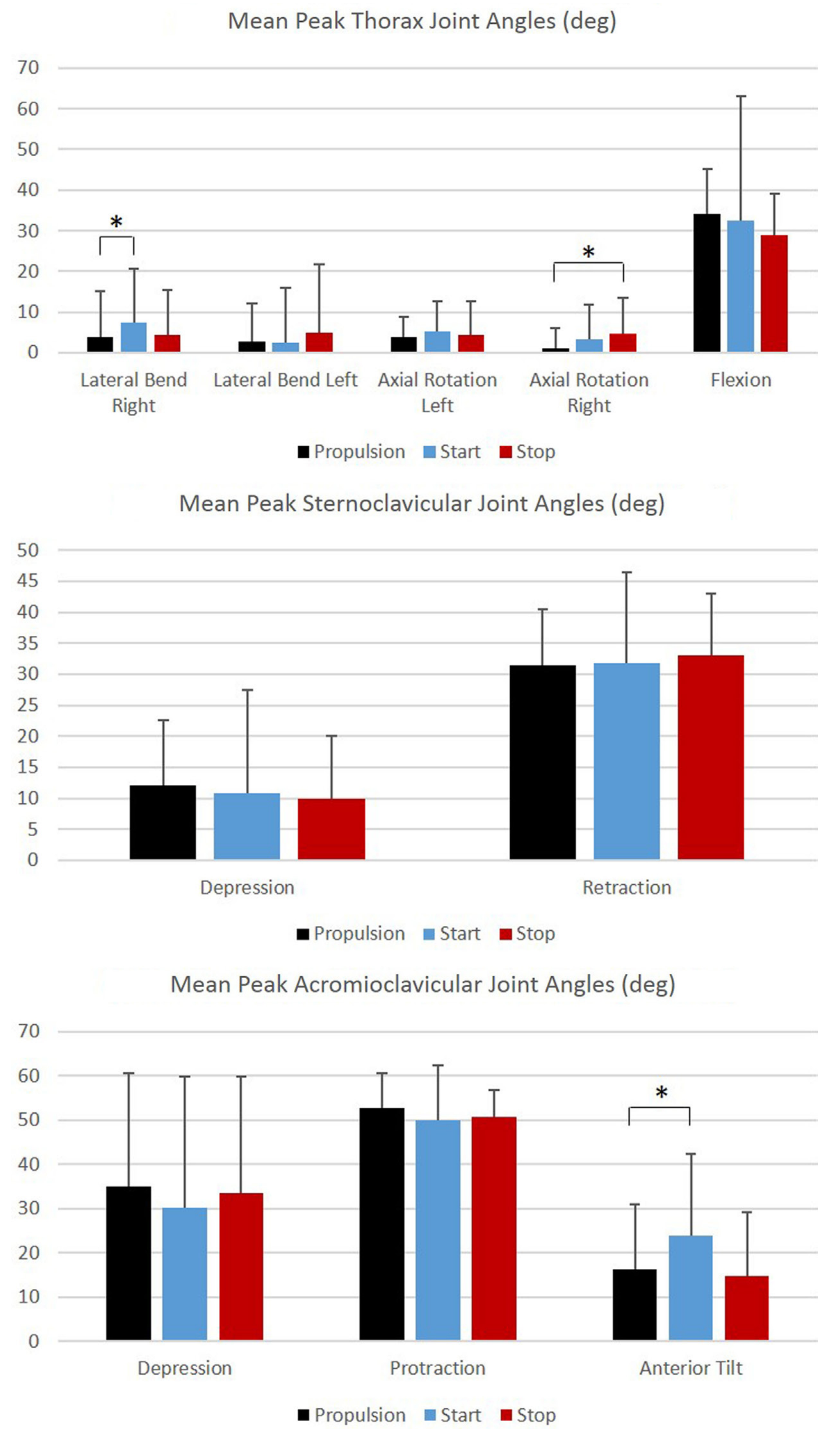

FIGURE 5 | Group mean peak joint angles (degrees) for the thorax, sternoclavicular, and acromioclavicular joints during each functional mobility task, propulsion (black), start (blue), and stop (red). One SD is represented by the thin vertical bar. Tasks connected by an asterisk are statistically significantly different ($p < 0.01$).

adult manual wheelchair users to use the semicircular stroke pattern during propulsion (Boninger et al., 2005), each of the four stroke patterns that have been identified and classified in adults (Shimada et al., 1998; Boninger et al., 2002, 2005) were used during propulsion within this pediatric population. In **Figures 12A–D**, each depict one representative stroke cycle from four different subjects, which clearly identifies with one of the four categories of adult stroke patterns. However, there were also some stroke

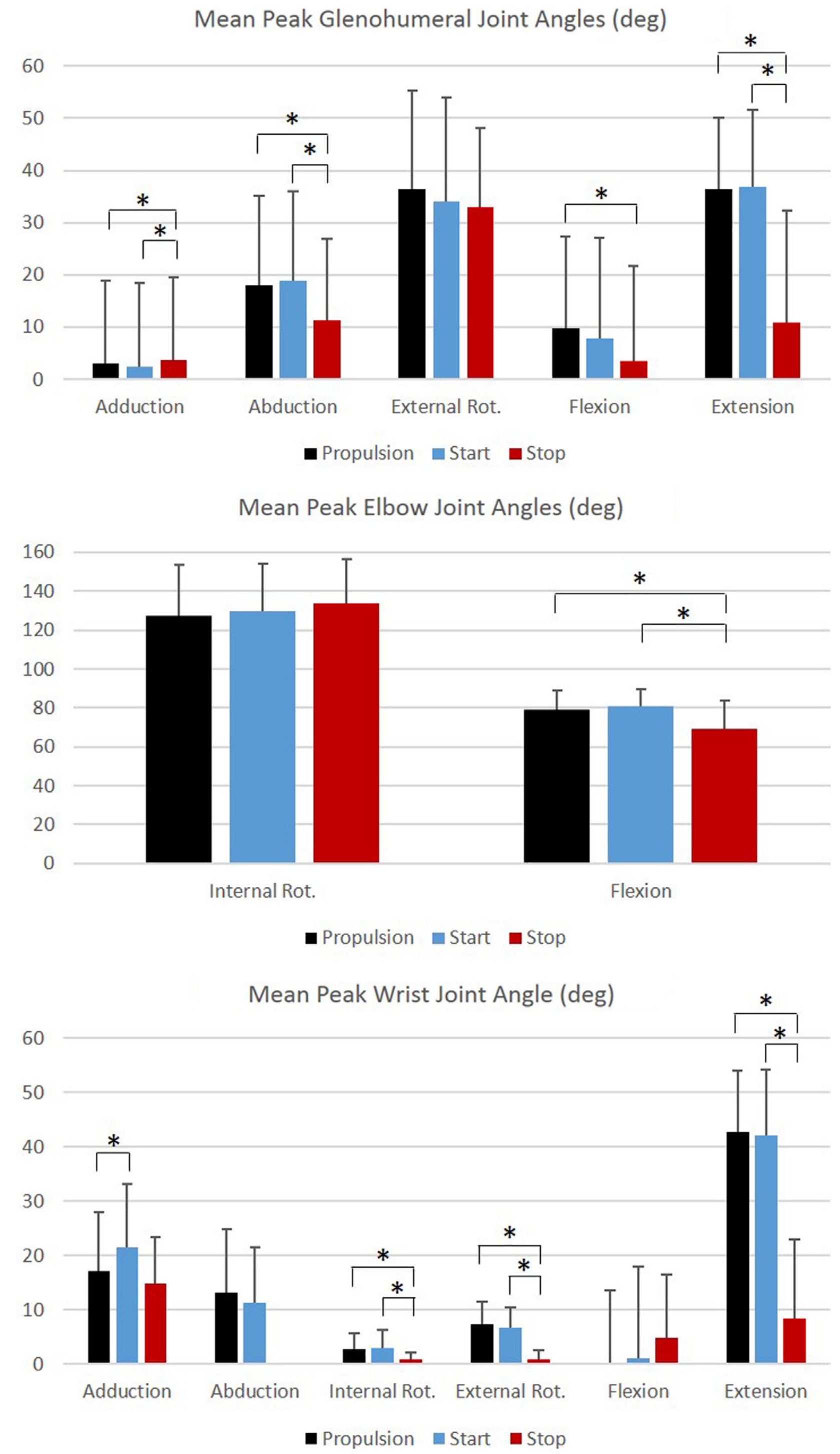

FIGURE 6 | Group mean peak joint angles (degrees) for the glenohumeral, elbow, and wrist joints during each functional mobility task, propulsion (black), start (blue), and stop (red). One SD is represented by the thin vertical bar. Tasks connected by an asterisk are statistically significantly different ($p < 0.01$).

patterns utilized by the children that do not appear to be properly represented by one of the four current adult classifications, an example is seen in **Figure 12E**. While this pattern follows the current definition of the single looping over propulsion pattern, "identified by the hands rising above the hand rim during the recovery phase" (Boninger et al., 2002), when comparing it to the typical depiction of adult single looping over propulsion pattern, **Figure 12B**, the two patterns have strikingly different features,

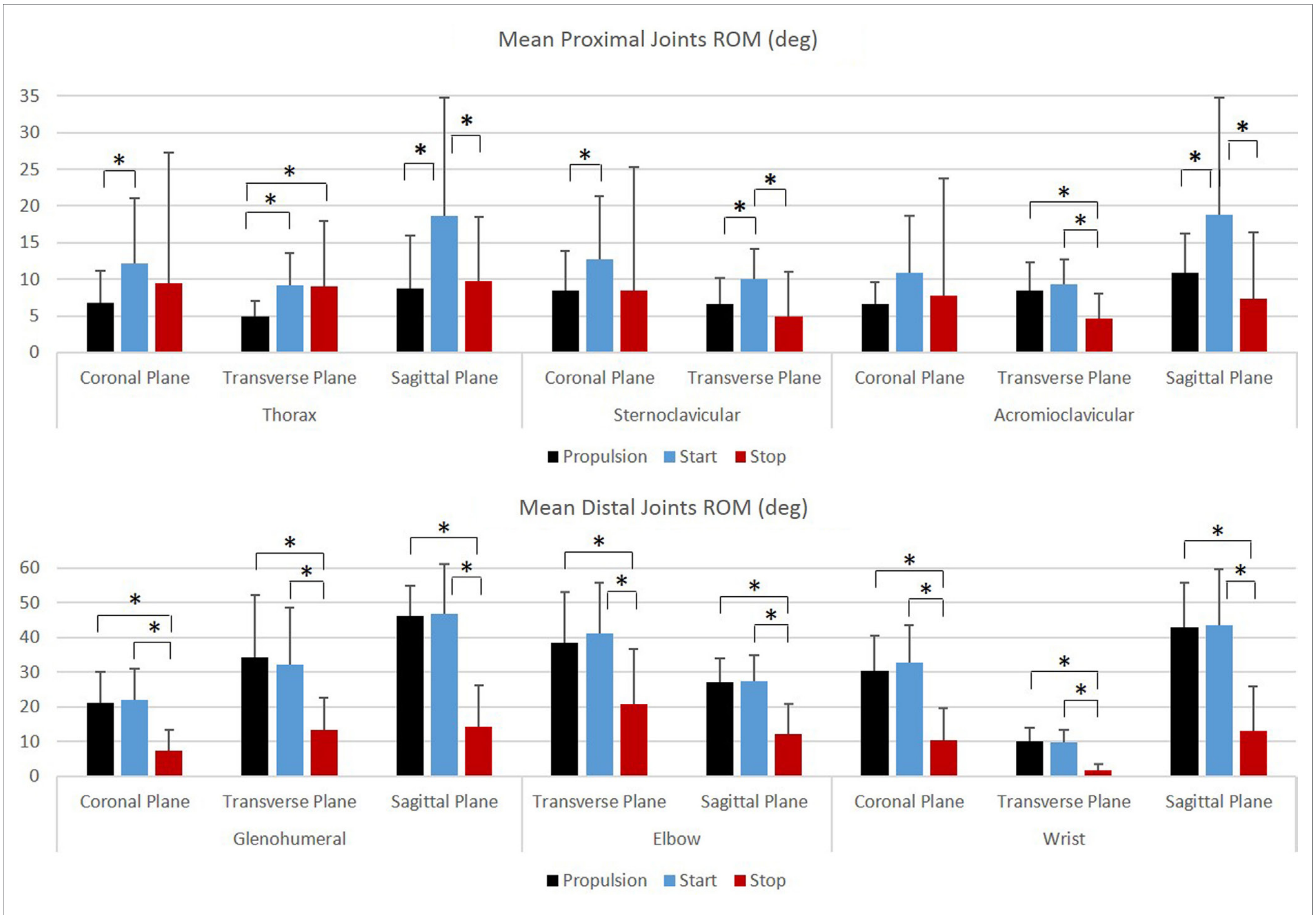

FIGURE 7 | Group mean joint ranges of motion (degrees) for the proximal joints (top row: thorax, sternoclavicular, and acromioclavicular) and the distal joints (bottom row: glenohumeral, elbow, and wrist) during each functional mobility task, propulsion (black), start (blue), and stop (red). One SD is represented by the thin vertical bar. Tasks connected by an asterisk are statistically significantly different ($p < 0.01$).

particularly in the later stages of the recovery phase prior to hand contact. Of additional interest is that multiple subjects used more than one stroke pattern throughout the propulsion task trials. Some subjects used different patterns between trials, and some used two or more stroke patterns within the same trial. Therefore, a primary stroke pattern was not evident.

Pain and Health-Related Quality of Life

One individual reported pain, which was minimal (15 on a scale of 0–100). Mean physical component summary scores (PCS) and mental health component summary scores (MCS) acquired with the SF-12 were 44.3 (6.4) and 56.3 (8.2), respectively (normal = 50), indicating lower than normal physical health and higher than normal mental health in this population.

Discussion

This work provides a unique characterization of joint dynamics and clinical outcomes during pediatric manual wheelchair propulsion, start, and stop tasks. This work is the first of its kind to quantify upper extremity wheeled biomechanics during functional tasks in children. Our group led efforts to investigate pediatric wheelchair propulsion (Schnorenberg et al., 2014; Slavens et al., 2015); however, functional tasks should also be considered. Sonenblum et al. (2012) found that manual wheelchair users were wheeling for only about 10% of the time they spent seated in their wheelchairs per day. Additionally, Cooper et al. (2008) determined that children completed 167 start/stop tasks/1000 m traveled in a day, with an average daily distance of 1600 m, thus, children are completing over 250 start and stop tasks a day, on average. Due to these findings, functional tasks, such as starting and stopping, are presented here. These tasks may be more challenging than propulsion and it is important to understand the joint demands during these functional tasks for improved rehabilitation and treatment planning. Our work is the first to use quantitative methods for determining pediatric joint kinematics and kinetics during functional manual wheelchair mobility, pain, and function. The results of our findings have implications for a comprehensive approach to evaluating pediatric wheelchair mobility.

Overall, the GH joint displayed the largest ROM of 47° (flexion–extension) during the start task and the largest force of 10.6% body

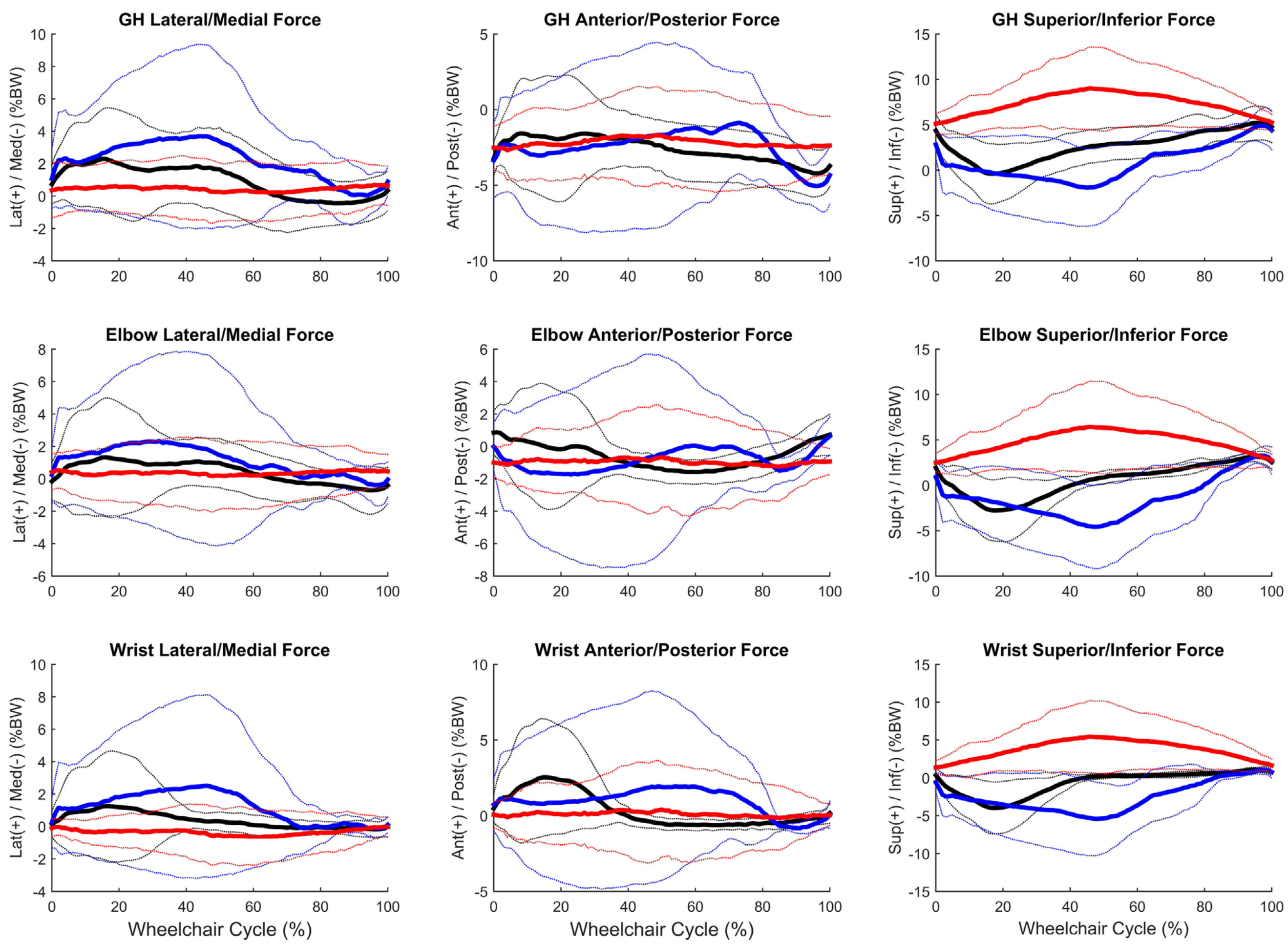

FIGURE 8 | Group mean (bold) and ±1 SD for the glenohumeral joint forces (top row), elbow joint forces (middle row), and wrist joint forces (bottom row) during the steady-state propulsion (black), start stroke (blue), and stopping stroke (red). All forces are normalized to percentage of body weight (% BW).

weight in the superior direction during the stop task. The elbow displayed the largest peak moment of 1.8% body weight × height in flexion during the start task. Propulsion, starting, and stopping tasks proved to be very different biomechanically, which suggests that clinicians should consider all three tasks when developing rehabilitation protocols and strategies for improving long-term health. GH, elbow, and wrist joint ROMs, were significantly smaller in all three planes, between the propulsion and stopping tasks, and between the starting and stopping tasks. Thus, propelling and starting a wheelchair utilize similar motion demands and magnitudes of the GH, elbow, and wrist joints, while stopping a wheelchair is significantly different. When analyzing the thorax, sternoclavicular, and acromioclavicular joints, there were significant joint ROM differences among all tasks. The start task had the largest ROM amongst the three tasks for all three joints in all planes of motion; however, was only significantly larger in the sagittal plane of the thorax and acromioclavicular joints, and the transverse plane of the sternoclavicular joint. Additionally, the start task ROM was significantly greater than the propulsion ROM in the coronal and transverse planes of the thorax and the coronal plane of the sternoclavicular joint. This shows that while the distal upper extremity joints (GH, elbow, and wrist) are similar between propulsion and start, the body must employ more of the proximal upper extremities (thorax, sternoclavicular, and acromioclavicular) when starting the manual wheelchair. Overall, the start task demands the largest ROM, which is expected due to the nature of beginning movement of the wheel and overcoming inertia. Once the wheel is in motion, as during propulsion, less ROM is needed to keep the wheelchair moving. ROM during starting and stopping is significantly different between tasks in the sagittal plane of all joints, which is also the plane in which the greatest amount of movement occurs during manual wheelchair use.

Peak joint forces and moments provide insight to joint demands and potential risk for injury and overuse. We have successfully quantified upper extremity joint forces and moments during wheelchair propulsion, starting, and stopping. These dynamic tasks were found to be significantly different from one another for GH, elbow, and wrist joint kinetics. All tasks were significantly

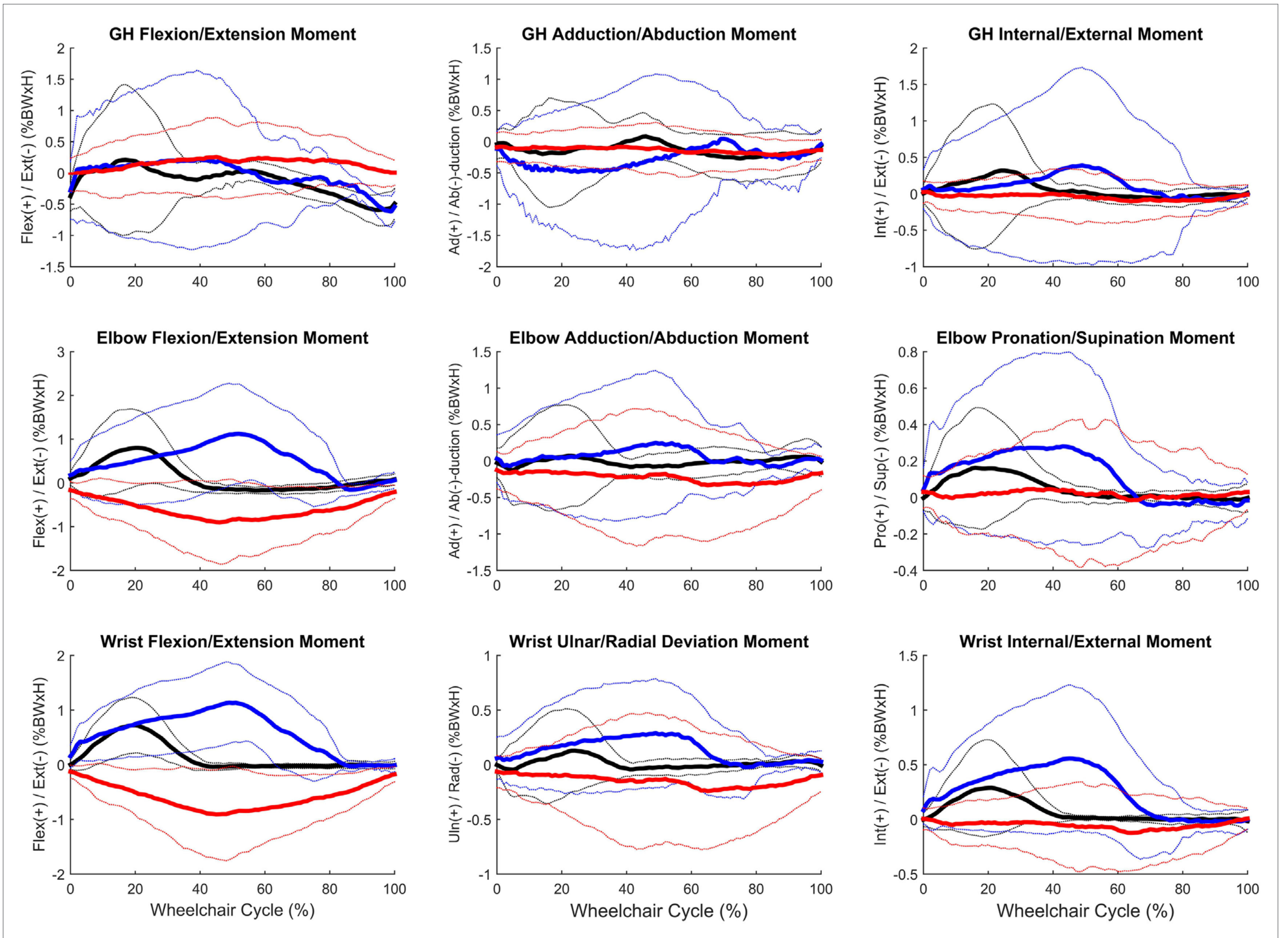

FIGURE 9 | Group mean (bold) and ±1 SD for the glenohumeral joint moments (top row), elbow joint moments (middle row), and wrist joint moments (bottom row) during the steady-state propulsion (black), start stroke (blue), and stopping stroke (red). All moments are normalized to percentage of body weight multiplied by height (% BW × H).

different from one another for the posterior and lateral GH joint forces and the lateral wrist joint force. Propulsion and starting proved to be significantly different from stopping for all GH joint forces, with only the superiorly directed force greatest during the stop task. The start task demanded the largest amount of force at the GH, elbow, and wrist joints in all planes and directions, with the exception of superior force. While the stop task generally had the lowest joint forces, it had the statistically highest superior joint force across all tasks for all three joints. Additionally, the stop task had the largest overall mean peak force, at 10.6% BW superiorly directed, as well as high superiorly directed joint forces for the elbow (7.9% BW) and the wrist (7.1% BW) joints. We can deduce that subjects placed their hands anteriorly and low on the wheelchair handrim when applying braking grasps, resulting in a pulling of the arm and the resulting high superior joint forces. As quantified here, large amounts of tension are placed on the GH, elbow, and wrist joint during stopping and large amounts of compression force act on the joints during starting. Clinically interesting, propulsion often demonstrates smaller joint force demands than starting or stopping tasks. Despite this, most research has been focused on propulsion. This reiterates the importance of understanding functional wheelchair mobility tasks and their impact on joint force demands. When designing rehabilitation protocols, all functional tasks should be taken into consideration. Propulsion alone should not be the only mobility task considered for wheelchair users when assessing and planning rehabilitation. Particular concern arises with functional tasks since larger joint forces and moments occur during these tasks as compared to propulsion. Further research is warranted to determine the effect of functional tasks on muscle and soft tissue of the shoulder, elbow, and wrist.

Largest joint moments occurred during flexion of the GH, elbow, and wrist joints. When examining the joint moments, they were the highest during the start task. This also supports the notion that the start task may be the most demanding of the tasks. Significant differences among all tasks were seen during GH abduction, elbow, and wrist flexion, and wrist internal rotation moments. Extension moments were significantly different in all joints between propulsion

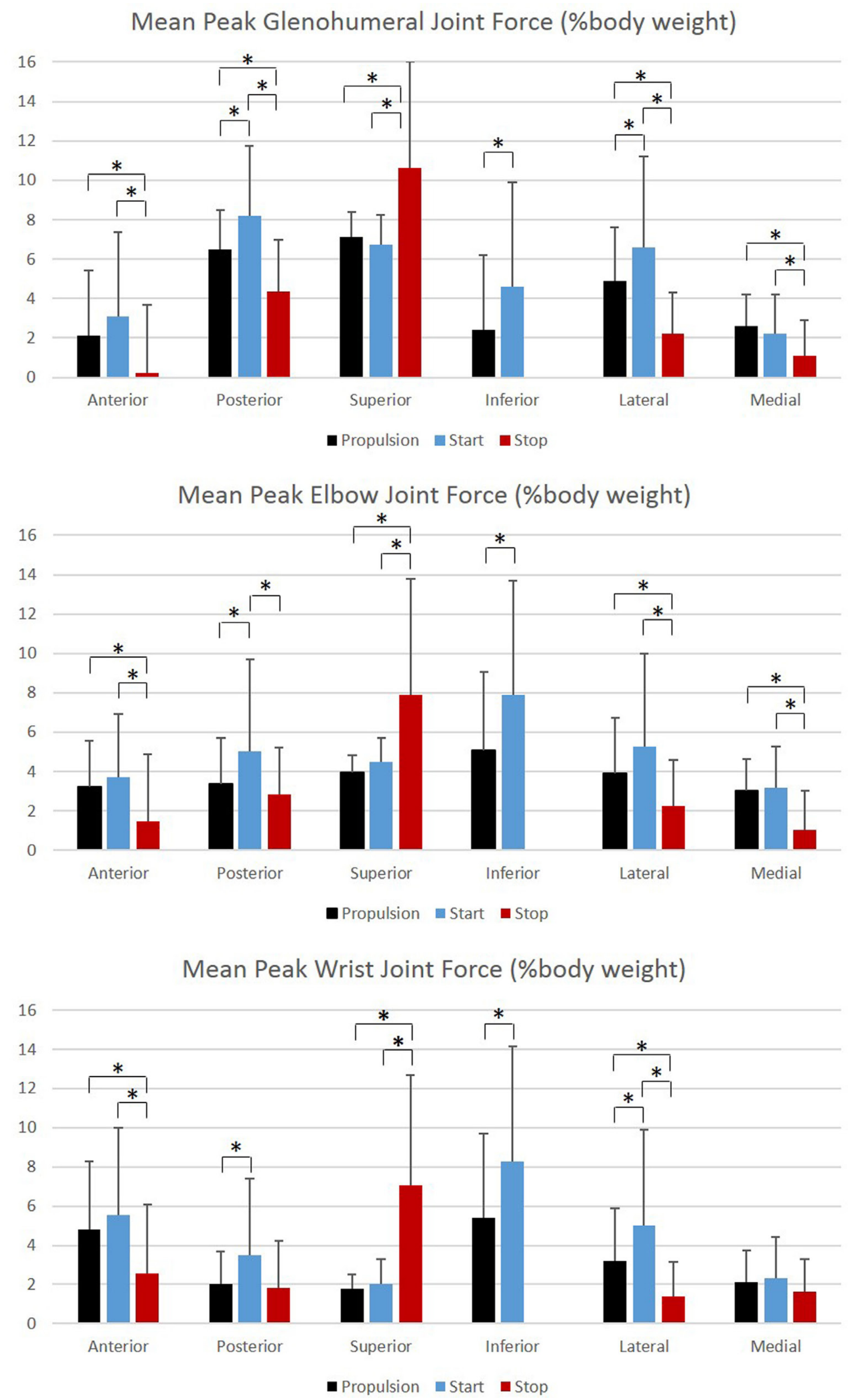

FIGURE 10 | Group mean peak joint forces (% BW) for the glenohumeral, elbow, and wrist joints during each functional mobility task, propulsion (black), start (blue), and stop (red). One SD is represented by the thin vertical bar. Tasks connected by an asterisk are statistically significantly different ($p < 0.01$).

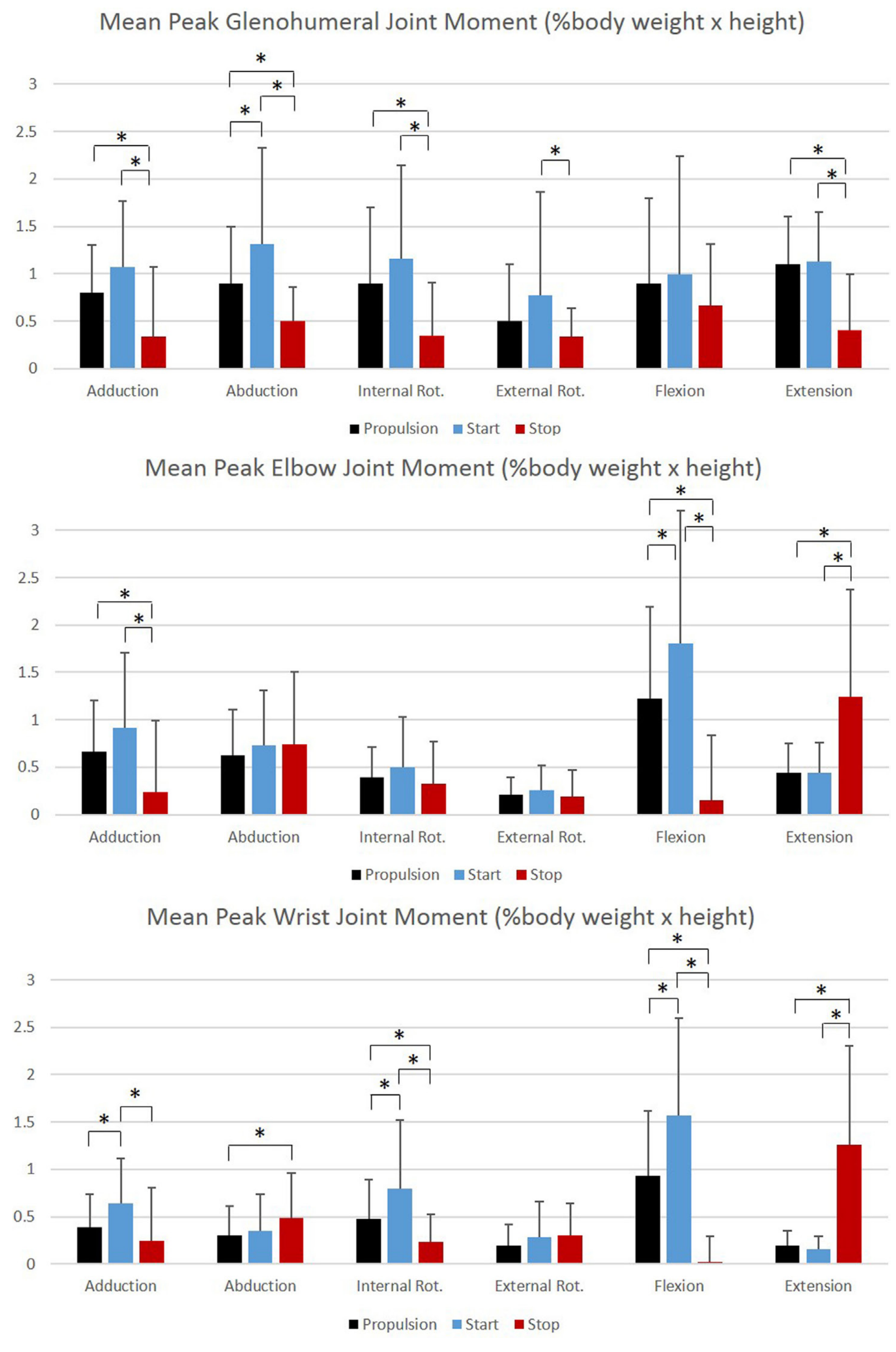

FIGURE 11 | Group mean peak joint moments (% BW × H) for the glenohumeral, elbow, and wrist joints during each functional mobility task, propulsion (black), start (blue), and stop (red). One SD is represented by the thin vertical bar. Tasks connected by an asterisk are statistically significantly different ($p < 0.01$).

and stopping and starting and stopping. Large variability should be noted, particularly during flexion and at the GH joint.

We successfully identified multiple stroke patterns in this pediatric group of wheelchair users with SCI. In addition to the standard four patterns displayed by adults (i.e., semicircular, ARC, single looping over propulsion, and double looping over propulsion), we also identified a pattern which may require its own classification. Additionally, within subject variability was observed,

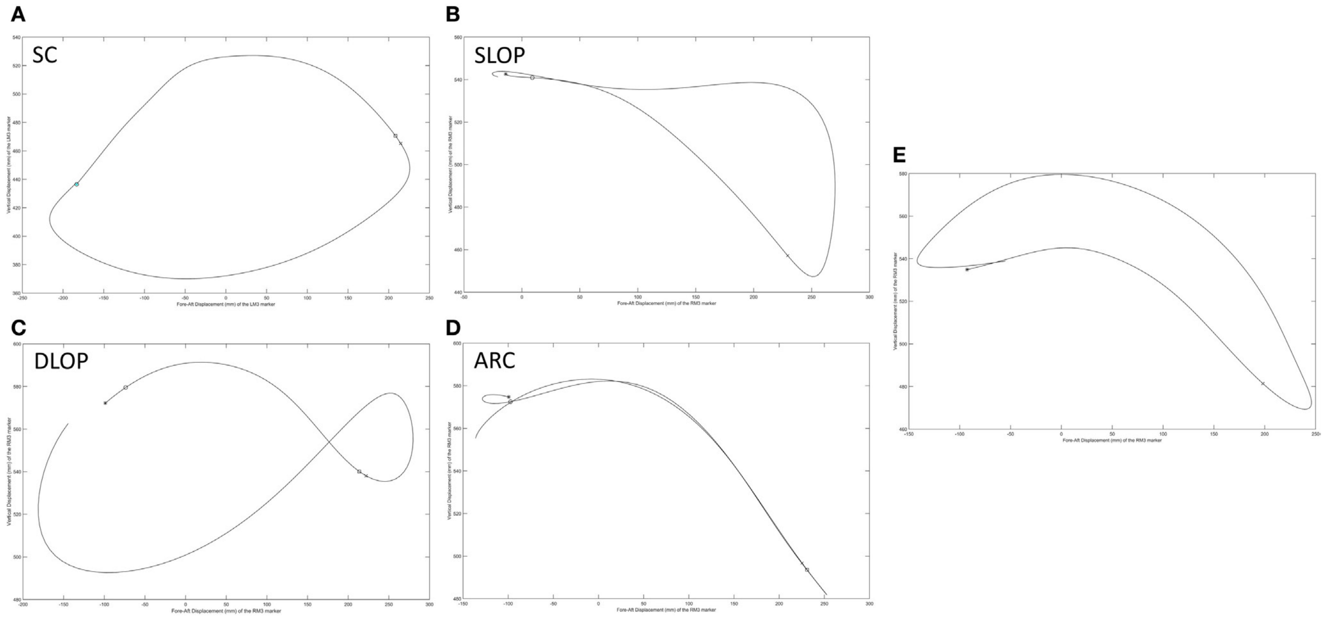

FIGURE 12 | Representative stroke patterns observed by individuals during the propulsion task. **(A–D)** Correspond to the four patterns previously identified and classified in adult users: **(A)** semicircular (SC), **(B)** single looping over propulsion (SLOP), **(C)** double looping over propulsion (DLOP), and **(D)** arcing (ARC). **(E)** Does not appear to readily fall into one of these categories.

with some subjects altering their propulsion pattern between and within propulsion trials. Pediatric stroke patterns and the demonstrated variability in movement should be further investigated to determine the most appropriate patterns for particular ages of users, tasks, environments, and levels of injury. Furthermore, additional research is warranted to determine if pediatric subjects should be trained differently than adults. Given these initial findings, it may be beneficial for pediatric subjects to use different stroke patterns than adults as well as a variety of stroke patterns to decrease pain and risk of injury over the lifespan.

The VAS was applied in the study since it serves as the standard outcome tool for clinical pain assessment at Shriners Hospital for Children – Chicago. One subject reported pain, which was minimal. This alludes to the idea that pain has either not yet developed in this group of participants or that the high variability in joint dynamics, as quantified here, is serving as protection to the joints. If so, these movement patterns and variability should be investigated to determine if they could be utilized long term into adulthood to minimize the risk of future pain and injury. Correlation of pain with biomechanical metrics and clinical history (e.g., time since injury and level of injury) is suggested. Further research is underway with a larger population to address these questions. The results of this work also support investigating additional pediatric pain assessment tools that may be more sensitive to upper extremity joint pain or pain during manual wheelchair mobility.

Mean physical health scores (PCS) and mental health scores (MCS) acquired with the SF-12 were 44.3 and 56.3, respectively (normal = 50), indicating lower than normal physical health and higher than normal mental health in this population. Additional outcomes measures are suggested for future assessment of health-related quality of life and correlation with biomechanical and clinical history data.

Although much work has been done for adult wheelchair mobility, there has been limited research on pediatric wheeled mobility, much less on functional tasks. Morrow et al. (2010) investigated intersegmental GH joint demands during functional tasks in adult manual wheelchair users with SCI and noted only GH joint external rotation and extension moments to be greater during starting than propulsion and found no differences among the tasks for GH joint forces. The results, we have found, suggest differences occur between children and adults, which may be attributed to musculoskeletal development and maturation. We believe children should be investigated separately and more comprehensively than adults with additional consideration for musculoskeletal developmental changes, environmental influences, wheelchair size, and strength (Boninger, 2002). We have found that the variability of manual wheelchair propulsion patterns in the pediatric population is quite significant, which may be advantageous in reducing cumulative upper extremity joint demands and pain. Research is in progress, exploring differences in the biomechanics of task performance between children and adults.

Future Directions

This work was the first of its kind to investigate the biomechanics of wheeled mobility tasks in a pediatric population. A larger population is warranted to fully understand the correlation among biomechanics, upper extremity joint pain, function, and health-related quality of life. Work is currently underway to elucidate the relationships amongst these areas with a larger population of pediatric manual wheelchair users. This knowledge will ultimately lead to improved clinical decision-making and rehabilitation paradigms.

Furthermore, evaluation of pediatric wheelchair mobility is essential to determine biomechanical, functional, and joint integrity differences between children and adults. Our work demonstrates that children perform highly variable movement patterns during propulsion, start, and stop tasks, some patterns of which are unlike those classified in adults. A comparison of pediatric and adult biomechanical variability may prove to be essential for improving the health and quality of life of manual wheelchair users. The large variability of joint dynamics (motions, forces, and moments) characterized in this study may relate to age, level of injury, or lack of pain presented by this pediatric population. Additionally, we believe that using a variety of stroke patterns may serve as overuse protection for the shoulder. Additional research directions include determining the rotator cuff muscle activations and forces, which will attempt to clarify the underlying musculoskeletal and tissue effects from pediatric wheeled mobility. Further research is underway to address these questions in a larger population of pediatric manual wheelchair users. The insight gained from this research has the potential to impact pediatric manual wheelchair training, usage, and rehabilitation guidelines.

Conclusion

Biomechanics of functional manual wheelchair mobility were quantified in children with SCI. Overall, propulsion, starting, and stopping tasks during manual wheelchair use were significantly different biomechanically. Starting a wheelchair appears to be the most demanding task on the upper extremity, while stopping appears to be the least demanding task. However, due to the unique biomechanical demands of each task and patient, clinicians should consider all functional tasks when planning rehabilitation treatment and longer-term mobility strategies. This work also infers that pediatric manual wheelchair users with SCI are different from adult manual wheelchair users and require rehabilitation tailored to their specific needs.

Acknowledgments

The authors would like to greatly thank Adam Graf, Joeseph J. Krzak, Kathryn Reiners, and Lianna Hawi for their contributions to this work. The contents of this article were developed under a grant from the Health and Human Services Administration for Community Living, Award number 90RE5006-01-00. However, these contents do not necessarily represent the policy of the Health and Human Services Administration for Community Living, and you should not assume endorsement by the Federal Government. Research reported in this publication was also supported by the Eunice Kennedy Shriver National Institute of Child Health and Human Development of the National Institutes of Health under Award Number K12HD073945.

References

Ballinger, D., Rintala, D., and Hart, K. (2000). The relation of shoulder pain and range-of-motion problems to functional limitations, disability, and perceived health of men with spinal cord injury: a multifaceted longitudinal study. *Arch. Phys. Med. Rehabil.* 81, 1575–1581. doi:10.1053/apmr.2000.18216

Boninger, M., Koontz, A., Sisto, S., Dyson-Hudson, T., Chang, M., Price, R., et al. (2005). Pushrim biomechanics and injury prevention in spinal cord injury: recommendations based on CULP-SCI investigations. *J. Rehabil. Res. Dev.* 42(3 Suppl. 1), 9–19. doi:10.1682/JRRD.2004.08.0103

Boninger, M., Souza, A., Cooper, R., Fitzgerald, S., Koontz, A., and Fay, B. (2002). Propulsion patterns and pushrim biomechanics in manual wheelchair propulsion. *Arch. Phys. Med. Rehabil.* 83, 718–723. doi:10.1053/apmr.2002.32455

Boninger, M., Towers, J., Cooper, R., Dicianno, B., and Munin, M. (2001). Shoulder imaging abnormalities in individuals with paraplegia. *J. Rehabil. Res. Dev.* 38, 401–408.

Brault, M. W., and U.S. Census Bureau. (2012). *Americans with Disabilities: 2010*. Washington, DC: U.S. Dept. of Commerce, Economics and Statistics Administration, U.S. Census Bureau.

Campbell, A. C., Lloyd, D. G., Alderson, J. A., and Elliott, B. C. (2009). MRI development and validation of two new predictive methods of glenohumeral joint centre location identification and comparison with established techniques. *J. Biomech.* 42, 1527–1532. doi:10.1016/j.jbiomech.2009.03.039

Case-Smith, J., and O'Brien, J. C. (2013). *Occupational Therapy for Children*. Maryland Heights, MO: Elsevier Health Sciences.

Cooper, R. A., Tolerico, M., Kaminski, B. A., Spaeth, D., Ding, D., and Cooper, R. (2008). Quantifying wheelchair activity of children: a pilot study. *Am. J. Phys. Med. Rehabil.* 87, 977–983. doi:10.1097/PHM.0b013e31818dfe74

Hingtgen, B. A., McGuire, J. R., Wang, M., and Harris, G. F. (2006). A upper extremity kinematic model for evaluation of hemiparetic stroke. 39, 681–688. doi:10.1016/j.jbiomech.2005.01.008

Hwang, M., Zebracki, K., Chlan, K. M., and Vogel, L. C. (2014). Longitudinal changes in medical complications in adults with pediatric-onset spinal cord injury. *J. Spinal Cord Med.* 37, 171–178. doi:10.1179/2045772313Y.0000000150

Jensen, R. K. (1989). Changes in segment inertia proportions between 4 and 20 years. *J. Biomech.* 22, 529–536. doi:10.1016/0021-9290(89)90301-1

Kaye, H., Kang, T., and LaPlante, M. (2000). *Mobility Device Use in the United States, in Disability Statistics Report*. Washington, DC: U.S.D.O. Education. National Institute on Disability and Rehabilitation Research.

Koontz, A. M., Cooper, R. A., Boninger, M. L., Yang, Y., Impink, B. G., and van der Woude, L. H. (2005). A kinetic analysis of manual wheelchair propulsion during start-up on select indoor and outdoor surfaces. *J. Rehabil. Res. Dev.* 42, 447–458. doi:10.1682/JRRD.2004.08.0106

Kwarciak, A. M., Sisto, S. A., Yarossi, M., Price, R., Komaroff, E., and Boninger, M. L. (2009). Redefining the manual wheelchair stroke cycle: identification and impact of nonpropulsive pushrim contact. *Arch. Phys. Med. Rehabil.* 90, 20–26. doi:10.1016/j.apmr.2008.07.013

Lal, S. (1998). Premature degenerative shoulder changes in spinal cord injury patients. *Spinal Cord* 36, 186–189. doi:10.1038/sj.sc.3100608

Mercer, J., Boninger, M., Koontz, A., Ren, D., Dyson-Hudson, T., and Cooper, R. (2006). Shoulder joint kinetics and pathology in manual wheelchair users. *Clin. Biomech. (Bristol, Avon)* 21, 781–789. doi:10.1016/j.clinbiomech.2006.04.010

Morrow, M. M., Hurd, W. J., Kaufman, K. R., and An, K. N. (2010). Shoulder demands in manual wheelchair users across a spectrum of activities. *J. Electromyogr. Kinesiol.* 20, 61–67. doi:10.1016/j.jelekin.2009.02.001

Nguyen, T. C., and Baker, R. (2004). Two methods of calculating thorax kinematics in children with myelomeningocele. *Clin. Biomech. (Bristol, Avon)* 19, 1060–1065. doi:10.1016/j.clinbiomech.2004.07.004

Office of Public Health Assessment. (2004). *Health Status in Utah: The Medical Outcomes Study SF-12 (2001 Utah Health Status Survey Report)*. Salt Lake City, UT: Utah Department of Health.

Pentland, W., and Twomey, L. (1991). The weight-bearing upper extremity in women with long term paraplegia. *Paraplegia* 29, 521–530. doi:10.1038/sc.1991.75

Petuskey, K., Bagley, A., Abdala, E., James, M. A., and Rab, G. (2007). Upper extremity kinematics during functional activities: three-dimensional studies in a normal pediatric population. *Gait Posture* 25, 573–579. doi:10.1016/j.gaitpost.2006.06.006

Rice, I., Impink, B., Niyonkuru, C., and Boninger, M. (2009). Manual wheelchair stroke characteristics during an extended period of propulsion. *Spinal Cord* 47, 413–417. doi:10.1038/sc.2008.139

Riddick-Grisham, S., and Deming, L. (2011). *Pediatric Life Care Planning and Case Management*, 2nd Edn. Boca Raton, FL: Taylor & Francis.

Schnorenberg, A. J., Slavens, B. A., Wang, M., Vogel, L. C., Smith, P. A., and Harris, G. F. (2014). Biomechanical model for evaluation of pediatric upper extremity joint dynamics during wheelchair mobility. *J. Biomech.* 47, 269–276. doi:10.1016/j.jbiomech.2013.11.014

Senk, M., and Cheze, L. (2010). A new method for motion capture of the scapula using an optoelectronic tracking device: a feasibility study. *Comput. Methods Biomech. Biomed. Eng.* 13, 397–401. doi:10.1080/10255840903263945

Shimada, S. D., Robertson, R. N., Bonninger, M. L., and Cooper, R. A. (1998). Kinematic characterization of wheelchair propulsion. *J. Rehabil. Res. Dev.* 35, 210–218.

Sie, I. H., Waters, R. L., Adkins, R. H., and Gellman, H. (1992). Upper extremity pain in the postrehabilitation spinal cord injured patient. *Arch. Phys. Med. Rehabil.* 73, 44–48.

Slavens, B. A., Schnorenberg, A. J., Aurit, C. M., Graf, A., Krzak, J. J., Reiners, K., et al. (2015). Evaluation of pediatric manual wheelchair mobility using advanced biomechanical methods. *Biomed Res. Int.* 2015, 634768. doi:10.1155/2015/634768

Sonenblum, S. E., Sprigle, S., and Lopez, R. A. (2012). Manual wheelchair use: bouts of mobility in everyday life. *Rehabil. Res. Pract.* 2012, 753165. doi:10.1155/2012/753165

Vitale, M. G., Goss, J. M., Matsumoto, H., and Roye, D. P. J. (2006). Epidemiology of pediatric spinal cord injury in the United States: years 1997 and 2000. *J. Pediatr. Orthop.* 26, 745–749. doi:10.1097/01.bpo.0000235400.49536.83

Vogel, L., Chlan, K., Zebracki, K., and Anderson, C. (2011). Long-term outcomes of adults with pediatric-onset spinal cord injuries as a function of neurological impairment. *J. Spinal Cord Med.* 34, 60–66. doi:10.1179/107902610X12883422813787

Vogel, L. C., Hickey, K. J., Klaas, S. J., and Anderson, C. J. (2004). Unique issues in pediatric spinal cord injury. *Orthop. Nurs.* 23, 300–308. doi:10.1097/00006416-200409000-00004

Wewers, M. E., and Lowe, N. K. (1990). A critical review of visual analogue scales in the measurement of clinical phenomena. *Res. Nurs. Health* 13, 227–236. doi:10.1002/nur.4770130405

Woltring, H. J. (1986). A Fortran package for generalized, cross-validatory spline smoothing and differentiation. *Adv. Eng. Softw.* 8, 104–113. doi:10.1016/0141-1195(86)90098-7

Wu, G., van der Helm, F. C., Veeger, H. E., Makhsous, M., Van Roy, P., Anglin, C., et al. (2005). ISB recommendation on definitions of joint coordinate systems of various joints for the reporting of human joint motion – part II: shoulder, elbow, wrist and hand. *J. Biomech.* 38, 981–992. doi:10.1016/j.jbiomech.2004.03.033

Yang, J., Boninger, M., Leath, J., Fitzgerald, S., Dyson-Hudson, T., and Chang, M. (2009). Carpal tunnel syndrome in manual wheelchair users with spinal cord injury: a cross-sectional multicenter study. *Am. J. Phys. Med. Rehabil.* 88, 1007–1016. doi:10.1097/PHM.0b013e3181bbddc9

Conflict of Interest Statement: The authors declare that the research was conducted in the absence of any commercial or financial relationships that could be construed as a potential conflict of interest.

frontiers in Bioengineering and Biotechnology

ORIGINAL RESEARCH
published: 18 May 2015
doi: 10.3389/fbioe.2015.00068

Influence of handrim wheelchair propulsion training in adolescent wheelchair users, a pilot study

Jennifer L. Dysterheft, Ian M. Rice and Laura A. Rice*

Wheelchair Biomechanics Performance Laboratory, Department of Kinesiology and Community Health, University of Illinois Urbana-Champaign, Urbana, IL, USA

Ten full-time adolescent wheelchair users (ages 13–18) completed a total of three propulsion trials on carpet and tile surfaces, at a self-selected velocity, and on a concrete surface, at a controlled velocity. All trials were performed in their personal wheelchair with force and moment sensing wheels attached bilaterally. The first two trials on each surface were used as pre-intervention control trials. The third trial was performed after receiving training on proper propulsion technique. Peak resultant force, contact angle, stroke frequency, and velocity were recorded during all trials for primary analysis. Carpet and tile trials resulted in significant increases in contact angle and peak total force with decreased stroke frequency after training. During the velocity controlled trials on concrete, significant increases in contact angle occurred, as well as decreases in stroke frequency after training. Overall, the use of a training video and verbal feedback may help to improve short-term propulsion technique in adolescent wheelchair users and decrease the risk of developing upper limb pain and injury.

Keywords: manual wheelchair, propulsion, biomechanics, training, adolescents

OPEN ACCESS

Edited by:
Philip Santos Requejo, Rancho Los Amigos National Rehabilitation Center, USA

Reviewed by:
Marcos Duarte, Federal University of ABC, Brazil
Henrique De Amorim Almeida, Polytechnic Institute of Leiria, Portugal

****Correspondence:***
Ian M. Rice, Wheelchair Biomechanics Performance Laboratory, Department of Kinesiology and Community Health, University of Illinois Urbana-Champaign, 906 South Goodwin Avenue, Urbana, IL 61802, USA
ianrice@illinois.edu

Specialty section:
This article was submitted to Biomechanics, a section of the journal Frontiers in Bioengineering and Biotechnology

Received: *16 March 2015*
Accepted: *30 April 2015*
Published: *18 May 2015*

Citation:
Dysterheft JL, Rice IM and Rice LA (2015) Influence of handrim wheelchair propulsion training in adolescent wheelchair users, a pilot study. Front. Bioeng. Biotechnol. 3:68. doi: 10.3389/fbioe.2015.00068

Introduction

Manual wheelchair propulsion (MWP) for daily mobility places significant demands on the upper limbs. While performing everyday tasks, such as propulsion and transferring, manual wheelchair users (MWUs) repetitively experience large loads through the shoulders and wrists (Bayley et al., 1987; Nash et al., 2001). As a consequence, MWUs experience disproportionately high rates of overuse injury and pain (Burnham and Steadward, 1994; Curtis et al., 1995; Ballinger et al., 2000). For example, nearly 70% of individuals who regularly use a manual wheelchair will experience upper limb pain, at the wrists or shoulders (Bayley et al., 1987; Gellman et al., 1988; Wylie and Chakera, 1988; Burnham and Steadward, 1994; Rice et al., 2013). The consequences of overuse injuries and pain may greatly impact MWUs' functional capacity and mobility, negatively influencing independence and quality of life (Gutierrez et al., 2007).

With upper limb pain and injury becoming increasingly common, the Consortium for Spinal Cord Medicine (CSCM) has recommended that MWUs use a low frequency, long and smooth stroke during the propulsive phase to decrease force exerted at a given velocity while allowing the hand to drift down and back below the handrim during recovery (Consortium for Spinal Cord Medicine, 2005). These recommendations are meant to minimize task repetition as well as the magnitude of propulsive forces through use of a larger contact angle (Boninger et al., 2005; Medicine PVoACfSC, 2005). Contact angle is the angle along the arc of the handrim, from contact to release. A larger *Contact Angle* is recommended, as it has the potential to reduce the number of strokes needed to maintain a given speed, therefore reducing *Stroke Frequency* and the number of repetitive motions performed by the upper limbs. Additionally, *Peak Resultant Force* is the occurrence of the highest vector sum of component forces (Fx, Fy, Fz) applied to the handrim during propulsion. Elevated peak forces experienced at the shoulder during propulsion often contribute to joint damage and overuse injuries as well (Shimada et al., 1998; Nyland et al., 2000; Vanlandewijck et al., 2001). Therefore, it is reasonable to surmise that utilizing techniques to minimize peak forces may help reduce the risk of pain and injury development.

Although these recommendations are well documented, alarmingly, children who use manual wheelchairs rarely receive formal training on safe and effective wheelchair propulsion techniques (Sawatzky et al., 2012). Lack of training may heighten the risk of injury development; however, training interventions have successfully improved propulsion technique in adult MWU (Rice et al., 2010, 2013). Most importantly, these studies produced substantial positive changes in contact angle, stroke frequency, and peak forces with video training and verbal feedback (Rice et al., 2010, 2013). While the literature on adult propulsion biomechanics and training is well developed, few have explored technique modification strategies in adolescent MWUs. Although basic skill and resistance training strategies have produced some positive results in adolescent MWUs (O'Connell and Barnhart, 1995; Sawatzky et al., 2012), it remains unclear if children can benefit from training approaches, proven successful in adults. If propulsion mechanics can be improved early in life, prior to technique consolidation, it may set adolescent MWUs on a healthy trajectory into adulthood.

The purpose of this study was to examine the safety and effectiveness of a propulsion technique training system, in adolescent MWU's, which has been used previously to successfully train adults. The system is a practical approach based on instructional video and verbal feedback. The goal of training was to instruct adolescent users to maximize contact angle, while minimizing stroke frequency at the handrim (Rice et al., 2010, 2013). If successful, the training system will represent a low-cost practical approach to minimizing upper limb pain and injury development in adolescent MWU's. Additionally, results may help to determine if adolescent wheelchair users display stroke mechanics changes similar to those seen in adults. Based on previous literature, it was hypothesized that with training, adolescents would react similarly to adults, displaying increased contact angle with reductions in stroke frequency and peak force at the handrim.

Materials and Methods

Participants

The University of Illinois at Urbana-Champaign's Institutional Review Board (IRB) approved all procedures prior to experimentation. Informed consent was attained from parents while assent was gathered from adolescent study participants. Inclusion criteria specified for participation included individuals 8–18 years of age who independently propelled a manual wheelchair as their primary mode of mobility (>40 h/week of wheelchair use). Additionally, all participants were free of any upper extremity condition or disability that could be worsened by physical activity and, participants with a spinal cord injury >2 years post-injury. A convenience sample of 10 adolescents (7 male, 3 female; 15.8 ± 1.6 years) recruited from the University of Illinois Youth Wheelchair Skills Camp, volunteered to participate in the study. Participant demographics are presented in **Table 1**.

Equipment

For data collection, force and moment sensing Clinical SMARTwheels (SMARTwheel; Three Rivers Holdings, Mesa, AZ, USA) (Asato et al., 1993) were fitted bilaterally to replace both wheels on the participants' personal, everyday wheelchairs (**Figure 1**). The right SMARTwheel was used for data collection, while the left served as a dummy wheel to parallel weight and inertial characteristics. While the SMARTwheel is slightly heavier than a standard wheel, it does not alter the feel or setup of a participant's personal chair (Cooper et al., 1997).

Protocol

Pain Assessment

First, participants completed the wheelchair users shoulder pain index (WUSPI) survey. The WUSPI (Curtis et al., 1995, 1999), a reliable and valid 15-item questionnaire was used to quantify the current level of pain in all participants (Curtis et al., 1995). Participants completed the WUSPI prior to propulsion activities. Additionally, the tool was sent to participants 3 months after data collection to examine the possible influence of training on

TABLE 1 | Participant demographics.

Participant ID	Age	Gender	Diagnosis/ injury level	Wheelchair use	Years using manual chair	WUSPI pre-intervention	WUSPI post-intervention
1	16	M	SB	Full time	16	6.4	6
2	15	M	CMT	Full time	9	0	SNR
3	14	F	SCI (C7)	Full time	10	23.1	4.1
4	13	F	SB	Full time	12	1.8	0
5	15	F	Amp	Full time	10	0.4	0
6	17	M	SB	Full time	6	22.8	26
7	17	M	SB	Full time	15	6	2.6
8	18	M	SCI	Full time	3	3.1	SNR
9	17	M	SCI (T5)	Full time	10	35.5	SNR
10	16	M	SB	Full time	16	0	0

SB, spina bifida; SCI, spinal cord injury (injury level); Amp, amputee; CMT, Charcot–Marie–Tooth disease; SNR, post-intervention survey not returned (no scores).

FIGURE 1 | Clinical SMARTwheel. Clinical SMARTwheels used for data collection replaced both wheels on participants' personal chairs. [a]denotes training intervention emphasis of using a large contact angle, along with decreased stroke frequency and forces.

Trial 1	Trial 2	Trial 3	Trial 4
*Baseline Propulsion Test Carpet Tile Concrete	*Repeat Trial 1	Training Intervention	*Posttest Repeat Trial 1

*Surface trials performed in a random order

FIGURE 2 | Experimental study design.

shoulder pain (the extent to which pain resulted from or was worsened by participation in the study).

Propulsion Assessment

With SMARTwheels, participants were instructed to push at a natural, self-selected pace over flat, industrial grade carpeted, and tiled surfaces, two times each (**Figure 2**). A self-selected speed was chosen deliberately to examine propulsion mechanics occurring at natural and comfortable pace, as well as to maximize the safety of adolescent participants. Participants also performed two speed controlled trials over a flat concrete surface. Based on the self-selected speeds from existing literature, a target velocity of 1.5 m/s was selected (Van der Woude et al., 1986; Bednarczyk and Sanderson, 1995). This pace is slightly slower than previous studies to ensure all participants could safely and comfortably maintain the speed. Participants were instructed to match the speed of a researcher using a wheelchair equipped with a Garmin Edge 800 GPS Speedometer.

All trials/surfaces were completed in random order for a distance of 15 m to allow completion of five steady-state strokes. Rest periods were not needed between surface trial repeats due to the low intensity and short distances; however, 5 min of recovery were provided in the time needed to change between surfaces. Additionally, researchers provided no feedback or commentary on propulsion mechanics or techniques during these trials as they occurred prior to training. After participants were exposed to the intervention (described below), propulsion was evaluated on each surface one additional time. Data were collected during the entire propulsion period for all trials on each surface. Due to the small sample size, participants served as their own control, where trials one and two constituted baseline data collection used for comparison with the third, post-intervention trial.

Intervention

After participants completed the first two trials over all three surfaces, they participated in the training intervention. The intervention consisted of a short training video (5 min) (Rice et al., 2013), which allowed for independent viewing. Participants were encouraged to use low frequency, long and smooth strokes (large contact angle) during the propulsive phase to decrease force exerted at a given velocity (Consortium for Spinal Cord Medicine, 2005). Additionally, subjects were encouraged to match the speed of the handrim upon contact to minimize braking torques that slows the wheel. Both contact angle and stroke frequency were defined and discussed in the video. As a visual aid, the video contained a MWU propelling on a dynamometer, demonstrating these techniques. For additional motivation, the video emphasized the importance of using proper technique to preserve upper limb health, independence, and quality of life. Upon completion of the video, researchers discussed and reemphasized the primary components of the video. During this time, participants were given the opportunity to ask researchers any questions and practice the new propulsion techniques. During this practice, participants received basic feedback from researchers.

Data Reduction

The propulsion performance variables selected for analysis were peak resultant force (Newton), contact angle (Degree), and stroke frequency (strokes per second) because of their association with upper limb pain and injury development. Participants' average velocity (m/s) was recorded for each trial as well. Mean intra-individual variability was calculated for each performance variable during velocity controlled concrete trials to quantify potential motor learning strategies as a function of training. Coefficient of variation (CV) was only calculated for the speed controlled trials to minimize the potential occurrence of variation changes due to velocity fluctuations. CV (%) was calculated as the percentage of SD with respect to the mean. Data from the Clinical SMARTwheel were collected from forces and moments applied to the handrim at a sampling frequency of 240 Hz. All variables were calculated as the mean values of five steady-state strokes.

Statistical Analysis

All statistical analyses were performed using SPSS (v.20.0 SPSS Inc., Chicago, IL, USA). Differences in normally distributed propulsion and intra-individual variation variables during the trials were analyzed separately using multiple one-way repeated measures ANOVAs with Bonferroni adjusted *post hoc* testing. Variables that violated the Shapiro–Wilk test of normality ($p < 0.05$) were analyzed using non-parametric Freidman's tests with Bonferroni corrections for pairwise comparisons. To examine possible effects or changes of speed, a one-way repeated measures ANOVA was performed on the average velocity of each trial. The first two, pre-intervention trials were analyzed separately to better differentiate effects of the intervention from possible practice effects that may have occurred due to repetition and practice (De Groot et al., 2002, 2008; Vegter et al., 2014). All variable analysis was performed separately for each surface. All WUSPI data from the pre-intervention and 3 month post-intervention follow-up ($n = 7$) were compared using a paired samples t-test.

The criterion to reject the null hypothesis was $p < 0.05$ and sample effect sizes are interpreted as small ($\eta^2 < 0.20$), moderate ($\eta^2 \sim 0.50$), and large ($\eta^2 > 0.80$). All descriptive statistics are reported as Mean (Standard Deviation) [M(SD)].

Results

Propulsion Performance

Descriptive statistics are reported in **Tables 2–4**. Of the variables from the carpet trials (**Table 2**), stroke frequency (trial 1: $p < 0.01$) violated the Shapiro–Wilk test of normality and was therefore analyzed using Freidman's tests. Results indicated that during the carpeted trials, after the intervention, statistically significant increases occurred in peak resultant force ($p < 0.01$, $\eta^2 = 0.48$) and contact angle ($p = 0.04$, $\eta^2 = 0.30$) with decreased stroke frequency ($p = 0.048$, $\eta^2 = 0.22$). Separate analysis of the average velocity for each of the trials revealed significant differences in speed during the self-selected trials ($p = 0.02$, $\eta^2 = 0.35$).

From the tile trials (see **Table 3**), peak resultant force (trial 1: $p = 0.02$) and stroke frequency (trial 2: $p < 0.01$) violated the Shapiro–Wilk test of normality and were therefore analyzed using Freidman's tests. Results of the tile trials indicated that after the intervention, statistically significant increases in contact angle ($p = 0.02$, $\eta^2 = 0.34$) and peak resultant force ($p = 0.03$, $\eta^2 = 0.44$) occurred, as well as a significantly decreased stroke frequency ($p = 0.03$, $\eta^2 = 0.22$). Differences in velocity were not found to be statistically significant between the tile trials ($p = 0.28$, $\eta^2 = 0.13$).

No variables from the speed controlled concrete trials violated the Shapiro–Wilk test of normality. Results (**Table 4**) demonstrate statistically significant increases in contact angle ($p = 0.02$, $\eta^2 = 0.36$) with decreased in stroke frequency ($p = 0.04$, $\eta^2 = 0.39$) after training. A trend was observed for increases in peak force ($p = 0.05$, $\eta^2 = 0.28$). No significant differences were observed in average velocity between trials ($p = 0.54$, $\eta^2 = 0.07$).

Intra-Individual Variability Performance

Dependent variables from the velocity controlled concrete trials were analyzed with a one-way repeated-measure ANOVA. Statistically significant changes were found only in peak resultant force variation ($p = 0.02$, $\eta^2 = 0.35$) (**Table 5**). No other significant changes were observed in contact angle ($p = 0.30$, $\eta^2 = 0.12$), stroke frequency ($p = 0.32$, $\eta^2 = 0.12$), and velocity ($p = 0.84$, $\eta^2 = 0.20$).

Shoulder Pain

Results of the paired samples t-test revealed no significant change in WUSPI scores from pre-testing (8.64 [10.09]) to

TABLE 2 | Carpet propulsion trials.

Performance variable	Trial 1 *M* (SD)	Trial 2 *M* (SD)	Trial 3 *M* (SD)	*F*	ω^2
Parametric results					
Peak resultant force (N)	49.96 (16.67)	51.90 (14.0)	60.99 (18.36)	8.19*	0.32
Contact angle (Deg)	71.29 (19.22)	78.80 (21.45)	82.66 (16.38)	3.80*	0.16
Velocity (m/s)	1.12 (0.21)	1.17 (0.15)	1.33 (0.28)	4.83*	0.35
Non-parametric results				X^2	
Stroke frequency (stroke/s)	0.82 (0.09)	0.84 (0.10)	0.76 (0.12)	6.05*	0.09

*$p < 0.05$.

TABLE 3 | Tile propulsion trials.

Performance variable	Trial 1 *M* (SD)	Trial 2 *M* (SD)	Trial 3 *M* (SD)	*F*	ω^2
Parametric results					
Contact angle (Deg)	67.90 (18.68)	73.94 (21.20)	81.28 (18.59)	4.60*	0.19
Velocity (m/s)	1.07 (0.10)	1.08 (0.13)	1.14 (0.17)	1.37	0.13
Non-parametric results				X^2	
Peak resultant force (N)	46.95 (15.68)	46.37 (9.90)	59.37 (19.43)	7.40*	0.29
Stroke frequency (stroke/s)	0.80 (0.08)	0.80 (0.11)	0.72 (0.08)	7.32*	0.08

*$p < 0.05$.

TABLE 4 | Outdoor propulsion trials.

Performance variable	Trial 1 *M* (SD)	Trial 2 *M* (SD)	Trial 3 *M* (SD)	*F*	ω^2
Parametric results					
Contact angle (Deg)	69.28 (16.73)	72.26 (12.66)	84.13 (17.77)	5.14*	0.22
Peak resultant force (N)	59.85 (21.08)	51.19 (15.80)	67.10 (26.59)	3.45	0.14
Stroke frequency (stroke/s)	0.94 (0.08)	0.87 (0.09)	0.75 (0.16)	5.71*	0.24
Velocity (m/s)	1.46 (0.07)	1.46 (0.06)	1.45 (0.07)	0.06	0.03

*$p < 0.05$.

TABLE 5 | Outdoor propulsion trials: variability results.

Performance variable	Trial 1 *M* (SD)	Trial 2 *M* (SD)	Trial 3 *M* (SD)	*F*	ω^2
Parametric results					
Contact angle (Deg)	18.93 (9.97)	19.18 (10.74)	12.97 (9.03)	1.31	0.02
Peak resultant force (N)	17.79 (8.66)	24.81 (8.11)	16.86 (8.68)*	4.76	0.20
Stroke frequency (stroke/s)	13.58 (11.41)	19.40 (10.22)	14.75 (11.36)	1.20	0.01
Velocity (m/s)	4.30 (2.60)	4.03 (2.60)	3.49 (2.04)	0.18	0.06

*$p < 0.05$.

the 3 month follow-up (5.53 [9.32]), $t(6) = 1.13$, $p = 0.30$ (**Table 1**). Three participants did not return the WUSPI, 3 months post-intervention ($n = 7$).

Discussion

The purpose of this study was to examine the influence of wheelchair training on adolescent propulsion technique to reduce the risk of upper limb pain and injury development. Because few studies have implemented training protocols on adolescent wheelchair users, another goal of the study was to determine if adolescents demonstrated propulsion technique changes similar to those seen in adult wheelchair users. Consistent with our hypothesis, changes occurred in participants' propulsion technique following the intervention, similar to those found in adult wheelchair users (Rice et al., 2010, 2013). Specifically, participants demonstrated increased contact angle, with decreases in stroke frequency across all surfaces and speeds, with moderate effect sizes. Additionally, when velocity was controlled a trend toward increased peak force was observed, however, small in magnitude.

During both the carpet and tile trials, significant increases were observed in contact angle, which likely resulted in participants' significant decrease in stroke frequency (see **Figures 3–4**). Although more recent literature on adults has observed decreases in force application with training, increases in peak forces occurred during the carpet and tile trials in the current study. In the study by Rice et al. (2013), similar short-term increases in force occurred; however, with further time and training, participants peak force levels subsided 3 months later. As previously observed in adults, the use of a larger contact angle may lead to a stroke where forces are distributed over a greater angular distance of the handrim. Based on the short-term similarities observed between adolescents in the current study and adults (increased short-term force application), it is possible that adolescent MWU may too learn to apply less peak force utilizing a larger contact angle. Long-term propulsion technique follow-up has been scheduled to help clarify. Additionally, use of larger contact angle helped minimize stroke frequency to maintain similar speeds immediately in the current study supporting the protective ergonomic principle of task reduction (Boninger et al., 2000; Medicine PVoACfSC, 2005). Overall, the observed short-term similarities between previous adult literature and our adolescents may provide preliminary evidence children can benefit from similar training approaches.

Although the increased forces observed in the current study were small in magnitude, it is important to discuss their etiology due to the association with upper limb pathologies. A likely explanation for the increased forces occurring on carpet was due to increased average speeds (**Tables 2** and **3**). As observed in the concrete trials, when velocity was regulated, peak force remained relatively stable post-intervention, with only a slight trend toward a gain (**Table 4**). Additionally, it is important to note that although no intervention had taken place yet, notable differences in peak force occurred during the two initial concrete control trials (**Table 4**). Numerous factors may have played a role in these peak force changes, such as attempts to maintain a target speed, adaptation to the research environment, or natural variation of force application. It is possible that with additional trials, changes in peak force may have minimized from one trial to the next. However, for the sample population in general, these changes in performance suggest that further research is needed to examine performance consistency.

Intra-individual variability of the propulsion variables were found to be relatively stable over all three surfaces, both prior (trials 1–2) to and following training (trial 3). However, this may be a result of the very short time-period, and therefore the limited number of strokes, from which data were collected. In previous literature examining variability in MWP, data were collected for 3–12 min for each trial, allowing for an extensive number of propulsive strokes to be analyzed (Moon et al., 2013; Vegter et al., 2013, 2014). When learning a new skill, it is anticipated that reductions in variability may occur with time. As observed previously in

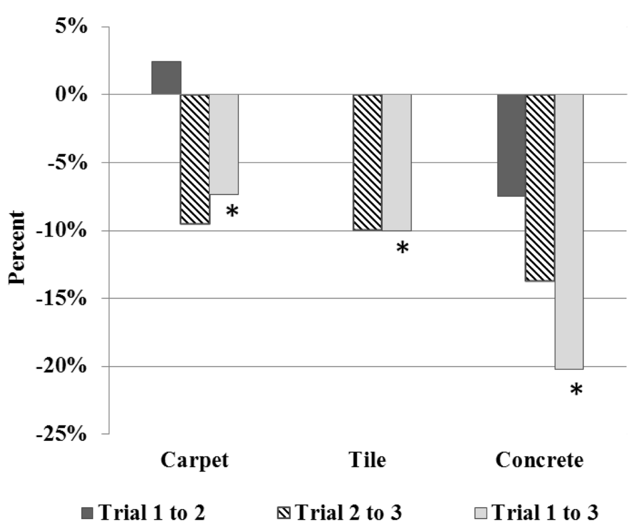

FIGURE 3 | Percentage change in stroke frequency over trials. *denotes significant change between trials, $p < 0.05$.

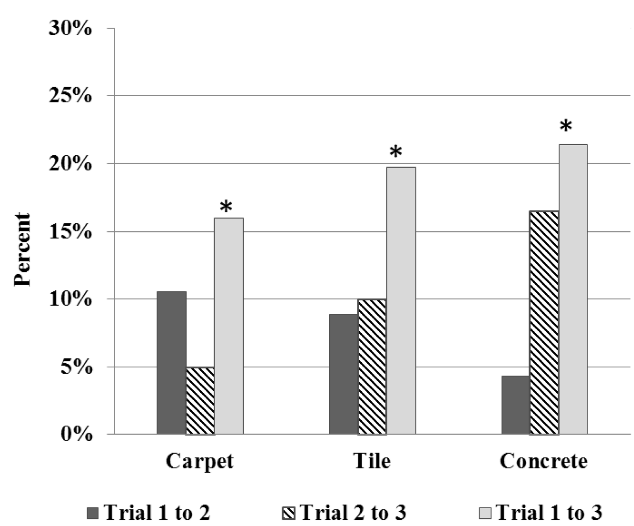

FIGURE 4 | Percentage change in contact angle over trials. *denotes significant change between trials, $p < 0.05$.

adults, the amount of variability in propulsion mechanics decrease more quickly in individuals who were considered to be faster learners (Bartlett et al., 2007; Wang et al., 2012; Vegter et al., 2013). However, it is also believed that a lack of variation in any repetitive movement results in an insufficient amount of time for the limbs to adapt or heal, thus resulting in overuse injuries (Bartlett et al., 2007). As individuals modify their movements slightly altering the distribution of movement stresses from one repetition to the next, a particular range of variability may serve as a protective measure against overuse injuries (Madeleine et al., 2008). Further research into the variability of both adolescent and adult wheelchair users may allow researchers to ascertain if a particular range is favorable.

Although not found to be statistically significant, baseline WUSPI scores revealed our participants had relatively low levels of shoulder pain prior to training and further reduced pain 3 months later (see **Table 1**). Importantly, due to our study design, we cannot conclude the pain reduction observed was directly related to our intervention. It is also possible the 3-month follow-up was biased because three individuals did not return their surveys. Future studies should explore pain reduction as a function of propulsion technique modification in larger groups of wheelchair users over time.

Although significant changes were found in contact angle and stroke frequency, the changes may have been modest in comparison to a less active population. However, even with wheelchair athletics experience, our participants demonstrated room for improvement. The literature supports that experienced MWUs have been observed to use larger contact angles and lower peak forces in comparison to non-experienced groups (Robertson et al., 1996; Kotajarvi et al., 2004).

As we move forward with this line of research, it will be critical to include larger more diverse groups of younger MWUs to both maximize generalizability and to sufficiently power future investigations. Additionally, we plan to shift outcome measures away from the short-term influence of training observed in a laboratory setting to the long-term effects occurring at home and in the community. Use of minimally obtrusive technologies like accelerometers has enormous potential in this context. For example, vector counts accumulated though wrist worn accelerometers are shown to have a linear association with energy expenditure during propulsion (Learmonth et al., 2015) and may offer a more detailed account of how improved technique translates to physical activity.

Limitations

As the current study was one of the first pilot investigations of propulsion training in adolescent wheelchair users, numerous limitations exist. Obtaining a sufficiently large sample size of younger wheelchair users can be challenging and likely explains the lack of literature on the topic. Similarly, our small, relatively homogenous sample size of active wheelchair users was a significant limitation, which influenced our statistical approach. Consequently, a repeated measures design was implemented where individuals served as their own control, which may have reduced power, as well as inflating the possibility of Type II error. Additionally, because no long-term data were collected, it is not possible to determine if learned propulsion techniques would persist or if reductions in peak force would eventually occur. Additionally, wheelchair characteristics were not collected, which may have influenced technique modification. Finally, the small number of strokes analyzed may have decreased our ability to detect fluctuations in intra-individual variation. Future examination will include longer periods of data collection to confirm.

Conclusion

After a 5 min training video, adolescent wheelchair users experience significant positive changes in contact angle and stroke frequency similar to those seen in adults, which may prevent the development of upper limb pain and injury. Although short-term changes were similar to those seen in adults, future investigation is warranted on larger more age divers group of younger MWU to confirm differences with adults.

Acknowledgments

This study was supported by the University of Illinois Center on Health Aging, and Disability (CHAD) Award. Special thanks to research assistants Anna Ballazhi, Ethan Sanders.

References

Asato, K. T., Cooper, R. A., Robertson, R. N., and Ster, J. F. (1993). SMARTWheels: development and testing of a system for measuring manual wheelchair propulsion dynamics. *IEEE Trans. Biomed. Eng.* 40, 1320–1324. doi:10.1109/10.250587

Ballinger, D. A., Rintala, D. H., and Hart, K. A. (2000). The relation of shoulder pain and range-of-motion problems to functional limitations, disability, and perceived health of men with spinal cord injury: a multifaceted longitudinal study. *Arch. Phys. Med. Rehabil.* 81, 1575–1581. doi:10.1053/apmr.2000.18216

Bartlett, R., Wheat, J., and Robins, M. (2007). Is movement variability important for sports biomechanists? *Sports Biomech.* 6, 224–243. doi:10.1080/14763140701322994

Bayley, J. C., Cochran, T., and Sledge, C. (1987). The weight-bearing shoulder. The impingement syndrome in paraplegics. *J. Bone Joint Surg.* 69, 676–678.

Bednarczyk, J. H., and Sanderson, D. J. (1995). Limitations of kinematics in the assessment of wheelchair propulsion in adults and children with spinal cord injury. *Phys. Ther.* 75, 281–289.

Boninger, M. L., Baldwin, M., Cooper, R. A., Koontz, A., and Chan, L. (2000). Manual wheelchair pushrim biomechanics and axle position. *Arch. Phys. Med. Rehabil.* 81, 608–613. doi:10.1016/S0003-9993(00)90043-1

Boninger, M. L., Koontz, A. M., Sisto, S. A., Dyson-Hudson, T. A., Chang, M., Price, R., et al. (2005). Pushrim biomechanics and injury prevention in spinal cord injury: recommendations based on CULP-SCI investigations. *J. Rehabil. Res. Dev.* 42, 9. doi:10.1682/JRRD.2004.08.0103

Burnham, R. S., and Steadward, R. D. (1994). Upper extremity peripheral nerve entrapments among wheelchair athletes: prevalence, location, and risk factors. *Arch. Phys. Med. Rehabil.* 75, 519–524.

Consortium for Spinal Cord Medicine. (2005). *Preservation of Upper Limb Function Following Spinal Cord Injury: A Clinical Practice Guideline for Health-Care Professionals*. Washington, DC: Paralyzed Veterans of America.

Cooper, R. A., Robertson, R. N., VanSickle, D. P., Boninger, M. L., and Shimada, S. D. (1997). Methods for determining three-dimensional wheelchair pushrim forces and moments - a technical note. *J. Rehabil. Res. Dev.* 34, 162–170.

Curtis, K., Roach, K., Applegate, E. B., Amar, T., Benbow, C. S., Genecco, T. D., et al. (1995). Development of the wheelchair user's shoulder pain index (WUSPI). *Spinal Cord* 33, 290–293. doi:10.1038/sc.1995.65

Curtis, K. A., Drysdale, G. A., Lanza, R. D., Kolber, M., Vitolo, R. S., and West, R. (1999). Shoulder pain in wheelchair users with tetraplegia and paraplegia. *Arch. Phys. Med. Rehabil.* 80, 453–457. doi:10.1016/S0003-9993(99)90285-X

De Groot, S., De Bruin, M., Noomen, S., and Van der Woude, L. (2008). Mechanical efficiency and propulsion technique after 7 weeks of low-intensity wheelchair training. *Clin. Biomech.* 23, 434–441. doi:10.1016/j.clinbiomech.2007.11.001

De Groot, S., Veeger, D., Hollander, A. P., and Van der Woude, L. (2002). Wheelchair propulsion technique and mechanical efficiency after 3 wk of practice. *Med. Sci. Sports Exerc.* 34, 756–766. doi:10.1097/00005768-200205000-00005

Gellman, H., Chandler, D., Petrasek, J., Sie, I., Adkins, R., and Waters, R. (1988). Carpal tunnel syndrome in paraplegic patients. *J. Bone Joint Surg.* 70, 517–519.

Gutierrez, D. D., Thompson, L., Kemp, B., Mulroy, S. J., and Network PTCR. (2007). The relationship of shoulder pain intensity to quality of life, physical activity, and community participation in persons with paraplegia. *J. Spinal Cord Med.* 30, 251.

Kotajarvi, B. R., Sabick, M. B., An, K.-N., Zhao, K. D., Kaufman, K. R., and Basford, J. R. (2004). The effect of seat position on wheelchair propulsion biomechanics. *J. Rehabil. Res. Dev.* 41, 403–414. doi:10.1682/JRRD.2003.01.0008

Learmonth, Y. C., Kinnett-Hopkins, D., Rice, I. M., Dysterheft, J. L., and Motl, R. W. (2015). Accelerometer output and its association with energy expenditure during manual wheelchair propulsion. *Spinal Cord*. doi:10.1038/sc.2015.33

Madeleine, P., Mathiassen, S. E., and Arendt-Nielsen, L. (2008). Changes in the degree of motor variability associated with experimental and chronic neck-shoulder pain during a standardised repetitive arm movement. *Exp. Brain Res.* 185, 689–698. doi:10.1007/s00221-007-1199-2

Medicine PVoACfSC. (2005). Preservation of upper limb function following spinal cord injury: a clinical practice guideline for health-care professionals. *J. Spinal Cord Med.* 28, 434.

Moon, Y., Jayaraman, C., Hsu, I., Rice, I., Hsiao-Wecksler, E., and Sosnoff, J. (2013). Variability of peak shoulder force during wheelchair propulsion in manual wheelchair users with and without shoulder pain. *Clin. Biomech.* 28, 967–972. doi:10.1016/j.clinbiomech.2013.10.004

Nash, M. S., Jacobs, P. L., Mendez, A. J., and Goldberg, R. B. (2001). Circuit resistance training improves the atherogenic lipid profiles of persons with chronic paraplegia. *J. Spinal Cord Med.* 24, 2–9.

Nyland, J., Snouse, S. L., Anderson, M., Kelly, T., and Sterling, J. C. (2000). Soft tissue injuries to USA paralympians at the 1996 summer games. *Arch. Phys. Med. Rehabil.* 81, 368–373. doi:10.1016/S0003-9993(00)90086-8

O'Connell, D. G., and Barnhart, R. (1995). Improvement in wheelchair propulsion in pediatric wheelchair users through resistance training: a pilot study. *Arch. Phys. Med. Rehabil.* 76, 368–372. doi:10.1016/S0003-9993(95)80663-6

Rice, I., Gagnon, D., Gallagher, J., and Boninger, M. (2010). Hand rim wheelchair propulsion training using biomechanical real-time visual feedback based on motor learning theory principles. *J. Spinal Cord Med.* 33, 33.

Rice, I. M., Pohlig, R. T., Gallagher, J. D., and Boninger, M. L. (2013). Handrim wheelchair propulsion training effect on overground propulsion using biomechanical real-time visual feedback. *Arch. Phys. Med. Rehabil.* 94, 256–263. doi:10.1016/j.apmr.2012.09.014

Robertson, R. N., Boninger, M. L., Cooper, R. A., and Shimada, S. D. (1996). Pushrim forces and joint kinetics during wheelchair propulsion. *Arch. Phys. Med. Rehabil.* 77, 856–864. doi:10.1016/S0003-9993(96)90270-1

Sawatzky, B., Rushton, P. W., Denison, I., and McDonald, R. (2012). Wheelchair skills training programme for children: a pilot study. *Aust. Occup. Ther. J.* 59, 2–9. doi:10.1111/j.1440-1630.2011.00964.x

Shimada, S. D., Robertson, R. N., Bonninger, M. L., and Cooper, R. A. (1998). Kinematic characterization of wheelchair propulsion. *J. Rehabil. Res. Dev.* 35, 210–218.

Van der Woude, L., De Groot, G., Hollander, A., van Ingen, S. G., and Rozendal, R. (1986). Wheelchair ergonomics and physiological testing of prototypes. *Ergonomics* 29, 1561–1573. doi:10.1080/00140138608967269

Vanlandewijck, Y., Theisen, D., and Daly, D. (2001). Wheelchair propulsion biomechanics. *Sports Med.* 31, 339–367. doi:10.2165/00007256-200131050-00005

Vegter, R. J., Lamoth, C. J., De Groot, S., Veeger, D. H., and Van der Woude, L. H. (2013). Variability in bimanual wheelchair propulsion: consistency of two instrumented wheels during handrim wheelchair propulsion on a motor driven treadmill. *J. Neuroeng. Rehabil.* 10, 9. doi:10.1186/1743-0003-10-9

Vegter, R. J., Lamoth, C. J., de Groot, S., Veeger, D. H., and van der Woude, L. H. (2014). Inter-individual differences in the initial 80 minutes of motor learning of handrim wheelchair propulsion. *PLoS ONE* 9:e89729. doi:10.1371/journal.pone.0089729

Wang, L. P., Hamaker, E., and Bergeman, C. (2012). Investigating inter-individual differences in short-term intra-individual variability. *Psychol. Methods* 17, 567. doi:10.1037/a0029317

Wylie, E., and Chakera, T. (1988). Degenerative joint abnormalities in patients with paraplegia of duration greater than 20 years. *Spinal Cord* 26, 101–106. doi:10.1038/sc.1988.20

Conflict of Interest Statement: The authors declare that the research was conducted in the absence of any commercial or financial relationships that could be construed as a potential conflict of interest.

frontiers in Bioengineering and Biotechnology

ORIGINAL RESEARCH
published: 26 October 2015
doi: 10.3389/fbioe.2015.00171

Modifications in wheelchair propulsion technique with speed

Ian M. Russell[1], Shashank Raina[1], Philip S. Requejo[2], Rand R. Wilcox[3], Sara Mulroy[2] and Jill L. McNitt-Gray[1,4]*

[1] Department of Biomedical Engineering, University of Southern California, Los Angeles, CA, USA, [2] Pathokinesiology Laboratory, Rancho Los Amigos National Rehabilitation Center, Downey, CA, USA, [3] Department of Psychology, University of Southern California, Los Angeles, CA, USA, [4] Department of Biological Sciences, University of Southern California, Los Angeles, CA, USA

Objective: Repetitive loading of the upper limb joints during manual wheelchair (WC) propulsion (WCP) has been identified as a factor that contributes to shoulder pain, leading to loss of independence and decreased quality of life. The purpose of this study was to determine how individual manual WC users with paraplegia modify propulsion mechanics to accommodate expected increases in reaction forces (RFs) generated at the pushrim with self-selected increases in WCP speed.

Methods: Upper extremity kinematics and pushrim RFs were measured for 40 experienced manual WC users with paraplegia while propelling on a stationary ergometer at self-selected free and fast propulsion speeds. Upper extremity kinematics and kinetics were compared within subject between propulsion speeds. Between group and within-subject differences were determined ($\alpha = 0.05$).

Results: Increased propulsion speed was accompanied by increases in RF magnitude (22 of 40, >10 N) and shoulder net joint moment (NJM, 15 of 40, >10 Nm) and decreases in pushrim contact duration. Within-subject comparison indicated that 27% of participants modified their WCP mechanics with increases in speed by regulating RF orientation relative to the upper extremity segments.

Conclusions: Reorientation of the RF relative to the upper extremity segments can be used as an effective strategy for mitigating rotational demands (NJM) imposed on the shoulder at increased propulsion speeds. Identification of propulsion strategies that individuals can use to effectively accommodate for increases in RFs is an important step toward preserving musculoskeletal health of the shoulder and improving health-related quality of life.

Keywords: biomechanics, spinal cord injury, shoulder pain, wheelchair, rehabilitation, propulsion, joint kinetics, upper extremity

Edited by:
Tarun Goswami, Wright State University, USA

Reviewed by:
Henrique De Amorim Almeida, Polytechnic Institute of Leiria, Portugal
Yen-Sheng Lin, Rehabilitation Institute of Chicago, USA

***Correspondence:**
Ian M. Russell
ian.m.russell@gmail.com

Specialty section:
This article was submitted to Biomechanics, a section of the journal Frontiers in Bioengineering and Biotechnology

Received: *08 July 2015*
Accepted: *12 October 2015*
Published: *26 October 2015*

Citation:
Russell IM, Raina S, Requejo PS, Wilcox RR, Mulroy S and McNitt-Gray JL (2015) Modifications in wheelchair propulsion technique with speed. Front. Bioeng. Biotechnol. 3:171. doi: 10.3389/fbioe.2015.00171

INTRODUCTION

Preserving shoulder function in individuals with spinal cord injury (SCI) continues to be a significant problem (Gutierrez et al., 2007; Alm et al., 2008). Effective interaction between an individual and their manual wheelchair (WC) is essential to preserving quality of life, specifically shoulder function and overall health (Curtis et al., 1999; Gutierrez et al., 2007). Although the clinical problem of shoulder pain in individuals with SCI was identified more than three decades ago, the prevalence remains high (Silfverskiold and Waters, 1991; Pentland and Twomey, 1994; Jain et al., 2010). Researchers and clinicians have attributed shoulder pain in the SCI population to the repetitive mechanical loading of the upper limb as a consequence of lower extremity paralysis (Bayley et al., 1987; Dalyan et al., 1999). In individuals with paraplegia, shoulder pain can occur within the first year and the incidence increases with time post-injury (35% at 5 years, 70% at 20 years, Sie et al., 1992). Due to the detrimental impact on functional mobility and the difficulty in treatment of shoulder pain, effective preventative strategies must be determined for *each* WC user. The activities that provoke the highest pain responses for full-time manual WC users tend to be those that are repetitive and generate high shoulder forces, such as manual wheelchair propulsion (WCP) (Curtis et al., 1999).

Manual WCP is a cyclic task that requires repetitive generation of propulsive forces on the pushrim of the WC. Generation of these reaction forces (RFs) applied at the pushrim involves coordinated activation of muscles responsible for simultaneously maintaining shoulder joint stability and controlling shoulder rotation. Structural stability of the shoulder joint is provided by a shallow humeral head socket (glenoid cavity) and a fibrous labrum (Inman et al., 1944). During WCP, the elbow is positioned below the shoulder. In this segment configuration, the joint capsule tends to be loose and the reinforcing ligaments are slack in absence of a RF, thereby creating the need for shoulder muscles to maintain joint stability (Mulroy et al., 1996). Simultaneously, activation of the upper extremity muscles must be coordinated to produce the shoulder and elbow net joint moments (NJMs) needed to generate propulsive RFs on the pushrim (Robertson et al., 1996; Kulig et al., 1998; Koontz et al., 2002). Imposing both joint stability and moment generation requirements on muscles in the shoulder region during WCP increases the susceptibility to neuromuscular fatigue (Kulig et al., 1998; Koontz et al., 2002). A weakened muscle within the shoulder girdle complex can result in an inadequate dynamic stability of the shoulder particularly during intervals when large RFs are required during WCP (McCully et al., 2007). Loss of dynamic stability causes stress on the shoulder structures and other joints of the upper limb and can lead to the development of shoulder pain (Curtis et al., 1999; Gironda et al., 2004; Samuelsson et al., 2004; Alm et al., 2008).

As part of daily living, manual WC users need to regulate WCP speed. On average, increases in WCP speed has been reported to significantly increase RF magnitudes, decrease hand contact duration, affect wrist angular position on pushrim (Kulig et al., 1998; Koontz et al., 2002; Veeger et al., 2002), and influence the mechanical demand imposed on muscles controlling shoulder stabilization and rotation during WCP (Kulig et al., 1998; Koontz et al., 2002). Increases in WCP speed can also lead to disproportionate increases in shoulder NJMs during hand contact (Veeger et al., 2002). Understanding how an individual can effectively interact with the pushrim to achieve required increases in WCP speed provides insights into how modifications in multijoint control of the upper limb can accommodate for increased mechanical demand imposed on the shoulder. Model simulation results indicate that modifications in RF orientation relative to the upper extremity segments can effectively redistribute load away from the shoulder while maintaining WCP speed (Munaretto et al., 2012, 2013). To date, the techniques used by individuals with SCI to accomplish the changes in propulsion speeds have been difficult to discern from group mean data of peak NJMs reported during WCP (Kulig et al., 1998, 2001; Koontz et al., 2002; Mercer et al., 2006).

In this study, we used a within-subject experimental design to determine how individual manual WC users with paraplegia modify WCP mechanics to accommodate expected increases in RF generated at the pushrim with self-selected increases in propulsion speed. As found previously, we expect that RF magnitude, shoulder net joint force (NJF), and shoulder NJM during WCP would increase whereas contact duration would decrease with increases in speed (Kulig et al., 1998; Koontz et al., 2002; Veeger et al., 2002). Consistent with that found in other impulse generating tasks (McNitt-Gray et al., 2001; Mathiyakom et al., 2005) and experimental-based model simulations of WCP (Munaretto et al., 2012), we hypothesized that the orientation of RF relative to the forearm and upper arm would affect the mechanical demand imposed on the upper extremity with increases in WCP speed. We anticipated that individuals with paraplegia would use different WCP techniques to accommodate the need to increase WCP speed. Modifications in WCP technique between free and self-selected fast WCP speeds were characterized by identifying within-subject differences in upper extremity joint kinetics at peak push during hand contact with the pushrim. Identification of effective load distribution strategies that an individual can use during manual WCP at different speeds provides evidence to support clinical decisions as to how and when to explore modifications in WCP technique as a means of preserving shoulder function in individuals with SCI.

MATERIALS AND METHODS

Participants

Forty participants (32 male and eight female) with complete SCI who were experienced manual WC users with paraplegia (T2-L3) from the outpatient clinics of the Rancho Los Amigos National Rehabilitation Center volunteered to participate. Each participant was provided informed consent in accordance with the Institutional Review Board. Individuals were excluded from participation if they reported a history of shoulder pain that altered performance of daily activities or required medical treatment. Average (SD) weight of participants was 74.5 (18) kg, average height was 1.73 (0.1) m and average age was 35 years (range: 18–62 years). The mean time since occurrence of the injury was 8.25 years (range: 2–20 years).

Instrumentation

For this study, the majority of the participants propelled their own WC using an ergometer (27 of 40). In cases when the individual's WC did not fit the ergometer set-up (13 of 40), the individual used a rigid frame, lightweight Quickie GPV WC with either a 16″ or 18″ seat, depending on the size of the participant. Horizontal and vertical axle positions were matched to that of the individual's WC. The height of the footrest, seat back, and inertial parameter of the test WC were also adjusted to match the participant's own WC. Each participant used their own seat cushion. The WC was positioned on a stationary ergometer, consisting of a support frame and split rollers, allowing separate rotation of each wheel. The rollers were coupled by means of a differential to an alternator and a modified Velodyne® bicycle ergometer that computer-controlled the resistance. To quantify the friction force between the tire and ergometer rollers, a coast down test (from 182 to 35 m/min) with the participant sitting in the test WC on top of the ergometer was used. Removable flywheels proportional to the weight of both the person and the WC were used to simulate the translational inertia of "over ground" propulsion. Further details about the ergometer instrumentation and calibration steps are described in previous papers (Mulroy et al., 2004, 2005; Requejo et al., 2008; Lighthall-Haubert et al., 2009). RF applied by the hand to the pushrim was measured using three strain gage force transducers at 200 Hz (SmartWheel, Three Rivers Holdings, Mesa, AZ, USA).

Data Collection

Three-dimensional trunk, right-side upper extremity and wheel kinematics were collected with active infra-red markers using a CODA motion analysis system (6-camera, CODA Motion Analysis system, 100 Hz) for 10 s of WCP at two speed conditions. Markers were placed on the trunk at the manubrium, the xiphoid process, the spinous process of T3 and T10 vertebrae, greater tubercle of the humerus, lateral epicondyle, medial epicondyle, deltoid tuberosity, middle of the forearm, radial styloid, ulnar styloid, head of the third metacarpal, and head of the fifth metacarpal. Three reflective markers were also placed on the right wheel.

Experimental Protocol

Prior to data collection, participants were given adequate time to become accustomed to the WC and experimental conditions. Each participant performed WCP at their self-selected free speed, as they do normally when traversing a tiled floor, and at a self-selected fast speed, as if they are in a hurry to not miss an important appointment. Preceding the start of data collection, participants propelled for 30 s to avoid the propulsion initiation period. Force and kinematic data were then collected for 10 s (6–10 push cycles) at each speed condition with no additional load applied to the ergometer rollers (i.e., level ground over a tiled surface).

Data Processing and Analysis

The kinematic and force data of consecutive propulsion cycles during the data collection interval (10 s) were analyzed using Visual3D[d] and Matlab[f]. The number of propulsion cycles analyzed for each subject was the maximum number of propulsion cycles captured in the 10-s window common to all subjects for that condition (5 for free and 6 for fast). Kinematic data were filtered in Visual3D using a sixth order low-pass filter with a cutoff frequency of 8 Hz (Cooper et al., 2002). Four segments were constructed based on the ISB standard definitions (Wu et al., 2005). The thorax segment was defined using markers placed at the xiphoid, manubrium, T3, and T10 vertebrae. The upper arm segment was constructed with the marker at the humeral head, a non-collinear marker on the upper arm, and the lateral humeral epicondyle marker. The forearm segment was created using the lateral humeral epicondyle marker, a non-collinear marker on the forearm, and the marker on the ulnar styloid process. The hand segment was created using the markers of the radial styloid, ulnar styloid, the head of the third metacarpal. Segment inertia parameters were based on body segment parameters (de Leva, 1996).

Cycle duration, defined as the elapsed time between successive hand-pushrim contacts, was determined using measured pushrim RF data. Contact phase of the cycle was defined from the point in time when the vertical component of the RF exceeded 3 N to the time of rim release, when the RF reduced to below 3 N. To characterize differences in initiation of hand contact with the pushrim and propulsion generation strategies between individuals, the number of peaks in RF observed during the contact phase were noted (**Figure 1**). The contact phase was further divided into sub-phases: the impact (IP) phase when present and a propulsion-generating phase(s) (PGP). The IP was defined as the interval immediately after pushrim contact (from initial hand contact to time of next local minimum) and was typically not associated with substantial torque acting to rotate the wheel. Time of peak push was identified as the time of the maximum peak in the vertical RF measured during PGP.

Kinematic and RF at the pushrim were synchronized at time of initial contact with the pushrim and used to calculate 3D NJM and NJF at the elbow and shoulder (100 Hz) using inverse dynamics in Visual3D. The magnitudes of the RF, NJF, and NJM at the elbow and shoulder are reported for peak push as the average of the six points around the peak in vertical RF during the PGP. The relative contribution of the elbow and shoulder to the mechanical demand imposed on the upper extremity was determined for peak push by the NJM at each joint divided by the sum of the NJMs at both joints (shoulder and elbow). The orientation of the RF relative to the forearm and upper arm was expressed by the angle of the resultant RF projected into the arm plane (created by the wrist, elbow, and shoulder).

Statistics

The probabilities for each variable being less during the free condition than the fast condition when comparing across propulsion conditions was calculated using a Sign Test. Assuming local independence for trials and that the free and fast conditions were independent for each subject, these comparisons were repeated for each variable for within-subject statistical significance as well (R, open-source). A p-value was then calculated for each subject using Cliff's analog of the Wilcoxon–Mann–Whitney test (Cliff, 1996). A modified, step-down Fisher-type method was then applied to control the familywise error rate of $\alpha = 0.05$ over multiple comparisons (Wilcox and Clark, 2015). This within-subject analysis was used to determine which subjects had statistically significant changes when comparing their self-selected free propulsion cycles to their self-selected fast propulsion cycles.

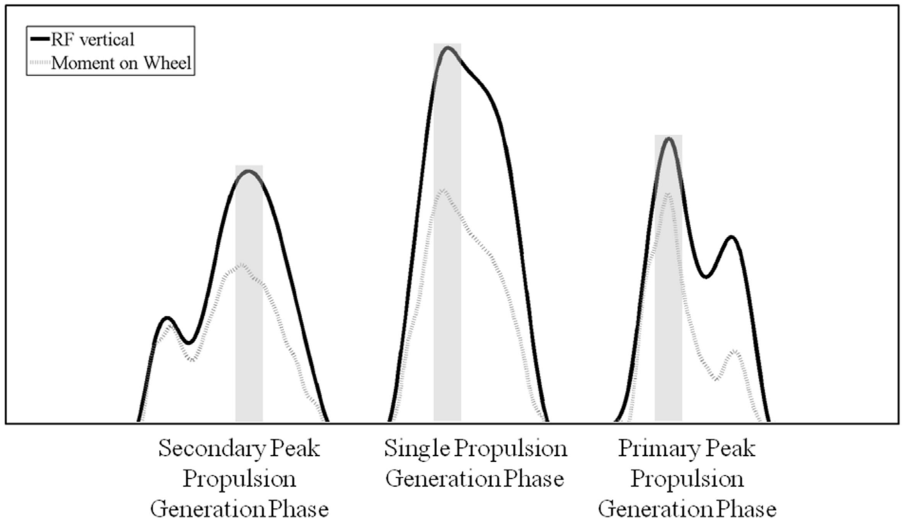

FIGURE 1 | Vertical reaction force and moment on the wheel for three example propulsion cycles illustrating the three different propulsion strategies seen in the data. The shaded regions show the duration around peak averaged to define peak push.

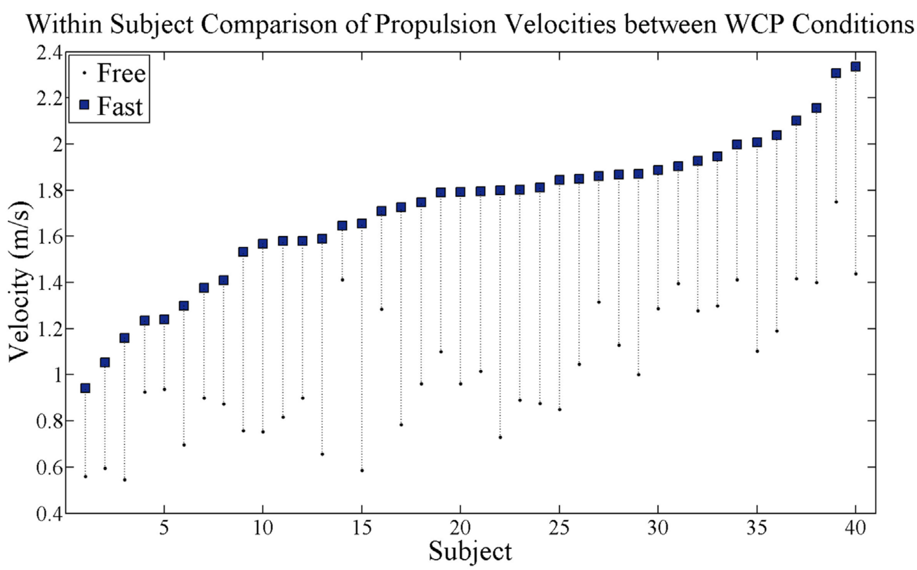

FIGURE 2 | Within-subject comparison of self-selected wheelchair propulsion velocity. Black dots are velocity at free speed condition and blue squares are velocity at fast speed condition. Dotted vertical lines connect each subject's free and fast velocities and show velocity increase. All subjects successfully increased propulsion velocity.

RESULTS

Consistent with the experimental design, all of the 40 participants significantly increased their WCP speed between free and fast conditions across all participants ($p = 0.0001$, **Figure 2**). Mean velocity across all participants during free condition was 1.02 m/s (0.3) and mean velocity across all participants during fast condition was 1.72 m/s (0.3). The velocity increase between free and fast conditions was on average 0.70 (0.2) m/s across participants.

As expected, hand-rim contact duration significantly decreased with increases in WCP speed across all participants ($p = 0.0001$, **Figure 3**). Within-subject comparisons indicated that 39 of the 40 participants reduced contact duration with increases in WCP speed. Of those 39 participants, 18 reduced contact duration by 0.20 s or more.

The resultant RF magnitude at peak push significantly increased for the fast as compared to the free WCP condition across all participants ($p = 0.0001$) (**Figure 4**). Within-subject

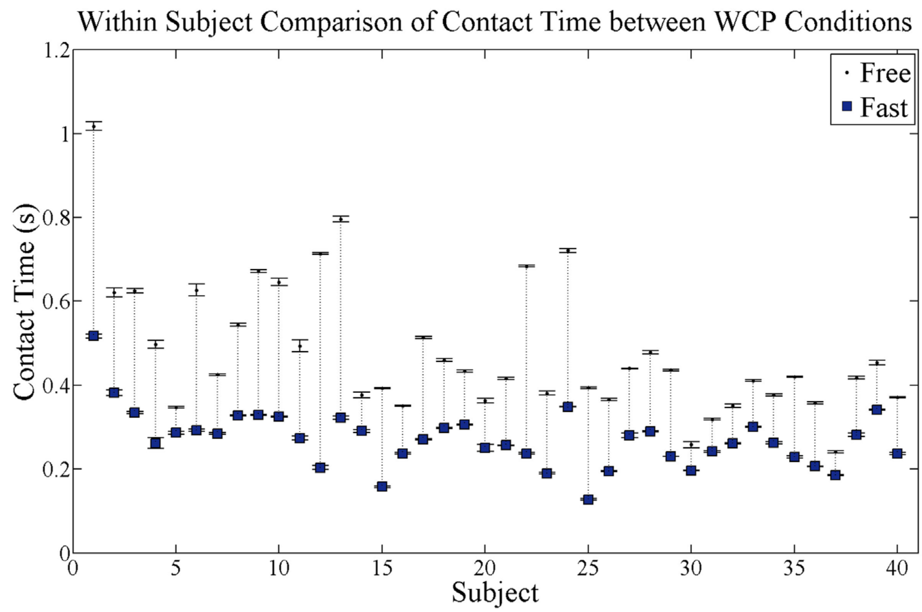

FIGURE 3 | Within-subject comparison of average contact time for each subject for both self-selected free and fast speed conditions. Black dots are contact time at free speed condition and blue squares are contact time at fast speed condition. SE bars are shown for both conditions. Dotted vertical lines connect each subject's free and fast contact times and show magnitude of the change in contact time. Within-subject comparison found 32 of the 40 participants significantly reduced contact duration.

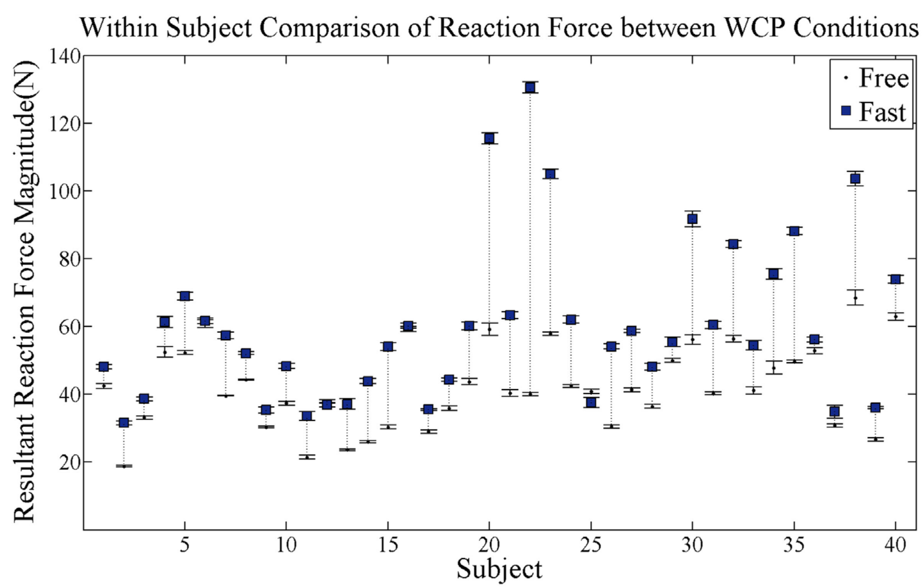

FIGURE 4 | Within-subject comparison of average resultant RF magnitude at peak push for each subject for both self-selected free and fast speed conditions. Black dots are average RF magnitude at free speed condition and blue squares are average RF magnitude at fast speed condition. SE bars are shown for both conditions. Dotted vertical lines connect each subject's free and fast RF magnitudes and show magnitude change in RF. Within-subject comparison found 26 of the 40 participants increased resultant RF at peak push.

comparisons indicated that 26 of the 40 participants increased resultant RF at peak push between the free and fast conditions. Of those 26 participants, 22 increased the resultant RF by 10 N or more.

The resultant shoulder NJM at peak push significantly increased in the fast as compared to free WCP conditions across all participants ($p = 0.0001$) (**Figure 5**). Within-subject comparison revealed that 30 of 40 participants increased resultant

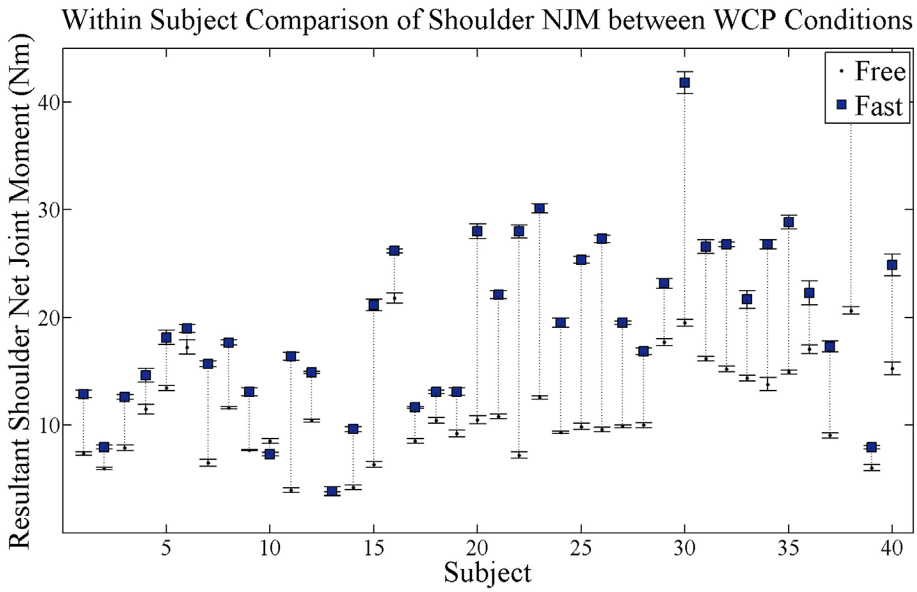

FIGURE 5 | Within-subject comparison of average resultant NJM magnitude on the shoulder at peak push for each subject for both self-selected free and fast speed conditions. Black dots are average shoulder NJM magnitude at free speed condition and blue squares are average shoulder NJM magnitude at fast speed condition. SE bars are shown for both conditions. Dotted vertical lines connect each subject's free and fast NJM magnitudes and show magnitude change in NJM. Within-subject comparison revealed that 30 of 40 participants showed a significant increase in resultant NJM on the shoulder with increases in WCP speed.

shoulder NJM with increases in WCP speed, with 15 participants increasing shoulder NJM by 10 Nm or more.

The resultant shoulder NJF at the time of peak push significantly increased in the fast as compared to free WCP conditions across all participants ($p = 0.0001$) (**Figure 6**). On average, resultant shoulder NJF increased by 23 N when propelling under the fast as compared to the free WCP condition.

As hypothesized, orientation of RF relative to the forearm and upper arm affected the mechanical demand imposed on the upper extremity with increases in WCP speed. Increases in RF magnitude did not necessarily result in proportionate increases in shoulder NJM within subject (**Figure 7**). For example, in the fast WCP condition, subjects A and B both generated relatively large RFs (130 and 92 N, respectively) but different techniques led to different magnitudes in shoulder NJMs (**Figure 7**). Subject A oriented the RF anterior to forearm resulting in an elbow extensor NJM and a shoulder flexor NJM of 28 Nm. In contrast, Subject B RF was more aligned with the forearm resulting in an elbow flexor NJM and a shoulder flexor NJM of 41 Nm.

Increase is WCP speed, from free to self-selected fast, was accomplished using different techniques within subject. In some cases, increases in WCP speed were associated with significant increase in RF magnitude without modifications in upper extremity kinematics (12 of 40). In other cases, individuals significantly modified RF orientation, forearm orientation, or both, resulting in modifications in mechanical demand imposed on the shoulder. More vertical orientations of the forearm at peak push was associated with hand positions more posterior on the pushrim, whereas more horizontal orientation of the forearm at peak push was associated with hand positions that were more anterior on the pushrim. No significant within-subject differences in elbow angle at peak push were noted between WCP speeds, suggesting muscle lengths were maintained across WCP conditions.

In some cases, individuals were able to mitigate increases in the rotational demand imposed on the shoulder with increases in WCP speed, whereas others were not. For example, the three exemplar participants achieved comparable fast WCP velocities with comparable RF magnitudes at peak push (**Figure 8A**). However, the magnitude of the shoulder NJM depended on the proximal distal moments created by the NJFs about the center of mass (CM) of the forearm and upper arm segments as well as the adjacent joint NJM at the elbow. When the RF is oriented *anterior* to the forearm CM, an elbow extensor NJM is needed to achieve the observed motion. The elbow extensor NJM applied to the upper arm contributes to the reduction in magnitude of the shoulder NJM. In contrast, when the RF is oriented *posterior* to the forearm CM, an elbow flexor NJM is needed to achieve the observed motion. The elbow flexor NJM applied to the upper arm contributes to the increase in magnitude of the shoulder NJM.

In the free WCP condition, the RF orientation relative to the forearm CM at peak push varied across all participants [anterior (17), aligned (10 within 5°), posterior (13), **Figure 8B**]. Likewise, in the fast propulsion condition, the RF orientation relative to the forearm CM at peak push tended to be evenly distributed across all participants [anterior (15), aligned (9 within 5°), posterior (16)].

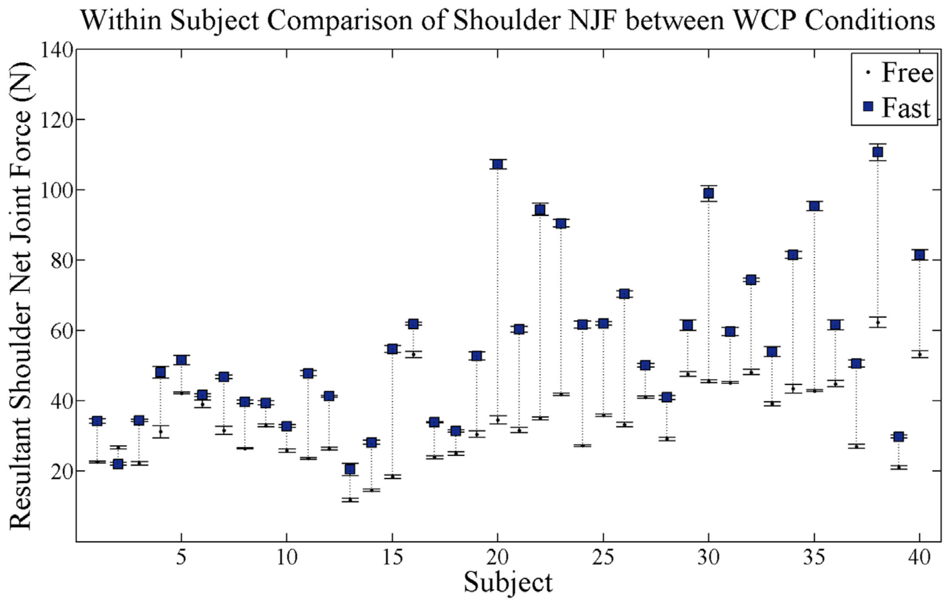

FIGURE 6 | Within-subject comparison of average resultant shoulder NJF magnitude at peak push for each subject for both self-selected free and fast speed conditions. Black dots are average shoulder NJF magnitude at free speed condition and blue squares are average shoulder NJF magnitude at fast speed condition. SE bars are shown for both conditions. Dotted vertical lines connect each subject's free and fast NJF magnitudes and show magnitude change in NJF.

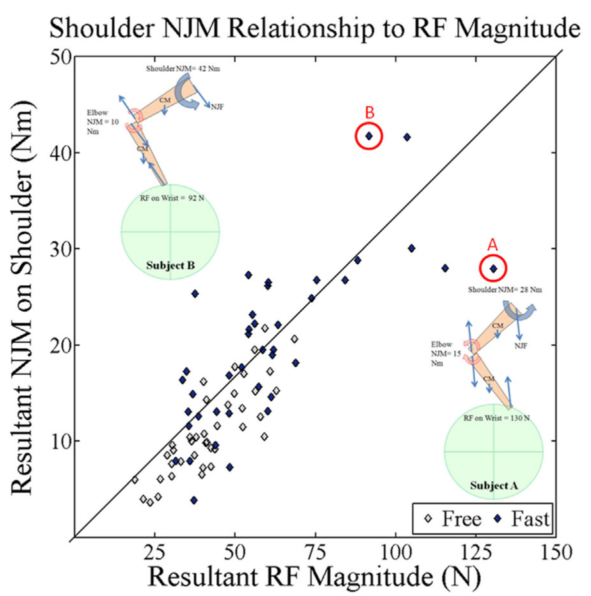

FIGURE 7 | Average resultant NJM magnitude on the shoulder at peak push for each subject for both self-selected free and fast speed conditions plotted against average resultant RF magnitude at peak push for each subject. Diagonal line represents a 1:1 relationship, meaning that a twofold increase in RF would lead to a twofold increase in NJM on the shoulder. At the higher RF magnitudes, a few subjects deviate further from this relationship. Subjects A and B illustrate how RF orientation relative to upper extremity can affect shoulder NJMs relationship to RF magnitude.

Within-subject comparison in RF orientation relative to the forearm CM at peak push indicated that shifts in orientation varied with WCP speed. Within-subject analysis indicated 11 of 40 participants made a significant shift in RF orientation relative to the forearm at peak push when increasing WCP speed. Six of 11 shifted RF in a direction consistent with increasing the shoulder NJM (**Figure 8A**), while five of 11 participants shifted RF in a direction consistent with decreasing the shoulder NJM. Nine of 11 participants modified the RF orientation relative to the forearm by more than 10°.

On an average, there were no consistent shifts across all participants in distribution of the total arm moment across the upper extremity when increasing WCP speed. Within-subject comparisons indicated that 10 of 40 participants showed a significant increase in the relative contribution of resultant shoulder NJM to the total arm moment. The largest shift in load distribution (reduction in shoulder NJM contribution to total arm moment by 30%) was accomplished by orienting RF more anterior to forearm (13–27°) and more aligned with the upper arm (28°).

No significant shifts in RF alignment with the arm plane at peak push were observed between WCP conditions across all participants. Within-subject analysis revealed that five of the 40 participants showed a statistically significant shift in RF alignment (re-alignment of RF relative to arm plane >5%) with increases in WCP speed. The RF was less aligned with the arm plane for four of five of those participants, thereby contributing to out of plane shoulder NJMs.

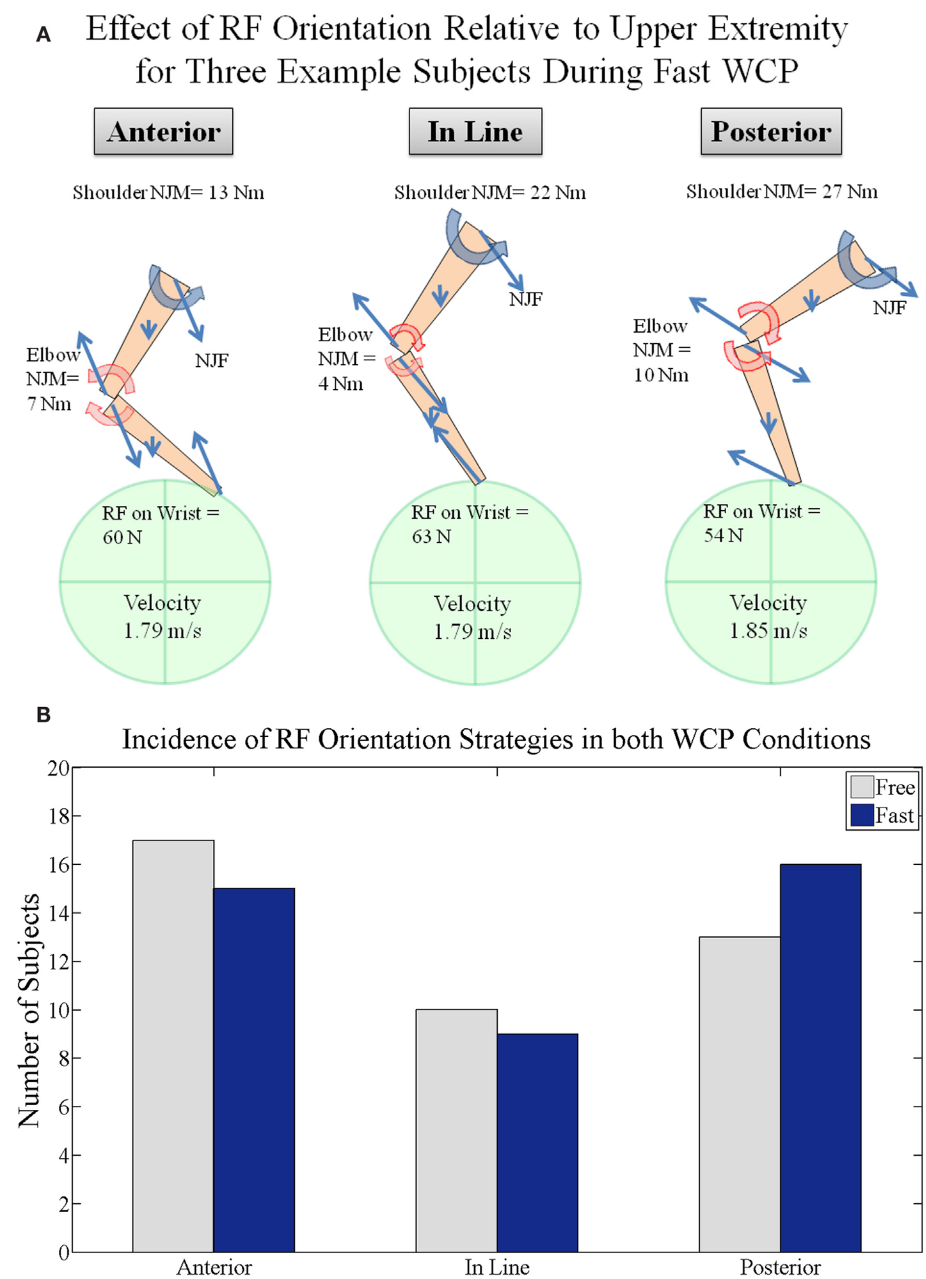

FIGURE 8 | (A) Effect of RF orientation relative to the upper extremity segments for three example subjects with comparable propulsion velocities and RF magnitudes. Free body diagrams are drawn for fast speed condition at the time of peak push. Note elbow NJMs are in opposite directions for the anterior and posterior examples and how that affects shoulder NJM. **(B)** Population grouping of RF component orientation in the armplane (plane that connects shoulder, elbow, and wrist) relative to the upper extremity at the time of peak push. Orientation is grouped into posterior (more than 5° behind the forearm), anterior (more than 5° in front of the forearm), and in line (within 5° posterior or anterior).

DISCUSSION

During daily activities, manual WC users often encounter situations that result in increases in the mechanical demand imposed on the upper extremity, such as speeding up, going up ramps, or traversing carpets and grass. Understanding the different techniques individual's use during tasks with increased upper extremity demands is important for identifying manual WCP strategies that can help preserve shoulder function, maintain independence, and improve quality of life. The results of this study indicate that increases in RF magnitudes associated with increases in WCP speed do not necessarily translate into comparable increases in shoulder NJMs. The magnitude of the shoulder NJM depends on the proximal distal moments created by the NJFs about the CM of the forearm and upper arm segments as well as the adjacent joint NJM at the elbow. Within-subject analysis indicated more than 25% of the participants made a significant shift in RF orientation relative to the forearm at peak push when increasing WCP speed. In approximately half of these cases, reorienting the RF relative to the upper extremity segments was used as an effective strategy for mitigating rotational mechanical demand imposed on the shoulder at increased WCP speeds. In the other cases, the shift in RF orientation relative to the forearm at peak push at increased WCP speeds contributed to increases in the shoulder NJM and reductions in the vertical component of the shoulder NJF. By investigating WCP technique modifications in response to increases in WCP speed using a within-subject design, preferential shifts in mechanical loading imposed on the shoulder can be determined. This knowledge of self-selected load mitigation strategies may prove fruitful in guiding clinical decisions that aim to identify strategies for preserving shoulder function in individuals with SCI.

The self-selected free and fast propulsion velocities attained in our sample population are comparable to those found in Kulig et al. (1998). Joint kinetics in this study was also found to be in line with magnitudes previously reported in the literature (Kulig et al., 1998; Koontz et al., 2002; Veeger et al., 2002; Collinger et al., 2008). In this study, an ergometer was used to achieve self-selected steady-state WCP speeds for multiple cycles. To minimize limitations associated with this experimental set-up, a within-subject design was used as a means for each individual to serve as their own control. Consistent with previously reported group mean data (Kulig et al., 1998; Koontz et al., 2002; Veeger et al., 2002; Collinger et al., 2008), the resultant RF as well as the resultant shoulder NJM and NJF at peak push significantly increased in the fast WCP speed condition when compared to free WCP across subjects.

In order to increase WCP speed, the tangential component of the RF being applied to the pushrim must increase in magnitude, particularly if the pushrim contact duration decreases with WCP speed. The participants in this study increased WCP speed using a variety of different techniques. Some participants increased WCP speed by amplifying RF magnitude without modifications in upper extremity kinematics. Whereas other individuals significantly modified RF orientation, forearm orientation, or both, resulting in modifications in mechanical demand imposed on the shoulder. Minimal changes in elbow angle at peak push were observed across speeds, suggesting individuals may have chosen to maintain a preferred muscle length when generating RF at peak push. Results of this study illustrated how choice of orientation of RF relative to the upper extremity affected mechanical demand on the shoulder. Orientation of RF anterior to the forearm CM created an elbow extensor NJM, which contributed to a reduction in shoulder NJM magnitude. Conversely, when RF was oriented posterior to the forearm CM the resulting elbow flexor NJM contributed to an increase in shoulder NJM magnitude. These results suggest that individuals choosing to modify WCP technique by shifting the RF more anterior to the forearm CM may favor reductions in shoulder NJM over increases in the vertical component of the RF, and vice versa. Identification of preferences toward a particular load mitigation strategy may prove fruitful in guiding clinical decisions that aim to identify strategies for preserving shoulder function in individuals with SCI.

The experimental results of this study are consistent with the model simulation results (Munaretto et al., 2012, 2013) that demonstrate at a particular WCP speed, increases in resultant pushrim RF can occur without comparable increase in shoulder NJM. The magnitude of the shoulder NJM is dependent on the proximal distal moments created by the NJFs at the elbow and shoulder and the elbow NJM (**Figure 8**). The magnitude of the proximal and distal moments is dependent on the magnitude of the NJFs and their orientation relative the upper arm. Redirection of the RF relative to the upper extremity, as shown in both the experimental and model simulation results, can serve as a potential strategy to redistribute load imposed on the upper extremity. Simulation results indicate that WCP speed can be maintained with minimal changes in shoulder NJM even if the corresponding RF doubles in magnitude, provided the RF is reoriented relative to the forearm and upper arm. These results indicate that alignment of the RF anterior to the forearm can mitigate the effect of higher pushrim forces on shoulder NJM magnitude. This strategy may prove to be an effective means of redistributing the mechanical loads imposed on the upper extremity joints during WCP.

Maintaining shoulder health requires more than reducing mechanical demand. Certain scapular and glenohumeral orientations have been associated with reducing subacromial space, which increases the potential risk of shoulder impingement syndrome. Previous research by Morrow et al. (2011) and Raina et al. (2012) found that WCP placed the scapula in some of these potentially dangerous orientations that could contribute to the development shoulder impingement. More specifically, Raina's study showed that with increases in propulsion force, WC user's scapula tended to move into anterior tilt, downward rotation, and protraction. All of these positions are associated with reduced subacromial space. If this scapular movement occurs in conjunction with upward motion of the humerus in the glenoid cavity, there is potential for impingement of the supraspinatus. The superiorly directed forces transmitted along the axis of the humerus could have a negative long-term consequence if not adequately controlled by muscles crossing the shoulder complex (Mulroy et al., 2005). However, further research must be done with more accurate methods of subacromial space estimation to see if the scapular movement found in WCP is clinically relevant (Raina et al., 2012). Any recommendation in technique modification must consider the ability of the individual to control RF and segment motion during task performance to avoid detrimental loading (McNitt-Gray, 2000).

By examining how individual WC users organized their upper limb coordination to accommodate increases in mechanical demands, effective multijoint control strategies for increasing WCP speed without substantial increases in the shoulder NJM was identified. Future studies will examine how this WCP technique may benefit those with different upper extremity control capabilities and will explore the relative contribution of these factors in regulating shoulder loads during WCP. For individuals unable to modify WCP technique by reorienting pushrim RF relative to the upper extremity segments, customized modifications in WC configuration, including optimal seat height (Kotajarvi et al., 2004), axle horizontal positions (Mulroy et al., 2005), and seat angle (Desroches et al., 2006), are alternative ways of redistributing the mechanical demands within the upper extremity joints.

SUPPLIERS

a. Digital Equipment Corporation, Cambridge, MA, USA.
b. Quickie GPV; Sunrise Medical, Quickie Designs Inc., 2842 Business Park Avenue, Fresno, CA 93727, USA.
c. Velodyne bicycle ergometer; Schwinn Bicycle Company, 217 N. Jefferson Street, Chicago, IL 60661, USA.
d. VICON (Oxford Metrics Ltd, Oxford, England).
e. C-Motion, Inc., 15821-A Crabbs Branch Way, Rockville, MD 20855, USA.
f. The MathWorks, Inc., 3 Apple Hill Drive, Natick, MA 01760-2098, USA.
g. R Programming Language. Link www.r-project.org.

ACKNOWLEDGMENTS

This study was supported by a grant from the National Institute of Health (R01 HD049774). This project was supported by SC CTSI (NIH/NCATS) through Grant UL1TR000130. Its contents are solely the responsibility of the authors and do not necessarily represent the official views of the NIH.

REFERENCES

Alm, M., Saraste, H., and Norrbrink, C. (2008). Shoulder pain in persons with thoracic spinal cord injury: prevalence and characteristics. *J. Rehabil. Med.* 40, 277–283. doi:10.2340/16501977-0173

Bayley, J. C., Cochran, T. P., and Sledge, C. B. (1987). The weight-bearing shoulder. The impingement syndrome in paraplegics. *J. Bone Joint Surg. Am.* 69, 676–678.

Cliff, N. (1996). Answering ordinal questions with ordinal data using ordinal statistics. *Multivar. Behav. Res.* 31, 331–350. doi:10.1207/s15327906mbr3103_4

Collinger, J. L., Boninger, M. L., Koontz, A. M., Price, R., Sisto, S. A., Tolerico, M. L., et al. (2008). Shoulder biomechanics during the push phase of wheelchair propulsion: a multisite study of persons with paraplegia. *Arch. Phys. Med. Rehabil.* 89, 667–676. doi:10.1016/j.apmr.2007.09.052

Cooper, R. A., DiGiovine, C. P., Boninger, M. L., Shimada, S. D., Koontz, A. M., and Baldwin, M. A. (2002). Filter frequency selection for manual wheelchair biomechanics. *J. Rehabil. Res. Dev.* 39, 323–336.

Curtis, K. A., Drysdale, G. A., Lanza, R. D., Kolber, M., Vitolo, R. S., and West, R. (1999). Shoulder pain in wheelchair users with tetraplegia and paraplegia. *Arch. Phys. Med. Rehabil.* 80, 453–457. doi:10.1016/S0003-9993(99)90285-X

Dalyan, M., Cardenas, D. D., and Gerard, B. (1999). Upper extremity pain after spinal cord injury. *Spinal Cord* 37, 191–195. doi:10.1038/sj.sc.3100802

de Leva, P. (1996). Adjustments to Zatsiorsky-Seluyanov's segment inertia parameters. *J. Biomech.* 29, 1223–1230. doi:10.1016/0021-9290(95)00178-6

Desroches, G., Aissaoui, R., and Bourbonnais, D. (2006). Effect of system tilt and seat-to-backrest angles on load sustained by shoulder during wheelchair propulsion. *J. Rehabil. Res. Dev.* 43, 871–882. doi:10.1682/JRRD.2005.12.0178

Gironda, R. J., Clark, M. E., Neugaard, B., and Nelson, A. (2004). Upper limb pain in a national sample of veterans with paraplegia. *J. Spinal Cord Med.* 27, 120–127.

Gutierrez, D. D., Thompson, L., Kemp, B., and Mulroy, S. J. (2007). The relationship of shoulder pain intensity to quality of life, physical activity, and community participation in persons with paraplegia. *J. Spinal Cord Med.* 30, 251–255.

Inman, V. T., Saunders, J. B., and Abbott, L. C. (1944). Observations on the function of the shoulder joint. *J. Bone Joint Surg.* 26A, 3–30.

Jain, N. B., Higgins, L. D., Katz, J. N., and Garshick, E. (2010). Association of shoulder pain with the use of mobility devices in persons with chronic spinal cord injury. *Platin. Met. Rev* 2, 896–900. doi:10.1016/j.pmrj.2010.05.004

Koontz, A. M., Cooper, R. A., Boninger, M. L., Souza, A. L., and Fay, B. T. (2002). Shoulder kinematics and kinetics during two speeds of wheelchair propulsion. *J. Rehabil. Res. Dev.* 39, 635–650.

Kotajarvi, B. R., Sabick, M. B., An, K. N., Zhao, K. D., Kaufman, K. R., and Basford, J. R. (2004). The effect of seat position on wheelchair propulsion biomechanics. *J. Rehabil. Res. Dev.* 41, 403–414. doi:10.1682/JRRD.2003.01.0008

Kulig, K., Newsam, C. J., Mulroy, S. J., Rao, S., Gronley, J. K., Bontrager, E. L., et al. (2001). The effect of level of spinal cord injury on shoulder joint kinetics during manual wheelchair propulsion. *Clin. Biomech.* 16, 744–751. doi:10.1016/S0268-0033(01)00066-3

Kulig, K., Rao, S. S., Mulroy, S. J., Newsam, C. J., Gronley, J. K., Bontrager, E. L., et al. (1998). Shoulder joint kinetics during the push phase of wheelchair propulsion. *Clin. Orthop. Relat. Res.* 354, 132–143. doi:10.1097/00003086-199809000-00016

Lighthall-Haubert, L., Requejo, P. S., Mulroy, S. J., Newsam, C. J., Bontrager, E., Gronley, J. K., et al. (2009). Comparison of shoulder muscle electromyographic activity during standard manual wheelchair and push-rim activated power assisted wheelchair propulsion in persons with complete tetraplegia. *Arch. Phys. Med. Rehabil.* 90, 1904–1915. doi:10.1016/j.apmr.2009.05.023

Mathiyakom, W., McNitt-Gray, J. L., Requejo, P. S., and Costa, K. E. (2005). Modifying center of mass trajectory during sit-to-stand tasks redistributes the mechanical demand across the lower extremity joints. *J Clin Biomech.* 20, 105–111. doi:10.1016/j.clinbiomech.2004.08.005

McCully, S. P., Suprak, D. N., Kosek, P., and Karduna, A. R. (2007). Suprascapular nerve block results in a compensatory increase in deltoid muscle activity. *J. Biomech.* 40, 1839–1846. doi:10.1016/j.jbiomech.2006.07.010

McNitt-Gray, J. L. (2000). Subject specific coordination of two- and one-joint muscles during landings suggests multiple control criteria. *Motor Control* 4, 84–88. discussion 97–116.

McNitt-Gray, J. L., Hester, D. M., Mathiyakom, W., and Munkasy, B. A. (2001). Mechanical demand and multijoint control during landing depend on orientation of the body segments relative to the reaction force. *J. Biomech.* 34, 1471–1482. doi:10.1016/S0021-9290(01)00110-5

Mercer, J. L., Boninger, M., Koontz, A., Ren, D., Dyson-Hudson, T., and Cooper, R. (2006). Shoulder joint kinetics and pathology in manual wheelchair users. *Clin Biomech (Bristol, Avon)* 21, 781–789. doi:10.1016/j.clinbiomech.2006.04.010

Morrow, M. M. B., Kaufman, K. R., and An, K. N. (2011). Scapula kinematics and associated impingement risk in manual wheelchair users during propulsion and a weight relief lift. *Clin. Biomech.* 26, 352–357. doi:10.1016/j.clinbiomech.2010.12.001

Mulroy, S. J., Farrokhi, S., Newsam, C. J., and Perry, J. (2004). Effects of spinal cord injury level on the activity of shoulder muscles during wheelchair propulsion: an electromyographic study. *Arch. Phys. Med. Rehabil.* 85, 925–934. doi:10.1016/j.apmr.2003.08.090

Mulroy, S. J., Gronley, J. K., Newsam, C. J., and Perry, J. (1996). Electromyographic activity of shoulder muscles during wheelchair propulsion by paraplegic persons. *Arch. Phys. Med. Rehabil.* 77, 187–193. doi:10.1016/S0003-9993(96)90166-5

Mulroy, S. J., Newsam, C. J., Gutierrez, D. D., Requejo, P., Gronley, J. K., Haubert, L. L., et al. (2005). Effect of fore-aft seat position on shoulder demands during wheelchair propulsion: Part 1. A kinetic analysis. *J. Spinal Cord Med.* 28, 214–221.

Munaretto, J. M., McNitt-Gray, J. L., Flashner, H., and Requejo, P. S. (2012). Simulated effect of reaction force redirection on the upper extremity mechanical demand imposed during manual wheelchair propulsion. *Clin. Biomech. (Bristol, Avon)* 27, 255–262. doi:10.1016/j.clinbiomech.2011.10.001

Munaretto, J. M., McNitt-Gray, J. L., Flashner, H., and Requejo, P. S. (2013). Reconfiguration of the upper extremity relative to the pushrim affects load distribution during wheelchair propulsion. *Med. Eng. Phys.* 35, 1141–1149. doi:10.1016/j.medengphy.2012.12.002

Pentland, W. E., and Twomey, L. T. (1994). Upper limb function in persons with long term paraplegia and implications for independence: Part II. *Paraplegia* 32, 219–224. doi:10.1038/sc.1994.41

Raina, S., McNitt-Gray, J. L., Mulroy, S., and Requejo, P. S. (2012). Effect of increased load on scapular kinematics during manual wheelchair propulsion in individuals with paraplegia and tetraplegia. *Hum. Mov. Sci.* 31, 397–407. doi:10.1016/j.humov.2011.05.006

Requejo, P. S., Lee, S. E., Mulroy, S. J., Haubert, L. L., Bontrager, E. L., Gronley, J. K., et al. (2008). Shoulder muscular demand during lever-activated vs pushrim wheelchair propulsion in persons with spinal cord injury. *J. Spinal Cord Med.* 31, 568–577.

Robertson, R. N., Boninger, M. L., Cooper, R. A., and Shimada, S. D. (1996). Pushrim forces and joint kinetics during wheelchair propulsion. *Arch. Phys. Med. Rehabil.* 77, 856–864. doi:10.1016/S0003-9993(96)90270-1

Samuelsson, K. A., Tropp, H., and Gerdle, B. (2004). Shoulder pain and its consequences in paraplegic spinal cord-injured, wheelchair users. *Spinal Cord* 42, 41–46. doi:10.1038/sj.sc.3101490

Sie, I. H., Waters, R. L., Adkins, R. H., and Gellman, H. (1992). Upper extremity pain in the postrehabilitation spinal cord injured patient. *Arch. Phys. Med. Rehabil.* 73, 44–48.

Silfverskiold, J., and Waters, R. L. (1991). Shoulder pain and functional disability in spinal cord injury patients. *Clin. Orthop. Relat. Res.* 272, 141–145.

Veeger, H. E., Rozendaal, L. A., and van der Helm, F. C. (2002). Load on the shoulder in low intensity wheelchair propulsion. *Clin. Biomech. (Bristol, Avon)* 17, 211–218. doi:10.1016/S0268-0033(02)00008-6

Wilcox, R. R., and Clark, F. (2015). Robust multiple comparisons based on combined probabilities from independent tests. *J. Data Sci.* 13, 43–52.

Wu, G., van der Helm, F. C., Veeger, H. E., Makhsous, M., Van Roy, P., Anglin, C., et al. (2005). ISB recommendation on definitions of joint coordinate systems of various joints for the reporting of human joint motion – Part II: shoulder, elbow, wrist and hand. *J. Biomech.* 38, 981–992. doi:10.1016/j.jbiomech.2004.05.042

Conflict of Interest Statement: The authors declare that the research was conducted in the absence of any commercial or financial relationships that could be construed as a potential conflict of interest.

frontiers in Bioengineering and Biotechnology

PERSPECTIVE
published: 27 July 2015
doi: 10.3389/fbioe.2015.00105

Variability in wheelchair propulsion: a new window into an old problem

Jacob J. Sosnoff[1], Ian M. Rice[1], Elizabeth T. Hsiao-Wecksler[2], Iris M. K. Hsu[2], Chandrasekaran Jayaraman[3] and Yaejin Moon[1]*

[1] Department of Kinesiology and Community Health, University of Illinois at Urbana-Champaign, Urbana, IL, USA, [2] Department of Mechanical Engineering and Sciences, University of Illinois at Urbana-Champaign, Urbana, IL, USA, [3] Department of Industrial and Enterprise Systems Engineering, University of Illinois at Urbana-Champaign, Urbana, IL, USA

Manual wheelchair users are at great risk for the development of upper extremity injury and pain. Any loss of upper limb function due to pain adversely impacts the independence and mobility of manual wheelchair users. There is growing theoretical and empirical evidence that fluctuations in movement (i.e., motor variability) are related to musculoskeletal pain. This perspectives paper discusses a local review on several investigations examining the association between variability in wheelchair propulsion and shoulder pain in manual wheelchair users. The experimental data reviewed highlights that the variability of wheelchair propulsion is impacted by shoulder pain in manual wheelchair users. We maintain that inclusion of these metrics in future research on wheelchair propulsion and upper limb pain may yield novel data. Several promising avenues for future research based on this collective work are discussed.

Keywords: motor variability, complexity, wheelchair biomechanics, injuries, kinematics, kinetics

OPEN ACCESS

Edited by:
Philip Santos Requejo, Rancho Los Amigos National Rehabilitation Center, USA

Reviewed by:
Henrique De Amorim Almeida, Polytechnic Institute of Leiria, Portugal
Elizabeth B. Torres, Rutgers University, USA

****Correspondence:***
Ian M. Rice, Department of Kinesiology and Community Health, University of Illinois at Urbana-Champaign, 303 Freer Hall, 906 South Goodwin Avenue, Urbana, IL 61801, USA
ianrice@illinois.edu

Specialty section:
This article was submitted to Biomechanics, a section of the journal Frontiers in Bioengineering and Biotechnology

Received: *04 May 2015*
Accepted: *10 July 2015*
Published: *27 July 2015*

Citation:
Sosnoff JJ, Rice IM, Hsiao-Wecksler ET, Hsu IMK, Jayaraman C and Moon Y (2015) Variability in wheelchair propulsion: a new window into an old problem. Front. Bioeng. Biotechnol. 3:105. doi: 10.3389/fbioe.2015.00105

There are an estimated 1.5 million manual wheelchair users in the United States (LaPlante and Kaye, 2010). Manual wheelchair users use their upper limbs for mobility and most functional activities. Unfortunately, the human upper limb is not specialized for the repetitive loading required for wheelchair propulsion. This requirement predisposes manual wheelchair users for upper limb pathology. Indeed, up to 70% of manual wheelchair users report upper limb pain (Nichols et al., 1979; Curtis et al., 1999; Gironda et al., 2004), which is mainly manifested in the shoulder and wrist (Dalyan et al., 1999). Furthermore, even in manual wheelchair users who do not report pain, there is evidence of degenerative changes in the shoulder (Lal, 1998), suggesting that it is just a matter of time before these asymptomatic individuals will experience pain.

Upper limb pain in wheelchair users has been linked to difficulty in performing activities of daily living (Dalyan et al., 1999), decreased physical activity, and decreased quality of life (Gutierrez et al., 2007). Overall, any loss of upper limb function due to pain adversely impacts the independence and mobility of manual wheelchair users. It has been speculated that a decrease in independence and mobility results in greater health care costs and an increased risk for secondary morbidity (cardiovascular disease, obesity, etc.) (Silfverskiold and Waters, 1991; Pentland and Twomey, 1994).

The development of upper limb pain in wheelchair users is a multifaceted process (Dyson-Hudson and Kirshblum, 2004). It has been suggested that upper limb pain is related to functional level (Curtis et al., 1999), duration of wheelchair use, wheelchair design (van der Woude et al., 2006), body weight (Sinnott et al., 2000; Collinger et al., 2008), propulsion mechanics (Koontz et al., 2002; Mercer et al., 2006), muscle coordination (Burnham et al., 1993; Kotajarvi et al., 2002), age (Fullerton et al., 2003), and gender (Lal, 1998; Gutierrez et al., 2007). The multi-factorial nature of the possible mechanisms and associated variables creates a daunting task for researchers and clinicians.

Variability as a Potential Indicator of Upper Extremity Injury

Recently, analysis of motor variability has been utilized as a new approach to understand ergonomic repetitive strain injuries (Srinivasan and Mathiassen, 2012). Although variability measures have been included in investigations focusing on learning of wheelchair propulsion in non-wheelchair users (Vegter et al., 2013, 2014), variability analysis has not been incorporated in investigations of upper extremity pain in manual wheelchair users. To fully understand the potential value of variability analysis to shoulder pain and wheelchair propulsion, it is worthwhile to briefly review this approach.

First and foremost, it is essential to appreciate that variability is inherent within all physiological systems. Despite its ubiquitous status, fluctuations in physiological output including motor variability were historically seen as a nuisance to scientific inquiry; something to be experimentally minimized or altogether eliminated (Newell and Corcos, 1993). However, this approach to variability tends to ignore that variability specifically within an individual can provide important information concerning health and function.

The introduction of non-linear dynamics and chaos theory to motor control and rehabilitation science led to the observation that variability (operationalized as fluctuations of physiological output within an individual) can provide unique information concerning the control and health of the neuromuscular system (Lipsitz, 2004; Sosnoff and Newell, 2006a). Aberrations in health are frequently denoted by a change in within individual variability (Sosnoff and Newell, 2006b). Examining variability in health has led to important insights in understanding the development of overuse injuries. Optimal musculoskeletal health results from repetitive sub-maximal loading with a certain amount of variability in frequency (i.e., timing) and rate of loading (i.e., force application) (Hamill et al., 1999). It is maintained that a lack of variation results in insufficient time to adapt (i.e., heal) between loading occasions. To date, a relation between kinematic variability and skeletal injury has been demonstrated in individuals with knee (Hamill et al., 1999), shoulder (Madeleine et al., 2008), and low-back pain (Lamoth et al., 2006).

For instance, a series of investigations examining upper limb occupational tasks, such as butchering, have reported an increase in arm movement variability in individuals with musculoskeletal pain (Madeleine et al., 2008; Lomond and Cote, 2011). Additionally, studies examining repetitive reaching tasks demonstrate that subjects with shoulder pain exhibited higher relative variability in their kinematics than those without pain (Lomond and Cote, 2010, 2011). Based on this collective body of work, we have speculated that variability in wheelchair propulsion is related to shoulder pain in manual wheelchair users. The purpose of this local review is to discuss published and unpublished research examining variability in wheelchair propulsion as a function of shoulder pain from our research group.

Variability and Wheelchair Propulsion: Recent Investigations

Recently, our research group at the University of Illinois at Urbana-Champaign supported by the National Institute of Health (#1R21HD066129-01A1) has set out to apply variability analyses to wheelchair propulsion. Specifically, we have conducted several investigations examining the association between variability in wheelchair propulsion and shoulder pain in manual wheelchair users.

Experimental Set Up

The data incorporated into these investigations (Moon et al., 2013; Jayaraman et al., 2014; Rice et al., 2014a) were derived from the same experimental set up. For brevity, the experimental setup and methodology will be described prior to detailing the actual investigations. Specifically, experienced manual wheelchair users with a range of physical disabilities propelled their own wheelchairs that where equipped with force sensing wheels (Smartwheels™) at a steady state pace on a dynamometer at three different speeds (self-selected, 0.7 m/s, 1.1 m/s) for 3 min. The use of force sensing wheels allowed for the determination of temporal–spatial and kinetic data relating to wheelchair propulsion. Additionally, we collected kinematic data on arm motion using a 10 camera motion capture system (Raptor Digital RealTime System, Motion Analysis Co., Santa Rosa, CA, USA), which tracked reflective markers on the participant's upper body bony landmarks. Based on international society of biomechanics recommendations (Wu et al., 2005), 18 reflective markers were attached bilaterally, at specific bony landmarks on the following locations: third metacarpophalangeal joint (i.e., middle finger knuckle), radial styloid (outside of writs), ulnar styloid (inside of wrist), olecronon process (tip of elbow), lateral epicondyl, acromion (front of shoulder), sternal notch (chest), C7 vertebrae (base of neck), T3 vertebrae (base of skull), T6 vertebrae (middle region of the spine), and jaw.

Wheelchair Propulsion Variability: Experimental Data

Figure 1A depicts the resultant force profile over 2 min of wheelchair propulsion of an individual with spinal cord injury. Subtle variations in the force profile between individual pushes are evident. Traditionally, researchers have averaged across the force profile of individual push cycles. Our first investigation sought to determine whether intra-individual variability of kinetic and temporal–spatial parameters of wheelchair propulsion was distinct in manual wheelchair users with and without shoulder pain (Rice et al., 2014a).

In this investigation, data from 26 adults [with shoulder pain ($n = 13$) and without shoulder pain ($n = 13$)] with a range of physical disabilities who use a manual wheelchair for mobility were analyzed. Specifically, intra-individual mean, SD, and coefficient of variation of (CV = mean/SD) of kinetic and temporal–spatial metrics were determined for salient spatiotemporal events (e.g., push time, peak push force, etc.).

Consistent with previous research (Mercer et al., 2006; Collinger et al., 2008), shoulder pain had no influence on mean

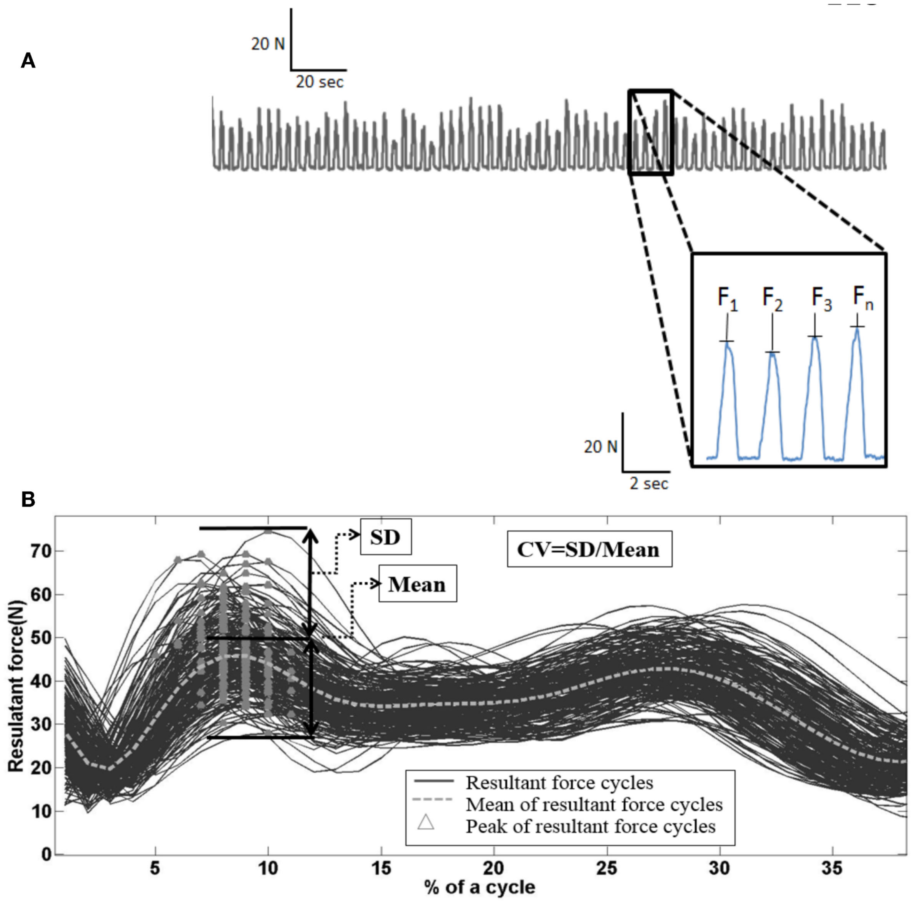

FIGURE 1 | (A) Peak hand-rim resultant force profile as a function of time during steady state wheelchair propulsion. Inset illustrates subtle variations in peak force over four pushes. **(B)** Resultant shoulder force output during the push phase of ~300 pushes of steady state wheelchair propulsion. Dashed line depicts mean resultant force, while triangles depict individual cycle peak resultant shoulder force.

kinetic and temporal–spatial propulsion variables at the hand-rim. However, significant group differences were found in relative variability (i.e., CV). Specifically, individuals with shoulder pain displayed less relative variability in their cycle-to-cycle peak resultant force and push time than individuals without shoulder pain. These preliminary results suggest that intra-individual variability analysis is sensitive to shoulder pain.

In a subsequent investigation, our research team examined the variability of peak resultant force acting on the shoulder during the push phase of wheelchair propulsion in individuals with and without self-reported shoulder pain (Moon et al., 2013). **Figure 1B** illustrates resultant force acting on the shoulder of a participant during steady state wheelchair propulsion. It is apparent in the figure that there are significant fluctuations in peak force from cycle to cycle. Propulsion data from 24 manual wheelchair users (13 with pain, 11 without pain) were included in the investigation. Peak resultant shoulder forces in the push phase were calculated using inverse dynamics. Mean, SD, and coefficient of variation of cycle-to-cycle peak resultant forces were calculated and analyzed as a function of shoulder pain.

Consistent with previous reports (Mercer et al., 2006; Collinger et al., 2008), we found no difference in mean peak shoulder resultant force between pain groups [no pain (41.38 ± 3.06 N) versus pain (44.16 ± 3.06 N)]. However, the pain group had significantly smaller variability of peak resultant force than the no pain group. These observations further raise the possibility that variability during the push phase of wheelchair propulsion maybe related to upper limb pain in manual wheelchair users.

In another investigation, we focused on intra-individual variability during the recovery phase of wheelchair propulsion as a function of shoulder pain (Jayaraman et al., 2014). Given that the recovery stroke is dependent upon the propulsion pattern employed (Sanderson and Sommer, 1985; Shimada et al., 1998), this investigation only included individuals who utilized a semi-circular propulsion pattern. Specifically, data from 10 experienced adult manual wheelchair users with spinal cord injury (5 with shoulder pain; 5 without shoulder pain) were analyzed. Intra-individual kinematic spatial variability of the steady state wrist motion during the recovery phase was determined using principal component analysis (PCA). PCA belongs to the factor analysis family and is a statistical decomposition technique used to identify patterns in data, thus, highlighting data similarities and differences (Daffertshofer et al., 2004).

Utilizing this technique, the kinematic spatial variability was calculated at 10% intervals along the wrist recovery path. Spatial variability was found to be highest at the start and end of the

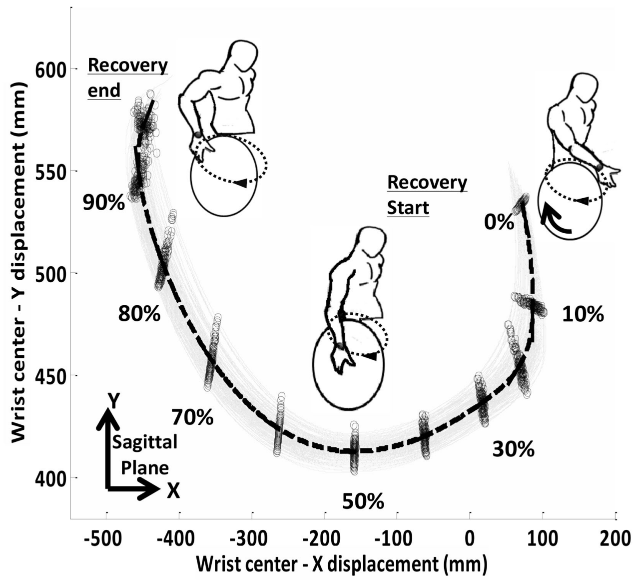

FIGURE 2 | Wrist recovery trajectories during semi-circular pattern wheelchair propulsion. Wrist cycle-to-cycle recovery trajectories ("gray solid lines"). The mean wrist recovery trajectory is shown by the bold dashed line. The wrist positions orthogonal to mean recovery trajectory for which PCA was computed (0–100% at every 10% interval along the recovery path) is denoted by ("o").

recovery path and lowest during the middle of the recovery path (**Figure 2**). Additionally, individuals with shoulder pain displayed significantly higher kinematic spatial variability than individuals without shoulder pain at the start (at 10% interval) of the recovery phase.

This pilot investigation further highlights that the analysis of intra-individual variability during manual wheelchair propulsion can distinguish between those with and without shoulder pain. It provides further evidence that variability analysis of wheelchair propulsion may offer a new approach to examine the impact of shoulder pain.

It is important to note that the association between pain and variability was distinct between the investigations that focused on push and recovery phase of wheelchair propulsion. Indeed, the first two investigations (Moon et al., 2013; Rice et al., 2014a) reported that those with shoulder pain had less variability than those without out; however, the investigation that exclusively focused on recovery phase demonstrated that those with pain had greater variability in their movement. There are several potential explanations for this discrepancy. Perhaps, the most straightforward is the difference in kinetics versus kinematics. It is possible that participants constrained their movement when applying pressure to the hand-rim in an effort to stay in a "pain free/minimization" zone. However, when their arm is unconstrained, they are more variable. Indeed, research focusing on unconstrained reaching tasks has demonstrated that those with shoulder injury/pain have greater kinematic variability than those without pain (Lomond and Cote, 2010, 2011). It is important to note that, Hamill et al. (2012) have theorized that musculoskeletal injury, such as shoulder pain in manual wheelchair users, can develop from either too little or too much motor variability. The complex relationship between motor variability and musculoskeletal injury warrants further investigation.

The collective findings also highlight that the importance of identifying the appropriate wheelchair propulsion variable to investigate. The variables that we have examined were based on previous reports (Morrow et al., 2009) and accepted practice in the field. It is quite possible that variability of other measures is more informative. For instance, it has been suggested that the variability of the interaction between segments or joints (i.e., coordinative variability) plays a key role in patella-femoral pain syndrome (Hamill et al., 2012). Further work is necessary to determine the appropriate variables of study.

Novel Approaches to Examine Variability in Wheelchair Propulsion

In addition to the published investigations detailed above, we have also conducted several preliminary analyses focusing on novel variability metrics. For instance, recently, we have sought to determine whether temporal variations between strokes are random or rather have some quantifiable structure, such as walking (Hausdorff, 2007). In this preliminary investigation data from 13 experienced adult manual wheelchair users with spinal cord injury were analyzed. A time series of resultant force at hand-rim was computed from the raw SMARTWheel data. To maintain consistency on the number of data points analyzed across individuals, only data from 100 cycles from each participant were used. Based on the occurrence of peak resultant force event on each cycle, two measures were extracted, namely, (1) a time series of cycle peak resultant force amplitude (PFR) and (2) a time series of inter-push time interval between peak resultant force (IPT) (Figure S1 in Supplementary Material). To investigate if the temporal variability observed in peak resultant force and inter-push time were random or had time-dependent structure, 1000 randomly shuffled surrogate time series were produced from each original time series. Each surrogate time series has the same distributional properties (mean and variance) as its corresponding original time series except that the order of occurrence of data points is randomized. Following the generation of surrogate time series, sample entropy (SampEn) of the original and each of its surrogate time series were computed. SampEn, is a metric that quantifies the regularity of a time series (Yentes et al., 2013). The SampEn of each original time series was then compared to the mean SampEn of surrogated counter parts (Paired t-test, two-tailed, $\alpha = 0.05$).

As expected, the original and surrogated data had identical mean (SD) of peak resultant force and inter-push time as 57.21 (16.63) N and 1.15 (0.22) s, respectively. Statistical analysis revealed that the SampEn of the original time series was significantly different than the surrogated time series for both peak resultant force and inter-push interval (p's < 0.05). The mean sample entropy for the surrogate time series [PFR: 2.13 (0.12); IPT: 2.02 (0.26)] was higher than that obtained from the original time series [PFR: 2.07 (0.13); IPT: 1.87 (0.25)]. These preliminary results indicate that time- and amplitude-dependent variability in resultant force observed in wheelchair propulsion are not random and have quantifiable structure. A significant limitation of this pilot investigation is that the time series of propulsion data is relatively small ($n = 100$ data points) for this type of analysis. It remains to be determined whether or not this structure is informative of upper extremity injury or other adverse consequences of wheelchair propulsion.

In another analytical approach, we examined the variability of arm motion during wheelchair propulsion utilizing phase portraits (Hsu et al., 2012). Phase portraits, which are graphical representations of position relative to velocity, can be used to explore the dynamics of a system over multiple cycles. We implement techniques developed to examine changes in variability and complexity in the shape of phase portraits. Variability was quantified by examining fluctuations of the centroid of each phase portrait over multiple cycles, specifically by calculating the confidence area and drift of the centroid. Complexity of the portrait was quantified by determining the portrait shape's frequency content using Fourier-based methods (DiBerardino et al., 2010). In this preliminary analysis, phase portraits of shoulder flexion–extension angular position versus angular velocity were examined as function of propulsion speed (see Figure S2 in Supplementary Material).

Data from nine experienced manual wheelchair users were analyzed in this pilot analysis. Variability parameters had mixed results with propulsion speed. There was a trend for the centroid area to increase with speed; whereas there was no significant change in centroid drift. Complexity of the phase portrait shape decreased significantly with speed. These results support prior work that propulsion speed impacts shoulder biomechanics (McGregor et al., 2009). Future work needs to determine if variability and complexity metrics of phase portrait are sensitive to shoulder pain similar to other metrics that we have utilized.

Limitations

Despite the novelty of this body of research, it was not without limitations. Specifically, these investigations included individuals who were manual wheelchair users, regardless of disability. Consequently, it is possible that differences in propulsion variability between pain groups was due to different disability being represented in each group and not shoulder pain *per se*. We do note that removal of participants without spinal dysfunction did not change the observe results in any of the reported studies and that ~80% of the sample were individuals with spinal dysfunction. The data were collected on a roller dynamometer, so it is not clear if these differences in propulsion variability would occur in over ground propulsion. Additionally, the use dynamometer precludes examination of some viable metrics, such as left-right coupling of steering (Vegter et al., 2013). It is also important to note that these investigations, classified individuals based on self-report of shoulder pain and no radiological information was collected. Future research utilize other measures of upper extremity pain are warranted. The association between pain in other joints, such as the wrist and elbow, and propulsion variability is not clear. Perhaps, the largest limitation is that this research is cross-sectional in nature, so no conclusions regarding causation can be made. We note that although these are significant limitations they are relatively common to wheelchair propulsion research.

Future Steps in Variability Analysis in Wheelchair Propulsion

The reviewed work highlights that variability of wheelchair propulsion maybe related to shoulder pain. We maintain that these metrics should be included in future research on wheelchair propulsion and upper limb pain. There are several promising avenues for future research based on this collective work.

The most important and perhaps most difficult step is to examine whether within individual variability in wheelchair propulsion is predictive of development of shoulder pain. We note that the majority of investigations that have attempted to determine predictors of shoulder pain in manual wheelchair users have been inconclusive (Mercer et al., 2006; Collinger et al., 2008).

It would also be worthwhile to examine whether training can alter wheelchair propulsion variability. Propulsion training is often viewed as a low-cost high-impact rehabilitation approach in upper limb preservation in manual wheelchair users (Boninger et al., 2005; de Groot et al., 2008; Rice et al., 2014b). Although variability of wheelchair propulsion has been examined in novice wheelchairs users as a function of training (de Groot et al., 2003), it is not clear if there would be changes in propulsion variability in experienced users with targeted training.

Just as variability analyses have provided insight into musculoskeletal injury in the ambulatory population (Hamill et al., 2012; Srinivasan and Mathiassen, 2012), we maintain that this approach has much promise in wheelchair users. Despite this promise of this theoretical view, there is much research to be done. We maintain that these series of investigation are a move in the right direction to understanding upper extremity pain in manual wheelchair users.

Supplementary Material

The Supplementary Material for this article can be found online at http://journal.frontiersin.org/article/10.3389/fbioe.2015.00105

References

Boninger, M. L., Koontz, A. M., Sisto, S. A., Dyson-Hudson, T. A., Chang, M., Price, R., et al. (2005). Pushrim biomechanics and injury prevention in spinal cord injury: recommendations based on CULP-SCI investigations. *J. Rehabil. Res. Dev.* 42, 9–19. doi:10.1682/JRRD.2004.08.0103

Burnham, R. S., May, L., Nelson, E., Steadward, R., and Reid, D. C. (1993). Shoulder pain in wheelchair athletes. The role of muscle imbalance. *Am. J. Sports Med.* 21, 238–242. doi:10.1177/036354659302100213

Collinger, J. L., Boninger, M. L., Koontz, A. M., Price, R., Sisto, S. A., Tolerico, M. L., et al. (2008). Shoulder biomechanics during the push phase of wheelchair propulsion: a multisite study of persons with paraplegia. *Arch. Phys. Med. Rehabil.* 89, 667–676. doi:10.1016/j.apmr.2007.09.052

Curtis, K. A., Tyner, T. M., Zachary, L., Lentell, G., Brink, D., Didyk, T., et al. (1999). Effect of a standard exercise protocol on shoulder pain in long-term wheelchair users. *Spinal Cord* 37, 421–429. doi:10.1038/sj.sc.3100860

Daffertshofer, A., Lamoth, C. J., Meijer, O. G., and Beek, P. J. (2004). PCA in studying coordination and variability: a tutorial. *Clin. Biomech. (Bristol, Avon)* 19, 415–428. doi:10.1016/j.clinbiomech.2004.01.005

Dalyan, M., Cardenas, D. D., and Gerard, B. (1999). Upper extremity pain after spinal cord injury. *Spinal Cord* 37, 191–195. doi:10.1038/sj.sc.3100802 de Groot, S., de Bruin, M., Noomen, S. P., and van der Woude, L. H. (2008). Mechanical efficiency and propulsion technique after 7 weeks of low-intensity wheelchair training. *Clin. Biomech. (Bristol, Avon)* 23, 434–441. doi:10.1016/j.clinbiomech.2007.11.001

de Groot, S., Veeger, H. E., Hollander, A. P., and van der Woude, L. H. (2003). Adaptations in physiology and propulsion techniques during the initial phase of learning manual wheelchair propulsion. *Am. J. Phys. Med. Rehabil.* 82, 504–510. doi:10.1097/01.PHM.0000069941.77921.AA

DiBerardino, L. A. III, Polk, J. D., Rosengren, K. S., Spencer-Smith, J. B., and Hsiao-Wecksler, E. T. (2010). Quantifying complexity and variability in phase portraits of gait. *Clin. Biomech. (Bristol, Avon)* 25, 552–556. doi:10.1016/j.clinbiomech.2010.03.007

Dyson-Hudson, T. A., and Kirshblum, S. C. (2004). Shoulder pain in chronic spinal cord injury, part I: epidemiology, etiology, and pathomechanics. *J. Spinal Cord Med.* 27, 4–17.

Fullerton, H. D., Borckardt, J. J., and Alfano, A. P. (2003). Shoulder pain: a comparison of wheelchair athletes and nonathletic wheelchair users. *Med. Sci. Sports Exerc.* 35, 1958–1961. doi:10.1249/01.MSS.0000099082.54522.55

Gironda, R. J., Clark, M. E., Neugaard, B., and Nelson, A. (2004). Upper limb pain in a national sample of veterans with paraplegia. *J. Spinal Cord Med.* 27, 120–127.

Gutierrez, D. D., Thompson, L., Kemp, B., and Mulroy, S. J. (2007). The relationship of shoulder pain intensity to quality of life, physical activity, and community participation in persons with paraplegia. *J. Spinal Cord Med.* 30, 251–255.

Hamill, J., Palmer, C., and Van Emmerik, R. E. (2012). Coordinative variability and overuse injury. *Sports Med. Arthrosc. Rehabil. Ther. Technol.* 4, 45. doi:10.1186/1758-2555-4-45

Hamill, J., van Emmerik, R. E., Heiderscheit, B. C., and Li, L. (1999). A dynamical systems approach to lower extremity running injuries. *Clin. Biomech. (Bristol, Avon)* 14, 297–308. doi:10.1016/S0268-0033(98)90092-4

Hausdorff, J. M. (2007). Gait dynamics, fractals and falls: finding meaning in the stride-to-stride fluctuations of human walking. *Hum. Mov. Sci.* 26, 555–589. doi:10.1016/j.humov.2007.05.003

Hsu, I. M.-K., Jayaraman, C., Culp, S., Rice, I. M., Hsiao-Wecksler, E. T., and Sosnoff, J. J. (2012). *Variability and Complexity of Shoulder Motion During Wheelchair Propulsion RESNA Annual Conference*. Baltimore, MD.

Jayaraman, C., Moon, Y., Rice, I. M., Hsiao-Wecksler, E. T., Beck, C. L., and Sosnoff, J. J. (2014). Shoulder pain and cycle to cycle kinematic spatial variability during recovery phase in manual wheelchair users: a pilot investigation. *PLoS One* 9:e89794. doi:10.1371/journal.pone.0089794

Koontz, A. M., Cooper, R. A., Boninger, M. L., Souza, A. L., and Fay, B. T. (2002). Shoulder kinematics and kinetics during two speeds of wheelchair propulsion. *J. Rehabil. Res. Dev.* 39, 635–649.

Kotajarvi, B. R., Basford, J. R., and An, K. N. (2002). Upper-extremity torque production in men with paraplegia who use wheelchairs. *Arch. Phys. Med. Rehabil.* 83, 441–446. doi:10.1053/apmr.2002.6685

Lal, S. (1998). Premature degenerative shoulder changes in spinal cord injury patients. *Spinal Cord* 36, 186–189. doi:10.1038/sj.sc.3100608

Lamoth, C. J., Daffertshofer, A., Meijer, O. G., and Beek, P. J. (2006). How do persons with chronic low back pain speed up and slow down? Trunk-pelvis coordination and lumbar erector spinae activity during gait. *Gait Posture* 23, 230–239. doi:10.1016/j.gaitpost.2005.02.006

LaPlante, M. P., and Kaye, H. S. (2010). Demographics and trends in wheeled mobility equipment use and accessibility in the community. *Assist. Technol.* 22, 3–17. doi:10.1080/10400430903501413

Lipsitz, L. A. (2004). Physiological complexity, aging, and the path to frailty. *Sci. Aging Knowledge Environ.* 2004, e16. doi:10.1126/sageke.2004.16.pe16

Lomond, K. V., and Cote, J. N. (2010). Movement timing and reach to reach variability during a repetitive reaching task in persons with chronic neck/shoulder pain and healthy subjects. *Exp. Brain Res.* 206, 271–282. doi:10.1007/s00221-010-2405-1

Lomond, K. V., and Cote, J. N. (2011). Differences in posture-movement changes induced by repetitive arm motion in healthy and shoulder-injured individuals. *Clin. Biomech. (Bristol, Avon)* 26, 123–129. doi:10.1016/j.clinbiomech.2010.09.012

Madeleine, P., Mathiassen, S. E., and Arendt-Nielsen, L. (2008). Changes in the degree of motor variability associated with experimental and chronic neck-shoulder pain during a standardised repetitive arm movement. *Exp. Brain Res.* 185, 689–698. doi:10.1007/s00221-007-1199-2

McGregor, S. J., Busa, M. A., Skufca, J., Yaggie, J. A., and Bollt, E. M. (2009). Control entropy identifies differential changes in complexity of walking and running gait patterns with increasing speed in highly trained runners. *Chaos* 19, 026109. doi:10.1063/1.3147423

Mercer, J. L., Boninger, M., Koontz, A., Ren, D., Dyson-Hudson, T., and Cooper, R. (2006). Shoulder joint kinetics and pathology in manual wheelchair users. *Clin. Biomech. (Bristol, Avon)* 21, 781–789. doi:10.1016/j.clinbiomech.2006.04.010

Moon, Y., Jayaraman, C., Hsu, I. M., Rice, I. M., Hsiao-Wecksler, E. T., and Sosnoff, J. J. (2013). Variability of peak shoulder force during wheelchair propulsion in manual wheelchair users with and without shoulder pain. *Clin. Biomech. (Bristol, Avon)* 28, 967–972. doi:10.1016/j.clinbiomech.2013.10.004

Morrow, M. M., Hurd, W. J., Kaufman, K. R., and An, K. N. (2009). Upper-limb joint kinetics expression during wheelchair propulsion. *J. Rehabil. Res. Dev.* 46, 939–944. doi:10.1682/JRRD.2008.12.0165

Newell, K. M., and Corcos, D. M. (1993). *Variability and Motor Control*. Champaign, IL: Human Kinetics.

Nichols, P. J., Norman, P. A., and Ennis, J. R. (1979). Wheelchair user's shoulder? Shoulder pain in patients with spinal cord lesions. *Scand. J. Rehabil. Med.* 11, 29–32.

Pentland, W. E., and Twomey, L. T. (1994). Upper limb function in persons with long term paraplegia and implications for independence: part I. *Paraplegia* 32, 211–218. doi:10.1038/sc.1994.41

Rice, I. M., Jayaraman, C., Hsiao-Wecksler, E. T., and Sosnoff, J. J. (2014a). Relationship between shoulder pain and kinetic and temporal-spatial variability in wheelchair users. *Arch. Phys. Med. Rehabil.* 95, 699–704. doi:10.1016/j.apmr.2013.11.005

Rice, L. A., Smith, I., Kelleher, A. R., Greenwald, K., and Boninger, M. L. (2014b). Impact of a wheelchair education protocol based on practice guidelines for preservation of upper-limb function: a randomized trial. *Arch. Phys. Med. Rehabil.* 95, 10–19.e11. doi:10.1016/j.apmr.2013.06.028

Sanderson, D. J., and Sommer, H. J. III (1985). Kinematic features of wheelchair propulsion. *J. Biomech.* 18, 423–429. doi:10.1016/0021-9290(85)90277-5

Shimada, S. D., Robertson, R. N., Bonninger, M. L., and Cooper, R. A. (1998). Kinematic characterization of wheelchair propulsion. *J. Rehabil. Res. Dev.* 35, 210–218.

Silfverskiold, J., and Waters, R. L. (1991). Shoulder pain and functional disability in spinal cord injury patients. *Clin. Orthop. Relat. Res.* 272, 141–145.

Sinnott, K. A., Milburn, P., and McNaughton, H. (2000). Factors associated with thoracic spinal cord injury, lesion level and rotator cuff disorders. *Spinal Cord* 38, 748–753. doi:10.1038/sj.sc.3101095

Sosnoff, J. J., and Newell, K. M. (2006a). The generalization of perceptual-motor intra-individual variability in young and old adults. *J. Gerontol. B Psychol. Sci. Soc. Sci.* 61, 304–310. doi:10.1093/geronb/61.5.P304

Sosnoff, J. J., and Newell, K. M. (2006b). Are age-related increases in force variability due to decrements in strength? *Exp. Brain Res.* 174, 86–94. doi:10.1007/s00221-006-0422-x

Srinivasan, D., and Mathiassen, S. E. (2012). Motor variability in occupational health and performance. *Clin. Biomech. (Bristol, Avon)* 27, 979–993. doi:10.1016/j.clinbiomech.2012.08.007

van der Woude, L. H., de Groot, S., and Janssen, T. W. (2006). Manual wheelchairs: research and innovation in rehabilitation, sports, daily life and health. *Med. Eng. Phys.* 28, 905–915. doi:10.1016/j.medengphy.2005.12.001

Vegter, R. J., Lamoth, C. J., de Groot, S., Veeger, D. H., and van der Woude, L. H. (2013). Variability in bimanual wheelchair propulsion: consistency of two instrumented wheels during handrim wheelchair propulsion on a motor driven treadmill. *J. Neuroeng. Rehabil.* 10, 9. doi:10.1186/1743-0003-10-9

Vegter, R. J., Lamoth, C. J., de Groot, S., Veeger, D. H., and van der Woude, L. H. (2014). Inter-individual differences in the initial 80 minutes of motor learning of handrim wheelchair propulsion. *PLoS ONE* 9:e89729. doi:10.1371/journal.pone.0089729

Wu, G., van der Helm, F. C., Veeger, H. E., Makhsous, M., Van Roy, P., Anglin, C., et al. (2005). ISB recommendation on definitions of joint coordinate systems of various joints for the reporting of human joint motion – part II: shoulder, elbow, wrist and hand. *J. Biomech.* 38, 981–992. doi:10.1016/j.jbiomech.2004.05.042

Yentes, J. M., Hunt, N., Schmid, K. K., Kaipust, J. P., McGrath, D., and Stergiou, N. (2013). The appropriate use of approximate entropy and sample entropy with short data sets. *Ann. Biomed. Eng.* 41, 349–365. doi:10.1007/s10439-012-0668-3

Conflict of Interest Statement: The authors declare that the research was conducted in the absence of any commercial or financial relationships that could be construed as a potential conflict of interest.

frontiers in Bioengineering and Biotechnology

ORIGINAL RESEARCH
published: 11 June 2015
doi: 10.3389/fbioe.2015.00086

An investigation of bilateral symmetry during manual wheelchair propulsion

Shelby L. Soltau[1], *Jonathan S. Slowik*[1], *Philip S. Requejo*[2,3], *Sara J. Mulroy*[2] *and Richard R. Neptune*[1]*

[1] Department of Mechanical Engineering, The University of Texas at Austin, Austin, TX, USA, [2] Pathokinesiology Laboratory, Rancho Los Amigos National Rehabilitation Center, Downey, CA, USA, [3] Rehabilitation Engineering, Rancho Los Amigos National Rehabilitation Center, Downey, CA, USA

Studies of manual wheelchair propulsion often assume bilateral symmetry to simplify data collection, processing, and analysis. However, the validity of this assumption is unclear. Most investigations of wheelchair propulsion symmetry have been limited by a relatively small sample size and a focus on a single propulsion condition (e.g., level propulsion at self-selected speed). The purpose of this study was to evaluate bilateral symmetry during manual wheelchair propulsion in a large group of subjects across different propulsion conditions. Three-dimensional kinematics and handrim kinetics along with spatiotemporal variables were collected and processed from 80 subjects with paraplegia while propelling their wheelchairs on a stationary ergometer during three different conditions: level propulsion at their self-selected speed (free), level propulsion at their fastest comfortable speed (fast), and propulsion on an 8% grade at their level, self-selected speed (graded). All kinematic variables had significant side-to-side differences, primarily in the graded condition. Push angle was the only spatiotemporal variable with a significant side-to-side difference, and only during the graded condition. No kinetic variables had significant side-to-side differences. The magnitudes of the kinematic differences were low, with only one difference exceeding 5°. With differences of such small magnitude, the bilateral symmetry assumption appears to be reasonable during manual wheelchair propulsion in subjects without significant upper-extremity pain or impairment. However, larger asymmetries may exist in individuals with secondary injuries and pain in their upper extremity and different etiologies of their neurological impairment.

Keywords: asymmetry, side-to-side differences, hand dominance, speed, graded, biomechanics

OPEN ACCESS

Edited by:
Alireza Mashaghi, Delft University of Technology, Netherlands

Reviewed by:
Glen Lichtwark, The University of Queensland, Australia
Katherine Saul, North Carolina State University, USA

Correspondence:
Richard R. Neptune, Department of Mechanical Engineering, The University of Texas at Austin, 204 E. Dean Keeton Street, Stop C2200, Austin, TX 78712, USA
rneptune@mail.utexas.edu

Specialty section:
This article was submitted to Biomechanics, a section of the journal Frontiers in Bioengineering and Biotechnology

Received: *23 April 2015*
Accepted: *25 May 2015*
Published: *11 June 2015*

Citation:
Soltau SL, Slowik JS, Requejo PS, Mulroy SJ and Neptune RR (2015) An investigation of bilateral symmetry during manual wheelchair propulsion. Front. Bioeng. Biotechnol. 3:86. doi: 10.3389/fbioe.2015.00086

Introduction

Manual wheelchair propulsion is commonly assumed to be a symmetric task. The rationale for this assumption is that any asymmetry, combined with the uncoupled nature of the wheels, would make straight-line propulsion difficult (e.g., de Groot et al., 2002). Resulting steering corrections could lead to increased energy cost and other unfavorable effects (e.g., Vegter et al., 2013a), and therefore experienced manual wheelchair users likely develop symmetrical propulsion mechanics over time.

However, the prevalence of the symmetry assumption has also been influenced by the limitations in available data collection systems. Early single-camera systems only allowed the measurement of unilateral kinematics that were usually restricted to the sagittal plane (e.g., Sanderson and Sommer, 1985; Masse et al., 1992; Veeger et al., 1992). Experimental set-ups involving mirrors and/or an additional camera allowed measurement of frontal plane kinematics and the calculation of 3D kinematics (e.g., van der Woude et al., 1989; Veeger et al., 1989; Goosey et al., 1998). The collection of bilateral 3D kinematics (e.g., Rao et al., 1996; Shimada et al., 1998) eventually became standard with the proliferation of multi-camera systems. By this time, instrumented wheels and other devices that allow the measurement of handrim kinetics had also been developed (e.g., Asato et al., 1993; Rodgers et al., 1994; Wu et al., 1998). However, many current laboratories are equipped with only one instrumented wheel due to the high cost of these devices (e.g., Hurd et al., 2008a). Thus, bilateral measurements often require multiple trials in which the instrumented wheel is switched back and forth between sides, effectively doubling the time and effort necessary for data collection.

Even with bilateral data collection, studies often do not report results for both sides, but elect to either average the data across both limbs (e.g., Boninger et al., 2000) or select only one limb for analysis (e.g., Finley et al., 2004; Mercer et al., 2006; Gagnon et al., 2014). Among the studies that have examined side-to-side differences in propulsion mechanics, there is a lack of consensus regarding the presence of asymmetry. Some studies have suggested that there is no significant asymmetry in kinematic (e.g., Goosey and Campbell, 1998), kinetic (e.g., Hurd et al., 2008b), or spatiotemporal (e.g., de Groot et al., 2002) variables. However, others have found significant side-to-side differences in similar propulsion variables (Hurd et al., 2008a; Stephens and Engsberg, 2010). The lack of statistically significant differences in most previous studies may be due to small sample sizes ($n \leq 20$). In addition, studies have suggested that asymmetry may be present in specific individuals even if it is not detectable when comparing side-to-side group averages (e.g., Koontz et al., 2001; Schnorenberg et al., 2014).

Another limitation of previous studies is most have only examined side-to-side differences during one propulsion condition (e.g., level propulsion at self-selected speed). However, recent studies have suggested that the level of asymmetry may be influenced by the terrain (Hurd et al., 2008a, 2009). The purpose of this study was to evaluate bilateral symmetry during manual wheelchair propulsion in a large number of subjects across different propulsion conditions. These results have important implications for experimental setups in future analyses of wheelchair propulsion mechanics.

Materials and Methods

Subjects

Symmetry data were collected and analyzed from 80 individuals with paraplegia who were free of shoulder pain and used a manual wheelchair at least 50% of the time for community mobility (74 men, 6 women; age: 37.0 ± 9.9 years; time from injury: 9.0 ± 6.6 years; height: 1.72 ± 0.09 m; mass: 74.5 ± 16.9 kg). Dominant side was self-reported by each subject (74 right-handed, 6 left-handed). The participants were recruited from outpatient clinics at Rancho Los Amigos National Rehabilitation Center and provided written informed consent in accordance with the Institutional Review Board.

Data Collection

Participants propelled their wheelchair on a stationary ergometer (**Figure 1**) during three conditions (e.g., Lighthall-Haubert et al., 2009): level propulsion at their self-selected speed (free), level propulsion at their fastest comfortable speed (fast), and propulsion on an 8% grade at their level self-selected speed (graded). Subjects acclimated to each condition until they felt comfortable (at least 30 s of propulsion) and a 10-s trial was recorded for each condition. Data were collected separately from both the dominant and non-dominant sides, with the side tested first randomly selected. Three-dimensional handrim kinetics were collected using an instrumented handrim (SmartWheel; Three Rivers Holdings, Mesa, AZ, USA). Trunk, ipsilateral upper extremity, and wheel kinematics were collected using a CODA motion analysis system (Charnwood Dynamics Ltd., Leicestershire, UK) with 15 active markers placed on landmarks on the body and the wheel (**Figure 1**).

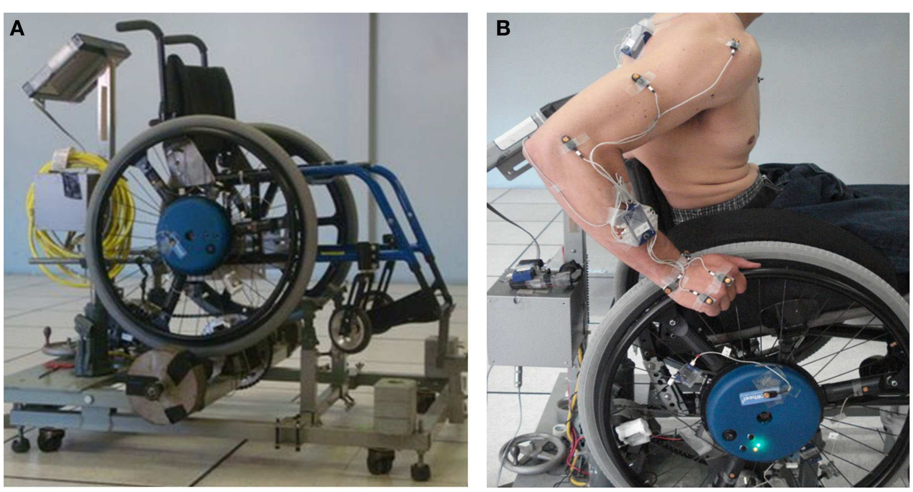

FIGURE 1 | Experimental setup: (A) Manual wheelchair ergometer consisting of supporting frame, controlling computer and split rollers. **(B)** Subject on ergometer with markers affixed to the body and wheel.

TABLE 1 | Definition of variables.

Variable name	Abbreviation	Calculation
Range of motion	ROM	Maximum angle–minimum angle
Propulsion moment (about wheel axle)	M_z	Direct Smart Wheel output
Anterior force	F_x	Direct Smart Wheel output
Superior force	F_y	Direct Smart Wheel output
Lateral force	F_z	Direct Smart Wheel output
Handrim radius	r	Measurement
Tangential force	$F_{\tan}$	$\frac{M_z}{r}$
Resultant force	F_{tot}	$\sqrt{F_x^2 + F_y^2 + F_z^2}$
Fraction of effective force	FEF	$\frac{F_{\tan}}{F_{\text{tot}}}$
Cycle time	CT	Based on M_z thresholds
Push time	PT	Based on M_z thresholds
Push percentage	PP	$\frac{PT}{CT}$
Push angle	θ	Angle between the positions of the hand at the start and end of the push phase (see **Figure 2**)
Number of loops	nloops	Based on the number of curve intersections
Signed area of the *i*th loop	A_i	Surveyor's formula (e.g., Braden, 1986)
Net radial thickness	NRT	$\frac{\sum_{i=1}^{\text{nloops}} A_i}{r\theta}$
Total radial thickness	TRT	$\frac{\sum_{i=1}^{nloops} \lvert A_i \rvert}{r\theta}$

Data Processing

Kinematic and kinetic data were processed in Visual3D (C-Motion, Inc., Germantown, MD, USA) using a low-pass, fourth-order, zero-lag Butterworth filter with cutoff frequencies of 8 and 10 Hz, respectively. A threshold of 1 Nm for the moment about the wheel axle was used to indicate the beginning and end of the push and recovery phases. Shoulder plane-of-elevation, shoulder elevation angle, shoulder internal-external rotation, elbow flexion-extension, and forearm pronation-supination angles were determined in accordance with International Society of Biomechanics recommendations (Wu et al., 2005). Range of motion values (ROMs) for these angles, peak and average tangential and resultant forces, fraction of effective force, cycle time, push percentage, and push angle were then calculated for each cycle and averaged across cycles for each subject during each condition (**Table 1**).

In addition, the third metacarpophalangeal joint center (MCP3) was located using a previously described method (Rao et al., 1996), and the MCP3 path was projected onto the plane of the handrim and averaged across cycles, resulting in a closed curve that details the full-cycle hand path or hand pattern (e.g., **Figure 2**; Boninger et al., 2002). Two objective, quantitative parameters were then calculated to characterize the hand pattern: net radial thickness (NRT) (a measurement of the displacement of the hand above the handrim) and total radial thickness (TRT) (a measurement of the distance between the hand and the handrim). For a detailed description of these parameters (NRT, TRT), see Slowik et al. (under review).

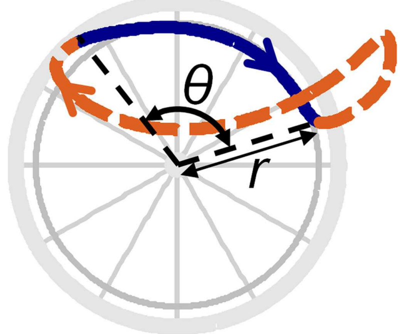

FIGURE 2 | Hand pattern variable definitions. The solid line denotes the hand path during push phase, while the dashed line denotes the hand path during recovery phase. The handrim radius is denoted by the variable *r* and push angle is denoted by θ.

Statistical Analyses

To determine if there was asymmetry in any of the measured variables, statistical analyses were performed in SPSS (IBM Corp., Armonk, NY, USA) using two-factor (condition, side) repeated measures ANOVAs with a Huynh–Feldt correction in the case of non-sphericity. The condition factor consisted of three levels (free, fast, and graded) and the side factor consisted of two levels (dominant and non-dominant). If there was a significant interaction effect, pairwise comparisons were performed using paired *t*-tests with a Bonferroni adjustment for multiple comparisons. The unadjusted threshold for statistical significance for all analyses was set at $\alpha = 0.05$. Condition main effects were not reported.

Results

Joint Kinematics

Almost all significant side-to-side differences occurred in the kinematic variables (**Table 2**). Elevation plane ROM had a significant interaction effect, particularly due to a larger dominant side value in the graded condition (condition*side interaction effect, $p = 0.006$; graded, dominant to non-dominant pairwise comparison, $p = 0.014$). Elevation angle ROM was larger on the dominant side than the non-dominant side (side main effect, $p = 0.015$). Shoulder rotation ROM was larger on the dominant side, particularly due to a larger dominant side value in the graded condition (side main effect, $p = 0.007$; condition*side effect, $p = 0.002$; graded, dominant to non-dominant pairwise comparison, $p < 0.001$). Elbow flexion ROM was larger on the dominant side than the non-dominant side (side main effect, $p = 0.044$). Forearm pronation ROM had a significant interaction effect, particularly due to a larger dominant side value in the graded condition (condition*side effect, $p < 0.001$; graded, dominant to non-dominant pairwise comparison, $p < 0.001$).

There were no other side main effects or interaction effects, and all differences were <5° except for shoulder rotation ROM during the graded condition (8°).

TABLE 2 | Mean (SD) values for examined propulsion variables. D indicates a dominant side value and ND indicates a non-dominant side value.

	Side	Free	Fast	Graded
JOINT KINEMATICS				
Elevation plane	D	72.6 (20.8)	81.3 (21.5)	85.7 (16.3)
ROM (°)○■	ND	72.4 (19.6)	81.6 (17.7)	81.8 (14.5)
Elevation angle	D	22.8 (7.2)	22.7 (7.8)	19.8 (7.6)
ROM (°) ▲	ND	21.7 (7.5)	21.7 (7.0)	18.8 (7.1)
Shoulder rotation	D	67.9 (22.5)	73.9 (21.5)	77.5 (17.3)
ROM (°) ▲ ○ ■	ND	64.2 (23.1)	70.8 (21.1)	69.5 (19.0)
Elbow flexion	D	45.7 (14.7)	52.7 (15.8)	60.3 (16.1)
ROM (°) ▲	ND	44.2 (16.2)	51.1 (16.0)	57.7 (16.9)
Forearm pronation	D	28.8 (10.5)	32.0 (12.6)	36.9 (15.1)
ROM (°) ○■	ND	28.9 (11.1)	31.4 (11.1)	32.4 (13.5)
HANDRIM KINETICS				
Average total	D	29.9 (7.7)	44.2 (13.1)	80.7 (18.1)
force (N)	ND	29.5 (7.8)	43.4 (12.6)	80.7 (19.7)
Average tangential	D	21.1 (5.3)	30.3 (7.8)	67.3 (13.9)
force (N)	ND	20.7 (5.3)	29.3 (7.3)	66.7 (14.7)
Peak total force (N)	D	45.2 (14.0)	77.7 (28.1)	127.1 (31.9)
	ND	44.6 (14.2)	74.8 (27.3)	127.1 (34.9)
Peak tangential	D	33.3 (10.5)	54.8 (16.4)	109.4 (26.2)
force (N)	ND	33.0 (10.5)	52.3 (15.5)	108.7 (26.6)
Fraction of effective	D	72.0 (11.4)	70.3 (10.7)	84.3 (9.5)
force (%)	ND	71.5 (11.0)	68.9 (9.8)	83.9 (9.7)
SPATIOTEMPORAL VARIABLES				
Cycle time (s)	D	1.15 (0.25)	0.78 (0.18)	0.79 (0.19)
	ND	1.12 (0.25)	0.77 (0.16)	0.78 (0.19)
Push percentage	D	36.0 (5.4)	32.0 (4.6)	55.6 (4.8)
(% cycle)	ND	35.5 (4.6)	31.9 (4.4)	55.2 (4.6)
Push angle (°) ○■	D	74.9 (15.5)	79.8 (14.5)	85.4 (14.9)
	ND	73.4 (16.2)	80.2 (13.9)	84.0 (15.4)
NRT (m)	D	−0.016 (0.055)	0.013 (0.049)	0.011 (0.023)
	ND	−0.012 (0.053)	0.010 (0.047)	0.011 (0.021)
TRT (m)	D	0.051 (0.038)	0.051 (0.035)	0.021 (0.019)
	ND	0.048 (0.039)	0.050 (0.030)	0.021 (0.014)

▲ denotes a significant side main effect.
*○ denotes a significant condition*side interaction effect.*
■ denotes a significant dominant to non-dominant pairwise comparison in the graded condition.

Handrim Kinetics

There were no significant side main effects or interaction effects in any of the kinetic variables.

Spatiotemporal Variables

Push angle had a significant interaction effect, particularly due to a larger dominant side value in the graded condition (condition*side effect, $p = 0.025$; graded, dominant to non-dominant pairwise comparison, $p = 0.033$). There were no other significant side main effects or interaction effects in the spatiotemporal variables.

Discussion

The results suggest that low levels of asymmetry may exist in manual wheelchair propulsion, and that these levels may increase in the graded condition when the demand on the upper extremity is increased. However, we did not find any statistically significant side-to-side differences in any of the kinetic variables, and only one spatiotemporal variable (push angle) showed a significant side-to-side difference. We did find significant side-to-side differences in the joint ROMs, with dominant side values larger than those of the non-dominant side. However, the mean differences were small, with only one difference being larger than 5°. In addition, side-to-side differences were often smaller than differences between individuals or between conditions. Thus, while the comparisons showed statistical significance, the clinical significance of these differences is likely not high.

The magnitudes of the side-to-side differences were similar to those reported by others. An early study investigating racing propulsion (Goosey and Campbell, 1998) reported a non-significant mean difference of approximately 2° in the elbow flexion ROM in a sample of seven experienced wheelchair users. Others investigated standard handrim propulsion and reported non-significant mean differences of <1 N in peak and average handrim forces in 20 experienced wheelchair users (Koontz et al., 2001). Another group performed a series of three studies (Hurd et al., 2008a,b, 2009), examining side-to-side differences in kinetic and temporal variables for standard handrim propulsion on different terrains (12–14 experienced wheelchair users). All studies showed similar magnitudes of differences to the present study. Using similar statistical methods (i.e., repeated measures ANOVAs and/or paired *t*-tests), Hurd et al. (2008b, 2009) found only a single significant side-to-side difference (in average instantaneous power for propulsion on aggregate concrete). The third study (Hurd et al., 2008a) utilized a symmetry index and suggested that statistically significant levels of asymmetry were present for all investigated variables and terrains.

The lack of consensus regarding symmetry differences is likely due to a combination of different sample sizes and statistical methods. The present study may have been able to find statistical significance where others had not due to the large sample size ($n = 80$). In addition, while symmetry indices have been utilized in the study of gait (e.g., Sadeghi et al., 2000) and have potential in the analysis of manual wheelchair propulsion, the particular symmetry index used by Hurd et al. (2008a) disregarded the direction of asymmetries by taking the absolute value of observed differences, which resulted in only positive values. The difference between their symmetry index and the one that they attempted to replicate (Kaufman et al., 1996) may have led to an overestimation of the across-subjects mean levels of asymmetry. It is unlikely that dominant side data will be identical to the non-dominant side data for any single subject, and any small side-to-side differences that otherwise may have been neutralized across subjects (including those due to normal levels of experimental uncertainty and motion variability) were instead preserved by examining the absolute value.

The results of this study, in combination with previous results in the literature, suggest that the assumption of symmetry is reasonable when analyzing wheelchair propulsion in groups of subjects without secondary injury or pain in their upper extremities. However, our study only included data from subjects with paraplegia, so our conclusions may not be generalizable to other patient populations. A previous study found more asymmetry in propulsion biomechanics in individuals with multiple sclerosis than in individuals with spinal cord injury and able-bodied subjects (Fay et al., 2004), thus reinforcing the need to consider symmetry in the context of specific populations. In addition, it may not be appropriate to assume symmetry in the study of individual subjects as larger asymmetries may be present in individual subject data than in group-averaged data (e.g., Koontz et al., 2001; Schnorenberg et al., 2014), a finding that is also confirmed in our data. Individuals were found to have larger asymmetries than the group average. Studies should also be careful in assuming symmetry for propulsion during more strenuous conditions as we found the largest levels of asymmetry in the graded condition and a previous study concluded that asymmetry increased when propelling over outdoor terrain compared to laboratory terrain (Hurd et al., 2008a).

A potential limitation of this study is that only one instrumented wheel was used during data collection. As a result, dominant and non-dominant variables were recorded during separate trials. However, potential systematic differences between trials (e.g., fatigue effects) were minimized by randomly selecting the trial order. While any remaining systematic differences between trials could lead to overestimation of asymmetry, we still only found low levels. In addition, the alternative of using two instrumented wheels during a single trial is not without its own limitations. The side-to-side mean differences in kinetic variables that we observed were smaller than the documented accuracy and precision of instrumented wheels (e.g., Cooper et al., 1997; Wu et al., 1998; Guo et al., 2011). Even after calibration, there can be small differences between measurements from individual wheels, which are supported by a recent study that found differences between individual measurement wheels during a single trial were larger than single wheel differences between trials (Vegter et al., 2013b).

Another potential limitation is that subjects did not propel the wheelchair overground, but instead used a stationary ergometer set up to replicate overground propulsion. Although ergometers are unable to perfectly replicate overground propulsion, they do provide controlled conditions for data collection and have been shown to produce steady-state propulsion mechanics consistent with overground data (e.g., Koontz et al., 2001). However, propulsion on an ergometer is less constrained compared to overground propulsion. While the average power delivered to each handrim must be equivalent during straight-line overground propulsion, no such steering requirement exists for ergometer propulsion (e.g., de Groot et al., 2005). However, this limitation would likely lead to an overestimation of asymmetry, so the use of an ergometer likely did not alter the study conclusions.

In summary, our results support the assumption of symmetry in manual wheelchair propulsion for studies that analyze groups of subjects without significant upper extremity pain or impairment. Small asymmetries likely exist in propulsion variables, and these may increase when propelling under more strenuous conditions. Thus, the validity of the symmetry assumption should be carefully considered in light of the specific research aims and methods.

Acknowledgments

This study was supported by NIH Grant R01 HD049774 and a National Science Foundation Graduate Research Fellowship under Grant DGE-1110007.

References

Asato, K. T., Cooper, R. A., Robertson, R. N., and Ster, J. F. (1993). SMARTWheels: development and testing of a system for measuring manual wheelchair propulsion dynamics. *IEEE Trans. Biomed. Eng.* 40, 1320–1324. doi:10.1109/10.250587

Boninger, M. L., Baldwin, M., Cooper, R. A., Koontz, A., and Chan, L. (2000). Manual wheelchair pushrim biomechanics and axle position. *Arch. Phys. Med. Rehabil.* 81, 608–613. doi:10.1016/S0003-9993(00)90043-1

Boninger, M. L., Souza, A. L., Cooper, R. A., Fitzgerald, S. G., Koontz, A. M., and Fay, B. T. (2002). Propulsion patterns and pushrim biomechanics in manual wheelchair propulsion. *Arch. Phys. Med. Rehabil.* 83, 718–723. doi:10.1053/apmr.2002.32455

Braden, B. (1986). The surveyor's area formula. *Coll. Math. J.* 17, 326–337. doi:10.2307/2686282

Cooper, R. A., Robertson, R. N., VanSickle, D. P., Boninger, M. L., and Shimada, S. D. (1997). Methods for determining three-dimensional wheelchair pushrim forces and moments: a technical note. *J. Rehabil. Res. Dev.* 34, 162–170.

de Groot, S., Veeger, D. H., Hollander, A. P., and Van der Woude, L. H. (2002). Wheelchair propulsion technique and mechanical efficiency after 3 weeks of practice. *Med. Sci. Sports Exerc.* 34, 756–766. doi:10.1097/00005768-200205000-00005

de Groot, S., Veeger, H. E., Hollander, A. P., and van der Woude, L. H. (2005). Influence of task complexity on mechanical efficiency and propulsion technique during learning of hand rim wheelchair propulsion. *Med. Eng. Phys.* 27, 41–49. doi:10.1016/j.medengphy.2004.08.007

Fay, B. T., Boninger, M. L., Fitzgerald, S. G., Souza, A. L., Cooper, R. A., and Koontz, A. M. (2004). Manual wheelchair pushrim dynamics in people with multiple sclerosis. *Arch. Phys. Med. Rehabil.* 85, 935–942. doi:10.1016/j.apmr.2003.08.093

Finley, M. A., Rasch, E. K., Keyser, R. E., and Rodgers, M. M. (2004). The biomechanics of wheelchair propulsion in individuals with and without upper-limb impairment. *J. Rehabil. Res. Dev.* 41, 385–394. doi:10.1682/JRRD.2004.03.0385

Gagnon, D. H., Babineau, A. C., Champagne, A., Desroches, G., and Aissaoui, R. (2014). Pushrim biomechanical changes with progressive increases in slope during motorized treadmill manual wheelchair propulsion in individuals with spinal cord injury. *J. Rehabil. Res. Dev.* 51, 789–802. doi:10.1682/JRRD.2013.07.0168

Goosey, V. L., and Campbell, I. G. (1998). Symmetry of the elbow kinematics during racing wheelchair propulsion. *Ergonomics* 41, 1810–1820. doi:10.1080/001401398185983

Goosey, V. L., Campbell, I. G., and Fowler, N. E. (1998). The relationship between three-dimensional wheelchair propulsion techniques and pushing economy. *J. Appl. Biomech.* 14, 412–427.

Guo, L., Kwarciak, A. M., Rodriguez, R., Sarkar, N., and Richter, W. M. (2011). Validation of a biofeedback system for wheelchair propulsion training. *Rehabil. Res. Pract.* 2011, 590780. doi:10.1155/2011/590780

Hurd, W. J., Morrow, M. M., Kaufman, K. R., and An, K. N. (2008a). Biomechanic evaluation of upper-extremity symmetry during manual wheelchair propulsion over varied terrain. *Arch. Phys. Med. Rehabil.* 89, 1996–2002. doi:10.1016/j.apmr.2008.03.020

Hurd, W. J., Morrow, M. M., Kaufman, K. R., and An, K. N. (2008b). Influence of varying level terrain on wheelchair propulsion biomechanics. *Am. J. Phys. Med. Rehabil.* 87, 984–991. doi:10.1097/PHM.0b013e31818a52cc

Hurd, W. J., Morrow, M. M., Kaufman, K. R., and An, K. N. (2009). Wheelchair propulsion demands during outdoor community ambulation. *J. Electromyogr. Kinesiol.* 19, 942–947. doi:10.1016/j.jelekin.2008.05.001

Kaufman, K. R., Miller, L. S., and Sutherland, D. H. (1996). Gait asymmetry in patients with limb-length inequality. *J. Pediatr. Orthop.* 16, 144–150. doi:10.1097/01241398-199603000-00002

Koontz, A. M., Cooper, R. A., and Boninger, M. L. (2001). An autoregressive modeling approach to analyzing wheelchair propulsion forces. *Med. Eng. Phys.* 23, 285–291. doi:10.1016/S1350-4533(00)00082-5

Lighthall-Haubert, L., Requejo, P. S., Mulroy, S. J., Newsam, C. J., Bontrager, E., Gronley, J. K., et al. (2009). Comparison of shoulder muscle electromyographic activity during standard manual wheelchair and push-rim activated power assisted wheelchair propulsion in persons with complete tetraplegia. *Arch. Phys. Med. Rehabil.* 90, 1904–1915. doi:10.1016/j.apmr.2009.05.023

Masse, L. C., Lamontagne, M., and O'Riain, M. D. (1992). Biomechanical analysis of wheelchair propulsion for various seating positions. *J. Rehabil. Res. Dev.* 29, 12–28. doi:10.1682/JRRD.1992.07.0012

Mercer, J. L., Boninger, M., Koontz, A., Ren, D., Dyson-Hudson, T., and Cooper, R. (2006). Shoulder joint kinetics and pathology in manual wheelchair users. *Clin. Biomech. (Bristol, Avon)* 21, 781–789. doi:10.1016/j.clinbiomech.2006.04.010

Rao, S. S., Bontrager, E. L., Gronley, J. K., Newsam, C. J., and Perry, J. (1996). Three-dimensional kinematics of wheelchair propulsion. *IEEE Trans. Rehabil. Eng.* 4, 152–160. doi:10.1109/86.536770

Rodgers, M. M., Gayle, G. W., Figoni, S. F., Kobayashi, M., Lieh, J., and Glaser, R. M. (1994). Biomechanics of wheelchair propulsion during fatigue. *Arch. Phys. Med. Rehabil.* 75, 85–93.

Sadeghi, H., Allard, P., Prince, F., and Labelle, H. (2000). Symmetry and limb dominance in able-bodied gait: a review. *Gait Posture* 12, 34–45. doi:10.1016/S0966-6362(00)00070-9

Sanderson, D. J., and Sommer, H. J. III (1985). Kinematic features of wheelchair propulsion. *J. Biomech.* 18, 423–429. doi:10.1016/0021-9290(85)90277-5

Schnorenberg, A. J., Slavens, B. A., Wang, M., Vogel, L. C., Smith, P. A., and Harris, G. F. (2014). Biomechanical model for evaluation of pediatric upper extremity joint dynamics during wheelchair mobility. *J. Biomech.* 47, 269–276. doi:10.1016/j.jbiomech.2013.11.014

Shimada, S. D., Robertson, R. N., Boninger, M. L., and Cooper, R. A. (1998). Kinematic characterization of wheelchair propulsion. *J. Rehabil. Res. Dev.* 35, 210–218.

Stephens, C. L., and Engsberg, J. R. (2010). Comparison of overground and treadmill propulsion patterns of manual wheelchair users with tetraplegia. *Disabil. Rehabil. Assist. Technol.* 5, 420–427. doi:10.3109/17483101003793420

van der Woude, L. H., Veeger, D. J., Rozendal, R. H., and Sargeant, T. J. (1989). Seat height in handrim wheelchair propulsion. *J. Rehabil. Res. Dev.* 26, 31–50.

Veeger, D., van der Woude, L. H., and Rozendal, R. H. (1989). The effect of rear wheel camber in manual wheelchair propulsion. *J. Rehabil. Res. Dev.* 26, 37–46.

Veeger, H. E., Lute, E. M., Roeleveld, K., and van der Woude, L. H. (1992). Differences in performance between trained and untrained subjects during a 30-s sprint test in a wheelchair ergometer. *Eur. J. Appl. Physiol. Occup. Physiol.* 64, 158–164. doi:10.1007/BF00717954

Vegter, R., de Groot, S., Lamoth, C., Veeger, D., and Van der Woude, L. (2013a). Initial skill acquisition of handrim wheelchair propulsion: a new perspective. *IEEE Trans. Neural. Syst. Rehabil. Eng.* 22, 104–113. doi:10.1109/TNSRE.2013.2280301

Vegter, R. J. K., Lamoth, C. J., de Groot, S., Veeger, D. H. E. J., and van der Woude, L. H. V. (2013b). Variability in bimanual wheelchair propulsion: consistency of two instrumented wheels during handrim wheelchair propulsion on a motor driven treadmill. *J. Neuroeng. Rehabil.* 10, 9. doi:10.1186/1743-0003-10-9

Wu, G., van der Helm, F. C., Veeger, H. E., Makhsous, M., Van Roy, P., Anglin, C., et al. (2005). ISB recommendation on definitions of joint coordinate systems of various joints for the reporting of human joint motion – part II: shoulder, elbow, wrist and hand. *J. Biomech.* 38, 981–992. doi:10.1016/j.jbiomech.2004.05.042

Wu, H. W., Berglund, L. J., Su, F. C., Yu, B., Westreich, A., Kim, K. J., et al. (1998). An instrumented wheel for kinetic analysis of wheelchair propulsion. *J. Biomech. Eng.* 120, 533–535. doi:10.1115/1.2798024

Conflict of Interest Statement: The authors declare that the research was conducted in the absence of any commercial or financial relationships that could be construed as a potential conflict of interest.

frontiers in Bioengineering and Biotechnology

ORIGINAL RESEARCH
published: 17 September 2015
doi: 10.3389/fbioe.2015.00139

Car transfer and wheelchair loading techniques in independent drivers with paraplegia

Lisa Lighthall Haubert[1], Sara J. Mulroy[1], Patricia E. Hatchett[1], Valerie J. Eberly[1], Somboon Maneekobkunwong[2], Joanne K. Gronley[1] and Philip S. Requejo[1,2]*

[1] Pathokinesiology Laboratory, Rancho Los Amigos National Rehabilitation Center, Downey, CA, USA, [2] Rehabilitation Engineering, Rancho Los Amigos National Rehabilitation Center, Downey, CA, USA

OPEN ACCESS

Edited by:
Jill L. McNitt-Gray,
University of Southern California, USA

Reviewed by:
Eli Carmeli,
Haifa University, Israel
Beverly Ann Rzigalinski,
Virginia College of Osteopathic Medicine, USA

***Correspondence:**
Lisa Lighthall Haubert,
Pathokinesiology Laboratory, Rancho Los Amigos National Rehabilitation Center, 7601 East Imperial Highway, Building 800, Room 33, Downey, CA 90242, USA
lisalhaubert@gmail.com

Specialty section:
This article was submitted to Biomechanics, a section of the journal Frontiers in Bioengineering and Biotechnology

Received: 06 July 2015
Accepted: 31 August 2015
Published: 17 September 2015

Citation:
Haubert LL, Mulroy SJ, Hatchett PE, Eberly VJ, Maneekobkunwong S, Gronley JK and Requejo PS (2015) Car transfer and wheelchair loading techniques in independent drivers with paraplegia. Front. Bioeng. Biotechnol. 3:139. doi: 10.3389/fbioe.2015.00139

Car transfers and wheelchair (WC) loading are crucial for independent community participation in persons with complete paraplegia from spinal cord injury, but are complex, physically demanding, and known to provoke shoulder pain. This study aimed to describe techniques and factors influencing car transfer and WC loading for individuals with paraplegia driving their own vehicles and using their personal WCs. Sedans were the most common vehicle driven (59%). Just over half (52%) of drivers place their right leg only into the vehicle prior to transfer. Overall, the leading hand was most frequently placed on the driver's seat (66%) prior to transfer and the trailing hand was most often place on the WC seat (48%). Vehicle height influenced leading hand placement but not leg placement such that drivers of higher profile vehicles were more likely to place their hand on the driver's seat than those who drove sedans. Body lift time was negatively correlated with level of injury and age and positively correlated with vehicle height and shoulder abduction strength. Drivers who transferred with their leading hand on the steering wheel had significantly higher levels of shoulder pain than those who placed their hand on the driver's seat or overhead. The majority of participants used both hands (62%) to load their WC frame, and overall, most loaded their frame into the back (62%) vs. the front seat. Sedan drivers were more likely to load their frame into the front seat than drivers of higher profile vehicles (53 vs. 17%). Average time to load the WC frame (10.7 s) was 20% of the total WC loading time and was not related to shoulder strength, frame weight, or demographic characteristics. Those who loaded their WC frame into the back seat had significantly weaker right shoulder internal rotators. Understanding car transfers and WC loading in independent drivers is crucial to prevent shoulder pain and injury and preserve community participation.

Keywords: spinal cord injury, paraplegia, car transfer, shoulder pain, depression transfers, wheelchair, independent drivers

Introduction

Shoulder pain is a common problem in individuals with spinal cord injury (SCI.) Its prevalence increases with time post-injury affecting as many as 70% of individuals by 20 years after SCI (Sie et al., 1992). The average age of onset of SCI is 41 years, and with advances in medicine, the life expectancy of individuals with SCI is approaching that of the non-disabled population[1]. Thus, persons with SCI have an extremely high likelihood of experiencing shoulder pain in their lifetime.

The development of shoulder pain in this population has been associated with the increase in upper limb weight-bearing demands for performance of transfers, pressure relief raises, and manual wheelchair (WC) propulsion. Shoulder pain negatively impacts independence and functional mobility, and is associated with significantly reduced subjective quality of life and physical activity in individuals with paraplegia (Gutierrez et al., 2007).

The demands of functional mobility on the shoulder joint following SCI have been explored in the laboratory, particularly during WC propulsion and depression raises and transfers. While depression transfers are performed less frequently than WC propulsion, median activity of key shoulder muscles is substantially greater, and glenohumeral contact forces are higher than that in WC propulsion. For instance, Perry et al. (1996) reported median pectoralis and infraspinatus major activity as high as 81 and 45% of maximum isometric contraction respectively, during the body lift of a level depression transfer in volunteers with low-level paraplegia vs. Mulroy et al. (2004) report median intensity of 34 and 20% during the push phase of self-selected free manual WC propulsion. Similarly, Van Drongelen et al. (2005) reported that the shoulder contact force was significantly greater (300%) during a weight relief lift than during level WC propulsion on an ergometer at 0.83 m/s.

Car transfers are the most demanding of transfers (Janssen et al., 1996), likely partly owing to the need to support the body across the gap between the WC and the car seat, resulting from the setback of the vehicle seat from the doorframe. Further, the vehicle seat is often higher than the WC seat, particularly for those transferring into higher profile vehicles, such as vans, SUVs, and trucks, increasing the demands on the trailing limb shoulder (Gagnon et al., 2008). Finally, for individuals driving independently, the need to load the WC into the vehicle presents an additional and substantial upper extremity demand. In spite of this increase in task demands, car transfer demands have not been documented in the literature.

Despite the high demands, car transfers are often a gateway to community mobility. Independent driving is the key to vocational engagement and community participation in individuals with SCI. Independent drivers with SCI were almost twice as likely to be engaged in a vocation (paid or volunteer work or school) as non-drivers (Hatchett et al., 2009) and demonstrated higher community reintegration and health-related quality of life scores compared to non-drivers (Norweg et al., 2011). Independent driving for persons who are dependent on a WC for mobility requires either car transfers or a modified van with a lift. Thus, the importance of understanding shoulder demands during car transfer and WC loading in order to prevent shoulder pain and injury and preserve independence and community participation for individuals with spinal cord injury is crucial.

The purpose of this study was to delineate the factors influencing car transfer and WC loading demands on the shoulders of individuals with paraplegia from SCI. We additionally endeavored to document transfer and WC loading times and techniques during transfer from individuals own WCs to their own vehicles.

[1]https://www.nscisc.uab.edu/, SCI Facts and Figures at a Glance, February 2012.

Materials and Methods

Volunteers with paraplegia resulting from SCI [American Spinal Injury Association Impairment Scale (AIS) A, B, or C] were recruited from outpatient clinics at Rancho Los Amigos National Rehabilitation Center (RLANRC) (a sample of convenience). Participants signed an informed consent approved by the Rancho Los Amigos Institutional Review Board prior to collection of observational data in the Pathokinesiology Laboratory and the parking lot at RLANRC. Individuals were at least 18 years of age with a minimum duration of paraplegia from SCI (AIS A, B, or C) of 2 years and maximum duration of 21 years. Volunteers were included if they pushed a manual WC for at least 50% of their locomotion and independently drove a vehicle and loaded their WC into their vehicle, according to self-report. Participants were excluded if they had cervical radiculopathy, adhesive capsulitis, a positive Codman's Drop Arm Test or a history of shoulder or upper limb traumatic injury, fracture or surgery impacting function at the time of consent. They were additionally excluded if they had comorbidities that could affect the integrity of their musculoskeletal system (e.g., rheumatoid arthritis, diabetes mellitus) and/or their body weight exceeded 250 lbs.

After reviewing and signing an informed consent in accordance with the Declaration of Helsinki, demographic data (personal factors), physical measurements, and WC measurements were collected from each participant. Vehicle measurements were taken prior to videotaping of the car transfer and WC loading. Demographic data included gender, age, level of and duration of SCI, and completeness of SCI. Physical measurements included body weight and height. WC measurements included weight of the WC frame and wheels, seat width, and seat height (from ground to the top of the WC cushion). Vehicle measurements included driver's seat height (from the ground), roof height (from the ground to the top of driver's door opening), and maximum driver's side door opening. Additionally, the distance of the gap between the right side of the WC seat and the left side of the driver's seat was measured once the volunteer had positioned their WC just prior to transferring into the vehicle. Vehicles were classified as one of the two heights: (1) low profile (sedans) and (2) high profile. The higher profile group consisted of (a) mid-height vehicles [vans and small to medium sports utility vehicles (SUVs)] and (b) high-profile vehicles (large trucks and SUVs), and were collapsed into one higher profile group for statistically meaningful results since only four volunteers drove high-profile vehicles (large trucks and SUVs). A Wheelchair User's Shoulder Pain Index (WUSPI) form was completed prior to bilateral shoulder strength testing.

Bilateral maximal isometric shoulder torques were measured in six directions (abduction, adduction, flexion, extension, external rotation, and internal rotation) using a Biodex System 3 Pro Dynamometer (Biodex Medical Systems, Inc., New York, NY, USA). Volunteers were tested in a seated position with the trunk and pelvis secured by two chest straps and a pelvic strap. Shoulder abduction and adduction were tested at 45° of shoulder abduction, the elbow and wrist extended to neutral, and the forearm pronated

90°. Shoulder flexion and extension were tested with the shoulder flexed 45° and the elbow, wrist, and forearm neutral. External and internal rotation were tested with the UE positioned in 90° of abduction, the elbow in 90° of flexion, the wrist neutral, and the forearm pronated. Each participant was instructed to push or pull against the lever arm using their maximum effort for a duration of 5 s. Following one 3-s practice repetition to familiarize the participant with the test, two trials were performed with a 10–15 s rest break between trials. The peak values for each of the two trials for each UE were averaged and then normalized to body weight.

Participants were videotaped while transferring into and out of their own vehicle and loading their personal WC into and out of the vehicle. Two to three video cameras were utilized to capture the functional tasks from different angles [driver's side sagittal view, passenger's side sagittal view, and driver's side diagonal (45–60° anterior to the sagittal plane)]. The driver's side and passenger doors and windows were open to allow adequate video capture of the tasks without obstruction by the vehicle. Video was captured at a rate of 30 frames/s and was initiated as the subject approached the vehicle in the WC just prior to stopping next to driver's seat of the vehicle to initiate the car transfer. Video recording was ended just after the volunteer loaded the last WC component in the vehicle and placed the hands on steering wheel, indicating completion of the loading task. Participants repeated the transfer and loading two times if they were able.

Videotape of each volunteer performing a transfer from their personal WC into the driver's seat of their usual vehicle as well as loading of their WC, utilizing their customary technique, into the vehicle were reviewed by one physical therapist with 15 years of experience. All participants removed and loaded the wheels and many removed the cushion and/or sideguards from the WC frame prior to loading the frame into the front or back seat of the their vehicle. Movement strategies and transfer and loading times were documented. During the transfer into the vehicle, placement of the lower limbs prior to transfer was documented, location of the right and left hand just prior to and during the transfer, and number of scoots prior to the body lift onto the driver's seat and afterward (just prior to WC loading) were recorded. Total transfer time (just after the WC is positioned to just prior to initiation of the reach for the WC for loading) and body lift time (from initiation of trunk lift to cessation of trunk descent) were quantified from time-stamped video. During WC loading, location of final resting place of the WC frame and components after loading into the vehicle was documented. Total loading time (from the initiation of reach for the WC to the placement of the last WC component in the vehicle and return to the driving position) and WC frame (heaviest component) loading time were quantified.

Statistics

Data were analyzed using SPSS 12.0 Software (SPSS, Inc., Chicago, IL, USA). Bivariate Pearson product-moment correlations (r) were calculated between body lift time and participant demographics including age, level of SCI, body weight, maximal isometric torques of the shoulder muscle groups, and characteristics of the WC and car including car seat height, WC to car height difference, and horizontal distance between WC seat and car (gap). Correlations were also calculated between WC frame loading time and participant demographics, isometric shoulder torques, and WC frame weight. Chi-square tests were used to assess associations between vehicle heights (low vs. high profile) and hand and leg placement strategies during transfer and WC frame placement during loading. One-way analyses of variance (ANOVAs) tests were conducted to compare isometric muscle torques of the shoulder muscles and WUSPI (shoulder pain) scores between participants who used the various patterns of hand placement for right and left hands and leg placement during the body lift phase of the transfer. If a significant main effect of hand or leg placement strategy was found, a Tukey's *post hoc* test was used to determine significance in pair-wise comparisons. An independent t-test was used to compare isometric muscle torques of the shoulder muscles and WUSPI (shoulder pain) scores between participants who loaded their WC frame in the front seat with those who placed it on the back seat. A p-value of 0.05 was used to denote statistical significance.

Results

Participants included four females and 25 males with T2 to L3 (2–15) paraplegia (mean = 9.1 ± 3.5, **Table 1**) and an average age of 40.2 ± 8.8 years and average time since injury of 14.9 ± 7.9 years. Average body weight was 73.2 kg. Average driver's seat height measured from the ground for the low-profile vehicles was 22 in, 28 in for the mid-height vehicles, and 36 in for the high profile. Most participants drove sedans (17 out of 29), seven drove mid-height, and five drove high profile vehicles. The average height difference between the WC seat and vehicle driver's seat was 3.7 ± 5.5 in and ranged from −3.5 to 16.0 in.

Description of Transfer Strategies

The majority of participants (15 out of 29) placed their right leg only into the car prior to the body lift phase of the transfer; five placed both legs in the car prior to the transfer, and eight transferred with their legs outside of the car (**Figures 1A–C**). The right or leading hand was most frequently placed on the driver's seat (19/29) during the body lift portion of the transfer, while seven transferred with the right hand on the steering wheel and three transferred with the right hand on the overhead door frame or grab bar (**Figures 1A–C**). The left hand or trailing hand was placed most frequently on the WC seat for the body lift (14/29), while three placed their left hand on the steering wheel of the car, two on the wheel of the WC, three on both the WC seat and wheel, five on the driver's side door, and two on the overhead door frame.

Vehicle height tended to influence hand placement but not leg placement strategy used during the body lift phase of car transfer. Drivers of higher profile vehicles were more likely to place their right hand on the driver's seat during the body lift than those who drove sedans (10/12 mid and high profile vs. 9/17 sedan) (Chi square = 2.88, $p = 0.09$) In contrast, those who drove a sedan were more likely to place their right hand on other locations [steering wheel (5/17) or overhead door frame (3/17)] than higher profile vehicle drivers (steering wheel 2/12). Sedan drivers were somewhat more likely to place their left hand on the WC seat or wheel than those who drove higher profile vehicles (13/17 vs. 6/12). A minority of sedan driver's (4/17) placed their left hand on various parts of the car (steering wheel = 2/17, overhead door frame = 1/17, and driver's door = 1/17). In contrast, half of the

TABLE 1 | Pearson product-moment correlations between body lift time and demographic, car/WC dimensions, and isometric shoulder torques.

Variable	Mean (SD)	Range (min–max)	Pearson correlation (r) with body lift time	p-Value of correlation
Age (years)	40.2 (8.8)	22.9–61.1	−0.294	0.061
Duration of SCI (years)	14.9 (7.9)	3.1–35.5	−0.002	0.500
Level of SCI (T2 = 2, T3 = 3, . . ., T12 = 12, L1 = 13, L2 = 14, L3 = 15)	9.1 (3.5)	2–15 (T2–L3)	**−0.490**	**0.004**
Body weight (kg)	73.2 (17.1)	44.0–120.3	−0.203	0.145
Car seat height (in)	25.8 (5.3)	19.0–38.3	**0.426**	**0.011**
WC seat to car seat height difference (in)	3.7 (5.5)	−3.5 to 16.0	**0.408**	**0.014**
Horizontal distance between WC seat and car seat (in)	11.8 (2.2)	7.0–16.8	0.015	0.471
Number of scoots prior to body lift	1.32 (0.91)	0–5	−0.086	0.331
Right adduction (Nm/kg × 100)	98.4 (32.7)	78.6–91.3	0.173	0.184
Right internal rotation (Nm/kg × 100)	46.3 (18.7)	42.4–50.4	0.015	0.468
Right external rotation (Nm/kg × 100)	46.5 (14.4)	39.2–45.6	0.298	0.058
Right flexion (Nm/kg × 100)	89.5 (28.4)	71.1–81.4	0.240	0.105
Right abduction (Nm/kg × 100)	73.7 (25.3)	59.9–69.6	**0.337**	**0.037**
Right extension (Nm/kg × 100)	94.6 (31.0)	77.2–90.6	0.165	0.196
Left adduction (Nm/kg × 100)	99.9 (34.0)	78.6–91.3	0.134	0.244
Left internal rotation (Nm/kg × 100)	50.9 (16.8)	42.4–50.4	0.083	0.334
Left external rotation (Nm/kg × 100)	48.1 (14.6)	39.2–45.6	0.257	0.089
Left flexion (Nm/kg × 100)	90.7 (26.1)	71.1–81.4	0.162	0.201
Left abduction (Nm/kg × 100)	75.8 (24.1)	59.9–69.6	**0.349**	**0.032**
Left extension (Nm/kg × 100)	89.5 (27.1)	77.2–90.6	0.100	0.302

Bold results indicate $p < 0.05$.

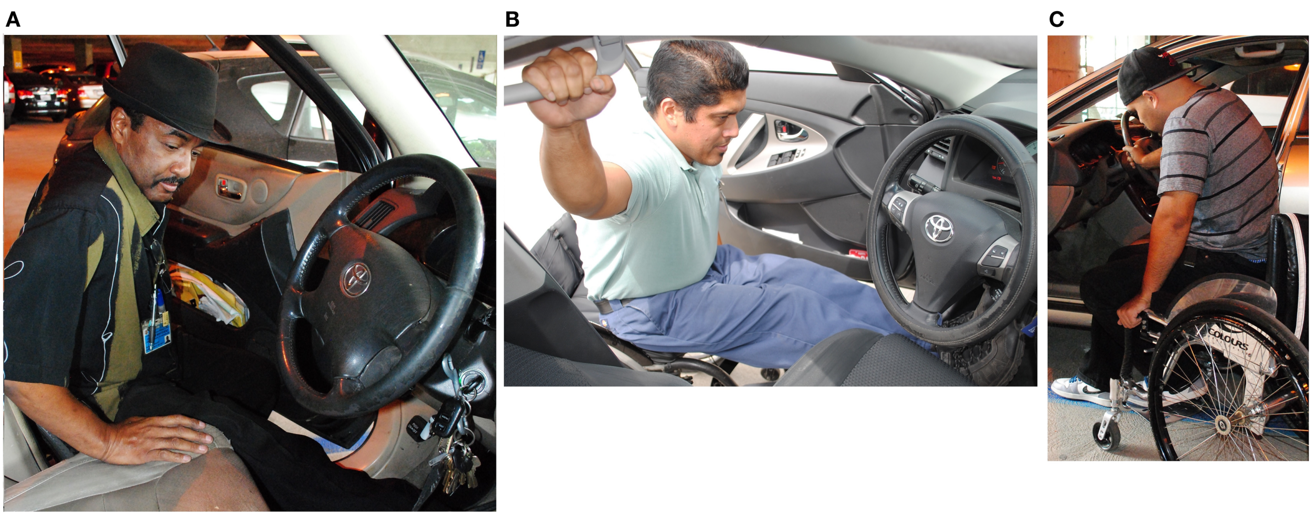

FIGURE 1 | (A) Car transfer into a mid-height vehicle with right leg inside and left leg outside of the vehicle and leading hand on the driver's seat. **(B)** Car transfer into a sedan with both legs in the vehicle and the leading hand on the grab bar. **(C)** Car transfer into a sedan with both legs outside of the vehicle and the leading hand on the steering wheel.

drivers of higher profile vehicles (6/12) placed their left hand on the vehicle: steering wheel = 1/12, overhead door frame = 1/12, and driver's door = 4/12. The association between car height and left hand placement did not reach statistical significance ($p = 0.14$). There was no association between car height and leg placement strategy.

Body Lift Time

Mean body lift time was 1.43 ± 0.5 s, <10% of total transfer time (mean = 17.8 ± 10.5 s). Body lift times were negatively correlated with levels of paraplegia ($r = -0.49$, $p = 0.004$) (**Table 1**; **Figure 2**) and positively correlated with car seat height ($r = 0.43$, $p = 0.011$) (**Figure 3**). In addition, right and left shoulder abduction strength was positively correlated with body lift time ($r = 0.34$, $p = 0.037$ and $r = 0.35$, $p = 0.032$, respectively) and age was negatively correlated ($r = -0.29$, $p = 0.061$). Younger and stronger persons had longer body lift times than older and weaker individuals.

Hand Placement and Shoulder Pain

Participants who placed their right hand on the steering wheel during transfer had higher WUSPI scores indicating more pain (9.9 ± 15.7), compared to those who placed their right hand on

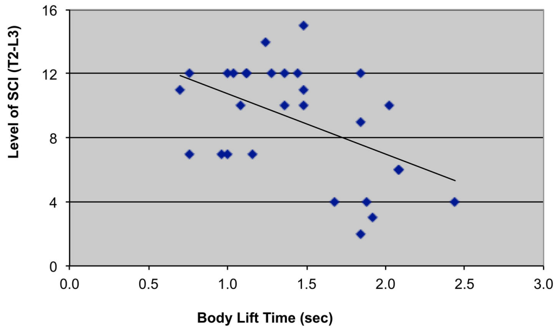

FIGURE 2 | Scatterplot with trend-line illustrating relationship between level of SCI (T2–L3) and body lift time (sec = seconds). T2 = 2, T3 = 3, T4 = 4, . . ., T12 = 12, LI = 13, L2 = 14, L3 = 15.

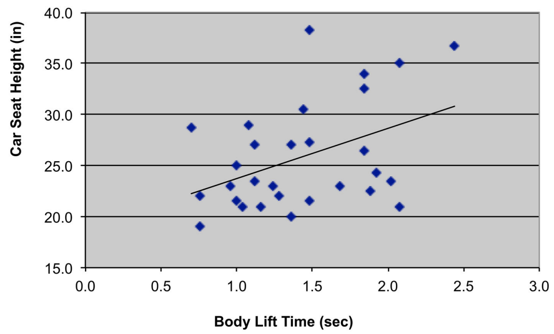

FIGURE 3 | Scatterplot with trend-line illustrating relationship between car seat height (in = inches) and body lift time (sec = seconds).

the driver's seat (1.3 ± 2.6) or overhead door frame (0.8 ± 1.3) ($p = 0.05$).

Description of WC Loading Strategies

Most participants used both hands to load the WC frame (18/29), seven used only one hand and four lifted part of the time with one hand and part of the time with both hands. Just under half of participants did not rest the frame momentarily on the car or their legs during loading (13/29) and more loaded their WC frame onto the back seat (18/29) than onto the front seat (11/29). Of those who drove a sedan, 53% (9/17) placed their WC frame on the front seat, while only 17% (2/12) who drove higher profile vehicles placed the frame in the front seat (Chi-square = 3.38, $p = 0.066$).

WC Frame Loading Time

The average time to load the WC frame into the vehicle was 10.7 ± 7.9 s, which was 20% of the total WC loading time of 49.5 ± 21.8 s. Mean weight of the WC frame was 7.7 ± 2.1 kg. WC frame loading time was not related to isometric shoulder torques, weight of the frame, or any demographic characteristic.

WC Frame Placement during Loading

Participants who customarily placed their WCs in the back seat had weaker muscle strength in the internal rotators of the right arm (28.1 ± 9.3 Nm/kg $\times$ 100) compared to those who placed their WCs in the front seat (40.2 ± 10.3 Nm/kg $\times$ 100) ($p = 0.003$).

Discussion

This study provides a descriptive analysis of customary movement strategies used by independent drivers with paraplegia from SCI to transfer from their WC into the driver's seat and to load their WC frame into their vehicle. The most physically demanding portion of a car transfer is the sub-phase when the body weight is lifted off of the WC seat with the arms and to a lesser extent, the legs and placed into the car seat. The duration of this high-intensity phase (body lift) was related both to the individual's level of SCI and to the height of the vehicle (**Figures 2** and **3**). Persons with lower levels of paraplegia spent less time in the body-lift phase of the transfer than those with higher paraplegia (**Figure 2**). A higher level of paraplegia results in a greater loss of innervation and strength in trunk muscles and has been associated with increased trunk flexion during "standard sitting pivot transfers" (depression transfers between two level, adjacent surfaces) (Desroches et al., 2013b). This increased trunk flexion was thought to increase stability by lowering the center of mass of the trunk and increasing the base of support. It also increased the average linear displacement of the body's center of mass (Desroches et al., 2013a), which could result in a longer duration of the body lift phase. The body lift phase of the transfer also was longer when transferring into cars with higher driver's seat heights, reflecting an increased demand on the shoulder with higher profile vehicles. Likely related was the association of younger age and stronger shoulder abductors with longer body lift times as younger and stronger persons tended to drive the higher profile vehicles.

The transfer times documented in the current study were similar but slightly longer than times reported in the literature for sitting pivot transfers. Sitting pivot transfers have been explored biomechanically in the laboratory by various groups (Allison et al., 1995, 1996; Perry et al., 1996; Allison, 1997; Allison and Singer, 1997; Nawoczenski et al., 2003; Gagnon et al., 2009; Desroches et al., 2012) and investigators differed in methodologies used to define the phases of transfer. For example, Nawoczenski et al. (2003) utilized angular and linear motion of the thorax to determine a preparatory, lift/pivot, and sit-back phase, while Gagnon et al. (2009) utilized a combination of kinematic and kinetic data to determine the pre-lift, lift, and post-lift phase of sitting pivot transfers. Additionally, sitting pivot transfers evaluated in the laboratory have consisted of transfers between levels, adjacent surfaces, unlike the typical car transfers assessed in the current study. Our goal was to define and quantify the most demanding portion of the car transfer, the body lift, which largely occurred from the lower WC surface to the driver's seat that was additionally separated by a horizontal gap of 9–17 in, which is substantially larger than the separation of surfaces in most studies of sitting pivot transfers.

In spite of the higher demands of the car transfer, the average duration of the body lift phase of the car transfer reported in this study was largely consistent with sitting pivot transfer times documented in the literature. While definitions and procedures for determination of phasing varied between studies, Desroches et al. (2012) found that the lift-pivot phase, the most comparable to the body-lift phase quantified in our study, averaged 0.72 ± 0.24 s (vs. the average body lift duration of 0.915 s (0.515–1.072 s) into the sedan in the current study. It follows that a car transfer, a more complex and demanding version of the sitting pivot transfer, would take longer, particularly in higher profile vehicles when both the horizontal and vertical distances traversed were greater than in sitting pivot transfers.

Leading hand placement was associated with shoulder pain during transfer into the driver's seat. Individuals who placed their leading hand on the steering wheel (24%) had significantly higher WUSPI scores than those who placed their hand on the driver's seat (66%) or overhead on the grab bar or doorframe (10%). This might be explained by the degree of elevation of the weight-bearing shoulder with the leading hand on the steering wheel, which is most consistent with average angles documented by Bey et al. (2007). Bey and colleagues utilized biplane X-rays and subject-specific CT models to determine that the supraspinatus tendon is in closest proximity to the acromion between 27.7° and 36.1° of elevation. These findings suggest that impingement of the subacromial structures might be more likely with the leading hand on the steering wheel, particularly with repetition of this high-demand task.

Strategies for hand placement, but not leg placement, were influenced by vehicle height. Eighty-three percent of those driving higher profile vehicles placed their leading hand on the driver's seat, while only 53% of sedan driver's utilized this technique. Given the larger discrepancy between the WC and driver's seat heights with higher profile vehicles, the leading hand may not be able to sufficiently reach the steering wheel or overhead grab bar or doorframe for theses transfers, except in taller individuals. Further, sedan drivers were more likely to place their trailing hand on the WC seat or wheel (77%) compared to higher profile vehicle drivers (50%). Individuals who routinely placed their WC frame onto the back seat of the car had isolated weakness in the internal rotator muscles of the right shoulder compared to those who placed their WC frame onto the front seat. Since the typical motion to place the frame into the back seat involves extreme external rotation with horizontal abduction of the shoulder, the internal rotators would need to control the weight of the frame during release. The typical shoulder position during release of the chair also happens to be the position to test for anterior instability of the shoulder. Gold et al. (2007) created a computer-generated model of the rotator cuff tendons from an open MRI during this test. They demonstrated that as the arm moves from a resting position at the side of the body to the extreme position of abduction and external rotation, the tendon of subscapularis, a primary internal rotator, is stretched significantly and lies directly beneath the acromion. Our participants are holding a WC frame that averages 7.7 kg so that the weakness of the internal rotation seen in those who put their chair in the back seat may well represent repetitive stretch-induced muscle injury.

Limitations

Determination of transfer phasing was conducted by observation of events from a videotape. Given that our goal was to explore and describe car transfers in the real-world, we did not record kinematic and kinetic data for more objective determination of transfer times. However, video tape of the transfer from two to three different angles was utilized by a single physical therapist with 15 years of experience for all subjects to maximize consistency and accuracy.

Our sample size of 29 participants was low, given the variation in car transfer strategies and vehicle heights and relatively few participants had shoulder pain. Consequently, the results should be viewed as a preliminary study. Additionally, since only four volunteers drove high profile vehicles (large trucks and SUVs), it was necessary to collapse the medium and high profile vehicle groups into one group for statistically meaningful results.

Conclusion

Documentation of the techniques utilized for car transfer from different WCs into a variety of vehicles and the loading of these WCs is a necessary preliminary step to optimize future biomechanical testing in the laboratory. We found that individuals with higher levels of injury, stronger shoulders, and higher profile vehicles had longer body lift times, relating to more demanding car transfers. Technique, particularly placing the leading hand on the steering wheel, was also associated with higher levels of shoulder pain. Placement of the WC frame, the heaviest component of the WC, into the back seat was associated with weakness in the internal rotators of the right shoulder, which may indicate injury from repetitive high demands on lengthened muscles. These findings illustrate the need to incorporate strength training into the weekly routines of individuals with SCI, a disability that places increased demands on the upper extremities. The ultimate goal is to determine optimal car transfer techniques to prevent shoulder pain and injury and maximize functional independence and participation for individuals aging with spinal cord injury.

Funding

Funded by NIDRR grant number H133E080024.

Acknowledgments

The authors would like to thank our study volunteers and staff in the Pathokinesiology Laboratory and Rehabilitation Engineering at Rancho Los Amigos National Rehabilitation Center.

References

Allison, G., Singer, K., and Marshall, R. (1995). Muscle activation patterns during transfers in individuals with spinal cord injury. *Aust. J. Physiother.* 41, 169–176. doi:10.1016/S0004-9514(14)60427-X

Allison, G. T. (1997). The ability to transfer in individuals with spinal cord injury. *Crit. Rev. Phys. Med. Rehabil.* 9, 131–151. doi:10.1615/CritRevPhysRehabilMed.v9.i2.20

Allison, G. T., and Singer, K. P. (1997). Assisted reach and transfers in individuals with tetraplegia: towards a solution. *Spinal Cord* 35, 217–222. doi:10.1038/sj.sc.3100393

Allison, G. T., Singer, K. P., and Marshall, R. N. (1996). Transfer movement strategies of individuals with spinal cord injuries. *Disabil. Rehabil.* 18, 35–41. doi:10.3109/09638289609167087

Bey, M. J., Brocks, S. K., Beierwaltes, W. N., Zauel, R., Kolowich, P. A., and Lock, T. R. (2007). In-vivo measurement of subacromial space width during shoulder elevation: technique and preliminary results in patients following unilateral rotator cuff repair. *Clin. Biomech.* 22, 767–773. doi:10.1016/j.clinbiomech.2007.04.006

Desroches, G., Gagnon, D., Nadeau, S., and Popovic, M. (2013a). Magnitude of forward trunk flexion influences upper limb muscular efforts and dynamic postural stability requirements during sitting pivot transfers in individuals with spinal cord injury. *J. Electromyogr. Kinesiol.* 23, 1325–1333. doi:10.1016/j.jelekin.2013.09.003

Desroches, G., Gagnon, D., Nadeau, S., and Popovic, M. R. (2013b). Effects of sensorimotor trunk impairments on trunk and upper limb joint kinematics and kinetics during sitting pivot transfers in individuals with a spinal cord injury. *Clin. Biomech.* 28, 1–9. doi:10.1016/j.clinbiomech.2012.11.001

Desroches, G., Vermette, M., Gourdou, P., and Gagnon, D. (2012). Development of an automated method to detect sitting pivot transfer phases using biomechanical variables: toward a standardized method. *J. Neuroeng. Rehabil.* 9, 7. doi:10.1186/1743-0003-9-7

Gagnon, D., Koontz, A. M., Brindle, E., Boninger, M. L., and Cooper, R. A. (2009). Does upper-limb muscular demand differ between preferred and nonpreferred sitting pivot transfer directions in individuals with a spinal cord injury? *J. Rehabil. Res. Dev.* 46, 1099–1108. doi:10.1682/JRRD.2009.02.0012

Gagnon, D., Nadeau, S., Noreau, L., Dehail, P., and Gravel, D. (2008). Quantification of reaction forces during sitting pivot transfers performed by individuals with spinal cord injury. *J. Rehabil. Med.* 40, 468–476. doi:10.2340/16501977-0192

Gold, G. E., Pappas, G. P., Blemker, S. S., Whalen, S. T., Campbell, G., McAdams, T. A., et al. (2007). Abduction and external rotation in shoulder impingement: an open MR study on healthy volunteers initial experience. *Radiology* 244, 815–822. doi:10.1148/radiol.2443060998

Gutierrez, D. D., Thompson, L., Kemp, B., and Mulroy, S. J. (2007). The relationship of shoulder pain intensity to quality of life, physical activity, and community participation in persons with paraplegia. *J. Spinal Cord Med.* 30, 251–255.

Hatchett, P. E., Mulroy, S. J., Requejo, P. S., Lighthall Haubert, L., Eberly, V. J., and Conners, S. G. (2009). “Impact of independent driving and chair lifting into a vehicle on community participation for individuals with paraplegia,” in *American Spinal Injury Association Conference Proceedings*. Downey, CA.

Janssen, T. W., van Oers, C. A., Veeger, H. E., Hollander, A. P., van der Woude, L. H., and Rozendal, R. H. (1996). *Relationship Between Physical Strain During Standardised ADL Tasks and Physical Capacity in Men with Spinal Cord Injuries. Paraplegia*, Vol. 34. Edinburgh, UK: International Medical Society of Paraplegia, Nature Publishing Group.

Mulroy, S. J., Farrokhi, S., Newsam, C. J., and Perry, J. (2004). Effects of spinal cord injury level on the activity of shoulder muscles during wheelchair propulsion: an electromyographic study. *Arch. Phys. Med. Rehabil.* 85, 925–934. doi:10.1016/j.apmr.2003.08.090

Nawoczenski, D. A., Clobes, S. M., Gore, S. L., Neu, J. L., Olsen, J. E., Borstad, J. D., et al. (2003). Three-dimensional shoulder kinematics during a pressure relief technique and wheelchair transfer. *Arch. Phys. Med. Rehabil.* 84, 1293–1300. doi:10.1016/S0003-9993(03)00260-0

Norweg, A., Jette, A. M., Houlihan, B., Ni, P., and Boninger, M. L. (2011). Patterns, predictors, and associated benefits of driving a modified vehicle after spinal cord injury: findings from the national spinal cord injury model systems. *Arch. Phys. Med. Rehabil.* 92, 477–483. doi:10.1016/j.apmr.2010.07.234

Perry, J., Gronley, J. K., Newsam, C. J., Reyes, M. L., and Mulroy, S. J. (1996). Electromyographic analysis of the shoulder muscles during depression transfers in subjects with low-level paraplegia. *Arch. Phys. Med. Rehabil.* 77, 350–355. doi:10.1016/S0003-9993(96)90083-0

Sie, I. H., Waters, R. L., Adkins, R. H., and Gellman, H. (1992). Upper extremity pain in the postrehabilitation spinal cord injured patient. *Arch. Phys. Med. Rehabil.* 73, 44–48.

Van Drongelen, S., Van Der Woude, L. H., Janssen, T. W., Angenot, E. L., Chadwick, E. K., and Veeger, D. H. (2005). Glenohumeral contact forces and muscle forces evaluated in wheelchair-related activities of daily living in able-bodied subjects versus subjects with paraplegia and tetraplegia. *Arch. Phys. Med. Rehabil.* 86, 1434–1440. doi:10.1016/j.apmr.2005.03.014

Conflict of Interest Statement: The authors declare that the research was conducted in the absence of any commercial or financial relationships that could be construed as a potential conflict of interest.

frontiers in
BIOENGINEERING AND BIOTECHNOLOGY

ORIGINAL RESEARCH ARTICLE
published: 15 December 2014
doi: 10.3389/fbioe.2014.00073

Three-dimensional kinematics of the human metatarsophalangeal joint during level walking

Sivangi Raychoudhury*, *Dan Hu* and *Lei Ren*

School of Mechanical, Aerospace and Civil Engineering, University of Manchester, Manchester, UK

Edited by:
Jill L. McNitt-Gray, University of Southern California, USA

Reviewed by:
Henrique De Amorim Almeida, Polytechnic Institute of Leiria, Portugal
Eiji Tanaka, The University of Tokushima Graduate School, Japan

****Correspondence:***
Lei Ren, School of Mechanical, Aerospace and Civil Engineering, University of Manchester, Manchester M13 9PL, UK
e-mail: lei.ren@manchester.ac.uk

The objective of this study is to investigate the three-dimensional (3D) kinematics of the functional rotation axis of the human metatarsophalangeal (MP) joint during level walking at different speeds. A 12 camera motion analysis system was used to capture the 3D motion of the foot segments and a six force plate array was employed to record the simultaneous ground reaction forces and moments. The 3D orientation and position of the functional axis (FA) of the MP joint were determined based on the relative motion data between the tarsometatarsi (hindfoot) and phalanges (forefoot) segments. From the results of a series of statistical analyses, it was found that the FA remains anterior to the anatomical axis (AA), defined as a line connecting the first and fifth metatarsal heads, with an average distance about 16% of the foot length across all walking speeds, and is also superior to the AA with an average distance about 2% of the foot length during normal and fast walking, whereas the FA shows a higher obliquity than the AA with an anteriorly more medial and superior orientation. This suggests that using the AA to represent the MP joint may result in overestimated MP joint moment and power and also underestimated muscle moment arms for MP extensor muscles. It was also found that walking speed has statistically significant effect on the position of the FA though the FA orientation remains unchanged with varying speed. The FA moves forwards and upwards toward a more anterior and more superior position with increased speed. This axis shift may help to increase the effective mechanical advantage of MP extensor muscles, maximize the locomotor efficiency, and also reduce the risk of injury. Those results may further our understanding of the contribution of the intrinsic foot structure to the propulsive function of the foot during locomotion at different speeds.

Keywords: metatarsophalangeal joint, three-dimensional kinematics, position and orientation, walking, ground reaction force

INTRODUCTION

The human foot is an enormously complex structure consisting of numerous bones, muscles, ligaments, and synovial joints. As the only body component in contact with the ground, it plays multiple crucial roles in attenuating ground impacts, maintaining locomotor stability, and generating propulsive powers during locomotion (Ker et al., 1987; Carrier et al., 1994; Ren et al., 2008a). Over the past decades, many experimental and computer simulation studies have been conducted to investigate the locomotor function of the human foot complex (Apkarian et al., 1989; Scott and Winter, 1993; Leardini et al., 1999; Gefen et al., 2000; Carson et al., 2001; MacWilliams et al., 2003; Nester et al., 2007; Ren et al., 2010; Qian et al., 2013). However, most of those studies have mainly concentrated on the biomechanics of the whole foot segment, whereas the specific functioning of the distal part of the foot has been much less frequently studied.

The metatarsophalangeal (MP) joint near the distal end of the foot may have multiple functions during locomotion (Bojsen-Møller and Lamoreux, 1979; Mann and Hagy, 1979; Stefanyshyn and Nigg, 1997). During walking, the MP joint undergoes progressive dorsiflexion in the stance phase, which tightens up the plantar aponeurosis to wrap around the metatarsal heads. This may help to elevate and stabilize the longitudinal arch of the foot by using the windlass mechanism of the plantar aponeurosis without muscle function (Mann and Hagy, 1979). The dorsiflexion of the MP joint in the late stance phase can noticeably reduce the moment arm of the ground reaction force compared to a single rigid foot lever. This may increase the effective mechanical advantage (EMA) of ankle dosriflexor muscles and hence reduce the muscular effort during push-off (Bojsen-Møller and Lamoreux, 1979; Biewener, 1989). In addition, it was found that the dorsiflexion of the MP joint tightens the connective tissue framework around the ball of the foot, and thereby constraints the relative motions of the skin to enable shear forces to be transmitted to the skeleton (Bojsen-Møller and Lamoreux, 1979).

The MP joint may play significant roles during rapid change of body movement because the toes help in balancing the body while the body is changing its motion rapidly (Mann and Hagy, 1979). It was found that the MP joint is a significant absorber of energy in sprinting, with increased energy absorption with increased speed (Stefanyshyn and Nigg, 1997). Furthermore, it was suggested that ankle and MP joints may provide a mechanism of varying the gear ratio of the ankle dorsiflexor muscles during running (Carrier et al., 1994). This may enhance locomotor performance during constant speed running by maintaining the muscles near the high-efficiency portion of the force–velocity curve.

To simplify the analyses, many of the previous studies have assumed that the MP joint rotates about an axis perpendicular to the sagittal plane, originating from the fifth metatarsal head (Stefanyshyn and Nigg, 1997, 1998). This two-dimensional assumption simplifies the motion of the MP joint and does not reflect the oblique nature of the MP joint. A recent study investigated the effect of the MP joint axis by comparing the calculated joint kinetic variables based on different MP joint axis definitions in sprinting (Smith et al., 2012). It was found that MP joint axis has a significant effect on calculated joint moment, power, and energy, and oblique joint axes result in less energy absorbed at the MP joint than a simplified perpendicular axis to the sagittal plane. It was suggested that an appropriate representation of the MP joint is necessary to better understand the MP joint during locomotion (Smith et al., 2012). However, most previous studies defined the MP joint axis mainly based on anatomical landmarks, e.g., the straight line connecting first and fifth metatarsal heads (Bojsen-Møller and Lamoreux, 1979; Smith et al., 2012). So far, little is known about the realistic orientation and position of the functional rotation axis of the MP joint during locomotion and how it changes with varying locomotor speed (Pohl et al., 2007).

The objective of this study is to investigate the three-dimensional (3D) kinematics of the human MP joint during level walking. The latest three-dimensional motion analysis technique was used to determine the position and orientation of the functional rotation axis of the MP joint in the stance phase of walking for multiple subjects at different speeds. Statistical analysis was conducted to evaluate the difference between the functional MP joint axis and the axis typically defined by the anatomical landmarks in literature. Moreover, the effect of walking speed on MP joint position and orientation was also analyzed statistically. This would provide useful information to improve our understanding of the *in vivo* biomechanical functioning of the human MP joint as well as the propulsive function of the foot during different speeds of locomotion. Furthermore, this may also help in innovating the design of sports and therapeutic footwear, prosthetic lower limbs, and robotic legs, which could be inspired from the nature design of the musculoskeletal system of the human body (Ren et al., 2014).

MATERIALS AND METHODS

GAIT MEASUREMENT

Six healthy male subjects with normal foot conformation (age: 26.67 ± 2.69 years; weight: 67.17 ± 10.29 kg; height: 175.0 ± 4.43 cm) from a population of postgraduate students, with no previous medical history of foot and lower limb injury, participated in the gait measurement in this study. The subjects provided informed consent in accordance with the policies of local institute ethical advisory committee. All the subjects were instructed to walk barefoot along an indoor walkway at their self-selected slow, normal, and fast walking speeds. A specially designed marker cluster system was mounted firmly on the right feet of the subjects to record the 3D segmental motions of the foot complex (see **Figure 1**).

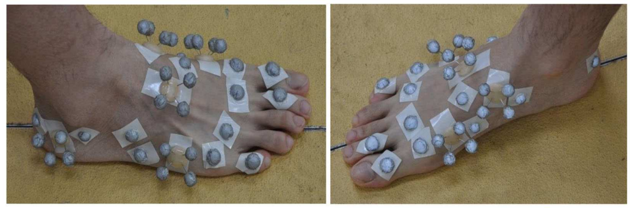

FIGURE 1 | The infrared marker cluster system used in this study to capture 3D foot motions. The foot was divided into two segments including tarsometatarsi (hindfoot) and phalanges (forefoot). A set of thermal plastic plates, each carrying four infrared markers, were used to capture the foot segmental motions. A number of hemispherical infrared markers were also attached on the anatomical landmarks.

A 12 infrared camera motion analysis system (Qualisys, Sweden) was used to capture 3D segmental motions at 150 Hz. Six force plates (Kistler, Switzerland) were used to record the simultaneous ground reaction forces and moments at 1000 Hz. A set of static calibration procedures were undertaken to locate the anatomical landmarks using a calibration wand and reflective markers according to the calibrated anatomical system technique (Cappozzo et al., 1995). The calibration markers were removed before the dynamic walking trials. For each walking speed, the measurement was repeated 15 times to ensure that representative walking data are recorded.

MP JOINT DEFINITION AND PARAMETERS

Five rigid body segments were defined to represent the lower limb: pelvis, right thigh, right shank, right tarsometatarsi (hindfoot), and right phalanges (forefoot). The 3D anatomical coordinate systems were defined for each individual segment based on the previous studies (Jenkyn and Nicol, 2007; Ren et al., 2008a, 2010). In this study, we have assumed that the five phalanges form a single rigid forefoot segment, whereas the MP joint is considered as a single hinge type joint. The anatomical axis (AA) of the MP joint was defined as the oblique line connecting the first metatarsal head and the fifth metatarsal head (see the blue line in **Figure 2A**), which is similar to those defined in previous studies (Boonpratatong and Ren, 2010; Graf et al., 2012; Smith et al., 2012). This axis divides the foot into two different segments: hindfoot and forefoot. On the other hand, the functional axis (FA) of the MP joint was defined as the rotational axis between the hindfoot segment and forefoot segment during stance phase of walking (see the red line in **Figure 2A**). A closed-form algorithm is employed to determine the 3D position and orientation of the FA of the MP joint (Gamage and Lasenby, 2002), which does not require manual adjustment of optimization parameters.

To represent the 3D orientation of the AA and FA of the MP joint, the 3D axes were projected to the *XOZ* and *XOY* planes of the foot local anatomical coordinate system (see **Figures 2C,D**), where the angles α and β were used to define the axis orientation with counter clockwise being positive based on the right-hand rule (see **Figures 2C,D**). In addition, to determine the 3D position of the AA and FA of the MP joint, the intersection point (x_a, y_a) between the AA and the *XOY* plane of the foot local coordinate system, or

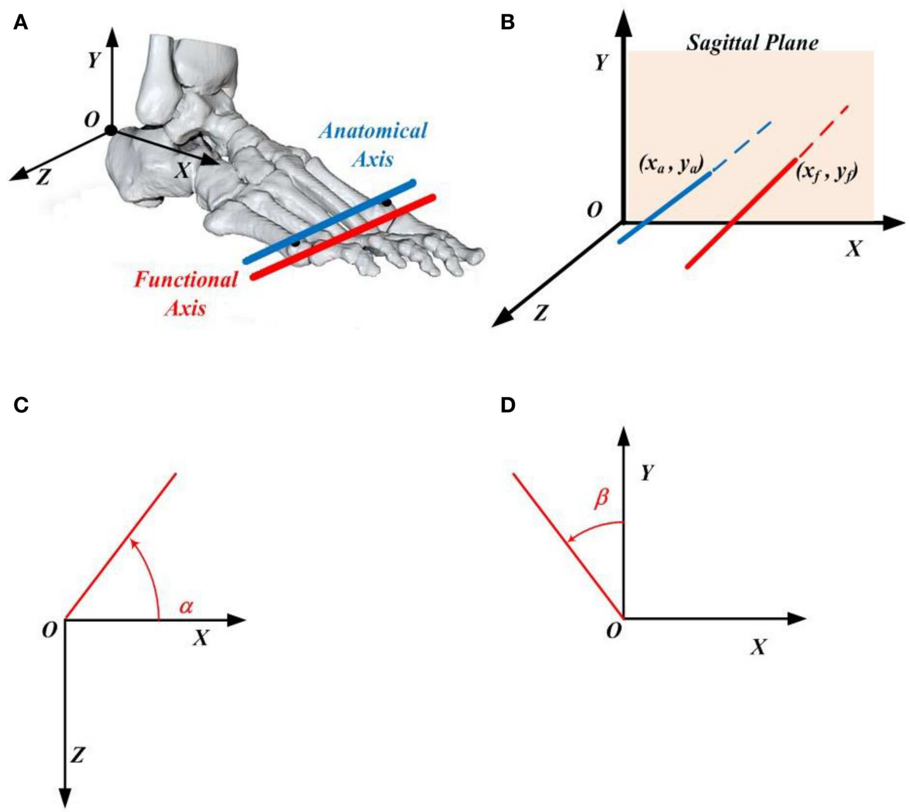

FIGURE 2 | (A) The functional axis (red) and anatomical axis (blue) of the metatarsophalangeal joint, where the anatomical axis is defined as the line connecting the first and fifth metatarsal heads. The origin of the foot local coordinate system situates on the upper ridge of the calcaneus bone. **(B)** The position of the functional axis is defined by its intersection point (x_f, y_f) with the *XOY* plane of the foot coordinate system, whereas the location of the anatomical axis is determined by its intersection point (x_a, y_a) with the *XOY* plane of the foot coordinate system. **(C)** Angle α made by the functional (or anatomical) axis with respect to the foot *X* axis when projected to the *XOZ* plane of the foot coordinate system. **(D)** Angle β made by the functional (or anatomical) axis with respect to the foot *Y* axis when projected to the *XOY* plane of the foot coordinate system.

the intersection point (x_f, y_f) between the FA and the *XOY* plane of the foot local coordinate system was used (see **Figure 2B**).

DATA ANALYSIS

The raw measured data were processed using GMAS software (Generalized Motion Analysis Software), a MATLAB based software package for 3D kinematic and kinetic analysis of biomechanical multi-body systems (Ren et al., 2005, 2008b). Trials with more than 10 consecutive missing frames were discarded. After the fill-gap processing, the data were filtered using a low pass zero lag fourth-order Butterworth digital filter with a cut-off frequency of 6.0 Hz.

Statistical analyses were conducted to investigate the 3D position and orientation differences between the AA and FA of the MP joint, and also the effect of walking speed on the AA and FA of the MP joint using SPSS 20.0 software (IBM, Armonk, New York, NY, USA). The effects of joint definition (AA or FA) and walking speed on joint position parameters (x, y) and orientation parameters (α, β) were analyzed using analysis of variance (ANOVA) with repeated measurements using a linear mixed model approach taking into account intra- and inter-subject variability. The different joint definitions and walking speeds were the fixed effects, and subjects and trials were random effects. Differences between the two joint definitions (AA and FA) and between each pair of walking speeds were tested using Fisher's least significant difference (LSD) multiple comparison based on the least-squared means, probability by considering $p < 0.05$ as statistically significant.

RESULTS

The measured data for all the six subjects were processed by using the method described in the preceding section. **Figure 3** shows the mean and standard deviation values of the MP joint AA position (x_a, y_a) and FA position (x_f, y_f) defined in the *XOY* plane of the foot local coordinate system, where the origin of the coordinate system is at the upper ridge of the calcaneus bone (Ren et al., 2010). The position data of both AA and FA axes for all the six subjects (from subject A to subject F) at all three different walking speeds (slow, normal, and fast) are presented in **Figure 3**. It can be seen that the FA is consistently anterior to the AA for all subjects across all the three walking speeds with an average position difference of 27.3 mm. In the inferior superior direction (along *Y* axis), both FA and AA positions are close to the origin, and

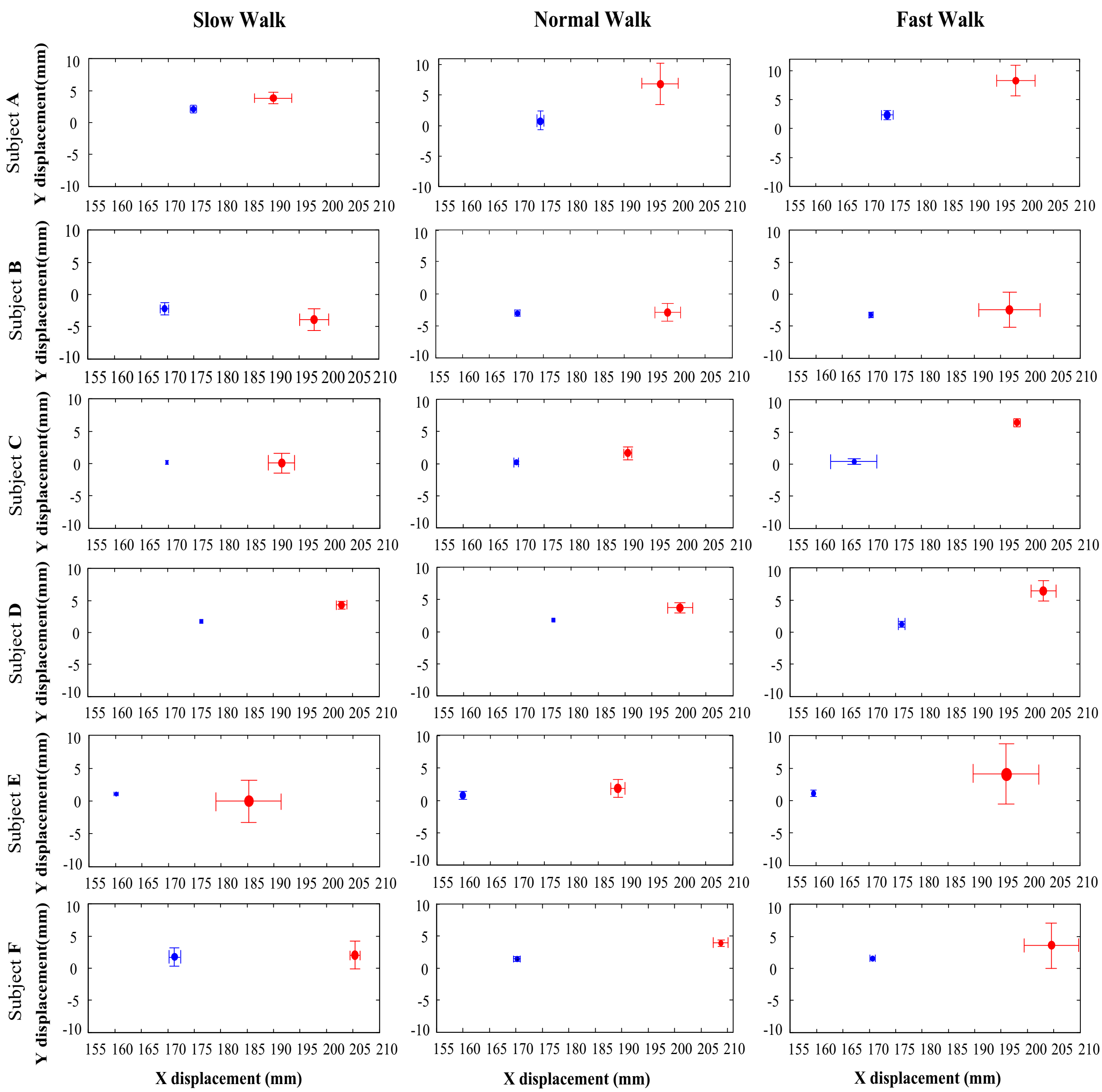

FIGURE 3 | The *x* and *y* positions of the anatomical axis (blue) and functional axis (red) of the MP joint in the *XOY* plane of the foot coordinate system, for all the six subjects (A to F) across all three walking speeds. The solid dots indicate the mean *x* and *y* positions, whereas the bars show the 1 SD zones.

there is no consistent trend in the relative position between the two axes. From the results shown in **Figure 3**, it appears that the FA of MP joint moves toward a more anterior and superior position with increased walking speed though the displacement in the inferior superior direction (along *Y* axis) is much less than the displacement in the posterior anterior direction (along *X* axis). In contrast to the trend of the FA, it seems that there is no apparent change in the AA position with increased walking speed for all the subjects.

Figure 4 shows the mean and the 1 SD zone of the orientation angle α of both AA and FA made with respect to the *X* axis in the *XOZ* plane of the foot coordinate system for all the subjects at all three walking speeds. It can be seen that both AA and FA axes are close to the direction of the foot *Z* axis. According to the right-hand rule, the positive angle α is measured starting from the *X* axis in a counter clockwise direction. From **Figure 4**, it appears that the FA has an orientation more inclined to the foot *Z* axis than the AA in the transverse plane for all the subjects. Also, it seems

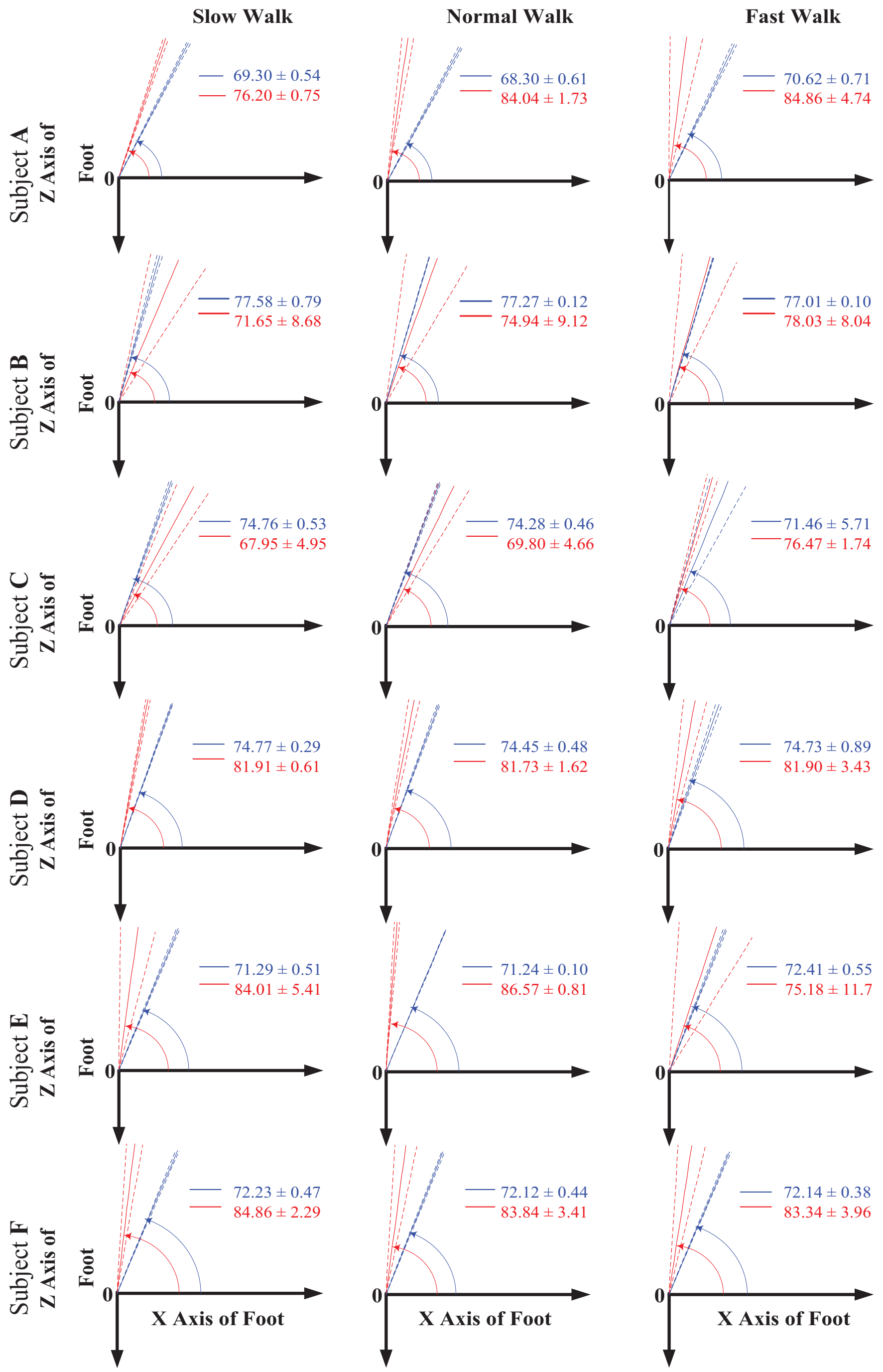

FIGURE 4 | The orientation angle α made by the functional axis (red) and anatomical axis (blue) with respect to the foot *X* axis when projected to the *XOZ* plane of the foot coordinate system for all the six subjects across all three walking speeds. The solid lines indicate the mean value of the angle, whereas the dash lines show the 1 SD zones.

that the obliquity of both AA and FA does not change obviously with changing speed.

Similarly, **Figure 5** shows the mean and the 1 SD zone of the orientation angle β of both AA and FA made with respect to the *Y* axis in the *XOY* plane of the foot coordinate system for all the subjects at all three walking speeds. According to the right-hand rule, the negative angle β is measured starting from the *Y* axis in a clockwise direction. It can be seen that the FA shows an apparently different orientation than the AA in the sagittal plane for all the subjects. The FA possesses a higher orientation angle β than the AA leading to a FA direction more inclined to the foot *Y* axis. From the results shown in **Figure 5**, it seems that the orientation angles

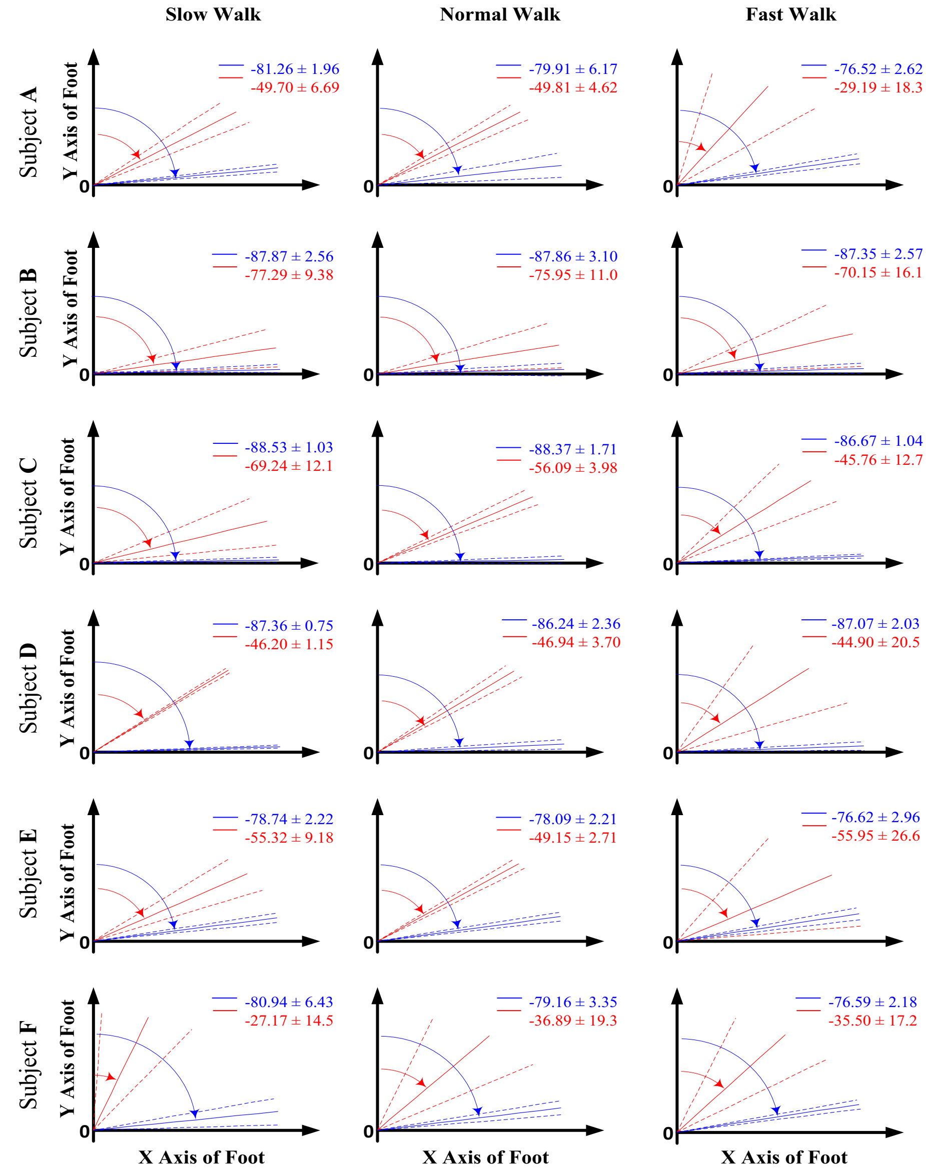

FIGURE 5 | The orientation angle β made by the functional axis (red) and anatomical axis (blue) with respect to the foot *Y* axis when projected to the *XOY* plane of the foot coordinate system for all the six subjects across all three walking speeds. The solid lines indicate the mean value of the angle, whereas the dash lines show the 1 SD zones.

in the sagittal plane for both AA and FA do not show particular changes with increased walking speed.

In **Table 1**, the statistical analysis result on the 3D position and orientation difference between the AA and FA of the MP joint is listed. The position parameters (x_a, y_a) and (x_f, y_f) are normalized by the foot length, defined as the distance between the upper ridge of the calcaneus bone and the midpoint between the first and fifth metatarsal heads. It can be seen that statistically significant differences were found for all the 3D orientation and position parameters across all three walking speeds, except for the vertical (in superior inferior direction) position parameter y at slow walking speed. The functional rotation axis, FA of the MP joint has a more anterior and superior position than that of the AA, especially during normal and fast walking. This position difference is more significant in superior inferior direction than in anterior posterior direction. The FA of the MP joint shows an anteriorly more medial and more superior orientation than the AA, which is defined as the straight line connecting the first and fifth metatarsal heads. This joint orientation angle difference is more significant in the sagittal plane than in the transverse plane.

The statistical analysis result investigating the effect of walking speed on the 3D position and orientation of the FA is shown in **Table 2**. It can be seen that the joint position in the anterior posterior direction shows statistically significant difference when

Table 1 | The result of the statistical analysis of the position and orientation difference between the functional axis (FA) and the anatomical axis (AA) of the MP joint.

		***x* Normalized by foot length**	***y* Normalized by foot length**	**α (degree)**	**β (degree)**
Slow walk	FA	1.1496 ± 0.0424^{a}	0.0050 ± 0.0193^{a}	77.8345 ± 7.9035^{a}	-52.6132 ± 24.7011^{a}
	AA	0.9989 ± 0.0100^{b}	0.0042 ± 0.0096^{a}	73.5031 ± 2.7248^{b}	-84.2468 ± 4.8971^{b}
Normal walk	FA	1.1619 ± 0.0415^{a}	0.0153 ± 0.0185^{a}	81.2593 ± 6.4280^{a}	-51.0727 ± 15.0268^{a}
	AA	0.9982 ± 0.0104^{b}	0.0029 ± 0.0098^{b}	72.8288 ± 2.8084^{b}	-82.7051 ± 5.2145^{b}
Fast walk	FA	1.1683 ± 0.0390^{a}	0.0250 ± 0.0250^{a}	80.0469 ± 6.3455^{a}	-47.2030 ± 23.4659^{a}
	AA	0.9942 ± 0.0187^{b}	0.0028 ± 0.0110^{b}	73.2755 ± 3.0998^{b}	-82.4910 ± 5.6568^{b}

Values are means ± s.e.m. for all trials and all subjects. Identical letters indicate axis groups within a column do not differ significantly from each other ($p > 0.05$).

Table 2 | The result of the statistical analysis of the effect of walking speed on the orientation and position of the functional axis (FA) of the MP joint.

	x_f Normalized by foot length	**y_f Normalized by foot length**	**α (degree)**	**β (degree)**
Slow walk	1.1496 ± 0.0424^{a}	0.0050 ± 0.0193^{a}	77.8345 ± 7.9035^{a}	-52.6132 ± 24.7011^{a}
Normal walk	1.1619 ± 0.0415^{ab}	0.0153 ± 0.0185^{b}	81.2593 ± 6.4280^{a}	-51.0727 ± 15.0268^{a}
Fast walk	1.1683 ± 0.0390^{b}	0.0250 ± 0.0250^{c}	80.0469 ± 6.3455^{a}	-47.2030 ± 23.4659^{a}

Values are means ± s.e.m. for all trials and all subjects. Identical letters indicate speed groups within a column do not differ significantly from each other ($p > 0.05$).

Table 3 | The result of the statistical analysis of the effect of walking speed on the orientation and position of the anatomical axis (AA) of the MP joint.

	x_a Normalized by foot length	**y_a Normalized by foot length**	**α (degree)**	**β (degree)**
Slow walk	0.9989 ± 0.0100^{a}	0.0042 ± 0.0096^{a}	73.5031 ± 2.7248^{a}	-84.2468 ± 4.8971^{a}
Normal walk	0.9982 ± 0.0104^{a}	0.0029 ± 0.0098^{b}	72.8288 ± 2.8084^{a}	-82.7051 ± 5.2145^{ab}
Fast walk	0.9942 ± 0.0187^{a}	0.0028 ± 0.0110^{ab}	73.2755 ± 3.0998^{a}	-82.4910 ± 5.6568^{b}

Values are means ± s.e.m. for all trials and all subjects. Identical letters indicate speed groups within a column do not differ significantly from each other ($p > 0.05$).

walking speed changes from slow to fast. The FA moves forwards toward a more anterior position with increased speed. More significant change can be seen in the superior inferior direction, the FA moves upwards toward a more superior position appreciably when walking speed increases. No statistically significant effects are found on the FA orientation angles in both the transverse (α) and sagittal (β) planes when walking speed increases from self-selected low to self-selected fast.

Similarly, **Table 3** shows the statistical analysis result examining the effect of walking speed on the 3D position and orientation of the AA of the MP joint. No statistically significant change is found in the AA position along the anterior posterior direction. When walking speed increases to normal, the AA position in the superior inferior direction moves apparently toward the inferior direction. There is no statistically significant effect found on the AA orientation angle in the transverse plane (α) with changing speed, whereas a slight increase of the AA orientation angle in the sagittal plane (β) was found when walking speed increases from slow to fast.

DISCUSSION

The objective of this study is to investigate the 3D orientation and location of the functional joint axis of the MP joint during walking at different speeds. Here, the functional joint axis of the MP joint is defined as the relative rotational axis between the phalanx segments and the hindfoot in the stance phase of walking. In the previous studies, the MP joint was normally defined as a line connecting the first (or second) and fifth metatarsal heads (Boonpratatong and Ren, 2010; Smith et al., 2012), and little is known about the realistic position of the functional joint axis of the MP joint.

Our results show that the 3D orientation and position of the FA of the MP joint is close to the AA defined by the line connecting first and fifth metatarsal heads. However, for the subjects tested in this study, there are some statistically significant differences between the FA and AA. The FA remains anterior to the AA with an average distance about 16% of the foot length across all walking speeds. In the vertical direction, the FA is superior to the AA with an average distance about 2% of the foot length during normal and fast walking, whereas, the FA shows a higher obliquity than AA with an anteriorly more medial and superior orientation. This suggests that using the AA to represent the MP joint may result in overestimated MP joint moment and power and also underestimated muscle moment arms for MP extensor muscles.

It was found that walking speed has statistically significant effect on the position of the FA though the FA orientation remains unchanged with varying speed. When walking speed increases, the FA moves forwards and upwards toward a more anterior and more superior position. This joint axis shift toward the ground reaction force vector in the late stance of walking will result in decreased moment arm of ground reaction force and also simultaneously increased moment arm of MP extensor muscles, and hence will increase the EMA of MP extensor muscles (Biewener, 1989, 1990, 2003; Biewener et al., 2004; Winter, 2005). In addition, a forward shift of the MP joint axis will result in an increased lever distance to the ankle joint, and may moderate the angular velocity increase with increasing walking speed. This may help to maintain the contraction velocity of the MP extensor muscles in the power optimal region (Biewener, 2003). It appears that a variable gear mechanism also exists in the MP joint especially in the late stance of walking (Carrier et al., 1994).

This study has some limitations. A single hinge type joint was assumed to represent the relative motion between the phalanges and the rearfoot throughout the stance phase of walking. As suggested by previous studies, two different axes may exist at the MP level during locomotion (Bojsen-Møller, 1978; Bojsen-Møller and Lamoreux, 1979). Our future works will involve the investigation of the 3D positions and transition of multiple MP axes. In addition, two rigid bodies (phalanges and hindfoot) were assumed to represent the motion of the foot complex by using multiple marker clusters in the gait measurement. However, in reality, some appreciable relative motions may occur between phalanges or the hindfoot bones. Thus, more complicated models may be needed in the future to better understand the 3D kinematics at MP joint. Furthermore, bone-pin markers rather than skin mounted markers may help to reduce the skin artifact involved in the gait measurement (Nester et al., 2007).

CONCLUSION

This study reveals many factors at the distal end of the foot, which may contribute to the locomotor function of the human foot complex. This includes not only the obliquely oriented functional rotation axis but also the relative position of the axis with respect to the hindfoot bones. The position of the FA of the MP joint is found to be anterior and superior to the AA with higher obliquity. Furthermore, with increasing speed the FA shifts more anterior. This forward and upward shift of the FA with increasing walking speed may help to moderate the muscular effort, maximize the locomotor efficiency, and reduce the risk of injury. This study may help us to better understand the contribution of the intrinsic foot structure to the propulsive function of the foot during locomotion at different speeds. Furthermore, this may also help in improving the design of sports and therapeutic footwears, prosthetic lower limbs, and robotic legs.

ACKNOWLEDGMENTS

The assistance and support of John R. Hutchinson on measurement data collection have been valuable.

REFERENCES

Apkarian, J., Naumann, S., and Cairns, B. (1989). A three dimensional kinematic and dynamic model of the lower limb. *J. Biomech.* 22, 143–155. doi:10.1016/0021-9290(89)90037-7

Biewener, A. A. (1989). Scaling body support in mammals: limb posture and muscle mechanics. *Science* 245, 45–48. doi:10.1126/science.2740914

Biewener, A. A. (1990). Biomechanics of mammalian terrestrial locomotion. *Science* 250, 1097–1103. doi:10.1126/science.2251499

Biewener, A. A. (2003). *Animal Locomotion*. New York: Oxford University Press Inc.

Biewener, A. A., Farley, C. T., Roberts, T. J., and Temaner, M. (2004). Muscle mechanical advantage of human walking and running: implications for energy cost. *J. Appl. Physiol.* 97, 2266–2274. doi:10.1152/japplphysiol.00003.2004

Bojsen-Møller, F. (1978). "The human foot a two speed construction," in *International Series of Biomechanics*, Vol. 6, eds E. Asmussen and K. Jorgensen. 261–266.

Bojsen-Møller, F., and Lamoreux, L. (1979). Significance of free dorsiflexion of the toes in walking. *Acta Orthop. Scand.* 50, 471–479. doi:10.3109/17453677908989792

Boonpratatong, A., and Ren, L. (2010). The human ankle-foot complex as a multi-configurable mechanism during the stance phase of walking. *J. Bionic Eng.* 7, 211–218. doi:10.1016/S1672-6529(10)60243-0

Cappozzo, A., Catani, F., Della, C. U., and Leardini, A. (1995). Position and orientation in space of bones during movement: anatomical frame definition and determination. *Clin. Biomech.* 10, 171–178. doi:10.1016/0268-0033(95)91394-T

Carrier, D. R., Heglund, N. C., and Earls, K. D. (1994). Variable gearing during locomotion in the human musculoskeletal system. *Science* 265, 651–653. doi:10.1126/science.8036513

Carson, M. C., Harrington, M. E., Thompson, N., O'Connor, J. J., and Theologis, T. N. (2001). Kinematic analysis of multi-segment foot model for research and clinical applications: a repeatability analysis. *J. Biomech.* 34, 1299–1307. doi:10.1016/S0021-9290(01)00101-4

Gamage, S. S., and Lasenby, J. (2002). New least squares solutions for estimating the average centre of rotation and the axis of rotation. *J. Biomech.* 35, 87–93. doi:10.1016/S0021-9290(01)00160-9

Gefen, A., Megido-Ravid, M., Itzchak, Y., and Arcan, M. (2000). Biomechanical analysis of the three-dimensional foot structure during gait: a basic tool for clinical applications. *J. Biomech.* 122, 630–639. doi:10.1115/1.1318904

Graf, E. S., Wright, I. C., and Stefanyshyn, D. J. (2012). Effect of relative marker movement on the calculation of the foot torsion axis using a combined Cardan angle and helical axis approach. *Comput. Math. Methods Med.* 2012, 368050. doi:10.1155/2012/368050

Jenkyn, T. R., and Nicol, A. C. (2007). A multi-segment kinematic model of the foot with a novel definition of forefoot motion for use in clinical gait analysis during walking. *J. Biomech.* 40, 3271–3278. doi:10.1016/j.jbiomech.2007.04.008

Ker, R. F., Bennett, M. B., Bibby, S. R., Kester, R. C., and Alexander, R. M. (1987). The spring in the arch of the human foot. *Nature* 325, 147–149. doi:10.1038/325147a0

Leardini, A., Benedetti, M. G., Catani, F., Simoncini, L., and Giannini, S. (1999). An anatomically based protocol for the description of foot segment kinematics during gait. *Clin. Biomech.* 14, 528–536. doi:10.1016/S0268-0033(99)00008-X

MacWilliams, B. A., Cowley, M., and Nicholson, D. E. (2003). Foot kinematics and kinetics during adolescent gait. *Gait Posture* 17, 214–224. doi:10.1016/S0966-6362(02)00103-0

Mann, R. A., and Hagy, J. L. (1979). The function of the toes in walking, jogging and running. *Clin. Orthop. Relat. Res.* 142, 501–510.

Nester, C. J., Liu, A., Ward, E., Howard, D., Cocheba, J., Derrick, T., et al. (2007). In vitro study of foot kinematics using a dynamic walking cadaver model. *J. Biomech.* 40, 1927–1937. doi:10.1016/j.jbiomech.2006.09.008

Pohl, M. B., Messenger, N., and Buckley, J. G. (2007). Forefoot, rearfoot and shank coupling: effect of variations in speed and mode of gait. *Gait Posture* 25, 295–302. doi:10.1016/j.gaitpost.2006.04.012

Qian, Z., Ren, L., Ding, Y., Hutchinson, J. R., and Ren, L. (2013). A dynamic finite element analysis of human foot complex in the sagittal plane during level walking. *PLoS ONE* 8:e79424. doi:10.1371/journal.pone.0079424

Ren, L., Howard, D., Ren, L., Nester, C., and Tian, L. (2008a). A phase-dependent hypothesis for locomotor functions of human foot complex. *J. Bionic Eng.* 5, 175–180. doi:10.1016/S1672-6529(08)60022-0

Ren, L., Jones, R. K., and Howard, D. (2008b). Whole body inverse dynamics over a complete gait cycle based only on measured kinematics. *J. Biomech.* 41, 2750–2759. doi:10.1016/j.jbiomech.2008.06.001

Ren, L., Howard, D., Ren, L., Nester, C., and Tian, L. (2010). A generic analytical foot rollover model for predicting translational ankle kinematic in gait simulation studies. *J. Biomech.* 43, 194–202. doi:10.1016/j.jbiomech.2009.09.027

Ren, L., Jones, R. K., and Howard, D. (2005). Dynamic analysis of load carriage biomechanics during level walking. *J. Biomech.* 38, 853–863. doi:10.1016/j.jbiomech.2004.04.030

Ren, L., Qian, Z., and Ren, L. (2014). Biomechanics of musculoskeletal system and its biomimetic implications: a review. *J. Bionic Eng.* 11, 159–175. doi:10.1016/S1672-6529(14)60033-0

Scott, S. H., and Winter, D. A. (1993). Biomechanical model of the human foot: kinematics and kinetics during the stance phase of walking. *J. Biomech.* 26, 1091–1104. doi:10.1016/S0021-9290(05)80008-9

Smith, G., Lake, M., Lees, A., and Worsfold, P. (2012). Measurement procedures affect the interpretation of the metatarsophalangeal joint function during accelerated sprinting. *J. Sports Sci.* 30, 1521–1527. doi:10.1080/02640414.2012.713501

Stefanyshyn, D. J., and Nigg, B. M. (1997). Mechanical energy contribution of the metatarsophalangeal joint to running and sprinting. *J. Biomech.* 20, 1081–1085. doi:10.1016/S0021-9290(97)00081-X

Stefanyshyn, D. J., and Nigg, B. M. (1998). Contribution of the lower extremity joints to mechanical energy in the running vertical jumps and running long jumps. *J. Sports Sci.* 16, 177–186. doi:10.1080/026404198366885

Winter, D. A. (2005). *The Biomechanics and Motor Control of Human Movement*, 3rd Edn. New Jersey: John Wiley and Sons, Inc.

Conflict of Interest Statement: The authors declare that the research was conducted in the absence of any commercial or financial relationships that could be construed as a potential conflict of interest.

Received: 30 August 2014; accepted: 01 December 2014; published online: 15 December 2014.

*Citation: Raychoudhury S, Hu D and Ren L (2014) Three-dimensional kinematics of the human metatarsophalangeal joint during level walking. Front. Bioeng. Biotechnol. **2**:73. doi: 10.3389/fbioe.2014.00073*

This article was submitted to Biomechanics, a section of the journal Frontiers in Bioengineering and Biotechnology.

Advantages of publishing in Frontiers

OPEN ACCESS
Articles are free to read, for greatest visibility

COLLABORATIVE PEER-REVIEW
Designed to be rigorous – yet also collaborative, fair and constructive

FAST PUBLICATION
Average 85 days from submission to publication (across all journals)

COPYRIGHT TO AUTHORS
No limit to article distribution and re-use

TRANSPARENT
Editors and reviewers acknowledged by name on published articles

SUPPORT
By our Swiss-based editorial team

IMPACT METRICS
Advanced metrics track your article's impact

GLOBAL SPREAD
5'100'000+ monthly article views and downloads

LOOP RESEARCH NETWORK
Our network increases readership for your article